

UNIVERSIDADE DE LISBOA, FACULDADE DE FARMÁCIA



**Novel Mitochondrial Electron Transport-Chain Inhibitors
as Potential Antimalarial Agents**

Tiago Correia de Oliveira Rodrigues

DOUTORAMENTO EM FARMÁCIA
(QUÍMICA FARMACÊUTICA E TERAPÊUTICA)

2010

UNIVERSIDADE DE LISBOA, FACULDADE DE FARMÁCIA



**Novel mitochondrial electron transport-chain inhibitors as
potential antimalarial agents**

Tiago Correia de Oliveira Rodrigues

Tese orientada pela Professora Doutora Francisca Lopes

**Dissertação apresentada à Faculdade de Farmácia da Universidade de Lisboa, com vista à
obtenção do grau de Doutor em Farmácia (Química Farmacêutica e Terapêutica)**

Lisboa, 2010

Este trabalho foi desenvolvido sob orientação da Professora Doutora Francisca Lopes, no *iMed.UL* (Research Institute for Medicines and Pharmaceutical Sciences) da Faculdade de Farmácia da Universidade de Lisboa.

O trabalho foi financiado pela Fundação para a Ciência e Tecnologia através da bolsa de doutoramento SFRH/BD/30689/2006 e do projecto PTDC/SAU-FCT/098734/2008.

This work was developed under scientific guidance of Dr. Francisca Lopes, at *iMed.UL* (Research Institute for Medicines and Pharmaceutical Sciences), Faculty of Pharmacy, University of Lisbon.

The work was financially supported by Fundação para a Ciência e Tecnologia, through the doctoral grant SFRH/BD/30689/2006, and project PTDC/SAU-FCT/098734/2008.

“But, on the other hand, every one who is seriously involved in the pursuit of science becomes convinced that a spirit is manifest in the laws of the Universe - a spirit vastly superior to that of man, and one in the face of which we with our modest powers must feel humble.”

Albert Einstein
(1879-1955)

To my wife, sister and parents

ACKNOWLEDGEMENTS

My PhD studies spanned roughly four years and many people crossed my path along the way. Several have proven essential for the completion of my work and I am grateful for the time they have made available to help me out, sometimes crippling their own work.

I want to sincerely thank my supervisor Dr. Francisca Lopes and Professor Rui Moreira for giving me the opportunity to do research in medicinal chemistry in the first place, while I was still a young undergraduate student. I would also wish to express my gratitude for presenting me with such an enthralling and challenging project, and with that, enabling me to learn a lot more on medicinal chemistry. Thank you so much for your sympathy, encouragement and guidance during all these years, and enlightening me through all your knowledge. Thanks are also owed for allowing me to try out my own ideas, which was great, even if they ended up in nothing.

I would also like to acknowledge Dr. Rita C. Guedes and Dr. Daniel dos Santos for introducing me to the computational chemistry world, which was key in the attempt of making a hybrid medicinal chemist out of me. Thank you so much for your patience, especially in the beginning, since I had no background in Linux whatsoever. The tools that I was taught were more than I had ever expected and our fruitful discussions helped me reach new heights.

I am also in debt with those whose work was indispensable to the completion of this project. I would like to thank Professor Phil J. Rosenthal and Dr. Jiri Gut (UCSF) for the antiplasmodial testing.

To Professor Paul M. O'Neill (University of Liverpool), Professor Steve Ward, Dr. Nick Fisher and Dr. Giancarlo Biagini (LSTMH) for their collaboration regarding the ongoing biochemical studies and insightful critics and suggestions.

To Dr. Filipa P. da Cruz, Dr. Miguel Prudêncio and Dr. Maria M. Mota (IMM) for the tests regarding the liver stage and the cytotoxicity assays.

To Dr. Maria do Rosário Bronze and Dr. Isabel Joglar for the mass spectra.

To RIAIDT at Santiago de Compostela, for performing the elemental analysis and mass spectroscopy experiments.

To Dr. Bruno Dacunha Marinho (University Santiago Compostela), for performing the X-Ray crystallography of my compounds, and his help in the preparation of the first paper.

To Fundação para a Ciência e Tecnologia (FCT), for funding; I will try to make sure it was well spent money.

I would also want to thank all the technical staff, Sr. Francisco and Lena, for helping me out with the material and ordering me reagents. I cross my fingers for Francisco's endeavour in becoming an EuroMillions winner ends shortly.

This project involved quite a lot of lab work and uncountable hours amid smelly solvents. I was fortunate to come across many funny and pleasant labmates; João, Ana, Rita and others, without whom, life at the lab would have been utterly bleak. I thank your interest in my work, abundant discussions and suggestions, and for encouraging me when the molecules didn't react the way they were supposed to... or at least in my mind.

I wish to express my deepest gratitude to my friends. Several pages would be necessary to go into details, but thanks are due to Helder for his friendship, and among other things, letting me play games on his laptop, discussing about science, UFOs and life in the outer Universe with me, while some of the reactions were refluxing downstairs. I am greatly in debt with you for listening about what was bothering me, and giving me your advice for both scientific and personal matters. I would also like to thank Rute, Su and Jalmira for their support and friendship. The list goes way beyond the limits of this section but rest assured that all of those that I did not mention have not been forgotten.

Acknowledgements are also due to my family in general, to whom this thesis is dedicated, particularly the loving memory of my ancestors; to my parents, for their love and continuous support in all its forms. I certainly wouldn't be here if you didn't encourage me to thrive in studies since I was very young, and motivating me whenever I was feeling miserable. I believe this is the result of a serious dedication to studies, and for that, this is also for you. I hope I have made you proud! I also thank my always little sister for her love and believing in me. She's been a focus in my life from the day she was born and I held her in my arms. There's more to life than pursuing PhD studies and you are the accurate example of how I feel about it.

I also thank my parents and brother-in-law for their love and always receiving me open-heartedly, for their understanding when I was absent working, and for cheering me up with their good-moods.

I praise God for the opportunity to get this far, for it is under His grace that we draw our path. I also thank the endless guidance and support; for giving me His hand and shedding light on me, especially in the darkest and seemingly unbearable moments of life. A million words are not enough to express my gratitude!

Finally, but certainly not least, I wish to thank my beloved wife Cláudia for her love and unconditional support; for being keystone. I wouldn't have got this far if it weren't for you. This is not only dedicated to you, but also your own accomplishment!

GENERAL INDEX

GENERAL INDEX	i
INDEX OF FIGURES	v
INDEX OF SCHEMES	viii
INDEX OF TABLES	xi
ABSTRACT	xiii
RESUMO	xiv
LIST OF ABBREVIATIONS AND SYMBOLOGY	xv

CHAPTER 1

1. INTRODUCTION	1
1.1 OVERVIEW OF MALARIA AND MITOCHONDRIAL DRUG TARGETS	1
1.2 THE ELECTRON TRANSPORT-CHAIN PATHWAY	2
1.3 CYTOCHROME <i>BC</i> ₁ INHIBITORS	3
1.3.1 <i>1,4-Naphthoquinones</i>	5
1.3.2 <i>4(1H)-Quinolones</i>	12
1.3.3 <i>Acridones</i>	14
1.3.4 <i>Acridinediones</i>	16
1.3.5 <i>4(1H)-Pyridones</i>	17
1.3.6 <i>(E)-β-Methoxyacrylates</i>	20
1.3.7 <i>Chalcones</i>	20
1.3.8 <i>8-Aminoquinolines</i>	22
1.3.9 <i>Miscellaneous</i>	22
1.4 AIMS OF THE THESIS	25

CHAPTER 2

2. PYRIDONIMINE SCAFFOLD	29
2.1 QUANTUM MECHANICAL STUDY	29

2.1.1 Brief overview on electronic structure methods and its use in the development of antimalarial drug candidates.....	29
2.1.2 Molecular geometry of 4-pyridonimines.....	29
2.1.3 Frontier orbital energies and densities.....	35
2.1.4 Molecular electrostatic potentials (MEP).....	38
2.2 MOLECULAR DOCKING.....	41
2.2.1 Brief overview on molecular docking.....	41
2.2.2 In silico cytochrome bc ₁ model validation.....	42
2.2.3 Docking of atovaquone, clopidol, and 2.1 into the active site.....	43
2.2.4 De novo structure-based design of 4-pyridonimines.....	44
2.3 SYNTHESIS.....	51
2.3.1 Rationale for Mannich-base 4-pyridonimines.....	51
2.3.2 4-Pyridinamines.....	52
2.3.3 4-Pyridonimines.....	54
2.3.4 Rationale for structure-based 4-pyridonimines.....	61
2.3.5 Intermediates for structure-base 4-pyridonimines.....	61
2.3.6 4-Pyridonimines.....	72
2.4 CONCLUSIONS.....	81

CHAPTER 3

3. QUINOLONIMINE SCAFFOLD	85
3.1 RATIONALE.....	85
3.2 SYNTHESIS.....	86
3.2.1 4,7-Dichloro-2-methylquinoline.....	86
3.2.2 Quinolinium salt intermediates.....	87
3.2.3 1-Nitro-4-phenoxybenzene intermediates.....	88
3.2.4 4-Phoxyanilines intermediates.....	90
3.2.5 4-Quinolonimines.....	91
3.3 CONCLUSIONS.....	106

CHAPTER 4

4. CHROMONE SCAFFOLD	109
-----------------------------------	------------

4.1 RATIONALE	109
4.2 SYNTHESIS.....	109
4.2.1 Retrosynthetic analysis of flavones	109
4.2.2 4-Phenoxybenzotrile and 4-phenoxybenzoic acid intermediates.....	110
4.2.3 Flavones	112
4.2.4 Retrosynthetic analysis of isoflavones.....	121
4.2.5 Attempted synthesis of isoflavones	122
4.2.6 Antiplasmodial activity and molecular docking.....	124
4.2.7 Anti-liver activity and cytotoxicity.....	126
4.3 CONCLUSIONS	128
CHAPTER 5	
5. VIRTUAL SCREENING STUDIES.....	131
5.1 BRIEF OVERVIEW ON VIRTUAL SCREENING	131
5.2 3D-PHARMACOPHORE MODEL GENERATION AND SCREENING.....	132
5.3 RECEPTOR-BASED VIRTUAL SCREENING	136
5.3 ANTIPLASMODIAL ACTIVITY	137
5.4 CONCLUSIONS	142
CHAPTER 6	
6. CONCLUSIONS AND PERSPECTIVES.....	145
CHAPTER 7	
7. EXPERIMENTAL SECTION	151
7.1 REAGENTS AND SOLVENTS	151
7.2 CHROMATOGRAPHY	151
7.3 EQUIPMENT	151
7.4 SYNTHESIS.....	152
7.4.1 Mannich-base side chain.....	152
7.4.2 4-(Pyridin-4-ylamino)phenols	153
7.4.3 4-Chloro-N-alkylpyridinium iodides.....	157

7.4.4 Mannich-base 4(1H)-pyridonimines	159
7.4.5 Intermediates of structure-base designed 4(1H)-pyridonimines	164
7.4.6 Structure-base designed 4(1H)-pyridonimines	175
7.4.7 Intermediates of 4(1H)-quinolonimines	182
7.4.8 4(1H)-Quinolonimines	185
7.4.9 Intermediates of flavones.....	191
7.4.10 Flavones.....	195
7.4.11 Intermediates for isoflavones.....	200
7.5 COMPUTATIONAL APPROACH	201
7.5.1 Quantum mechanical calculations	201
7.5.2 Molecular docking and virtual screening.....	202
7.6 HEMATIN BINDING STUDIES	204

APPENDICES

Appendix 1.....	209
APPENDIX 1.1 ENERGY-MINIMIZED STRUCTURES.....	209
APPENDIX 1.2 DOCKING POSE OF THE SYNTHESIZED MANNICH-BASE 4-PYRIDONIMINES.....	211
APPENDIX 1.3 X-RAY DATA FOR COMPOUND 2.8.....	212
Appendix 2.....	213
APPENDIX 2.1 X-RAY DATA FOR COMPOUND 3.22.....	213
APPENDIX 2.2 HEMATIN TITRATION WITH 4-QUINOLONIMINES.....	214
Appendix 3.....	218
APPENDIX 3.1 PHARMACOPHORE MODEL VALIDATION, RMSD	218
APPENDIX 3.2 MOE DATABASE: TOP 100 LIGANDS.....	219
APPENDIX 3.3 ZINC DATABASE: TOP 100 LIGANDS	224
REFERENCES.....	231

INDEX OF FIGURES

Figure 1.1 Mitochondrial electron transfer chain enzymes and the interplay with <i>Pf</i> DHODH from pyrimidine biosynthesis. (Adapted from http://sites.huji.ac.il/malaria/).....	3
Figure 1.2 Cytochrome <i>bc</i> ₁ complex. Image generated from PDB 1KYO, using PyMol ^[43, 46]	4
Figure 1.3 Atovaquone docked at the oxidation site of the yeast <i>bc</i> ₁ complex ^[58]	6
Figure 1.4 Structure of antimycin A and cytochrome <i>bc</i> ₁ interactions ^[164]	24
Figure 2.1 <i>In silico</i> optimized (<i>E</i>)- 2.8 (green) superimposed with VMD 1.8.6 ^[182] to the crystallized atomic coordinates (red, RMSD = 0.31Å).....	34
Figure 2.2 LUMOs of atovaquone, clopidol and compounds 2.1-17	36
Figure 2.3 HOMOs of atovaquone, clopidol and compounds 2.1-17	37
Figure 2.4 MEPs of atovaquone, clopidol, GW844520 and compounds 2.1-17	39
Figure 2.5 Binding poses of stigmatellin. In blue the crystallized structure and in green the docking prediction: (A) ChemScore; (B) GoldScore.....	42
Figure 2.6 Docking poses of (A) atovaquone; (B) clopidol (two possibilities); and (C) 2.1 . The molecular electrostatic potential of the Q _o pocket calculated through the APBS formalism is also displayed: in red the negative potential (dark red is -15 kT/e) and in blue the neutral potential.....	44
Figure 2.7 Binding mode of GW844520.....	44
Figure 2.8 Docking pose of (A) 2.18 and (B) 2.19	45
Figure 2.9 Docking poses of (A) 2.20 ; (B) 2.21 ; (C) 2.22 ; (D) 2.23 ; (E) 2.24 ; (F) 2.25 ; (G) 2.26 ; (H) 2.27 ; (I) 2.28	47
Figure 2.10 Docking poses of (A) 2.29 ; (B) 2.30 ; (C) 2.31 ; (D) 2.32 ; (E) 2.33 ; (F) 2.34 ; (G) 2.35 ; (H) 2.36 ; (I) 2.37 ; (J) 2.38 ; (K) 2.39 ; (L) 2.40	49
Figure 2.11 Docking poses for compounds 2.41-45	50
Figure 2.12 ORTEP view of the molecular structure of 2.8 , showing the labelling of all non-hydrogen atoms. Displacement ellipsoids for non-hydrogen atoms are shown at the 50% probability level. Hydrogen atoms have been omitted for clarity.....	59
Figure 2.13 2D NOESY spectrum of 2.123	73
Figure 2.14 Fragmentation pattern for 4-pyridonimines, exemplified by 2.129	76
Figure 2.15 Docking poses of (A) clopidol (purple), and GW844520 (blue); (B) 2.130 (purple), and 2.131 (blue).....	79

Figure 2.16 Antiplasmodial activity of compounds 2.124-138 at 10 μM (black bars) and 2 μM (grey bars) against liver stage <i>P. berghei</i> . The luminescence (bars) is given as percentage of control (MeOH) inhibition. The cytotoxicity was measured in fluorescence (dots) from the Alamar Blue test and is also given as percentage of control. Primaquine was tested at 5 μM . All concentrations were tested and missing bars account for the total suppression of parasite load.....	80
Figure 3.1 Predicted LogP for the 4-pyridonimine and 4-quinolonimine scaffolds.....	85
Figure 3.2 Fragmentation pattern for 4-quinolonimines, exemplified by 3.28 and 3.29.....	93
Figure 3.3 ORTEP view of the molecular structure of 3.22 , showing the labelling of all non-hydrogen atoms. Displacement ellipsoids for non-hydrogen atoms are shown at the 50% probability level.	94
Figure 3.4 Docking poses of 3.20 , 3.22 and 3.27 , with mesh highlighting the volume and shape of the ligands inside the Q_o binding site of cytochrome <i>bc_1</i>	97
Figure 3.5 Antiplasmodial activity of compounds 3.20-31 at 10 μM (black bars) and 2 μM (grey bars) against liver stage <i>P. berghei</i> . The luminescence (bars) is given as percentage of control (MeOH) inhibition. The cytotoxicity was measured in fluorescence (dots) from the Alamar Blue test and is also given as percentage of control. Primaquine was tested at 5 μM . All concentrations were tested and missing bars account for the total suppression of parasite load.....	98
Figure 3.6 (A) Spectroscopic changes in the Soret band (400 nm) when hematin is titrated with increasing concentrations of chloroquine (20 $^{\circ}\text{C}$, apparent pH 5.5, HEPES buffer with 40% DMSO); (B) Absorbance of chloroquine under the same experimental conditions as (A).	101
Figure 3.7 A) Spectroscopic changes in the Soret band (400 nm) when hematin is titrated with increasing concentrations of clopidol (20 $^{\circ}\text{C}$, apparent pH 5.5, HEPES buffer with 40% DMSO).	103
Figure 3.7 (cont.) (B) Variation of absorbance of hematin at 400 nm as a function of clopidol concentration. The solid line represents the best fit curve for the 1:1 stoichiometry model. The curve was corrected for dilution and absorbance of the ligand.....	104
Figure 3.8 (A) Spectroscopic changes in the Soret band (400 nm) when hematin is titrated with increasing concentrations of 3.28 (20 $^{\circ}\text{C}$, apparent pH 5.5, HEPES buffer with 40% DMSO).	104

Figure 3.8 (cont.) (B) Absorbance of 3.28 under the same experimental conditions as (A); (C) Variation of absorbance of hematin at 400 nm as a function of 3.28 concentration. The solid line represents the best fit curve for the 1:1 stoichiometry model. The curve was corrected for dilution and absorbance of the ligand.	105
Figure 4.1 Docking poses of (A) stigmatellin; (B) 4.12, 4.13, 4.15, 4.16 and 4.31	125
Figure 4.2 Antiplasmodial activity of compounds 4.12-21 and 4.31-32 against the liver stage of <i>P. berghei</i> . The luminescence (bars) is given as percentage of control (DMSO) inhibition. The cytotoxicity was measured in fluorescence (dots) from the Alamar Blue test and is also given as percentage of control. The compounds were tested in two concentrations: 10 μ M (black bars), 2 μ M (grey bars) and primaquine was tested at 5 μ M. Compound 4.34 was only tested at 10 μ M.	127
Figure 4.3 Dose-response curve of luminescence intensity, as a function of the logarithm of compound concentration. The red markers refer to $\log IC_{50}$	128
Figure 5.1 The ligand-receptor interactions for GW844520, 1.113 ; strong hydrophobic interactions can be seen between the side chain and hydrophobic aminoacid residues. Water molecules have not been included in docking calculations, but are likely to intervene as hydrogen-bond mediators.	132
Figure 5.2 Chemical structures of the training set selected for the pharmacophore modeling.	134
Figure 5.3 (A) shows the pharmacophore model used to screen the ZINC database; (B) shows the model used for the MOE database. Green spheres represent hydrophobic regions, orange represents aromatic regions, blue is a hydrogen-bond acceptor and its projection and purple represents hydrogen-bond donor and its projection.	134
Figure 5.4 Virtual screening protocol breakdown.	136
Figure 5.5 Structures of compounds selected from the virtual screening protocol.	138
Figure 5.6 Docking poses for selected compounds: (A) 5.6 ; (B) 5.7 ; (C) 5.10 ; (D) 5.11	141
Figure 5.6 (cont.) Docking poses for selected compounds: (E) 5.12 ; (F) 5.20 ; (G) 5.21 ; (H) 5.23	142
Figure A1.1 Energy-minimized structures of atovaquone, clopidol and compounds 2.1-17	209
Figure A1.2 Docking poses of 2.4, 2.6-8	211

INDEX OF SCHEMES

Scheme 2.1 Retrosynthetic analysis for Mannich-base derivatives.	51
Scheme 2.2 Synthesis of pyridin-4-amines 2.51-58 . Reagents and conditions: (i) DEA, CH ₂ O, EtOH, reflux 24h (ii) DEA, CH ₂ O, EtOH, reflux 48-72h (iii) HCl 6N, reflux overnight (iv) 4-chloropyridine, EtOH, reflux.	52
Scheme 2.3 Synthetic pathway to compounds 2.1 and 2.4-8 . Reagents and conditions: (i) a) dry THF or DMF, NaH, rt b) MeI; (ii) dry THF, alkyl iodide, rt or reflux; (iii) EtOH, 2.49 , reflux; (iv) DMF, MeI; (v) NaOH, rt.	55
Scheme 2.4 Retrosynthetic analysis of target 4-pyridonimines.	61
Scheme 2.5 Synthetic pathway to compounds 2.72-80 . Reagents and conditions: (i) dry benzene or toluene, PPh ₃ , reflux.	62
Scheme 2.6 Synthetic pathway of compounds 2.81-104 . Reagents and conditions: (i) a) dry benzene, <i>n</i> -BuLi, N ₂ , b) aldehyde, rt or reflux; (ii) NaOH, CH ₂ Cl ₂ , aldehyde, rt; (iii) NaOH, CH ₂ Cl ₂ , aldehyde, MW.	63
Scheme 2.7 Mechanism for <i>in situ</i> generation of H ₂	68
Scheme 2.8 Synthetic pathway to compounds 2.103-110 . Reagents and conditions: (i) CH ₂ Cl ₂ , MeOH, TES, Pd-C 10%, rt.	68
Scheme 2.9 Synthetic pathway to compounds 2.113-118 . Reagents and conditions: (i) dry toluene, TfOMe or TfOEt, rt.	70
Scheme 2.10 Synthetic pathway to compound 2.119 . Reagents and conditions: (i) NaOH, reflux; (ii) toluene, EtOTf, TEA, rt.	71
Scheme 2.11 Synthetic pathway for compound 2.121 and 2.122 . Reagents and conditions: (i) CH ₃ CN, TMSI, N ₂ , reflux; (ii) CH ₂ Cl ₂ , MeOH, NBS, rt, light.	72
Scheme 2.12 Synthetic pathway for compound 2.123 . Reagents and conditions: (i) a) DMF, NaH b) EtI.	72
Scheme 2.13 Synthetic pathway to compound 2.124-137 . Reagents and conditions: (i) EtOH, TEA, aniline, reflux.	73
Scheme 2.14 Synthetic pathway to compound 2.138 . Reagents and conditions: (i) CHCl ₃ , <i>m</i> CPBA, reflux (ii) EtOH, TEA, aniline, reflux.	75
Scheme 3.1 Retrosynthetic analysis of target 4-quinolonimines.	86

Scheme 3.2 Synthetic pathway for compound 3.2 . Reagents and conditions: (i) PPA, 3-chloroaniline, 110 °C (ii) 150 °C.	86
Scheme 3.3 Synthetic pathway to compound 3.1 . Reagents and conditions: (i) POCl ₃ , reflux.	87
Scheme 3.4 Attempted synthesis of 3.7	88
Scheme 3.5 Retrosynthetic analysis for the phenoxyanilines.	88
Scheme 3.6 Synthetic pathway to compounds 3.8-13 . Reagents and conditions: (i) DMF, Na ₂ CO ₃ , CuI, reflux.	89
Scheme 3.7 Synthetic pathway to compounds 3.14-19 . Reagents and conditions: (i) CH ₂ Cl ₂ , MeOH, TES, Pd-C 10%, rt; (ii) Sn, HCl, reflux.	90
Scheme 3.8 Synthetic pathway to compounds 3.20-32 . Reagents and conditions: (i) EtOH, TEA, aniline, reflux.	91
Scheme 3.9 Simulated glutathione attack to afford 3.33 . Reagents and conditions: (i) TEA, MeOH, rt.	96
Scheme 3.10 Models fitted to the experimental curves.	100
Scheme 4.1 Retrosynthetic analysis of target flavones.	110
Scheme 4.2 Synthetic pathway to compounds 4.1-4 . Reagents and conditions: (i) DMF, Na ₂ CO ₃ , CuI, nucleophile, reflux; (ii) DMF, Na ₂ CO ₃ , nucleophile, reflux.	111
Scheme 4.3 Synthetic pathway to compounds 4.9 . Reagents and conditions: (i) 2-hydroxyacetophenone, DCC, CH ₂ Cl ₂ , DMAP, rt (ii) a) SOCl ₂ , reflux; b) 2-hydroxyacetophenone, CH ₂ Cl ₂ , DMAP, rt; (iii) a) CH ₂ Cl ₂ , TEA, rt; b) ClCO ₂ Et, rt; c) 2-hydroxyacetophenone, DMAP, rt; (iv) 2-hydroxyacetophenone, dry pyridine, rt.	113
Scheme 4.4 Synthetic pathway for compounds 4.11 . Reagents and conditions: (i) Dry pyridine, 3-(trifluoromethyl)benzoyl chloride, DBU, reflux.	114
Scheme 4.5 Synthetic pathway to compound 4.28 . Reagents and conditions: (i) Sn, HCl, EtOH, reflux; (ii) dry pyridine, acetic anhydride, reflux; (iii) dry pyridine, DBU, [1,1'-biphenyl]-4-carbonyl chloride, reflux (iv) Similar to (iii), MW.	116
Scheme 4.6 Synthetic pathway to compounds 4.29 and 4.30 . Reagents and conditions: (i) NBS, AIBN, benzene, reflux 2 h; (ii) NBS, AIBN, benzene, reflux 24 h; (iii) MeOH, MeONa, reflux.	116
Scheme 4.7 Synthetic pathway to compounds 4.31-33 . Reagents and conditions: (i) NBS, benzoyl peroxide, CCl ₄ , reflux; (ii) NBS, ZrCl ₄ , CCl ₄ , rt; (iii) MeOH, MeONa, reflux.	117
Scheme 4.8 Fragmentation pattern of 4.12 and 4.20 as examples for the flavone series.	118

Scheme 4.9 Synthetic pathway to compounds 4.34 . Reagents and conditions: (i) Benzaldehyde, NaOH, reflux; (ii) Benzaldehyde, NaOH, rt.	119
Scheme 4.10 Synthetic pathway to compounds 4.35 and 4.36 . Reagents and conditions: (i) DMSO, I ₂ , MW; (ii) DMSO, I ₂ , reflux; (iii) PdCl ₂ , AcONa, AcOH, AIBN; (iv) H ₂ O ₂ 30%, NaOH, EtOH.	120
Scheme 4.11 Synthetic pathway to compound 4.37 . Reagents and conditions: (i) TEA, TBTU, NH(Me)OMe, rt; (ii) dry THF, LiAlH ₄ , -5 °C; (iii) EtOH, NaOH, acetophenone, rt.	120
Scheme 4.12 Retrosynthetic analysis of isoflavones.	121
Scheme 4.13 Synthetic procedure for 4.40 . Reagents and conditions: (i) DMF-DMA, 95 °C; (ii) CHCl ₃ , pyridine, I ₂ , rt.	122
Scheme 4.14 Synthetic procedure for 4.41 . Reagents and conditions: (i) DMF, CuI, 4-chlorophenol or 4-fluorophenol, Na ₂ CO ₃ , reflux.	122
Scheme 4.15 Synthetic procedure for compounds 4.42 and 4.43 . Reagents and conditions: (i) 4-(fluorophenyl)boronic acid, DME, H ₂ O, Na ₂ CO ₃ , Pd-C, 45 °C; (ii) 4-chlorophenol, CuI, Na ₂ CO ₃ , DMF, reflux.	123
Scheme 4.16 Alternative pathway to 4.43 , using the same reactions as in Scheme 4.15.	123
Scheme 4.17 Synthetic procedure for compounds 4.45 and 4.46 . Reagents and conditions: (i) DMF, Na ₂ CO ₃ , CuI, 3-(trifluoromethoxy)phenol, reflux; (ii) a) dry THF, <i>n</i> -BuLi, borate triisopropyl, -78 °C b) HCl 6N, rt; (iii) a) dry THF, Mg, N ₂ , I ₂ , reflux b) triisopropyl borate, -78 °C c) HCl 6N, rt.	123

INDEX OF TABLES

Table 1.1 <i>In vitro</i> activity of <i>Kigelia pinnata</i> compounds ^[86]	10
Table 1.2 Antiplasmodial <i>in vitro</i> activity of thiophenonaphthoquinone compounds against the BHz 26/28 chloroquine-resistant strain ^[87]	10
Table 1.3 <i>In vitro</i> activity of 1,4-naphthoquinone compounds ^[88]	11
Table 1.4 Antiplasmodial activity of ferrocenyl 1,4-naphthoquinone compounds ^[89]	12
Table 1.5 Antiplasmodial activities of 4(1 <i>H</i>)-quinolones ^[99]	13
Table 1.6 Antiplasmodial activities of acridone series ^[100]	15
Table 1.7 Antiplasmodial activities of 4(1 <i>H</i>)-pyridones: influence of side chain on activity ^[19]	17
Table 1.8 Antiplasmodial activities of phenoxyaryl-4(1 <i>H</i>)-pyridones ^[19]	19
Table 1.9 Antiplasmodial activities of β -methoxyacrylate against the K1 strain ^[131]	20
Table 1.10 Antiplasmodial activities of selected chalcones ^[134]	21
Table 2.1 Structures of compounds 2.1-17 (only the (<i>E</i>) conformer is explicitly included)	31
Table 2.2 Selected electronic properties	32
Table 2.3 Selected angle and dihedral angles	33
Table 2.4 Structures and GoldScores of compounds 2.20-28	46
Table 2.5 Structures and GoldScores of compounds 2.29-40	49
Table 2.6 Structures and GoldScores of compounds 2.41-45	51
Table 2.7 Synthesis of key intermediates 2.51-58	53
Table 2.8 Reaction conditions for the S _N Ar reactions and synthesis of 2.59	53
Table 2.9 Synthesis of compounds 2.62-69	55
Table 2.10 Synthesis of compounds 2.1 and 2.4-8	56
Table 2.11 Yields of the several species isolated from the alkylation of 2.56	57
Table 2.12 Antiplasmodial activity of 4-pyridonimines containing a Mannich-base side chain, 2.1 , 2.4 and 2.6-8	60
Table 2.13 Phosphonium salts synthesized	62
Table 2.14 Comparison of Wittig reaction methods, to acquire 2.81-83	64
Table 2.15 Reaction of nitro-substituted benzyltriphenyl phosphonium salts with aldehydes under standard PTC conditions at room temperature (Method B) and microwave-assisted synthesis (Method C)	65
Table 2.16 Comparative study, rt vs. MW, for the synthesis of 2.81	66

Table 2.17 Synthesis of alkenes 2.96-99 through Wittig chemistry.....	67
Table 2.18 Structure of compounds 2.101 and 2.102	68
Table 2.19 Structure of compounds 2.103-110	69
Table 2.20 Structure of compounds 2.111 and 2.112	70
Table 2.21 Structure and obtained yields for compounds 2.113-118	71
Table 2.22 Structure of 4-pyridonimines and yields.....	74
Table 2.23 Antiplasmodial activity against <i>P. falciparum</i> W2 and FCR3 strains.....	78
Table 3.1 Structure and yields of 3.4-6	87
Table 3.2 Structure and yields of 3.8-13	89
Table 3.3 Structure and yields for compounds 3.14-19	90
Table 3.4 Structure and yields of compounds 3.20-32	92
Table 3.5 Effect of R ² -R ⁴ and X substitutions in compounds 3.20-31 on the antiplasmodial activity against <i>P. falciparum</i> W2 strain and association constants (binding to FPIX in 1:1 stoichiometry).....	95
Table 4.1 Structure and yields of compounds 4.1-4	111
Table 4.2 Structure and yields of compounds 4.5-8	112
Table 4.3 Structure and yields (over 4 steps) of compounds 4.12-21 under standard heating conditions and MW-assisted synthesis.....	115
Table 4.4 Substituent effect on the antiplasmodial activity, against the W2 strain, of compounds 4.12-21, 4.31, 4.32	124
Table 5.1 Biological data for compounds selected from virtual screening.....	139
Table 7.1 Conditions for the synthesis of 2-(diethylaminomethyl)paracetamol.....	152
Table 7.2 Conditions for the synthesis of 4-(pyridin-4-ylamino)phenols.....	153
Table 7.3 Conditions for the synthesis of 2.53	154
Table 7.4 Conditions for the synthesis of 2.59	157

ABSTRACT

The bc_1 complex is an attractive a validated drug target in the fight against malaria. The mitochondrial electron transport-chain, in which this complex is involved, is fundamental in *Plasmodium* sp.. The parasites do not possess the requested enzymatic machinery to salvage pyrimidines from their metabolism and, therefore, have to perform *de novo* pyrimidine biosynthesis to enable their survival. Blockage of this pathway leads to their death. The present work focused on the development of novel inhibitors with structural similarity to known bc_1 complex antagonists. Also, this work aimed at delivering novel leads for drug development.

4-Pyridonimines with extended lipophilic side chains showed potential as isosteric replacements for 4(1*H*)-pyridones. The structure of those compounds was derived from structure-based design and they were active *in vitro* against *P. falciparum*. The most active compound presented an IC_{50} of *ca.* 1 μ M, and the mode of action was hypothesized through docking studies.

A series of 4-quinolonimines was also prepared. Those presented enhanced antiplasmodial activity in comparison to the previous set of compounds, with IC_{50} s ranging from 0.5 to 1 μ M. These also showed outstanding activity against the liver stage of *P. berghei*. Despite the mechanism of action not being clear at the moment, the compounds demonstrated to bind to hemozoin. However, the docking studies in the Q_0 site of the bc_1 complex also showed a good fit of the compounds.

Flavones were also synthesized with the aim of optimizing the antiplasmodial activity of stigmatellin. All compounds showed modest activity against both blood and liver stages, with the most active compound presenting an IC_{50} of 6 μ M against *P. falciparum* W2 strain.

Finally, the virtual screening study that was performed allowed the discovery of novel scaffolds with antiplasmodial activity. A combination of ligand- and receptor-based approaches was successful in retrieving 7 active compounds out of the 23 that were purchased. One of them presented an IC_{50} of 2 μ M *in vitro*.

KEYWORDS: Cytochrome bc_1 ; 4-pyridonimine; 4-quinolonimine; flavone; molecular docking; virtual screening.

RESUMO

O complexo bc_1 é um alvo terapêutico atractivo e validado na luta contra a malária. A cadeia transportadora de electrões, em que este complexo está envolvido, é fundamental em parasitas do género *Plasmodium* sp.. Os parasitas não possuem as enzimas necessárias para reciclar as pirimidinas vindas do metabolismo e, por isso, necessitam de sintetizá-las *de novo*, de forma a permitir a sobrevivência do parasita. O bloqueio desta via metabólica conduz à morte sua morte. O presente trabalho incidiu no desenvolvimento de novos inibidores com semelhança estrutural a antagonistas conhecidos do complexo bc_1 . De igual forma, este trabalho focou-se na descoberta de novos protótipos para o desenvolvimento de novos antimaláricos.

As 4-piridoniminas com cadeias lipofílicas longas mostraram potencial como isómeros das 4(1*H*)-piridonas. A estrutura dos primeiros foi derivada de estudos de *docking* molecular e apresentaram actividade *in vitro* contra *P. falciparum*. O composto mais activo possui um IC_{50} de aproximadamente 1 μ M e o seu modo de acção foi posto em hipótese por *docking* molecular.

Uma série de 4-quinoloniminas foi também preparada. Estas mostraram ser mais activas que a série de compostos anteriores, com IC_{50} entre 0,5 e 1 μ M, tendo mostrado também excelente actividade contra a fase hepática de *P. berghei*. Apesar do mecanismo de acção não ser claro neste momento, os compostos mostraram ligar-se à hematina. Contudo, os estudos de *docking* molecular no sítio Q_o do complexo bc_1 podem, igualmente, justificar as actividades obtidas.

Foi sintetizada uma série de flavonas com o intuito de otimizar a actividade antiplasmódica da estigmatelina. Todos os compostos obtidos mostraram actividade modesta contra as fases sanguínea e hepática, com o composto mais activo a apresentar um IC_{50} de 6 μ M contra a estirpe W2 de *P. falciparum*.

Finalmente, o estudo de *screening* virtual que foi efectuado permitiu a descoberta de novos núcleos com actividade antiplasmódica. A combinação de um método aplicando, de forma faseada, a informação de ligandos e do receptor resultou na obtenção de 7 compostos activos, de um total de 23 comprados. Um dos compostos apresentou um IC_{50} de 2 μ M *in vitro*.

PALAVRAS-CHAVE: Citocromo bc_1 ; 4-piridonimina; 4-quinolonimina; flavona; *docking* molecular; *screening* virtual.

LIST OF ABBREVIATIONS AND SYMBOLOGY

$\Delta\psi_m$	Mitochondrial Electrochemical Gradient
AcOEt	Ethyl acetate
ADMET	Absorption, Distribution, Metabolization, Excretion, Toxicity
AIBN	Azobisisobutyronitrile
ATP	Adenosine Triphosphate
B3LYP	Becke 3 Lee, Yang, Parr
br.d	Broad doublet
br.s	Broad singlet
C	Cysteine
COSY	Correlation Spectroscopy
CTH	Catalytic Transfer of Hydrogen
D	Aspartic Acid
d	Doublet
dd	Doublet of doublets
ddd	Doublet of doublet of doublets
DCC	Dicyclohexylcarbodiimide
DBU	1,8-Diazabicycloundec-7-ene
DEA	Diethylamine
DEPT	Distortionless Enhancement by Polarization Transfer
DFT	Density Function Theory
DMAP	Dimethylaminopyridine
DME	Dimethoxyethane
DMF	<i>N,N</i> -Dimethylformamide
DMF-DMA	<i>N,N</i> -Dimethylformamide-Dimethylacetal
DMSO	Dimethylsulfoxide
dq	Doublet of quartets
dt	Doublet of triplets
E	Glutamate
EI	Electronic Impact
Eq.	Equivalent
EtOH	Ethanol

F	Phenylalanine
FAB	Fast Atom Bombardment
FPIX	Ferriprotoporphyrin IX
G	Glycine
GFP	Green Fluorescent Protein
GOLD	Genetic Optimization for Ligand Docking
GSK	GlaxoSmithKline
H	Histidine
HOMO	Highest Occupied Molecular Orbital
HMQC	Heteronuclear Multiple Quantum Coherence
HTS	High-Throughput Screening
I	Isoleucine
IR	Infra-Red
ISP	Iron-Sulfur Protein
<i>J</i>	Coupling constant
K	Lysine
K_{ass}	Association constant
K_{d}	Dissociation constant
L	Leucine
$\log S_{\text{w}}$	Log Solubility in water
LUMO	Lowest Unoccupied Molecular Orbital
M	Methionine
m	Multiplet
<i>m</i> CPBA	<i>Meta</i> -chloroperbenzoic acid
MeOH	Methanol
MeONa	Sodium Methoxide
MEP	Molecular Electrostatic Potential
MOE	Molecular Operating Environment
mp	Melting point
mtETC	Mitochondrial Electron Transport-Chain
MW	Microwaves
NADH	Nicotinamide Adenine Dinucleotide
NBS	<i>N</i> -bromosuccinimide
<i>n</i> -BuLi	<i>n</i> -Butyl Lithium

NMR	Nuclear Magnetic Resonance
NOESY	Nuclear Overhauser Effect Spectroscopy
P	Proline
PDB	Protein Data Bank
<i>Pf</i> NDH2	Alternative type II NADH Dehydrogenase
<i>Pf</i> DHODH	Dihydroorotate Dehydrogenase
PPA	Polyphosphoric acid
PTC	Phase Transfer Catalysis
Py	Pyridine
q	Quartet
Q.E.	Quinine Equivalent
Q _i	Ubiquinone reduction site
Q _o	Ubiquinol oxidation site
RMSD	Root Mean Square Deviation
rt	Room temperature
s	Singlet
SAR	Structure-Activity Relationships
SDH	Succinate:ubiquinone oxireductase
S _N Ar	Nucleophilic Aromatic Substitution
S _N 2	Bimolecular Nucleophilic Substitution
T	Threonine
t	Triplet
TBTU	<i>O</i> -(Benzotriazol-1-yl)- <i>N,N,N',N'</i> -tetramethylauronium tetrafluoroborate
td	Triplet of doublets
TEA	Triethylamine
TES	Triethylsilane
THF	Tetrahydrofuran
TLC	Thin Layer Chromatography
TMSI	Trimethylsilane
tt	Triplet of triplets
V	Valine
VS	Virtual Screening
W	Tryptophan
Y	Tyrosine

CHAPTER 1

INTRODUCTION

1. INTRODUCTION

1.1 Overview of malaria and mitochondrial drug targets

Malaria remains a major infectious disease. Approximately half of the world's population is at risk of infection, with an estimated 300 million new cases annually, and 1 million deaths, mostly children under the age of five^[1-3]. Malaria is most prevalent in tropical areas and 90% of all cases occur in Africa, where the death toll is the highest among endemic regions^[4, 5]. Five species from the genus *Plasmodium* cause infection in humans, with *Plasmodium falciparum* being the most virulent, followed by *P. vivax*.

The life cycle of malaria parasites is complex and multi-staged. It includes an asexual cycle in humans and a sexual cycle in the *Anopheles* mosquito. In humans, it can be further distinguished into a liver and an erythrocytic stage^[6]. During the blood meal, the mosquito transfers sporozoites into the blood stream, which conceal from the host immune system by invading the hepatocytes. They convert to trophozoites, and divide into several schizonts. After rupture of the hepatocytes, the merozoites are released into the blood stream. These invade the erythrocytes and mature into a trophozoite. Then, the matured trophozoites divide into schizonts, and the merozoites are released into the blood stream to invade other red blood cells. With the rupture of the blood cells, parasitic waste and cell debris are released, causing the clinical symptoms of the disease. After a number of asexual life cycles, the merozoites eventually develop into sexual forms, which are transferred to the mosquito during another blood meal. These gametocytes undergo sexual reproduction within the mosquito mid-gut, producing sporozoites, which finally migrate to the salivary glands and are ready for a new infection^[6].

The swift emergence of multi-drug resistant strains is currently impairing both prophylaxis and chemotherapy. Thus, there is an urgent need to find novel drugs, for both known and new drug targets, that might overcome the clinical resistance to marketed antimalarials^[7-10].

Pyrimidine biosynthesis has long been known as a potential target for antimalarial chemotherapy^[11, 12] and presents a set of attractive drug targets. In higher organisms, the electron transport-chain is composed of four enzyme complexes, located in the inner mitochondrial membrane:

- a) NADH:ubiquinone oxidoreductase, complex I;
- b) Succinate:ubiquinone oxidoreductase, complex II, succinate dehydrogenase or SDH;
- c) Ubiquinol:cytochrome *c* oxidoreductase, complex III or cytochrome *bc*₁;
- d) Cytochrome *c* oxidase, complex IV^[13].

Complexes II through IV are conserved in *Plasmodia*, but an alternative type II NADH dehydrogenase (*Pf*NDH2) replaces complex I. Additionally, other oxidoreductases, such as dihydroorotate dehydrogenase (*Pf*DHODH) are present in the mitochondria and display an important role in *de novo* pyrimidine biosynthesis.

1.2 The electron transport-chain pathway

Unlike many eukaryotic cells, malaria parasites obtain almost all their ATP via glycolysis rather than oxidative phosphorylation in the mitochondrion^[14, 15]. Additionally, sequencing of the malarial genome has revealed that genes encoding enzymes from the pyrimidine biosynthetic pathway have been conserved, whereas those responsible for salvaging pyrimidines have not^[16]. Thus, malaria parasites rely completely on the *de novo* pyrimidine biosynthesis, essential for the formation of nucleic acids, glycoproteins and phospholipids. Despite its low activity, the mitochondrial electron transport-chain (mtETC) is responsible for maintaining an electrochemical gradient ($\Delta\psi_m$) across the mitochondrial membrane, as well as a constant pool of ubiquinone for pyrimidine biosynthesis^[17]. Therefore, the shutdown of the mtETC completely arrests crucial metabolic pathways within the microorganism, rendering these enzymes valid and attractive drug targets. Furthermore, these enzymatic complexes have proven to be structurally different from the homologous human enzymes, which gave rise to the recent interest from both academia and pharma industry^[18-20].

Three drug targets have been exploited for the discovery of selective inhibitors: *Pf*NDH2, SDH and cytochrome *bc*₁. The biochemistry, including mechanistic details for these enzymes have been reviewed elsewhere^[21, 22]. In short, *Pf*NDH2 catalyses the electron transfer from NADH to ubiquinone in a ping-pong fashion, to maintain a constant pool of NAD⁺ for reductive metabolic pathways such as glycolysis and the tricarboxylic acid cycle^[23]. On the other hand, SDH feeds electrons to complex III, which are ultimately transferred to the final complex^[24].

*Pf*DHODH is the fourth enzyme in the *de novo* biosynthesis of pyrimidines and catalyses the oxidation of dihydroorotate to orotate at the outer side of the inner mitochondrial membrane. The pair of electrons abstracted from dihydroorotate in this oxidation step is transferred through the flavin mononucleotide co-factor to ubiquinone, that was generated at the *bc*₁ complex^[25-27]. Moreover, it is thought that the main metabolic function of the mtETC is to regenerate the ubiquinone necessary for the final step of pyrimidine biosynthesis^[28]. Figure 1.1 shows these pathways.

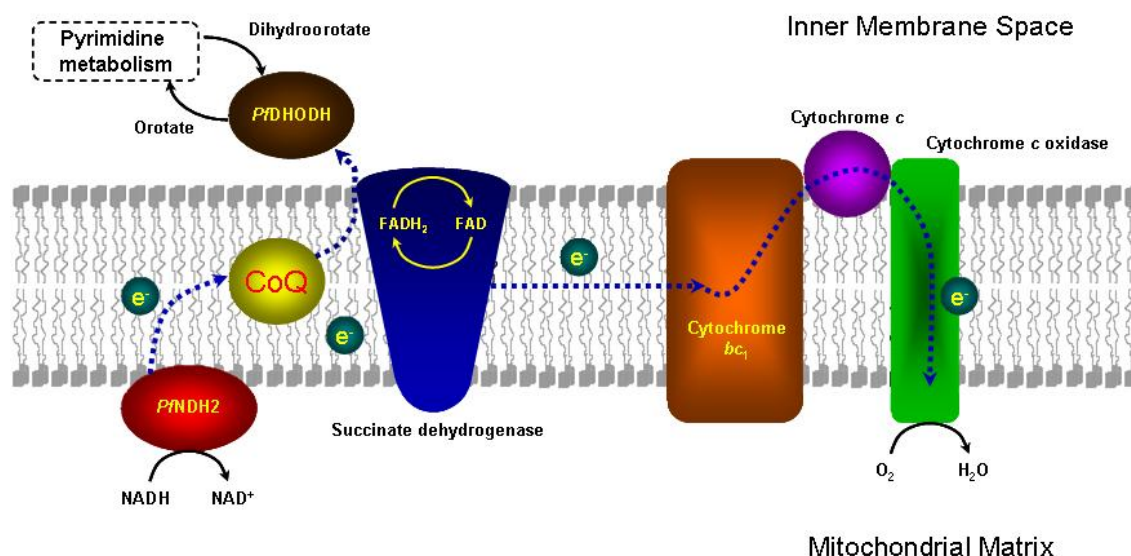


Figure 1.1 Mitochondrial electron transfer chain enzymes and the interplay with *PjDHODH* from pyrimidine biosynthesis. (Adapted from <http://sites.huji.ac.il/malaria/>).

1.3 Cytochrome bc_1 inhibitors

Cytochrome bc_1 represents the only enzyme complex common to almost all respiratory electron transfer-chains, from Archaea and Bacteria to Eukarya, and its structure has been extensively studied [29, 30]. Cytochrome bc_1 consists of 11 different polypeptides, three of which display catalytic functions: cytochrome *b*, cytochrome c_1 and the Rieske protein, or iron-sulfur protein (ISP), due to the iron-sulfur cluster present in it, Figure 1.2 [31]. The ISP is highly mobile and evidence suggests that this feature is crucial for the activity of the complex [32-35].

To date, the modified proton-motive Q cycle mechanism provides the most satisfactory model that accounts for electron transfer coupled to the proton translocation through cytochrome bc_1 . This is thoroughly reviewed elsewhere [21, 22, 34, 36-39]. Briefly, ubiquinol produced by dehydrogenases upstream to the bc_1 complex binds to the oxidation site (Q_o) where it is involved in the release of two protons, along with the loss of two electrons into the intermembrane space. Each electron follows a separate path, reducing two different acceptors: a) heme b_L located in cytochrome *b* and b) iron-sulfur cluster in the head domain of the Rieske protein. Next, heme b_L reduces heme b_H , also located within cytochrome *b*, which further recycles the electron through the reduction of ubiquinone to ubiquinol at the reduction site (Q_i). Meanwhile, the reduced ISP transfers an electron to the heme *c* group in cytochrome c_1 . This transfer is accomplished via a conformational shift, during which the histidine acceptor residue at the head group of the ISP rotates, allowing close

contact of the iron-sulfur cluster with heme *c*. This change is due to the shortening in length of the hinge segment of the ISP [21, 40].

The complex III from numerous organisms has been crystallized with several ligands bound to the oxidation and reduction sites, providing further insight into the complex function [31, 39, 41-45].

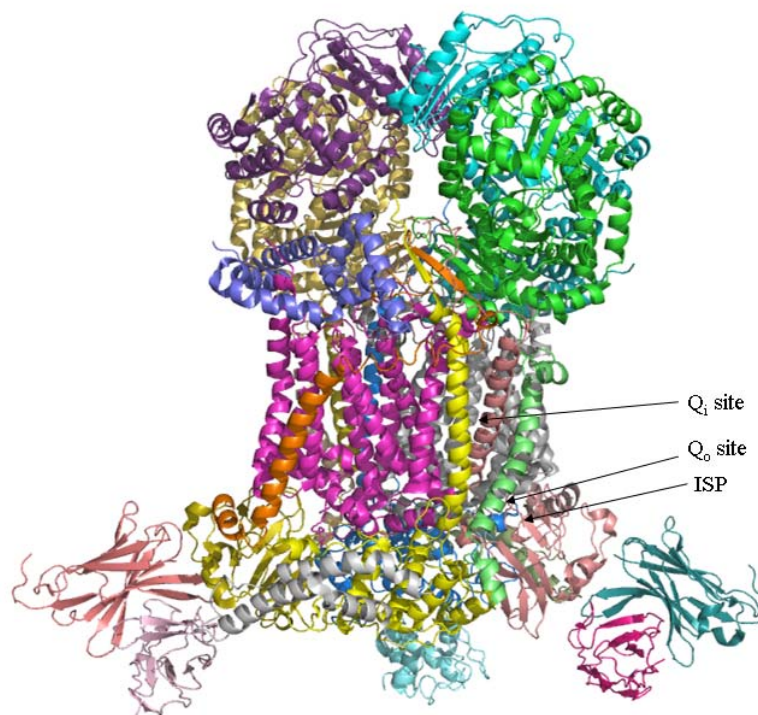


Figure 1.2 Cytochrome bc_1 complex. Image generated from PDB 1KYO, using PyMol [43, 46].

Cytochrome bc_1 has been the major drug target in the mtETC, and its inhibitors can be classified into four groups according to their binding points. Group I, which includes β -methoxyacrylates, bind to the Q_o site blocking electron transfer from ubiquinol to the ISP and electron transfer onto the b_L centre. Group II, which include hydroxyquinone derivatives, also bind to the Q_o site, inhibiting electron transfer from the ISP to cytochrome c_1 as well as electron transfer onto the b_L centre. Group III include Q_i site inhibitors, responsible for blocking electron transfer from the b_H centre to ubiquinone. Finally, a fourth group of chromone inhibitors also block the Q_o site, but with different properties from those of groups I and II [47].

1.3.1 1,4-Naphthoquinones

Currently, atovaquone, **1.1**, is the only drug targeting the bc_1 complex in clinical use [48-50]. However, high levels of resistance, related with point mutations in cytochrome *b*, have been observed for this drug. Consequently, in an attempt to improve its efficiency and decrease the mutation rate, the drug is now used in combination with proguanil. Mutations are predominantly restricted to a highly conserved 'PEWY' region, that helps recognition of ubiquinol, and is implied in the electron transfer within the Q_o site [13]. The most prevalent point mutations conferring clinical failure of atovaquone have been assigned to codon 268. A specific change of the *in vivo* wild-type tyrosine to asparagine or serine, Y268N/S, was found to increase the IC_{50} 800-10,000 fold, as a consequence of an altered fit and binding [51-53]. However, despite being sufficient, the Y268 mutation seems not to be necessary for treatment failure [51]. Mutation from methionine to isoleucine on residue 133, M133I, and from leucine to phenylalanine on residue 271, L271F, has generated resistance *in vitro* and can also be identified in several *Plasmodia* [54-56]. Other mutations in positions 258, 267, 272 and 280 have also resulted in a 1,000-fold increase of the drug's IC_{50} value [8, 57].

Due to the lack of a crystallized bc_1 complex from malaria parasites, molecular modeling studies regarding atovaquone binding to the bc_1 complex have been carried out with the homologous enzyme from *Saccharomyces cerevisiae*, because of the high sequence homology [58]. Atovaquone is a competitive inhibitor for ubiquinol that results in collapse of the parasitic mitochondrial membrane potential, but with no effect on the mammalian counterpart [17]. It binds when the soluble domain of the Rieske protein is proximal to cytochrome *b* and interacts directly with the ISP. This prevents mobilization to cytochrome c_1 and, consequently, impairs the $\Delta\psi_m$ [14, 49, 58, 59]. It has been predicted that this drug forms a hydrogen bond between the hydroxyl group on the naphthoquinone ring of the inhibitor and H181 at the ISP. A second water-mediated hydrogen bond between the carboxyl group of E272 and a carbonyl group from the quinone system is also expected, Figure 1.3 [58, 60, 61]. Other putative contact residues are I119, F123, Y126, M133, V140, I141, I144, I258, P260, F264, F267, Y268, L271, V284, L285 and L288 [59, 62, 63].

Atovaquone displays broad antiprotozoal activity, in the low nanomolar range, on several development stages of plasmodia. Moreover, synergism of atovaquone and other naphthoquinones with tetracyclines, dihydrofolate reductase inhibitors, and 4(1*H*)-pyridones has been reported for the W2 and D6 strains [64-67].

1,4-Naphthoquinones have long been known to possess antiplasmodial activity. Hydrolapachol, **1.2**, for instance, was first reported in the 1940s, and in the same decade the antiplasmodial screening of over 300 naphthoquinone derivatives was carried out by Fieser's group. Lengthening

the isoalkyl side chain of **1.2**, by insertion of methylene groups, increased the antimalarial activity in ducks, to a maximum at C₉. Longer side chains decreased activity. The same trend could be observed for the *n*-alkyl series and other related naphthoquinones. Compound **1.3** is almost twice as potent as its isoalkyl and *n*-alkyl counterparts. On the other hand, introduction of a ring into the side chain, e.g. **1.4**, shifted the activity peak to compounds with a higher number of carbons in the side chain, C₁₀ or C₁₁. When two rings are present, as in **1.5-7**, the maximum quinine equivalent, Q.E. - the ratio of dose of quinine, given in mg/kg, and that of the drug under assay which cause the first sharp drop in parasitemia in relation to untreated controls ^[68] - shifts to C₁₂ or C₁₃. All *trans* diastereomers are more potent than their *cis* isomers, and compound **1.7** with a Q.E. equal to 15.3 is the most potent molecule. Moreover, the 2-OH group seems indispensable for activity as loss of activity was observed with several other substituents: OMe, SH, Me, H, Cl and NHCOMe. The same trend was obtained when substitutions were made in the side chain, and in the naphthoquinone ring. Methyl groups reduced the activity of the compounds when introduced in the core scaffold ^[68-73].

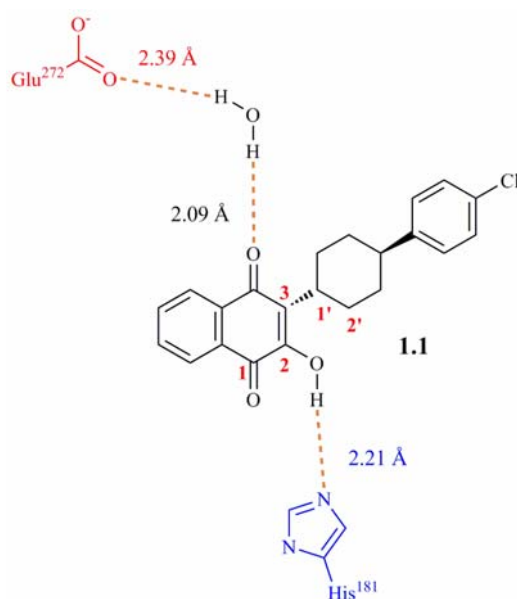
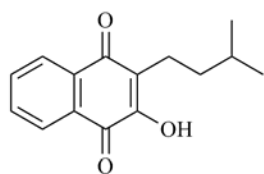
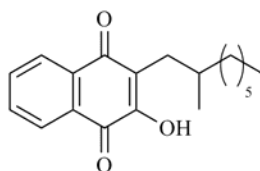
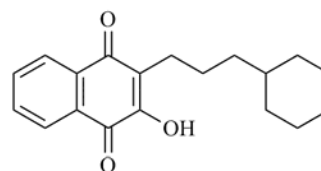
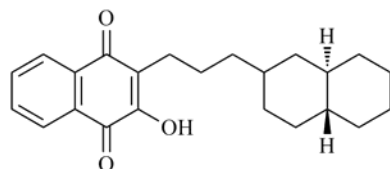
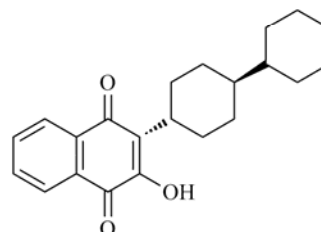
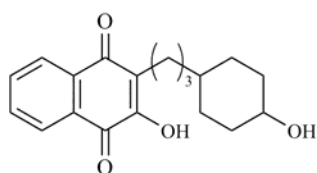
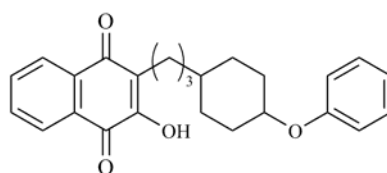
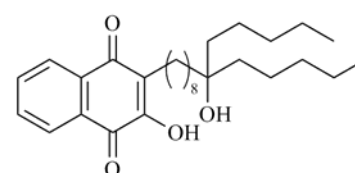


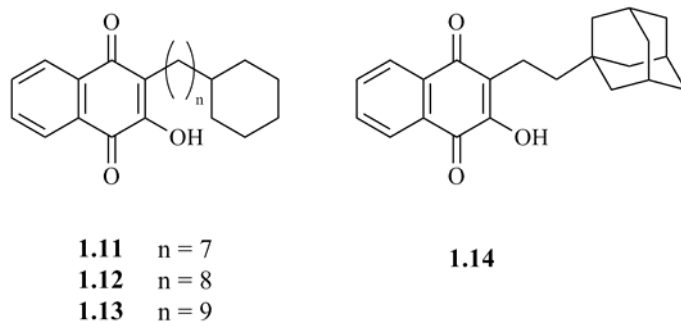
Figure 1.3 Atovaquone docked at the oxidation site of the yeast *bc*₁ complex ^[58].

Metabolism studies of naphthoquinones **1.3** and **1.4** demonstrated the oxidation of the side chains, yielding metabolites with significantly reduced antimalarial activity. In fact, compound **1.4** is rapidly metabolized, and any suppressive activity observed for this compound is due to its long-lived metabolite **1.8**. Thus, hydroxyl groups have been introduced in the following series, resulting in compounds metabolically more stable, despite having lower activity ^[70, 74].

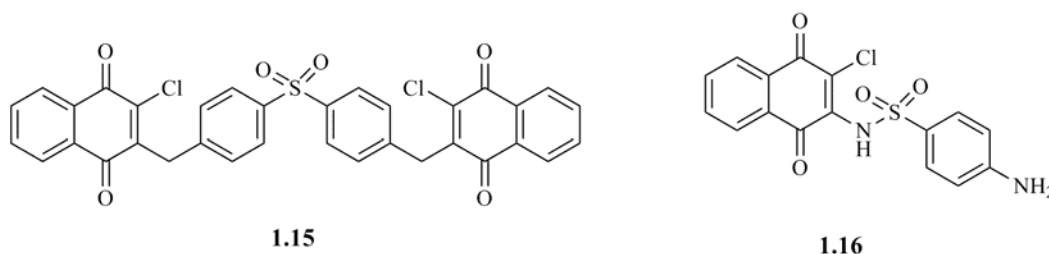
**1.2** Q.E. = 0.15**1.3** Q.E. = 2.1**1.4** Q.E. = 0.5**1.5** Q.E. = 1.2
1.6 (cis-5) Q.E. = 2.9**1.7** Q.E. = 15.3**1.8****1.9****1.10**

However, it was noted that an increase in the number of carbon atoms could compensate for any drop of activity, and the introduction of an aryl moiety afforded **1.9**, which was stable and as active as **1.4**. With these features in mind, a series of hydroxylated naphthoquinones were built, yielding lapinone **1.10** and other naphthoquinones alike, which displayed high activity and antirespiratory effect [70, 74-76].

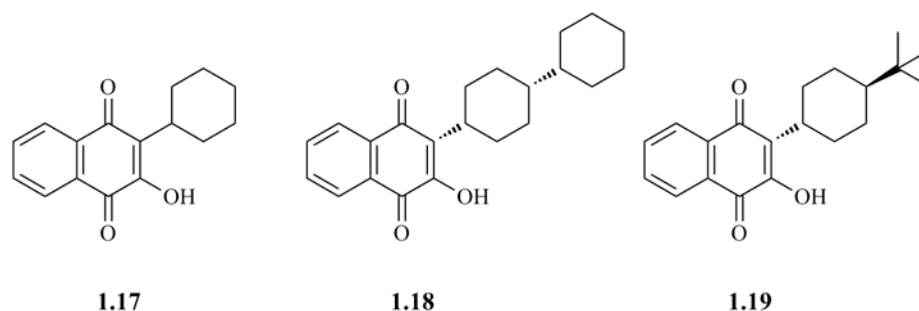
Due to the emergence of chloroquine resistant strains in the 1960s, a renewed interest in naphthoquinones emerged. The synthesis of 3-cyclohexylalkyl and adamantyl 2-hydroxy-1,4-naphthoquinone derivatives afforded compounds with good antimalarial activities against *P. berghei*. Using chloroquine as a control for suppression of malaria, over 28 days at 5 mg/kg, similar results were obtained for 25 mg/kg of **1.11**, and menoctone, **1.12**, derivatives, while decreased activity was observed for the 3-(ω -cyclohexylnonyl) homologue **1.13**. For the adamantyl series, activities were lower, and compound **1.14** cured mice at 40 mg/kg for a week, but at half dose only two of five mice were cleared from parasitemia. Indeed, for **1.14** relapse was noted after 14 days [77, 78].



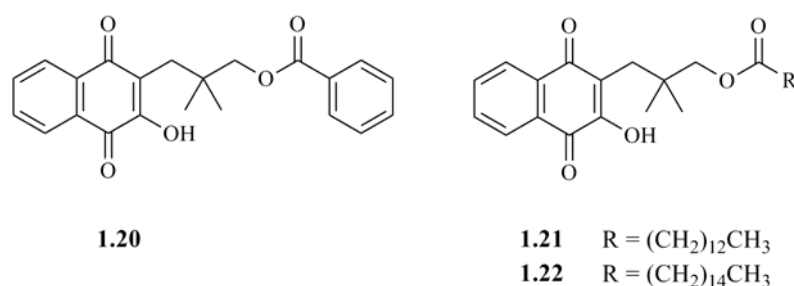
In another study, a series of sixty four 1,4-naphthoquinone derivatives were assayed for curative activity on *P. berghei*. From these, compounds **1.15** and **1.16** displayed good antimalarial activity [79].



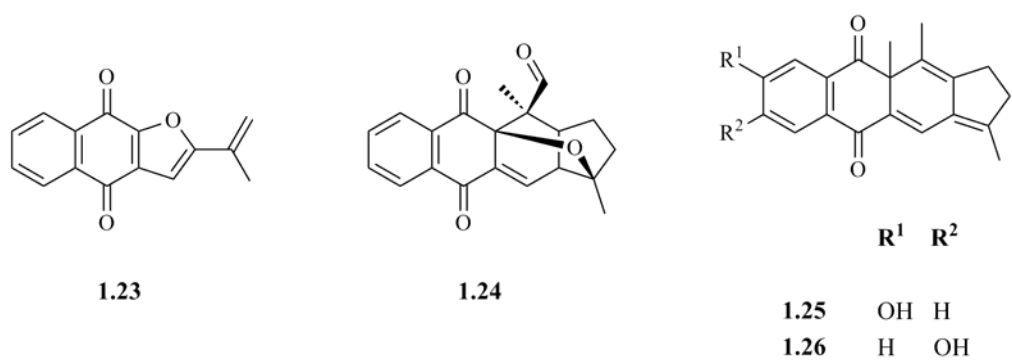
In 1981, the ongoing effort to find efficient and metabolism-resistant molecules led to the discovery of parvaquone, **1.17**, and its *cis*-dicyclohexyl analogue, **1.18**; these were equipotent, and ten times more active than their template menoetone. Introduction of oxygen and nitrogen atoms into the cycloalkyl substituent reduced activity^[80], while subsequent exploration of the cyclohexyl substituent afforded BW58C, **1.19**, a broad spectrum antiprotozoal. This was over 5,600 times more potent than **1.12**, over 1300 times more potent than **1.17**, and approximately 650-fold more active than chloroquine in *in vitro* assays. However, in *P. yoelii* infected mice, BW58C was only four times as active as chloroquine, with an ED₅₀ equal to 1.19 mg/kg, 7 x p.o. The diastereomer mixture of **1.19** also showed activity on *P. cynanolgi* and no apparent recrudescence was noted. Further studies revealed that it also had prophylactic activity against *P. berghei*. Nonetheless, in humans, the *tert*-butyl group is rapidly hydroxylated to a 1000-fold less active metabolite and further development was discontinued. Replacement of the *tert*-butyl by a 4-chlorophenyl group affords atovaquone, **1.1**^[81, 82]. Several structural modifications on atovaquone have been examined, either to improve activity or the formulation properties of tablets / i.v. dosage forms. Thus, derivatization of the hydroxyl group in **1.1** as a phosphate or carbamate yielded compounds that were shown to be useful for both treatment and prophylaxis of malaria^[83-85].



More recently, a series of 2-hydroxy-1,4-naphthoquinones derived from rhinacanthin, **1.20**, showed potent antiplasmodial activity. The optimum side chain length was found to have C₁₃, **1.21**, or C₁₅, **1.22**, with IC₅₀ values of 32 and 30 nM, respectively, against the K1 multi-drug resistant strain. It was also noted that the α -methyl substituent in the ester moiety was beneficial for antiplasmodial activity, when compared to its β and α -ethyl counterparts. Furthermore, the geminal methyl groups in the propyl chain are pivotal for the activity in this series. Compound **1.21** provided also specific Q_o site inhibition, IC₅₀ = 79.6 \pm 3.41 nM, against the homologous yeast *bc*₁ complex, and poor inhibition of the rat enzyme, IC₅₀ = 2,495 \pm 820 nM^[18].

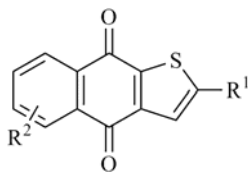


Additionally, a series of four unique naphthoquinones isolated from the rootbark of *Kigelia pinnata* demonstrated useful antiplasmodial activity. 2-(1-Hydroxyethyl)naphtho[2,3-*b*]furan-4,9-dione, **1.23**, was found to be the most active molecule, with IC₅₀ values of 627 nM and 718 nM against the K1 and T9-96 *P. falciparum* strains, respectively, Table 1.1. Isopinnatal, **1.24**, kigelinol, **1.25**, and isokigelinol, **1.26**, exhibited lower activities, especially the latter two. Moreover, despite the cytotoxicity of these compounds, the antiplasmodial activity was not due to *in vitro* cytotoxicity, as the selectivity indexes were of at least 10. The study also suggested that furanonaphthoquinones possessed much less affinity to parasitic mitochondria when compared to naphthoquinones, and that minor changes in furanonaphthoquinones would favour accumulation in the parasitic mitochondrial membrane. This would eventually increase the activity^[86].

**Table 1.1** *In vitro* activity of *Kigelia pinnata* compounds ^[86].

Compound	Antiplasmodial Activity	
	IC ₅₀ (nM)	
	K1 strain	T9-96 strain
1.23	627	718
1.24	763	1,552
1.25	16,660	15,200
1.26	15,200	11,930

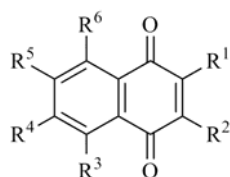
Similarly, fully synthetic thiophenonaphthoquinones **1.27-32** displayed moderate to good *in vitro* activity against *P. falciparum* at 0.2 µM, but were not active *in vivo*, Table 1.2 ^[87].

Table 1.2 Antiplasmodial *in vitro* activity of thiophenonaphthoquinone compounds against the BH2 26/28 chloroquine-resistant strain ^[87].

Compound	R ¹	R ²	% infection reduction at 0.2 µM
1.27	H	H	55
1.28	H	8-OMe	7
1.29	H	5-OMe	78
1.30	H	6-OMe	78
1.31	H	7,8-di-OMe	51
1.32	2-NO ₂	H	45

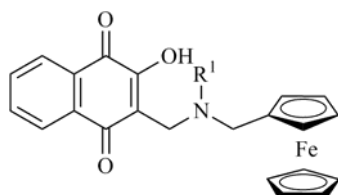
A series of amino-1,4-naphthoquinones was also tested for antiplasmodial activity and 2-amino-3-chloro-1,4-naphthoquinone, **1.33**, was the most potent compound with an IC_{50} of 180 nM against the W2 strain, Table 1.3. The presence of a primary amino group in R^1 appeared to be essential for activity, since substitution of that group for a halogen, **1.34**, decreased activity by 260-fold, while inclusion of other amino groups at R^2 , **1.35-37**, rendered compounds with only modest antiplasmodial activity^[88].

Table 1.3 *In vitro* activity of 1,4-naphthoquinone compounds^[88].



Compound	R^1	R^2	R^3	R^4	R^5	R^6	Antiplasmodial activity	
							IC_{50} (nM)	
							W2 strain	D6 strain
1.33	NH ₂	Cl	H	H	H	H	180	920
1.34	Cl	Cl	H	H	H	H	43,260	43,980
1.35	Cl	<i>N</i> -pyrrolidino	H	H	H	H	9,630	36,650
1.36	Cl	<i>N</i> -morpholino	H	H	H	H	31,960	115,140
1.37	H	<i>N</i> -anilino	H	H	H	H	47,670	63,970

Given that the use of metal complexes capable of enhancing the activity of biological compounds has become a relevant strategy, a small library of ferrocene derivatives of 1,4-naphthoquinone was built, incorporating a modified side chain of 6-8 carbons. Those displayed moderate antiplasmodial activity. The IC_{50} of compounds **1.38-40** was 3 to 6-fold higher than that of atovaquone, hinting that the ferrocene unit is damaging to activity, Table 1.4. Thus, it was suggested that this series do not act at the bc_1 complex level^[89].

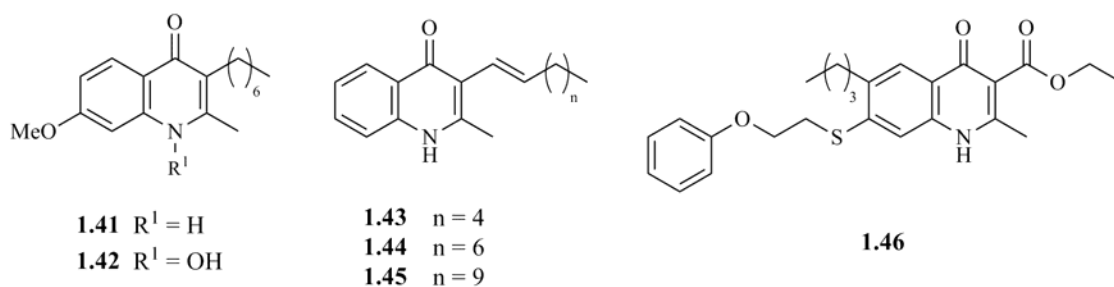
Table 1.4 Antiplasmodial activity of ferrocenyl 1,4-naphthoquinone compounds ^[89].

Compound	R ¹	IC ₅₀ (μM)	
		3D7 strain	Dd2 strain
1.38	(CH ₂) ₅ CH ₃	5 ± 0.4	2.5 ± 0.3
1.39	(CH ₂) ₆ CH ₃	2.5 ± 0.3	5 ± 0.4
1.40	(CH ₂) ₇ CH ₃	6.25 ± 1.5	6 ± 1.25
Atovaquone		0.6 ± 0.2	0.7 ± 0.35

1.3.2 4(1H)-Quinolones

4(1H)-Quinolones are also valuable antiprotozoal scaffolds, acting on the mitochondrial electron transport-chain ^[11, 90-92]. Much work, directed at improving both the antimalarial activity and the solubility of endochin, **1.41**, in water has been carried out. Structural modifications include carbonates, *N*-oxides, Mannich-bases and esters. Introduction of the *N*-hydroxyl group in the endochin molecule (BD26235), **1.42**, for example, resulted in increased water solubility and in improved antimalarial activity ^[90, 91, 93]. However, substitution of the alkyl side chain for a cyclopentyl group, or substitution of the methoxy group by a chlorine atom, results in appreciable loss of activity ^[94]. A separate study yielded more promising results, with some alkenylquinolones, **1.43-45**, displaying activity or curative properties on infected mice. Compound **1.45** had activity comparable to that of endochin, with an IC₅₀ of 5.7-16.6 nM, and displayed no cross resistance with some marketed antimalarials ^[95]. Additionally, elimination of the double bond in conjugation with the quinolone ring destroyed activity ^[96]. Compound **1.42**, on the other hand, proved to be non-toxic and was curative in infected chicks. BE11382, **1.46**, increased the mean survival time in parasite infected mice, suggesting that a substituent at C7 of 3-carboethoxy-4(1H)-quinolones may be beneficial ^[97].

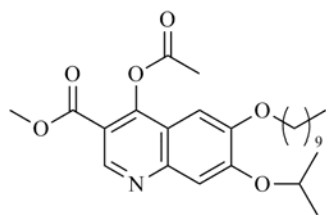
More recently, in a search for new scaffolds that comply with the structural features of the 4(1H)-quinolones, an *in silico* pharmacophore model was employed to screen virtual libraries of compounds ^[98]. Also, based on the structures of WR 194,905, **1.47**, and WR 197,236, **1.48**, a small set of compounds was synthesised and important structure activity relationships were drawn.



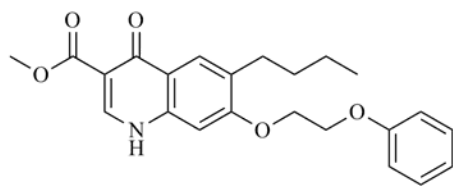
Simple quinolones without a long alkyl side chain yielded IC₅₀ values of 2.5 μM, **1.49**, 2.3 μM, **1.50**, and 325 nM, **1.51**, while compounds with longer side chains were active in the low nanomolar range, e.g. IC₅₀ 1.2 nM for **1.52**. Moreover, evidence suggests a mechanism of action similar to that of atovaquone, as significant cross resistance was attained against the Tm90-C2B strain. A 3-trifluorohexyl group also improved antimalarial activity by 70-fold over the corresponding unsubstituted counterpart, e.g. **1.53** vs. **1.50** and, more interestingly, no cross resistance to atovaquone was observed. Regarding the metabolism, this substituent may also be interesting since its terminal location is expected to block cytochrome P450 mediated oxidation. Other structure activity relationships that can be drawn are: substitution of 7-OMe for 7-OH reduces activity, and lengthening of the haloalkyl side chain increases it. This class of compounds also showed synergism with 4(1*H*)-pyridones and inhibition of oxygen consumption at the *bc*₁ complex level^[99]. A summary of antiplasmodial activities can be found in Table 1.5.

Table 1.5 Antiplasmodial activities of 4(1*H*)-quinolones^[99].

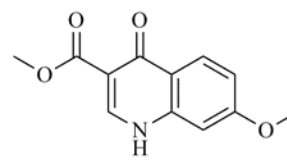
Compound	IC ₅₀ (nM)		
	D6 strain	Dd2 strain	Tm90-C2B strain
1.49	> 2,500	> 2,500	> 2,500
1.50	2,300	1,260	1,290
1.51	325	303	750
1.52	1.2	1.2	270
1.53	32	30	66
1.54	680	390	1,360
1.55	1.25	1.44	4.7
1.56	7.3	5.5	26.6
Endochin	3.2	2.8	17.4
Atovaquone	0.3	0.5	5,090



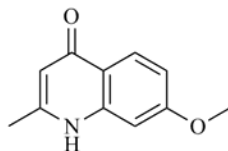
1.47



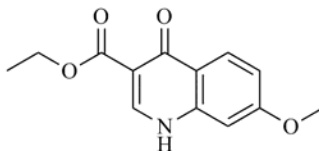
1.48



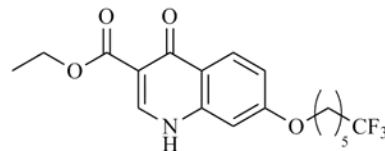
1.49



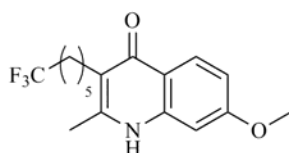
1.50



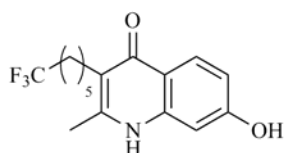
1.51



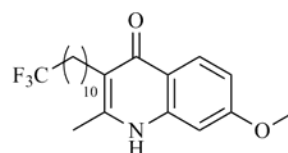
1.52



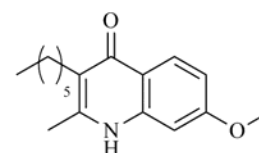
1.53



1.54



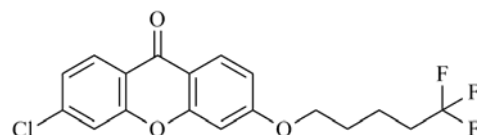
1.55



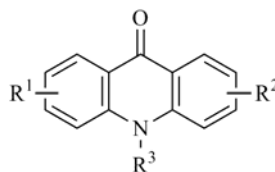
1.56

1.3.3 Acridones

Related acridones have also demonstrated potent antiplasmodial activity, Table 1.6 [100, 101]. These reveal structure activity trends identical to the quinolones; those containing a longer side chain and terminal CF_3 groups exhibit higher potencies, with IC_{50} s as low as ~ 1 pM, **1.78**. The ring nitrogen is also critical for activity, given the observed decrease in potency by over 50,000-fold when the nitrogen is replaced by oxygen; the xanthone **1.88** has an IC_{50} of 16 μM . It was also noted that alkylation of the nitrogen resulted in drop of activity, to a lesser extent, i.e. **1.85** [100].



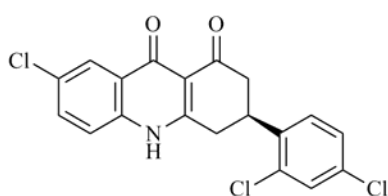
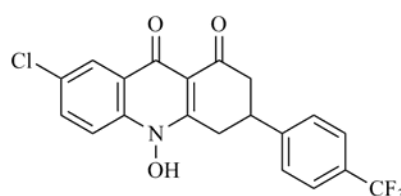
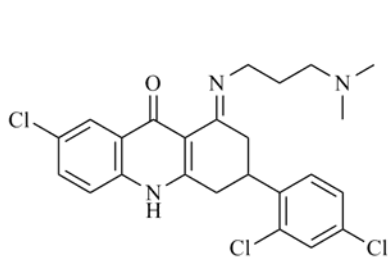
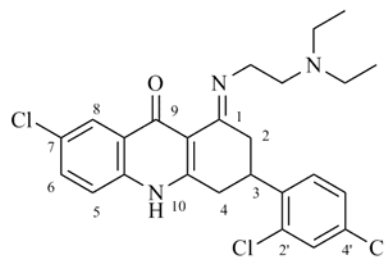
1.88

Table 1.6 Antiplasmodial activities of acridone series ^[100].

Compound	R ¹	R ²	R ³	IC ₅₀ (nM)	
				D6 strain	Dd2 strain
1.57	H	H	H	2,000	2,500
1.58	H	2-NH ₂	H	50,000	50,000
1.59	H	2-OMe	H	329	271
1.60	H	3-OMe	H	283	224
1.61	H	2-OH	H	9,000	4,400
1.62	H	3-OH	H	2,000	504
1.63	6-Cl	2-OMe	H	45	65
1.64	6-Cl	2-OH	H	190	260
1.65	6-Cl	2-O(CH ₂) ₄ CH ₂ Br	H	70	152
1.66	6-Cl	2-O(CH ₂) ₄ CH ₂ Cl	H	46	40
1.67	6-Cl	2-O(CH ₂) ₅ NMe ₂	H	67	95
1.68	6-Cl	3-OMe	H	76	192
1.69	6-Cl	3-OH	H	2,200	9,200
1.70	6-Cl	3-O(CH ₂) ₄ CH ₂ Br	H	27	54
1.71	6-Cl	3-O(CH ₂) ₄ CH ₂ Cl	H	12	13
1.72	6-Cl	3-O(CH ₂) ₃ CF ₃	H	1.0	1.2
1.73	6-Cl	3-O(CH ₂) ₄ CF ₃	H	0.3	0.5
1.74	H	3-O(CH ₂) ₄ CF ₃	H	0.5	0.3
1.75	6-Cl	3-O(CH ₂) ₅ CF ₃	H	0.06	0.07
1.76	6-Cl	2-O(CH ₂) ₅ CF ₃	H	10	15
1.77	6-Cl	3-O(CH ₂) ₄ CF ₂ CF ₃	H	0.02	0.02
1.78	6-Cl	3-O(CH ₂) ₄ CF(CF ₃) ₂	H	0.0015	0.0008
1.79	H	2-O(CH ₂) ₅ CF ₃	H	36	49
1.80	H	3-O(CH ₂) ₅ CF ₃	H	0.43	0.015
1.81	H	4-O(CH ₂) ₅ CF ₃	H	446	515
1.82	6-Cl	3-O(CH ₂) ₇ CF ₃	H	0.16	0.17
1.83	6-Cl	3-O(CH ₂) ₇ CH ₂ OH	H	2.2	3.5
1.84	6-Cl	3-O(CH ₂) ₁₀ CF ₃	H	0.023	0.025
1.85	6-Cl	3-O(CH ₂) ₄ CF ₃	Me	4,000	3,500
1.86	6-NO ₂	3-O(CH ₂) ₅ CF ₃	H	3.2	5.8
1.87	6-NH ₂	3-O(CH ₂) ₅ CF ₃	H	0.018	0.025

1.3.4 Acridinediones

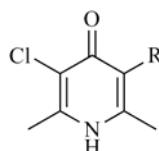
Acridinediones are another class of known potent antimalarials [102-104], that have been reported to inhibit the parasite respiratory pathway, causing a reduction of oxygen consumption. Acridinediones are predicted to block the bc_1 complex, but small changes into their structure affect not only their potency, but also their mechanism of action. While some inhibit the bc_1 complex others inhibit hemozoin polymerization [20, 64, 105, 106]. (*S*)-WR 249685, **1.89**, and racemic floxacrine, **1.90**, are two selective bc_1 complex inhibitors for *P. falciparum*. Their IC_{50} s for the enzyme are in the nanomolar range and consistent with whole cell growth inhibition. Additionally, data suggests mild cross resistance with atovaquone, associated to bc_1 complex mutations. This results in an increase of the IC_{50} s, which is an indication of Q_0 site blocking [20]. Compounds that lack the *N*-hydroxyl present in **1.90** have reduced antiplasmodial activity in general; *N*-allyl derivatives display modest activity, while the *N*-alkyl acridinediones are inactive. Replacement of the ketone function at the 1-position by an imine, afforded derivatives with comparable activities, and longer side chains on the imine moiety improved activity. Compounds **1.91** and **1.92** were curative in doses as low as 5 mg/kg in mice. Commonly, an aryl moiety at C3 is required for high potency, as alkyl substituents either yield compounds that are devoid of antiplasmodial activity or are marginally active. Electron withdrawing groups in the C3-aryl moiety also enhance potency, whereas electron donating groups diminish it. Interestingly, a methyl group at C2' of the aromatic ring is not deleterious, as opposed to bulkier substituents which decrease the potency. A chlorine located at C7 is also important for activity, but the lack of any substituents in positions C5 and C8 affords molecules with lowered effectiveness [107].

**1.89****1.90****1.91****1.92**

1.3.5 4(1H)-Pyridones

The novel class of 4(1H)-pyridones is based on clopidol, **1.93**. Clopidol is long known for its antiplasmodial (curative at 160 mg/kg) and anticoccidial activities through inhibition of mitochondrial respiration [108, 109]. However, its poor solubility in several solvents led to the synthesis of various derivatives [108, 110]. Currently, GlaxoSmithKline (GSK) is developing a series of clopidol analogues with more lipophilic side chains in an effort first disclosed in 1991 [111-113]. Compared to its lead, the *n*-octyl derivative **1.94** has enhanced activity *in vitro*, but is inactive *in vivo* due to metabolic degradation of the side chain, Table 1.7. Introduction of side chains less prone to metabolism, **1.95-99**, improved not only the *in vitro*, but also *in vivo* activities [19].

Table 1.7 Antiplasmodial activities of 4(1H)-pyridones: influence of side chain on activity [19].



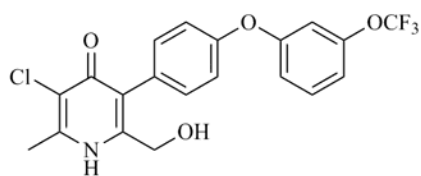
Compound	R	<i>P. falciparum</i> T9-96	<i>P. yoelii</i>
		IC ₅₀ (nM)	ED ₅₀ (mg/kg)
1.93	Cl	20,000	40
1.94	<i>n</i> -C ₈ H ₁₇	4,000	> 60
1.95	Ph	11,000	22
1.96		2,500	20
1.97		50	0.6
1.98		400	0.7
1.99		60	0.6
Atovaquone		3	0.03

Further structure-activity relationship (SAR) analysis on derivatives containing the 3-(4'-phenoxy)phenyl side chain was carried out. A halogen at C₅, either chlorine or bromine, leads to more potent derivatives. Though, other electron withdrawing substituents at that position do not improve activity, and electron donating moieties result in a significant increase of the IC₅₀, Table 1.8. Variation within the terminal aryl moiety does not influence activity significantly, and the phenoxy side chain is best positioned at 3' or 4'; a much reduced activity is observed for the 2'

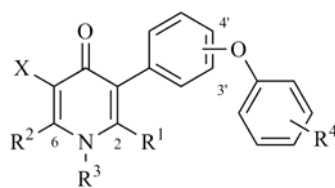
analogue, i.e. **1.120**. The methyl groups at C2 and C6 also appear to be critical, and significant loss of activity is achieved upon their withdrawal or their replacement by a trifluoromethoxy group. The *N*-oxide derivatives are 10-fold less active than their pyridone counterparts, e.g. **1.125** vs. **1.104** and **1.126** vs. **1.102** ^[19].

In addition to potent activity against erythrocytic stages of malaria, these compounds showed *in vitro* and *in vivo* activity against liver stages, making them amenable to prophylaxis ^[19, 114].

ADME studies on compound GW844520, **1.113**, revealed a half-life adequate for short duration of oral therapy, activity against resistant isolates, and no cross resistance with atovaquone, among other features. However, according to the MMV 2005 annual report its development was discontinued due to toxic properties ^[19, 115, 116]. GW308678, **1.110**, was then selected for further development, but unfortunately showed recrudescence at any dose up to 32 mg/kg ^[117]. Since 2006, two further patents from GSK have disclosed structural modifications of the lead compound: compounds with biaryl or related side chains at C3, and those containing modified side chains instead of methyl groups at C2 or C6 display promising *in vitro* antiplasmodial activities for advanced development ^[118, 119]. The MMV portfolio for the second quarter of 2010 includes one of those compounds, GSK932121, **1.127**, in phase I of clinical trials ^[120].



1.127

Table 1.8 Antiplasmodial activities of phenoxyaryl-4(1*H*)-pyridones ^[19].

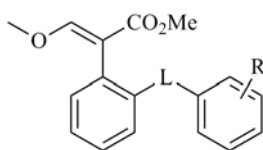
Compound	R ¹	R ²	R ³	X	Isomer	R ⁴	<i>P. falciparum</i>		<i>P. yoelii</i>
							IC ₅₀ (nM)		ED ₅₀
							T9-96	3D7A	(mg/kg)
1.100	Me	Me	H	Br	4-OAr	H	150	N.A.	4
1.101	Me	Me	H	Br	4-OAr	4-F	40	N.A.	0.6
1.102	Me	Me	H	H	4-OAr	4-Cl	250	N.A.	2.5
1.103	Me	Me	H	Cl	4-OAr	4-Cl	60	N.A.	1.7
1.104	Me	Me	H	Br	4-OAr	4-Cl	40	N.A.	0.3 (5)
1.105	Me	Me	H	Cl	4-OAr	3-Cl	30	N.A.	> 5
1.106	Me	Me	H	Br	4-OAr	3-Cl	30	N.A.	3.9
1.107	Me	Me	H	H	4-OAr	4-CF ₃	500	N.A.	1.3
1.108	Me	Me	H	Cl	4-OAr	4-CF ₃	60	N.A.	0.6
1.109	Me	Me	H	Br	4-OAr	4-CF ₃	30	N.A.	0.3 (1.1)
1.110	Me	Me	H	Cl	4-OAr	3-CF ₃	30	N.A.	0.2 (0.2-0.6)
1.111	Me	Me	H	Br	4-OAr	3-CF ₃	30	N.A.	0.6 (3.6)
1.112	Me	Me	H	H	4-OAr	4-OCF ₃	160	160	> 5
1.113	Me	Me	H	Cl	4-OAr	4-OCF ₃	30	5	0.2 (0.4-1.3)
1.114	Me	Me	H	Br	4-OAr	4-OCF ₃	30	8	0.3 (0.2-0.5)
1.115	Me	Me	H	CF ₃	4-OAr	4-OCF ₃	N.A.	30	N.A.
1.116	Me	Me	H	NO ₂	4-OAr	4-OCF ₃	N.A.	30	N.A.
1.117	Me	Me	H	OMe	4-OAr	3-CF ₃	N.A.	300	N.A.
1.118	Me	Me	H		4-OAr	4-OCF ₃	N.A.	1,290	N.A.
1.119	Me	Me	H	Br	3-OAr	4-OCF ₃	N.A.	7	N.A.
1.120	Me	Me	H	Br	2-OAr	4-OCF ₃	N.A.	400	N.A.
1.121	H	Me	H	Br	4-OAr	4-OCF ₃	N.A.	200	N.A.
1.122	Me	H	H	Br	4-OAr	4-OCF ₃	N.A.	110	N.A.
1.123	Me	CF ₃	H	Br	4-OAr	4-OCF ₃	N.A.	> 1,000	N.A.
1.124	H	CF ₃	H	Br	4-OAr	4-OCF ₃	N.A.	> 1,000	N.A.
1.125	Me	Me	OH	Br	4-OAr	4-Cl	450	N.A.	~ 1,000
1.126	Me	Me	OH	H	4-OAr	4-Cl	2,200	N.A.	> 1,000

N.A. - Not available

1.3.6 (*E*)- β -Methoxyacrylates

(*E*)- β -Methoxyacrylate is a scaffold known to inhibit the bc_1 complex. Compounds from this class have found applicability in tackling crop pathogens, and as tools for probing the function of the bc_1 complex [121-127]. Unlike other classes of inhibitors, ubiquinol still binds in the Q_o in presence of these inhibitors, but its electrons cannot be transferred to the ISP. A shift of the relative position of the natural ligand due to a conformational distortion of cytochrome *b*, induced by the binding of methoxyacrylates, appears to be the reason [128, 129]. In 1999, 252 compounds were first disclosed as having potent antimalarial activity on chloroquine sensitive and resistant strains, a step that led to some highly active compounds reported a year later [130, 131]. Compound **1.128** had shown useful antiplasmodial activity, but derivatives containing a longer linker, from two to four atoms, **1.129-133**, improved activity when compared to **1.128**, Table 1.9. The (*E,E*)-butadiene linker conferred the better activity to the compounds [131].

Table 1.9 Antiplasmodial activities of β -methoxyacrylate against the K1 strain [131].



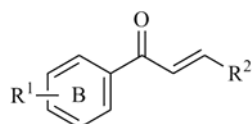
Compd.	L	R	IC ₅₀ (nM)	Compd.	L	R	IC ₅₀ (nM)
1.128		2-CF ₃	75.8	1.138		3-F	24.8
1.129		2-CF ₃	21.5	1.139		3-CF ₃	43.0
1.130		2-CF ₃	6.2	1.140		3-Br	48.6
1.131		2-CF ₃	1.6	1.141		4-Cl	5.6
1.132		2-CF ₃	0.39	1.142		2,4-diCF ₃	0.3
1.133		2-CF ₃	3.9	1.143		2,4-diCl	0.26
1.134		2-CF ₃	4.2	1.144		2,4-diMe	0.14
1.135		H	11.5	1.145		2-Cl, 4-F	0.51
1.136		2-Cl	1.1	1.146		3-OMe, 2-NO ₂	1.47
1.137		2-CN	4.6				

1.3.7 Chalcones

SAR studies with chalcones show that the most important features for antiplasmodial activity are the properties of ring B. Hydrophobicity and the size of substituents are critical. Hydroxylated

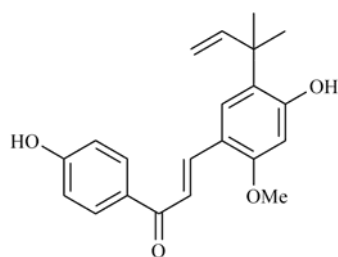
chalcones showed to be at least 2-fold less active when compared to the corresponding alkoxyated analogues [132, 133]. Recently, naphthyl and quinolinyl chalcone derivatives were reported to display submicromolar antiplasmodial activities, **1.147-154**, Table 1.10. Generally, quinolinyl and pyridinyl derivatives are preferred over naphthyl, and 2-quinolinyl over the remainder positional isomers *in vitro*. Quinolinyl derivatives presented activities in the low nanomolar range, whereas pyridinyl and naphthyl compounds displayed micromolar IC₅₀s. Both methoxy and halogenated chalcones afforded compounds with good activity and no difference was observed between chloro and fluoro analogues [134, 135]. Several other reviews report structural modifications on this attractive scaffold [136-139].

Table 1.10 Antiplasmodial activities of selected chalcones [134].



Compound	R ¹	R ²	IC ₅₀ (nM)	
			W2 strain	D6 strain
1.147	3,4-di-OMe	4-quinolinyl	0.50	0.88
1.148	2,5-di-Cl	3-quinolinyl	1.70	0.62
1.149	2,5-di-Cl	4-quinolinyl	0.23	0.19
1.150	3,4-di-Cl	4-quinolinyl	0.80	1.70
1.151	2-OMe, 5-F	2-quinolinyl	0.67	3.8
1.152	2-OMe, 5-F	3-quinolinyl	1.10	0.46
1.153	3-F, 4-OMe	4-quinolinyl	3.20	0.93
1.154	2-OMe, 5-Cl	3-quinolinyl	0.59	0.95

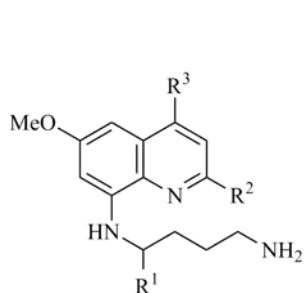
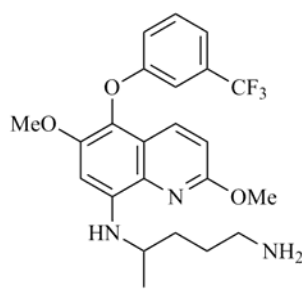
Licochalcone A, **1.155**, is a natural product from Chinese liquorice roots known to inhibit cytochrome *bc*₁, SDH and falcipain-2 [139-142]. No correlation between falcipain inhibition and antiplasmodial activity was found, but evidence of a strong inhibitory effect on the mtETC suggests that the main mechanism of action might involve the competitive blocking of multiple ubiquinone binding sites [143, 144]. Mi-Ichi and co-workers showed that complex II was sensitive to licochalcone A at an IC₅₀ value of 1.30 μM, i.e. 10-fold more potent than against the mammalian counterpart. Moreover, DHODH-cytochrome *c* activity was sensitive to licochalcone A with an IC₅₀ value of 100 nM, but *Pf*DHODH was not inhibited even at 100 μM, which means that the *bc*₁ complex is the main drug target [144].



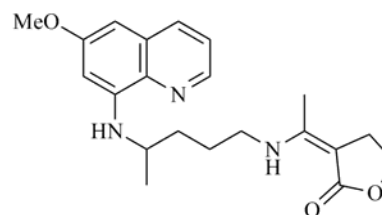
1.155

1.3.8 8-Aminoquinolines

8-Aminoquinolines have also been hypothesised to interact with the mtETC complex through inhibition of Q_0 / Q_i sites, due to the structural similarities with the natural ligand [145-147]. Primaquine, **1.156** and other 8-aminoquinoline representatives are, like atovaquone, effective in both *P. falciparum* prophylaxis and leishmaniasis [148-150]. Many related compounds were synthesised with respectable activities against murine, primate and avian malaria. Although interspecies differences in activity profiles were often observed [151-156]. For example, **1.157** and **1.158** showed causal prophylaxis and cured murine malaria at 20 mg/kg and 10 mg/kg, respectively [157, 158]. Presently, tafenoquine **1.159** and aablaquine **1.160** are in the final stages of clinical trials against *P. falciparum* and *P. vivax*. Further information on the subject can be found in a recent review of primaquine-based antimalarials [149].

1.156 $R^1 = \text{Me}, R^2 = R^3 = \text{H}$ 1.157 $R^1 = \text{Et}, R^2 = \text{H}, R^3 = \text{Me}$ 1.158 $R^1 = \text{Me}, R^2 = \text{C}(\text{CH}_3)_3, R^3 = \text{H}$ 

1.159



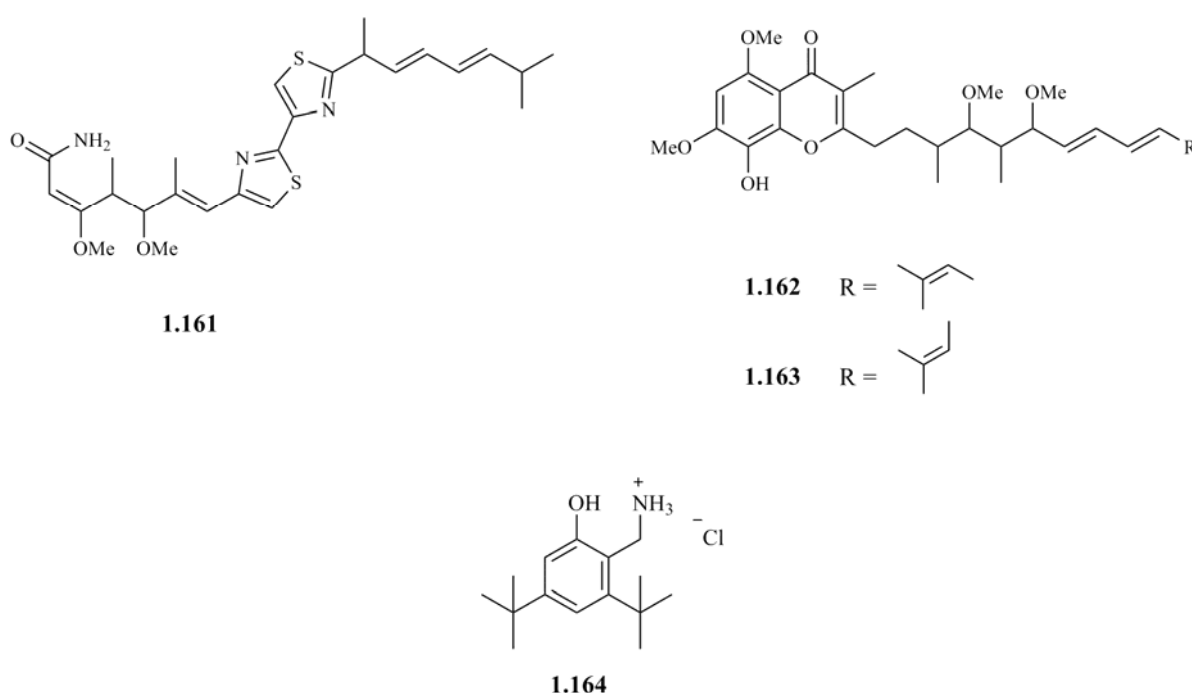
1.160

1.3.9 Miscellaneous

Myxothiazol, **1.161**, is a group I antibiotic and a potent antimalarial bc_1 complex inhibitor with an IC_{50} of 33 nM and 695 nM on the D6 and Tm90C2B (atovaquone resistant) strains, respectively [47, 159].

Stigmatellin A and B, **1.162** and **1.163**, block the Q_o site and present properties of both type I and II inhibitors^[160]. They bind to the heme *b_L* domain of cytochrome *b* as well as to the ISP, and contain a 5,7-dimethoxy-8-hydroxychromone system with an alkenyl side chain in position 2, responsible for the tight binding^[44]. Modification of the 8-hydroxy, 5-methoxy or 4-keto groups leads to partial or complete loss of inhibitory activity. On the other hand, reduction of the chromone to a chromanone system does not alter the potency significantly, nor this can be achieved by an alteration of the side chain, as long as the overall lipophilicity is not decreased. Hence the partition coefficient of the inhibitor between the aqueous phase and the membrane is of decisive importance^[47]. The IC₅₀s of 79.2 nM and 147.5 nM for D6 and Tm90C2B showed only a 2-fold loss of activity to an atovaquone resistant strain, suggesting different binding of that of atovaquone^[159].

MK-4815, **1.164**, has been identified to have antiplasmodial activity in whole parasite screens by Merck & Co. Inc. It has also demonstrated potency against *P. falciparum* malaria. Its mechanism of action appears to involve the mtETC of the parasite^[120].



Antimycin A, **1.165** Figure 1.4, is a dilactone salicylamide, and a potent inhibitor of the Q_i site of cytochrome *bc₁* with an IC₅₀ of 13 nM and 10.7 nM against D6 and Tm90C2B, respectively^[159, 161]. Crystal structures for bovine complex III inhibited by this molecule have been determined. A strong hydrogen bond network with the enzyme can be observed. The formamide oxygen hydrogen bonds with K227, through a water molecule, whereas the nitrogen acts as a hydrogen bond donor to D228, which also forms a hydrogen bond with the phenol group. A hydrogen bond between the

phenolic oxygen and the benzamide is responsible for the co-planarity of the system and the benzamide oxygen is involved in a water mediated hydrogen bond to H201 [162, 163].

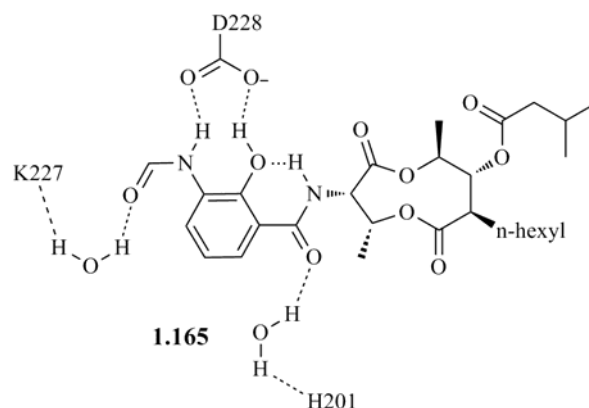
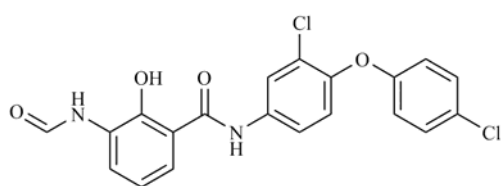
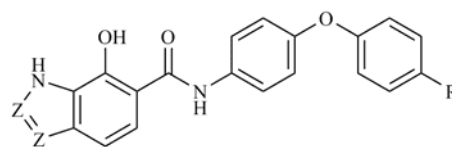


Figure 1.4 Structure of antimycin A and cytochrome bc_1 interactions [164].

SAR studies on antimycin A analogues suggest that the aromatic region is crucial for activity and the remainder of the molecule only contributes for proper solubility characteristics, as loss of activity is observed by varying the phenol acidity and withdrawal of the formamide group [165, 166]. Simpler analogues with the replacement of the dilactone moiety for biphenyl ethers, **1.166**, were prepared and showed comparable *in vitro* inhibitory potency to antimycin A. Therefore, the overall hydrophobicity is important for proper interaction and fitting in the active site [167]. However, since the reactivity of formamide could result in lower *in vivo* activity, a series ofazole-fused salicylamides were prepared to circumvent the drawbacks of the previous analogues. Benzotriazole and indole derivatives with a trifluoromethyl group, **1.167**, showed to possess identical activity to that of antimycin against the bc_1 complex, but low *in vivo* activity due to weak cell penetration [164].

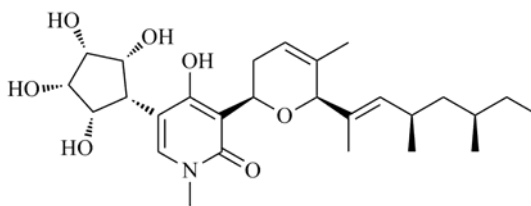


1.166



1.167 Z = CH or N
R = H or CF₃

Finally, funiculosin, **1.168**, a *N*-methyl-4-hydroxy-2-pyridone antibiotic with a hydrophobic side chain also inhibits the respiratory chain at the Q_i and Q_o sites [42, 168-170].



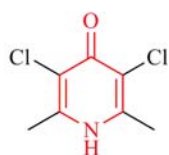
1.168

1.4 Aims of the thesis

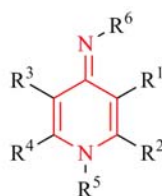
The primary goal of this project was to contribute to the ongoing research of mitochondrial cytochrome bc_1 inhibitors in malaria, providing information on what determinants are crucial for an effective blocking of the drug target.

To achieve the goal, the (1*H*-pyridin-4-ylidene)-amine (or 4-pyridonimine) scaffold, **1.169**, was chosen as a starting point for drug candidate optimization and development, based on the following observations:

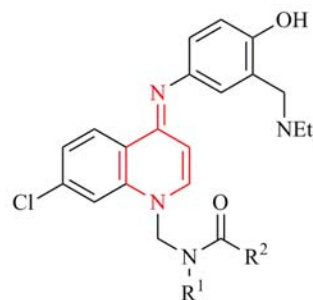
- Compounds with general structure **1.169** may represent bioisosteres of clopidol, **1.93**. Biososterism is an important tool in rational drug design and the imino group is considered to be a good replacement for the carbonyl group^[171];
- Compounds **1.169** derive from similar structures **1.170** that display good *in vitro* antiplasmodial activity, but poor chemical stability^[172]. The target compounds **1.169** do not contain the *N*-amidomethyl moiety, which is responsible for the reported chemical reactivity;
- This molecular simplification strategy allows the use of simple starting materials for the synthesis, a major issue for obtaining drugs at an affordable cost. Moreover, the proposed synthetic pathway allows the introduction of a large number of structural motifs.



1.93



1.169



1.170

This would be conducted by combining theoretical and experimental procedures. A computational chemistry study was carried out to assess the suitability of this scaffold as a 4(1*H*)-pyridone isostere. This study would also determine the major structural and electronic properties of the (1*H*-pyridin-4-ylidene)amine scaffold that might be relevant for the interaction with the molecular target in the parasite. The synthesis through simple building-blocks, *in vitro* evaluation against *P. falciparum* strains, and a biochemical model of the *bc*₁ complex, would provide the proof-of-concept and complete this task, chapters 2 and 3.

In a second phase, the SAR information withdrawn from the previous series and the literature would be used to design a new library of flavone and isoflavone derivatives. The scaffold was also chosen based on the following premises:

- a) Stigmatellin, **1.162-163**, is a natural chromone-based antibiotic with potent antiplasmodial activity^[159];
- b) Being a natural product, the access to stigmallin is limited and its chemical synthesis time-consuming and exquisitely difficult;
- c) The chromone ring in stigmatellin is responsible for binding to the Rieske protein and cytochrome *b*. The synthesis of the core scaffold can be achieved through appropriate starting materials in a straightforward manner, allowing at the same time the introduction of lipophilic, yet simpler side chains when compared to that of stigmatellin.

The *in vitro* evaluation of the flavone derivatives against different *P. falciparum* strains would provide information on which substituents would be best to carry on in scaffold optimization and future chemical synthesis, chapter 4.

Finally, with the aim of discovering novel scaffolds capable of inhibiting the *bc*₁ complex for future optimization, a virtual screening study would be carried out, chapter 5. Virtual screening is widely regarded as a valuable technique for lead discovery and presents advantages compared to high-throughput screening (HTS). The celerity and its less expensive nature, compared to HTS, make this an ideal approach for retrieval of new leads from libraries comprising several thousands of chemotypes. The validation of the procedure would be achieved from *in vitro* testing of the chosen ligands.

CHAPTER 2

PYRIDONIMINE SCAFFOLD

2. PYRIDONIMINE SCAFFOLD

2.1 Quantum mechanical study

2.1.1 Brief overview on electronic structure methods and its use in the development of antimalarial drug candidates

Electronic structure methods use laws of quantum mechanics for its calculations, i.e. the energy and related properties of a given molecule are obtained by solving the Schrödinger equation. Since the exact solution is not practical in most cases, several mathematical approximations are employed to its solution. Thus, according to the type of approximation, one can classify the electronic structure methods in:

- a) Semi-empirical methods, e.g. AM1, which use parameters derived from experimental data to simplify the equation;
- b) *ab initio* methods, which use no experimental data, and are based solely on the laws of quantum mechanics (first principles).

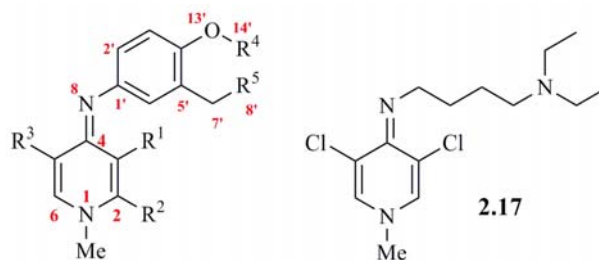
Density functional methods, or DFT, are similar to *ab initio* methods, and include the effects of electron correlation. Besides the method that one has to choose, there is also a basis set. The basis set is a mathematical representation of the molecular orbitals within a given molecule. Thus, it is possible to constrain the calculation with a smaller basis set. On the other hand, a larger basis set will represent more accurately the molecular orbitals, but the time required to achieve a result will be longer. Therefore, it is necessary to balance the time available to perform a calculation and the desired accuracy of the outcome^[173, 174]. In malaria these methods have been successfully employed to model inhibitors of the aggregation of hemozoin^[175-179].

This part of the work was developed in parallel with the synthesis of the Mannich-base 4-pyridonimines (Section 2.3) and aimed to study the electronic and molecular structures of those compounds, in order to establish relationships between the quantum chemical descriptors and the antiplasmodial activity of the molecules. Hence, all the synthesized compounds were studied as well as other 4-pyridonimines that could be easily obtained from the same synthetic pathway.

2.1.2 Molecular geometry of 4-pyridonimines

Most of the 4-pyridonimines presented in Table 2.1 were studied in their (*E*) and (*Z*) configurations. Also, several conformations were studied for each diastereoisomer to determine

which one corresponded to the global minimum of energy. The optimized conformations were found to be local minima on their potential energy surfaces, following a frequency calculation (Appendix 1.1 for the energy-minimized structures). Since the structurally-related amodiaquine is reported to present an intramolecular hydrogen bond between the phenolic oxygen and the nitrogen atoms from the diethylamino group as a free base^[180], this series of compounds was also optimized with this hydrogen bond. As expected, it was found that the conformers containing a hydrogen bond between the phenolic oxygen and the nitrogen from the diethylamino group provided lower energies, i.e. were more stable, when compared to the ones without such bond. Furthermore, the predicted pK_a values for the basic nitrogens on **2.1** are 11.3 for N8' and 12.5 for N8^[181]. Consequently, the protonated forms of this compound, **2.2** and **2.3**, were also studied, as they would present a probable ionization state in aqueous media. For the compounds that were studied in both their (*E*) and (*Z*) configuration it was found that the (*E*) diastereoisomers were more stable than their counterparts, Table 2.2, i.e. when the substituent was on R³ rather than on R¹. The only exception was compound **2.4**, where the (*Z*) diastereomer was marginally more stable than the (*E*) isomer. In this case, the predicted lower steric constraint might justify the obtained result. In fact, the C3-C4-N8 angle in (*Z*)-**2.4** was very similar to the one observed for (*E*)-**2.24**, Table 2.3. For a full analysis of the stereoelectronic properties, only the most stable diastereomer was chosen.

Table 2.1 Structures of compounds **2.1-17** (only the (*E*) conformer is explicitly included).

Compd	R ¹	R ²	R ³	R ⁴	R ⁵
2.1	H	H	H	H	NEt ₂
2.2	H	H	H	H	NHEt ₂ ⁺
2.3^a	H	H	H	H	NHEt ₂ ⁺
2.4	H	Me	H	H	NEt ₂
2.5	H	H	NH ₂	H	NEt ₂
2.6	H	H	Me	H	NEt ₂
2.7	H	Me	H	H	N(Me)Et ₂ ⁺
2.8	H	H	SO ₂ NMe ₂	Me	N(Me)Et ₂ ⁺
2.9	H	H	NO ₂	H	NEt ₂
2.10	H	H	F	H	NEt ₂
2.11	H	CN	H	H	NEt ₂
2.12	H	H	CO ₂ H	H	NEt ₂
2.13	Cl	H	Cl	H	NEt ₂
2.14	H	H	CF ₃	H	NEt ₂
2.15	H	H	OH	H	NEt ₂
2.16	H	H	Br	H	NEt ₂

^a Protonated on the imine nitrogen (atom N8).

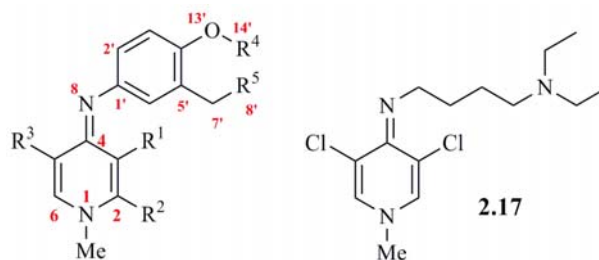
Table 2.2 Selected electronic properties.

Compound	E (Hartree) ^a	E _{HOMO} (Hartree)	E _{LUMO} (Hartree)	HOMO-LUMO Gap
Atovaquone	-1535.312321	-0.23889	-0.10860	-0.13029
Clopidol	-1321.198283	-0.22196	-0.02444	-0.19752
2.1	-900.750151	-0.15961	-0.01103	-0.14858
2.2	-901.146060	-0.26655	-0.11388	-0.15267
2.3	-901.473062	-0.44142	-0.27026	-0.17116
(E)-2.4	-940.036257	-0.15899	-0.00779	-0.15120
(Z)-2.4	-940.039605	-0.15859	-0.00776	-0.15083
(E)-2.5	-956.092729	-0.15475	-0.00954	-0.14521
(E)-2.6	-940.042220	-0.16024	-0.00966	-0.15058
(Z)-2.6	-940.033866	-0.15804	-0.00934	-0.14870
(E)-2.7	-979.707670	-0.25999	-0.11470	-0.14529
(Z)-2.7	-979.706674	-0.15859	-0.00776	-0.15083
(E)-2.8	-1662.139781	-0.27044	-0.11761	-0.15283
(Z)-2.8	-1662.133697	-0.27494	-0.11912	-0.15582
(E)-2.9	-1105.233082	-0.17632	-0.07052	-0.10580
(E)-2.10	-999.981523	-0.16475	-0.01886	-0.14589
(E)-2.11	-992.983733	-0.17469	-0.06170	-0.11299
(Z)-2.11	-992.983458	-0.17385	-0.06411	-0.10974
(E)-2.12	-1089.300945	-0.16713	-0.04130	-0.12583
2.13	-1819.936762	-0.16548	-0.03000	-0.13548
(E)-2.14	-1237.773631	-0.17023	-0.02608	-0.14415
(E)-2.15	-975.953891	-0.15755	-0.01131	-0.14624
(E)-2.16	-3471.857156	-0.16691	-0.02077	-0.14614
2.17	-1631.586747	-0.19225	-0.02402	-0.16823

^a Energy corrected to 298 K.

The Q_o site in cytochrome *bc*₁ adopts the shape of a curved tube ^[60]. As a consequence, both the substitution pattern, and the geometry of the molecule need to be addressed, and thus, the characterization of the molecules regarding their conformation and topology is of utmost importance, Table 2.3. These 4-pyridonimines displayed a positive C3-C4-N8 angle deviation from 120°, ranging from *ca.* 123° to 134°, regardless of the diastereoisomer, e.g. **2.4**, **2.6** and **2.8**. The C3-C4-N8 angle deviation from 120° was affected by the protonation state at N8 and N8'. For example, the neutral **2.1** presented an angle of 128.2°, while protonation at N8', e.g. **2.2**, decreased the angle by almost 5°. Additional protonation at the imine nitrogen N8, e.g. **2.3**, restored the C3-C4-N8 angle to a value similar to that of the neutral molecule.

Table 2.3 Selected angle and dihedral angles



Cpd	Angle (°)	Dihedral angle (°)	Cpd	Angle (°)	Dihedral angle (°)				
ATV ^a	C2-C3-C1'	122.4	C2-C3-C1'-C2'	-116.7	(E)-2.8	C3-C4-N8	128.1	C4-N8-C1'-C2'	-139.3
2.1	C3-C4-N8	128.2	C4-N8-C1'-C2'	-133.3		C4-N8-C1'	125.3		
	C4-N8-C1'	122.2			(E)-2.9	C3-C4-N8	126.2	C4-N8-C1'-C2'	-57.7
2.2	C3-C4-N8	123.5	C4-N8-C1'-C2'	-138.1		C4-N8-C1'	122.2		
	C4-N8-C1'	127.7			(E)-2.10	C3-C4-N8	129.3	C4-N8-C1'-C2'	-54.8
2.3	C3-C4-N8	127.9	C4-N8-C1'-C2'	-128.2		C4-N8-C1'	121.7		
	C4-N8-C1'	123.7			(E)-2.11	C3-C4-N8	129.0	C4-N8-C1'-C2'	-50.5
(Z)-2.4	C3-C4-N8	127.9	C4-N8-C1'-C2'	-129.3		C4-N8-C1'	122.5		
	C4-N8-C1'	122.0			(E)-2.12	C3-C4-N8	125.1	C4-N8-C1'-C2'	-62.3
(E)-2.4	C3-C4-N8	128.1	C4-N8-C1'-C2'	-56.6		C4-N8-C1'	122.1		
	C4-N8-C1'	121.8			2.13	C3-C4-N8	131.7	C4-N8-C1'-C2'	-132.3
2.5	C3-C4-N8	129.5	C4-N8-C1'-C2'	-50.3		C4-N8-C1'	127.8		
	C4-N8-C1'	123.0			(E)-2.14	C3-C4-N8	127.4	C4-N8-C1'-C2'	-56.8
(Z)-2.6	C3-C4-N8	130.1	C4-N8-C1'-C2'	-125.6		C4-N8-C1'	122.2		
	C4-N8-C1'	126.3			(E)-2.15	C3-C4-N8	128.6	C4-N8-C1'-C2'	-54.8
(E)-2.6	C3-C4-N8	127.6	C4-N8-C1'-C2'	-55.9		C4-N8-C1'	122.0		
	C4-N8-C1'	122.2			(E)-2.16	C3-C4-N8	127.9	C4-N8-C1'-C2'	-54.6
(Z)-2.7	C3-C4-N8	128.2	C4-N8-C1'-C2'	-44.0		C4-N8-C1'	122.5		
	C4-N8-C1'	124.2			2.17	C3-C4-N8	133.6	C4-N8-C1'-C2'	-96.2
(E)-2.7	C3-C4-N8	128.2	C4-N8-C1'-C2'	-143.2		C4-N8-C1'	127.4		
	C4-N8-C1'	123.8							
(Z)-2.8	C3-C4-N8	128.1	C4-N8-C1'-C2'	-117.5					
	C4-N8-C1'	125.3							

^a ATV - Atovaquone; Numbering in page 6.

Inspection of Table 2.3 allows the following observations regarding the predicted molecular structure of the studied compounds:

- The C3-C4-N8 angle is affected by the nature of substituents at the 4-pyridonimine moiety. Strong electron-donating substituents at C5 such as NH₂, **2.5**, and OH, **2.15**, result in an increase of the angle, when compared to the unsubstituted counterpart, **2.1**;
- Electron-withdrawing substituents such as NO₂, **2.9**, CO₂H, **2.12**, or CF₃, **2.14**, have the opposite effect, decreasing the C3-C4-N8 angle relatively to **2.1**;

- c) The presence of halogens at C3 does not affect significantly the C3-C4-N8 angle, i.e. **2.10** and **2.16**, but the simultaneous substitution to chlorine at C3 and C5, as in **2.13** and **2.17**, increases the C3-C4-N8 angle when compared to **2.1**;
- d) The nature of substituents in the 4-pyridonimine has practically no impact on the C4-N8-C1' angle, which reflects the distance between the substituent and the phenolic moiety. The only exceptions were found in molecules **2.13** and **2.17**, which presented a significant increase in the C4-N8-C1' angle, relatively to **2.1**. This reveals the impact of the steric hindrance imposed by the two chlorine atoms;
- e) The C4-N8-C1' angle increases when the diethylaminomethyl group is protonated, e.g. **2.2**;
- f) The nature and position of the substituents are responsible for a significant rotation around the N8-C1' bond, resulting in a wide range of dihedral angles. Compound **2.17** presents a narrower C4-N8-C1'-C6' dihedral angle, when compared to its aryl counterpart **2.13**;
- g) The predicted dihedral angles were not significantly different from the one observed for atovaquone, C2-C3-C1'-C2': -116.7°. Thus, it is expected that these compounds might fit in a highly convoluted Q_o site.

These geometry predictions are expected to be accurate as the crystals of **2.8** (Section 2.3.3) present bond lengths, angles and dihedral angles that are very similar to the *in silico* optimized (*E*)-**2.8**, Figure 2.1. Superimposing both structures a root mean square deviation (RMSD) of 0.31 Å is obtained. The marginally narrower C4-N8-C1' angle and the wider C4-N8-C1'-C6' dihedral angle in the optimized structure leads to a minor displacement of the 4-pyridonimine scaffold, compared to the crystallized molecule.

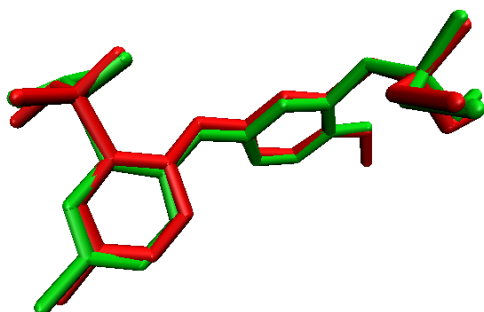


Figure 2.1 *In silico* optimized (*E*)-**2.8** (green) superimposed with VMD 1.8.6^[182] to the crystallized atomic coordinates (red, RMSD = 0.31Å).

2.1.3 Frontier orbital energies and densities

Frontier orbital electron densities on molecules provide a useful mean for the detailed characterization of donor-acceptor interactions. It has been shown that these orbitals play a major role in governing many chemical reactions. For example, they can account for the formation of many transfer complexes. The energy of the highest occupied molecular orbital (HOMO) is directly related to the ionization potential and characterizes the susceptibility of the molecule towards an attack by electrophiles. On the other hand, the lowest unoccupied molecular orbital (LUMO) is related with electron affinity, and gives an idea of the susceptibility of the molecule towards nucleophilic attack^[183].

The energies associated with the studied compounds were small, ranging between -0.27 eV and -0.16 eV for HOMO, and between -0.12 eV and -0.01 eV for LUMO, with exception of compound **2.3**. This indicates the fragile nature of bound electrons. Also, the small HOMO-LUMO gap permits electron exchange and transfer, making these compounds very reactive. Further analysis of the LUMOs in Figure 2.2 and Table 2.2 result in the following observations:

- a) Compounds with higher antiplasmodial activity, Table 2.12, are the ones with less negative HOMOs (~ -0.16 eV) and LUMOs (~ -0.01 eV), indicating that the substitutions that affect these energies could have a direct impact on the antiplasmodial activity;
- b) The LUMOs of clopidol and atovaquone show that the 4(1*H*)-pyridone and the quinone moieties are prone to nucleophilic attack, like all the 4-pyridonimine moieties within the most stable diastereomers studied. Interestingly, the LUMO of clopidol has a similar form to that of pyridinium salts^[184], which are also related to the 4-pyridonimines;
- c) The quaternary ammonium salts, where the diethylamino group is either methylated, **2.7** and **2.8**, or protonated, **2.2**, present the LUMOs located in the aryl moiety. The HOMOs show smaller energies, implying the susceptibility to nucleophilic attack in this region;
- d) The most pronounced similarities of the LUMO profile from 4-pyridonimines with clopidol occur when the scaffold presents no substituent, an electron-donor group or a halogen, as is the case of compounds **2.1**, **2.3-6**, **2.10**, **2.15**, and **2.16**;
- e) Non-halogen electron-withdrawing groups, i.e. **2.9**, **2.11**, **2.12** and **2.14**, appear to distort the symmetry observed for the remaining cases;
- f) Compounds **2.13** and **2.17** reveal a near-identical pattern, pinpointing that the side-chain may not be crucial for direct interaction with the active residues within cytochrome *b*. However, it might be essential to induce a correct docking pose within the Q_o site, through hydrophobic interactions, as might occur with atovaquone.

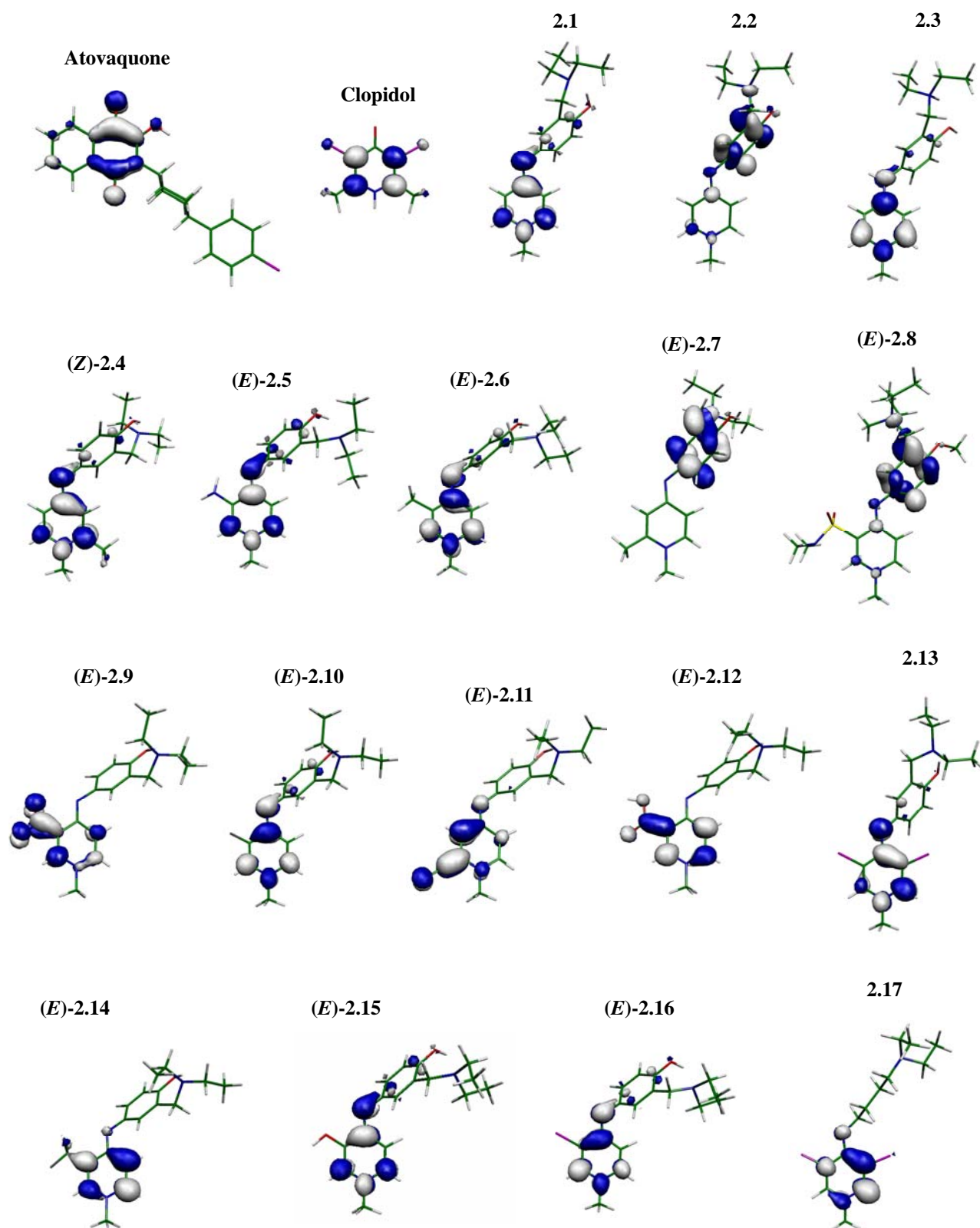


Figure 2.2 LUMOs of atovaquone, clopidol and compounds **2.1-17**.

On the other hand, analyzing HOMOs from Figure 2.3 and Table 2.2 one can see that:

- The energies are considerably lower for known bc_1 complex inhibitors than for the other molecules, except quaternary ammonium salt compounds which present higher values than atovaquone, i.e. **2.2**, **2.3**, (*E*)-**2.7** and (*E*)-**2.8**;
- HOMOs are located mainly at the aryl moiety, whereas in the charged molecules a more scattered pattern is shown, i. e. **2.2**, **2.7** and **2.8**. Further trends are less clear, though the pattern observed for clopidol was reproduced by compound (*E*)-**2.7**;
- The introduction of electron-donors on the 4-pyridonimine moiety results in the increase of the HOMO and LUMO energies.

The HOMO-LUMO gap, i. e., the difference in energy between these two orbitals, is an important kinetic stability index ^[185]. In this study, the energy gap was always higher for clopidol than for 4-pyridonimines, which suggests that these compounds are more reactive than clopidol. In contrast, the energy gap of 4-pyridonimines is higher than that of atovaquone, with the exception of compounds **2.9**, **2.11** and **2.12**. Those molecules contain electron withdrawing groups on the 4-pyridonimine moiety.

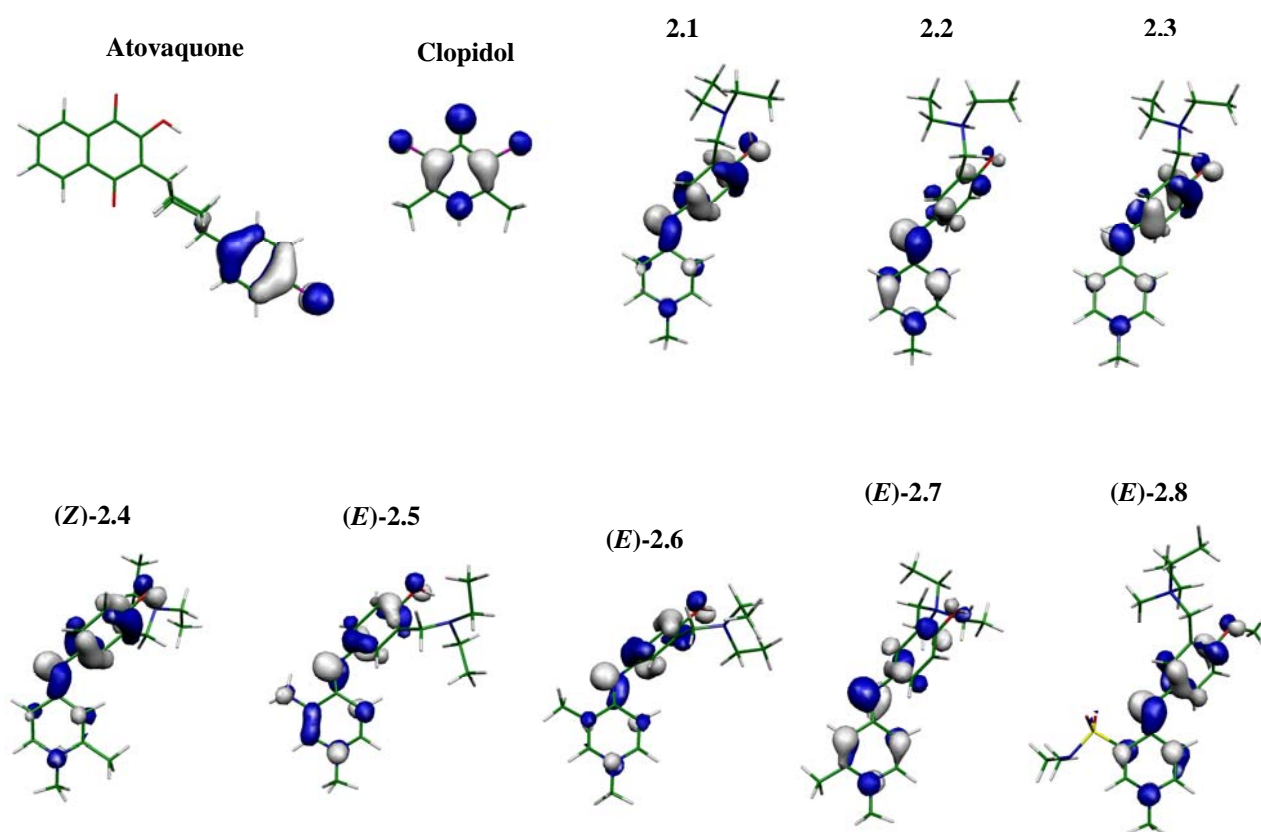


Figure 2.3 HOMOs of atovaquone, clopidol and compounds **2.1-17**.

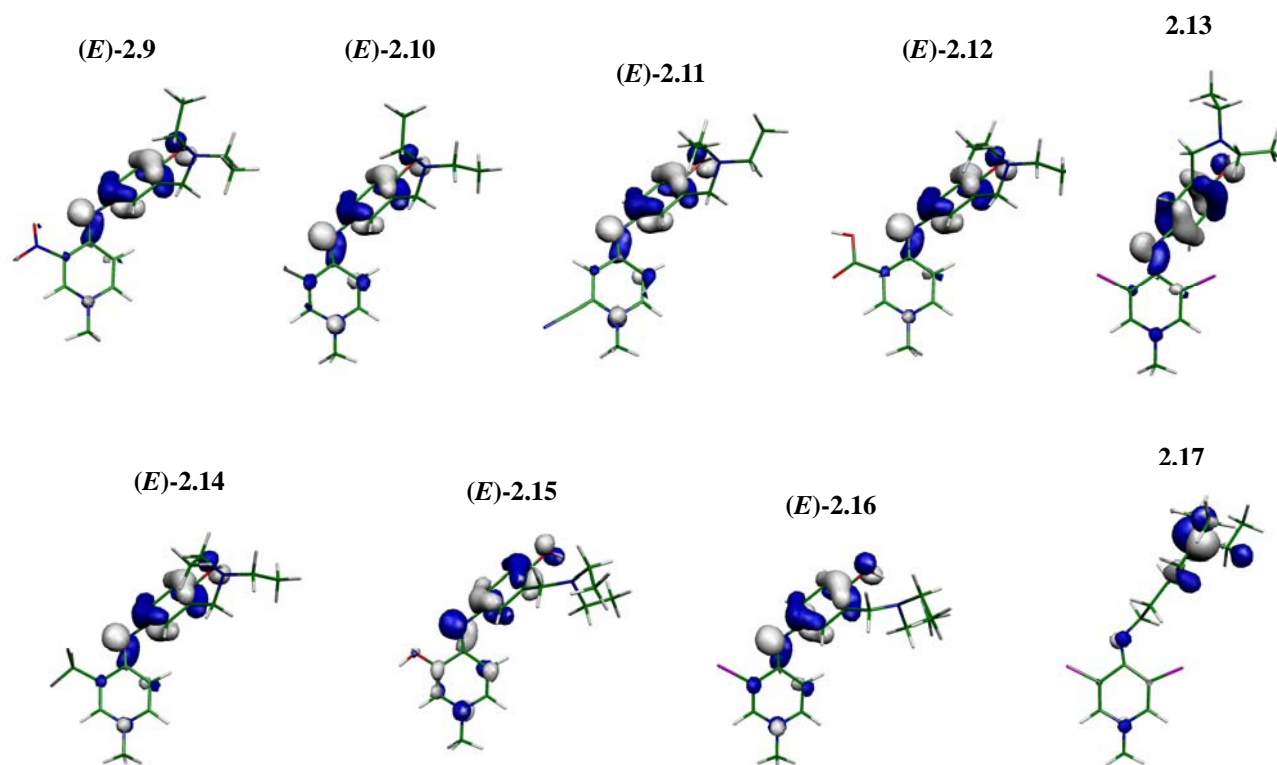


Figure 2.3 (cont.) HOMOs of atovaquone, clopidol and compounds 2.1-17.

2.1.4 Molecular electrostatic potentials (MEP)

Three-dimensional MEPs superimposed onto the total electron density provide useful information for the interpretation of long-range interactions between molecules, which helps to understand how a ligand binds to its receptor. Additionally, they provide useful information on the shape and size of the molecule^[186, 187]. In these colour-coded maps, regions given as red or orange represent areas with high electron density, whereas the blue areas represent electron-poor sites. It is also noteworthy that these MEPs are not static, i.e. interaction of the ligand in the binding pocket might change electron densities of both ligand and protein.

For atovaquone, Figure 2.4, one can observe that the naphthoquinone moiety is highly electron-rich on the oxygen atom areas, which have been described as essential to establish a hydrogen-bond at the Q_o site^[58]. On the other hand, the most negative potential on clopidol and GW844520 is ascribed to the oxygen and nitrogen atoms and, since the electron's distribution is rather different from that of atovaquone, it is expected that these might either interact differently or display a different orientation from atovaquone in the binding pocket.

Regarding the 4-pyridonimines the following observations can be made:

- a) Display either a straight or curled shape, and a very similar electrostatic potential pattern to the one observed for clopidol;
- b) The charge distribution pattern for these compounds suggests that the imine nitrogen atoms may participate in electrostatic interactions or hydrogen bonds;
- c) Every molecule presents two distinct regions: the 4-pyridonimine, which accounts for most of the slight differences observed between the molecules, due to the substitution pattern, and the aryl moiety that displays a very identical electrostatic potential distribution for every case, as long as it is not a quaternary ammonium salt, i.e. **2.2**, **2.3**, **2.7** and **2.8**;
- d) Generally, within the 4-pyridonimine moiety, the most negative potential is on the imine nitrogen, followed by the N1 nitrogen and, as expected, the heterocycle presents a neutral or positive electrostatic potential. This trend is most pronounced for those compounds that have strong electron-withdrawing substituents, i.e. **2.9**, **2.11**, **2.12**, and **2.14**;
- e) Regarding the aryl moiety, the most negative electrostatic potentials are ascribed to the phenolic oxygen and the nitrogen from the diethylamino group, while the aromatic system is mostly given as neutral, except for quaternary ammonium salts. In the latter case, the nitrogen from the diethylamino group presents a less negative or positive potential when compared to neutral molecules, which was expected, as a result of nitrogen quaternization, i.e. **2.2**, **2.3**, **2.7** and **2.8**.

Since all compounds showed the same electrostatic potential range, the 4-pyridonimines have, theoretically, the capability to interact in the active site in a similar way to clopidol and GW844520, as a consequence of their MEP profile identity. A good qualitative correlation between the activity of compounds **2.1**, **2.4**, **2.6-2.8**, Table 2.12, and the MEP profile was found. Charged molecules did not show antiplasmodial activity and displayed a very distinct potential distribution to that of clopidol. Neutral molecules, on the other hand, displayed better activity, probably as a consequence of the better identity of all electron-derived parameters studied here.

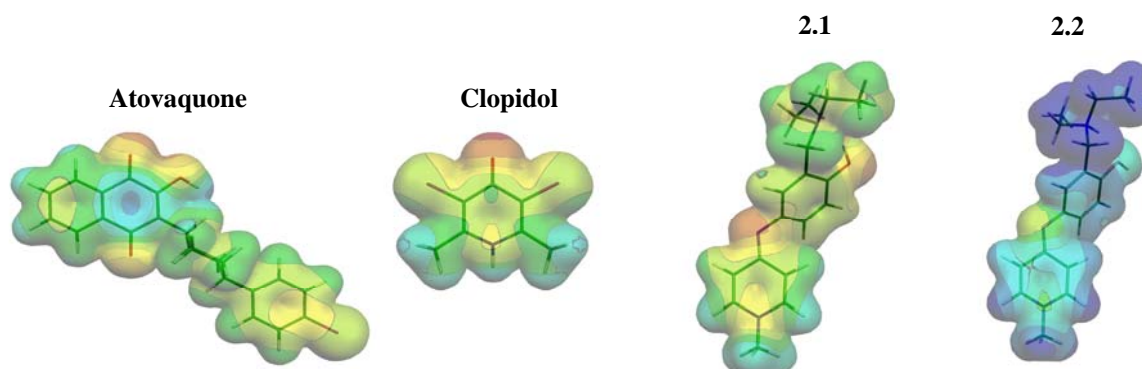


Figure 2.4 MEPs of atovaquone, clopidol, GW844520 and compounds **2.1-17**.

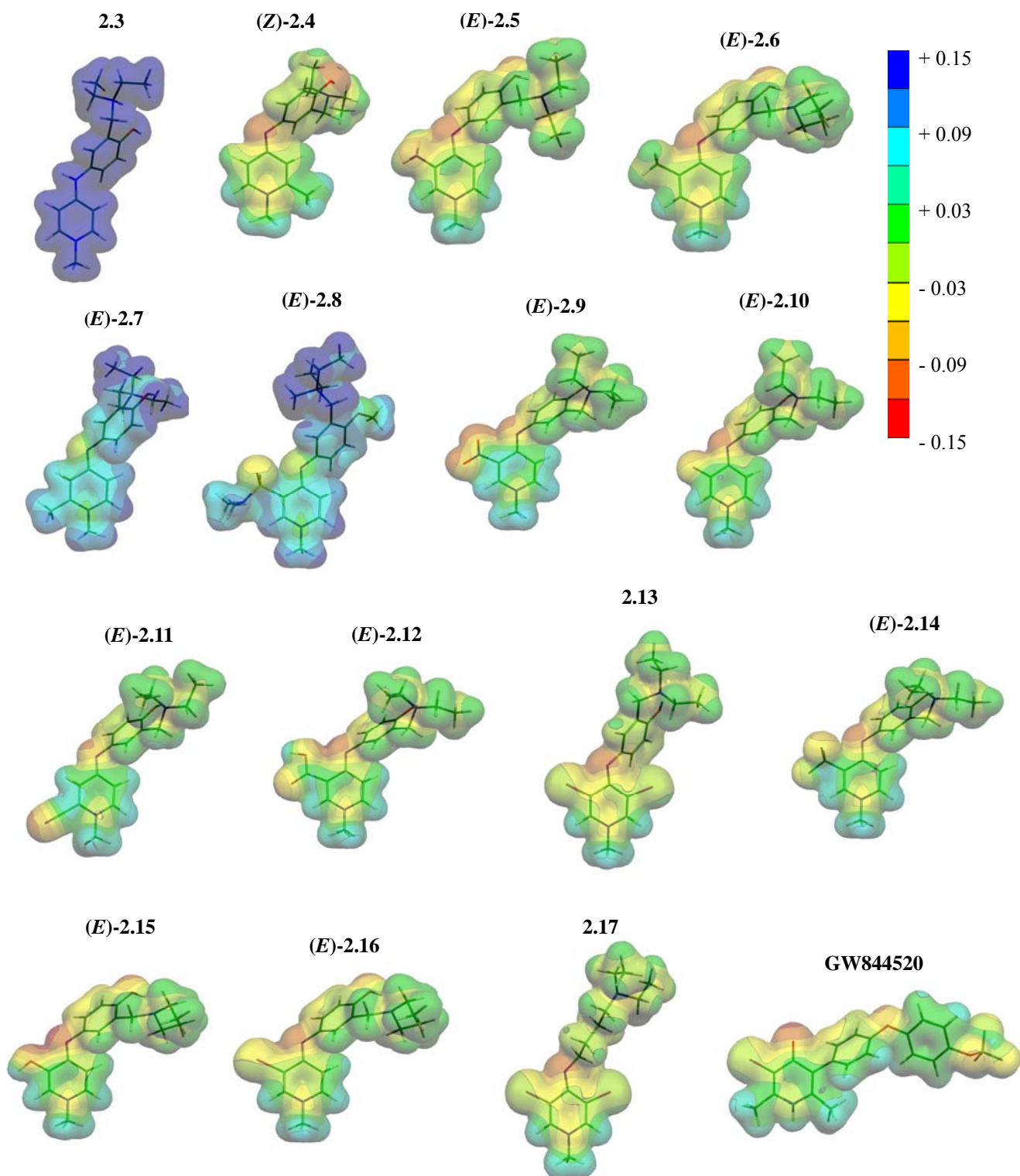


Figure 2.4 (cont.) MEPs of atovaquone, clopidol, GW844520 and compounds 2.1-17.

Finally, clopidol has a dipole moment of 8.48 D, whereas the 4-pyridonimines displayed a magnitude for the dipole moment ranging from 3.00 to 9.78 D. Despite most of the compounds

having a value in the same range as clopidol, between 7.4 and 8.6 D, no correlation with the biological activity of the synthesized Mannich-base 4-pyridonimines was found.

2.2 Molecular docking

2.2.1 Brief overview on molecular docking

Molecular docking of ligands into proteins is playing an increasingly important role in lead discovery and design, regardless of still being far from the goal of accurately predicting complex ligand-receptor interactions. This poses the greatest challenge in modern structure-based drug design, and is mainly due to the difficulty to model, in a reliable way, the protein flexibility, rather than ligand's flexibility^[188-190]. A number of docking programs are available, as well as search algorithms which assess and rationalize the ligand-protein interactions^[191].

GOLD (Genetic Optimisation for Ligand Docking) is a docking program that uses a genetic algorithm to dock flexible ligands into binding sites^[192]. Generally, it applies the concepts of genetic evolution, with each docking solution being encoded as a chromosome. The chromosomes of a population, with all the information about hydrogen bonds, hydrophobic points, etc., are given a score from the fitness to the binding site. These chromosomes are then ranked, in regard to their scores, and the fitter are iteratively optimized, through point mutations and cross-overs^[191]. GOLD offers several scoring functions: GoldScore, ChemScore, ASP and an user defined score. GoldScore^[193] is especially useful in predicting binding poses, and is composited by five components: protein-ligand hydrogen bond energy, protein-ligand van der Waals energy, ligand internal van der Waals energy, ligand torsional strain energy and ligand intramolecular hydrogen bond energy. ChemScore^[194] is derived empirically from measured binding affinities and is best suited to estimate the total free energy changes that occur from ligand binding. It has also been reported that GOLD, despite its good prediction of binding poses, is binding site-dependent and is not as good when the binding is predominantly driven by hydrophobic interactions^[195].

With the aim of optimizing the Mannich-base compounds, a structure-based approach was followed to identify which substituents would better fit the binding pocket. This was carried out in a stepwise trial-error procedure.

2.2.2 *In silico* cytochrome bc_1 model validation

Currently there is no available crystal structure of the bc_1 complex from *P. falciparum*, but a homology model has been reported [20]. To circumvent the lack of crystallized structures of the bc_1 complex from *Plasmodium* species, *Saccharomyces cerevisiae* has been used as surrogate, due to the high sequence identity between its cytochrome b and that of *Plasmodium* [58]. As a result, it has been successfully used to model *in silico* the binding mode of atovaquone to the Q_o site, and to study cytochrome b mutations that confer resistance to atovaquone in *Plasmodium* and *Pneumocystis* [58, 60].

The bc_1 complex co-crystallized with stigmatellin (PDB code: 1KYO [43]) was used for the molecular docking studies. It contains the functional homodimer with the Rieske iron-sulfur protein in close contact with cytochrome b , that is, correctly oriented for electron transport. However, the relatively low resolution of 2.97 Å makes it impossible to predict the position of crystallized waters. More recently, the new structure 3C5X with a resolution of 1.90 Å [44] was published by the same group as 1KYO, and those waters were allocated. However, due to the total superimposition of the two PDB files and the added computational demand to perform docking runs with water molecules, a simpler method without water molecules was kept, despite being reported that their presence results in better predictions [196-198].

The GoldScore and ChemScore algorithms were used in order to validate the docking model. Both performed well, and the pose from the crystallized stigmatellin was reproduced with a RMSD below 1.5 Å, Figure 2.5. This prediction was considered satisfactory as a RMSD of 2.0 Å is commonly considered the cut-off for a good prediction [199]. Moreover, the major differences between the two molecules came from the weakly interacting side chain at the periphery of the binding site.

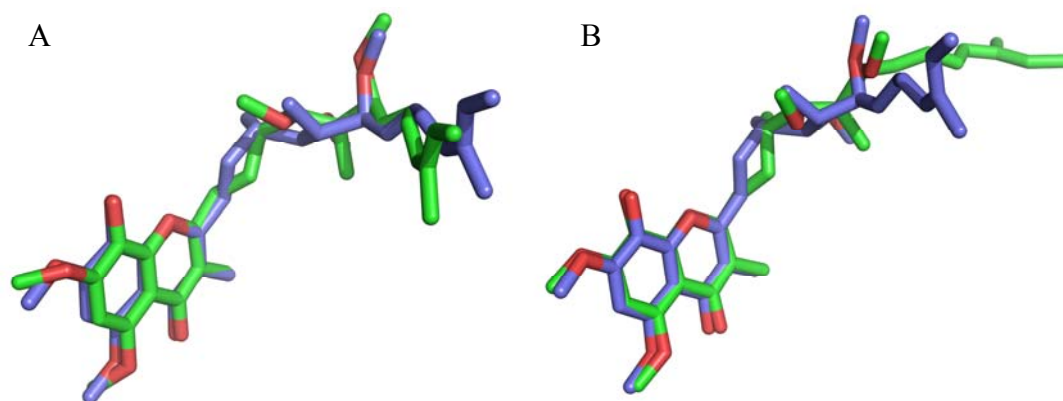


Figure 2.5 Binding poses of stigmatellin. In blue the crystallized structure and in green the docking prediction: (A) ChemScore; (B) GoldScore.

Since the two scoring algorithms performed well, the GoldScore was chosen to carry on with the docking studies due to the better superimposition in the chromone moiety, which is the pharmacophore.

2.2.3 Docking of atovaquone, clopidol, and 2.1 into the active site.

Atovaquone, clopidol and **2.1** were docked into the molecular electrostatic potential of cytochrome *bc*₁ Q_o binding site to identify important binding features, and correlate this information with the one obtained for 4-pyridonimines, Figure 2.6. The figure shows a highly negative binding pocket which becomes less negative or neutral in the hydrophobic channel leading to the Q_o centre. Moreover, a complementarity of the electrostatic potential between cytochrome *bc*₁ and the ligands is highlighted with this study. The positive ring of the naphthoquinone moiety, binds deep into the Q_o site, where the electrostatic potential is most negative, Figure 2.6 A. Also, the hydroxyl group interacts with the positive nitrogen of H181. Conversely, the hydrophobic side chain in atovaquone binds to a near-neutral part of the active site, which might be important to generate an ideal docking pose of the naphthoquinone moiety within the binding pocket. Thus, in addition to crucial hydrogen bonds with the E272 / H181 residues and hydrophobic contact ^[58], the electrostatic interactions might be fundamental for a stabilized Q_o-ligand complex. It is also possible to see that the hydroxyl group is within the distance for a hydrogen bond with H181, and the carbonyl oxygen atom at C4 of the quinone system, is at 3.97 Å of the oxygen atoms of E272, which can accommodate a water-mediated hydrogen bond. These interactions are consistent with another model of the yeast *bc*₁ complex with atovaquone bound in the Q_o binding site and provide further support to the model ^[58].

The docking results for compound **2.1**, Figure 2.6 C (Appendix 1.2 for other compounds), suggest a similar binding mode, with this scaffold complementing the most electronegative vicinity of the Q_o site and the aminophenol side chain, described previously as having a close to neutral electrostatic potential, stabilizing the protein-ligand complex through an hydrophobic interaction in the pocket channel.

Modeling the interaction of clopidol with *bc*₁ complex showed that the highest ranked binding pose presented the carbonyl oxygen atom at 2.41 Å of E272, which is also consistent with a water-mediated hydrogen bond, Figure 2.6 B. In addition, there are only weak van der Waals interactions between the methyl and chlorine groups of clopidol with the active site residues.

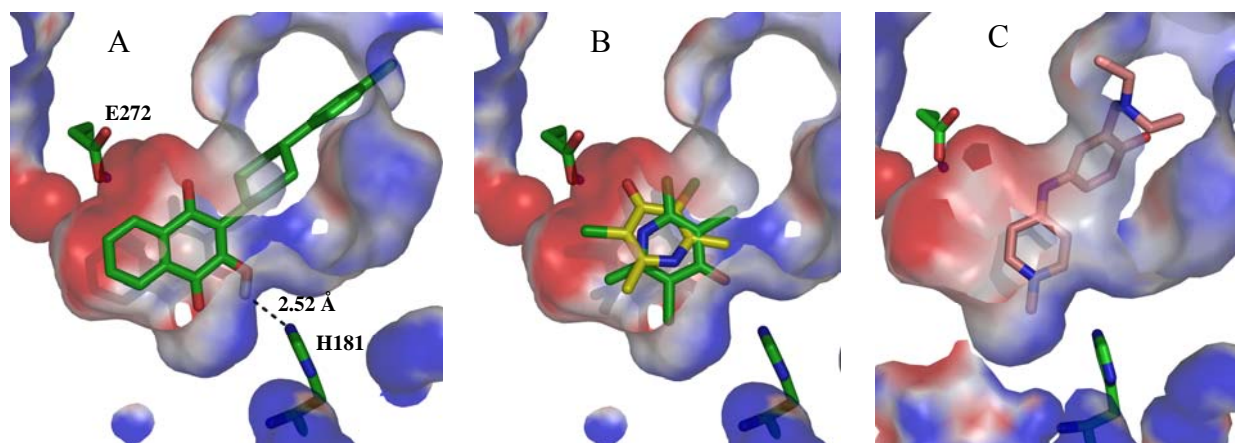


Figure 2.6 Docking poses of (A) atovaquone; (B) clopidol (two possibilities); and (C) **2.1**. The molecular electrostatic potential of the Q_o pocket calculated through the APBS formalism is also displayed: in red the negative potential (dark red is -15 kT/e) and in blue the neutral potential.

2.2.4 *De novo* structure-based design of 4-pyridonimines

With these results in hand it was intended to design a new series of pyridonimines that would better fit in the binding pocket, and present better antiplasmodial activity, consequently. Since it had been shown that the 4-pyridonimines displayed similar electronic properties to GW844520, a potent *bc*₁ complex inhibitor, this compound was first docked into the Q_o site, to understand the key binding interactions that the new series of 4-pyridonimines would have to mimic, Figure 2.7.

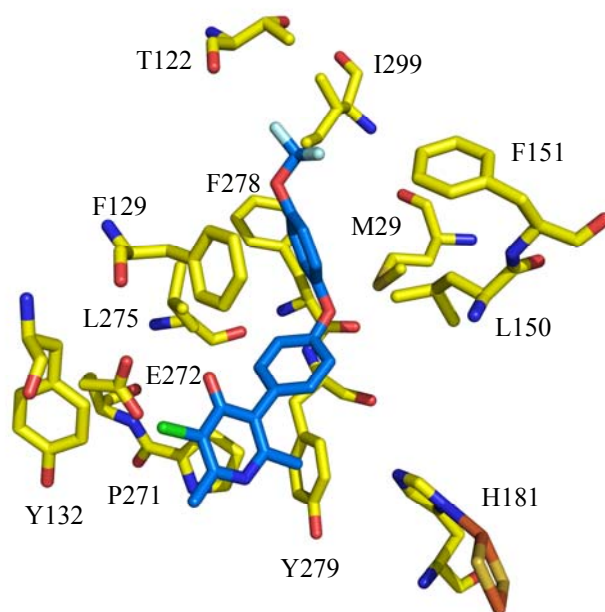


Figure 2.7 Binding mode of GW844520.

Docking in the bc_1 complex revealed that the top ranking solution presented the 4(*H*)-pyridone moiety within the binding site, and the side chain at C5 filling the hydrophobic channel. Enhanced van der Waals contacts between the side chain and P271, Y279, L150, F151, L275, M295 and I299 were observed, indicating that the bulk of the intermolecular interactions are essentially hydrophobic. Also, this compound occupied the whole extension of the binding site, maximizing the hydrophobic contact with the bc_1 complex. Despite the importance of the hydrophobic interactions, it is likely that hydrogen bonds in GW844520 play a role in inhibition. For **2.1** it is not predicted a full interaction in the binding pocket, and the aryl moiety appears not to display an optimal orientation, Figure 2.6 C. Presumably those factors have affected the inhibitory potency of this compound.

Compounds **2.18** and **2.19** were docked to understand if the pose of a quinoline-based compound would improve the hydrophobic contact within the Q_o site, Figure 2.8.

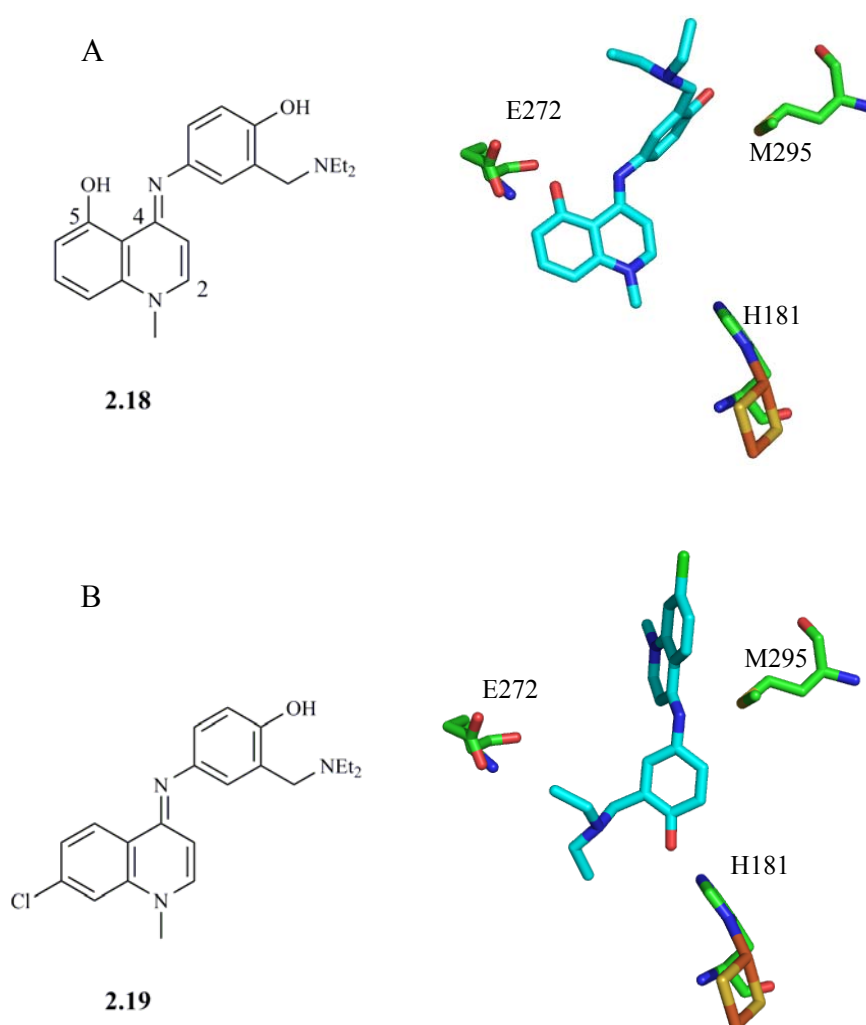
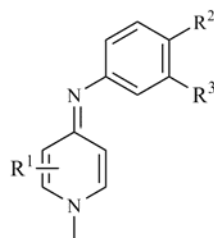


Figure 2.8 Docking pose of (A) **2.18** and (B) **2.19**.

Compound **2.18** displays a hydroxyl group on C5 to maximize binding interactions via hydrogen-bond to E272 residue (2.01 Å) and is also within interaction distance of M295 (1.77 Å). Though, the high torsional strain of the quinoline ring (GoldScore $S_{\text{int}} = -16.43$ for the best fit solution) is responsible for the low fitness value, GoldScore = 44.47. On the other hand, the amodiaquine derivative **2.19** does not display an ideal orientation in the binding pocket, and has an even lower GoldScore (42.43). Thus, quinoline molecules were discarded in this structure-base design approach, since their score was lower than that obtained for **2.1** (46.44).

In a second step of this approach, compounds **2.20-28** were tested, Table 2.4.

Table 2.4 Structures and GoldScores of compounds **2.20-28**.



Compound	R ¹	R ²	R ³	GoldScore
2.20	H	OH	OPh-4-Cl	53.73
2.21	H	OH	SPh-4-Cl	60.87
2.22	H	OH	NHPh-4-Cl	49.74
2.23	H	OH	CH ₂ Ph-4-Cl	57.06
2.24	H	OH	(CH ₂) ₂ Ph-4-Cl	57.59
2.25	H	OPh-4-Cl	OH	49.39
2.26	H	H	(CH ₂) ₂ Ph-4-Cl	61.59
2.27	2-NH ₂	OH	(CH ₂) ₂ Ph-4-Cl	54.88
2.28	2-NH ₂	H	(CH ₂) ₂ Ph-4-Cl	60.98

To optimize the hydrophobic interaction, a second aromatic ring was introduced and several spacers were tested, i.e. **2.20-24**. Moreover, chlorine was introduced at C4 of the terminal aryl to resemble atovaquone. From those compounds, **2.21** presented a better score, but the awkward pose inside the binding pocket, Figure 2.9 C, in addition to the possibility of metabolization into a sulfoxide, led to the rejection of that spacer in further optimizations. Compounds **2.20** and **2.22** displayed low GoldScore fitnesses (53.73 and 49.74, respectively) comparing to **2.23** and **2.24** (57.06 and 57.59, respectively) and were thus not optimized. However, as compound **2.23** is also

expected to be labile, and readily metabolized into a ketone, **2.24** was chosen for further optimization. Therefore, for this type of compounds it was found that the double methylene spacer was the most appropriate, as it led the inhibitor candidate to full occupancy of the active site, Figure 2.9 E. Interestingly, GSK has recently released the structure of *bc*₁ complex inhibitors displaying the same side chain ^[200]. Furthermore, the hydroxyl group appeared to be important in establishing interactions with the binding pocket, either with methionine or histidine residues. However, as the 4-aminophenol moiety may metabolize into a quinoneimine, this set of compounds were also prone to such metabolization, and deplete the human host from glutathione. Thus, compound **2.25** was docked in an isoquine-like approach, but without a good result. Next, compound **2.26** was docked and provided a very good score (61.59). This compound also allowed to conclude that the 4-hydroxyl group would not be essential for a good ligand-protein binding, as the score was higher than for **2.24** (57.59). That was also observed when an amino group was introduced at C2 in the 4-pyridonimine moiety, i.e. **2.27** vs. **2.28**. That substituent was introduced to optimize the ligand interaction with E272, but the best fit result predicted a better interaction with a methionine residue, Figure 2.9 H and I. Thus, as it could also compromise the synthesis of the target compounds, the introduction of a hydrogen donor / acceptor at C2 was abandoned.

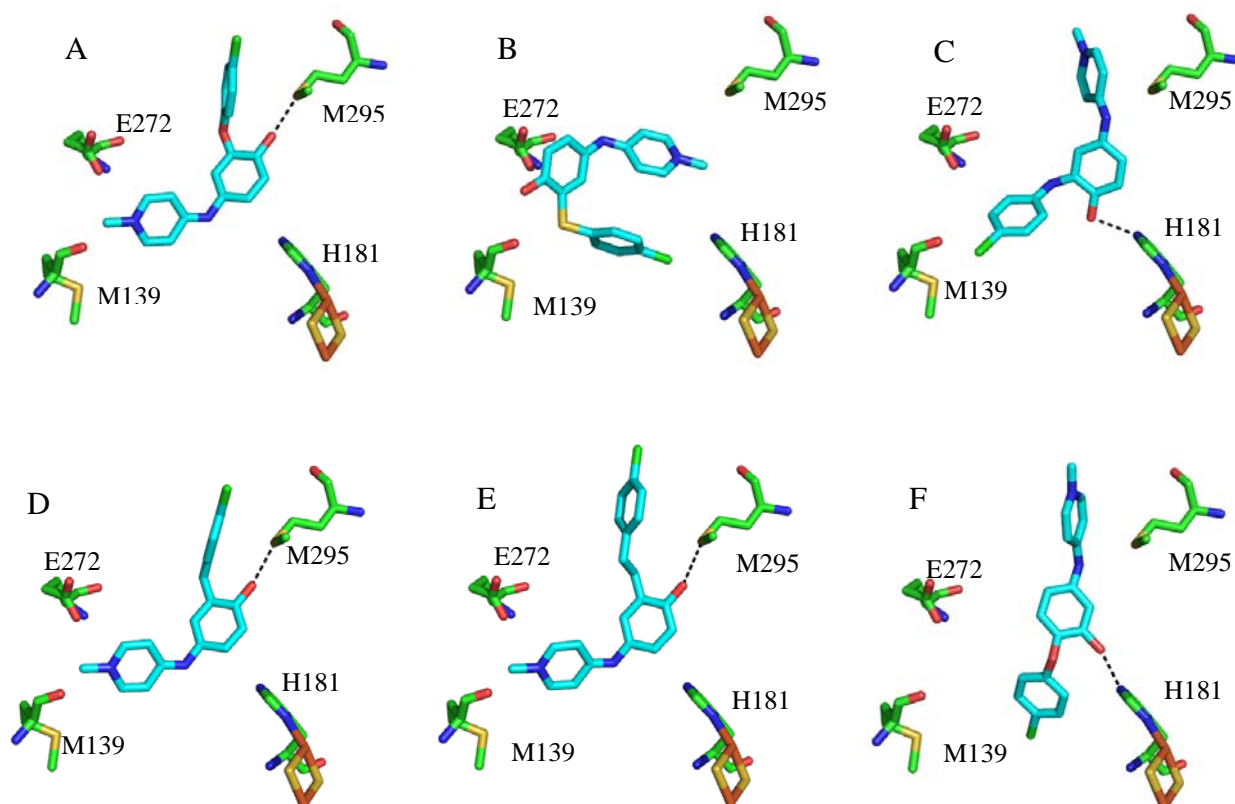


Figure 2.9 Docking poses of (A) **2.20**; (B) **2.21**; (C) **2.22**; (D) **2.23**; (E) **2.24**; (F) **2.25**; (G) **2.26**; (H) **2.27**; (I) **2.28**.

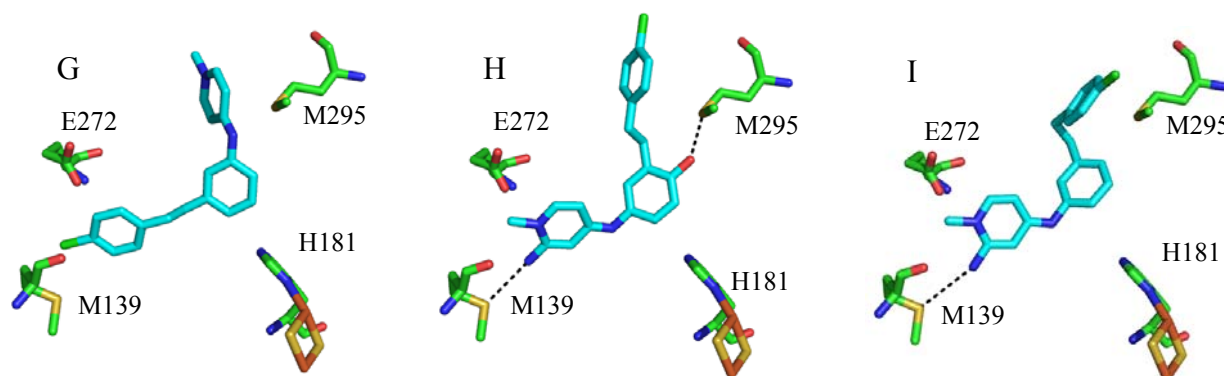
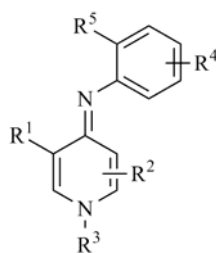
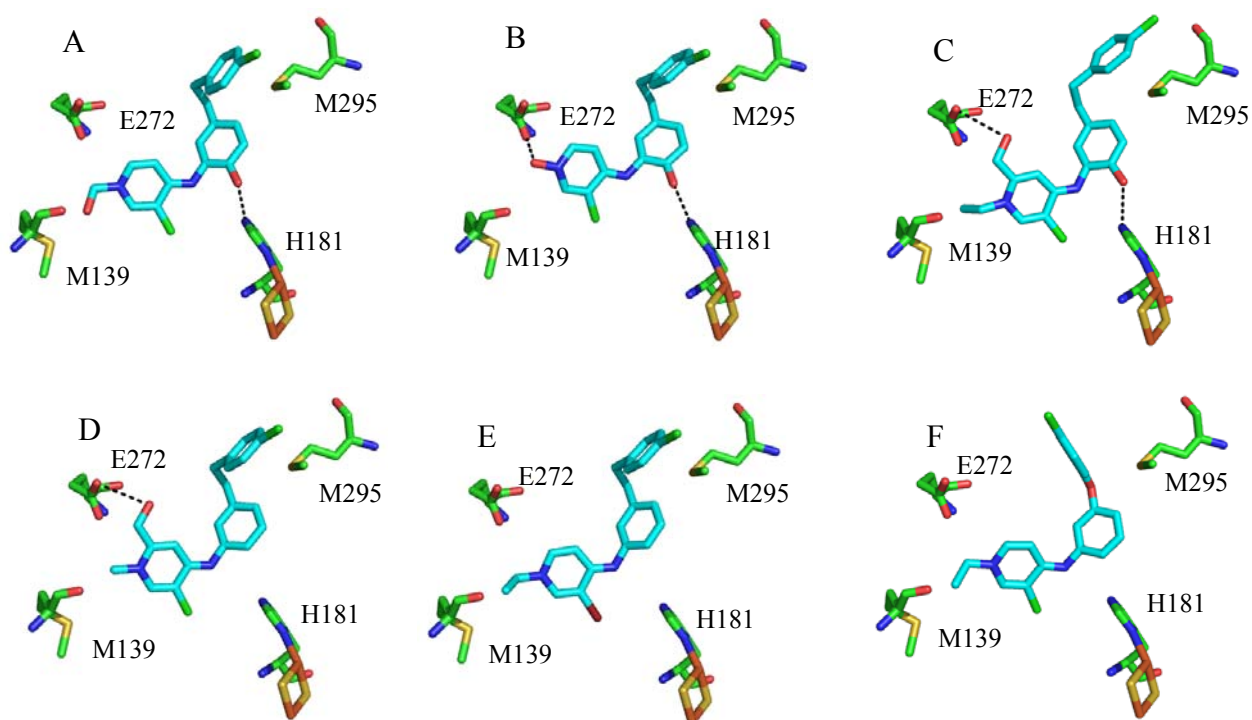


Figure 2.9 (cont.) Docking poses of (A) **2.20**; (B) **2.21**; (C) **2.22**; (D) **2.23**; (E) **2.24**; (F) **2.25**; (G) **2.26**; (H) **2.27**; (I) **2.28**.

As the skeleton for the potentially active compounds had been established, a series of minor changes were made to improve binding to the active pocket. A halogen was introduced at C3 to fit a small pocket in the active site and improved markedly the GoldScores, Table 2.5. In order to increase the possibility of a hydrogen bond with critical aminoacid residues, hydroxymethyl and hydroxyl groups were tested. It was noted that a hydroxyl group at R⁵ could establish a hydrogen bond with H181, Figure 2.10 A-C, whereas a hydroxymethyl group could interact with E272, Figure 2.10 C and D, but the score did not increase, i.e. **2.31** vs. **2.32**. Compound **2.33**, with a 3-Br substituent, gave the best score (68.78). Moreover, two stilbene derivatives were tested, as they would be intermediates in the synthetic pathway, but the rotation constraint given by the double bond did not favour fitting into the active site, i.e. **2.35** and **2.36**, Figure 2.10 G and H. **2.37** displayed a very good GoldScore, but the introduction of a second halogen decreased the score, i.e. **2.37** vs. **2.39**. That should be ascribed to the different orientation of the molecules in the active site and a poorer hydrophobic interaction, Figure 2.10 K and L. The simple substitution of *N*-methyl for *N*-ethyl, i.e. **2.37** vs. **2.38**, also benefited the fitness, as the resulting atom coordinates left the chlorine better accommodated. For 3,5-diCl compounds, **2.39** and **2.40**, this trend was not observed as a result of a different binding pose.

Table 2.5 Structures and GoldScores of compounds **2.29-40**.

Compound	R ¹	R ²	R ³	R ⁴	R ⁵	GoldScore
2.29	Cl	H	CH ₂ OH	3-(CH ₂) ₂ Ph-4-Cl	OH	64.62
2.30	Cl	H	OH	3-(CH ₂) ₂ Ph-4-Cl	OH	61.30
2.31	Cl	6-CH ₂ OH	Et	4-(CH ₂) ₂ Ph-4-Cl	OH	62.59
2.32	Cl	6-CH ₂ OH	Et	3-(CH ₂) ₂ Ph-4-Cl	H	62.72
2.33	Br	H	Et	3-(CH ₂) ₂ Ph-4-Cl	H	68.78
2.34	Cl	H	Et	3-OPh-4-Cl	H	61.71
2.35	Cl	H	Et	3-CHCHPh-4-Cl (<i>Z</i>)	H	38.91
2.36	Cl	H	Et	3-CHCHPh-4-Cl (<i>E</i>)	H	42.98
2.37	Cl	H	Me	3-(CH ₂) ₂ Ph-4-Cl	H	64.83
2.38	Cl	H	Et	3-(CH ₂) ₂ Ph-4-Cl	H	66.46
2.39	Cl	5-Cl	Me	3-(CH ₂) ₂ Ph-4-Cl	H	62.65
2.40	Cl	5-Cl	Et	3-(CH ₂) ₂ Ph-4-Cl	H	61.63

**Figure 2.10** Docking poses of (A) **2.29**; (B) **2.30**; (C) **2.31**; (D) **2.32**; (E) **2.33**; (F) **2.34**; (G) **2.35**; (H) **2.36**; (I) **2.37**; (J) **2.38**; (K) **2.39**; (L) **2.40**.

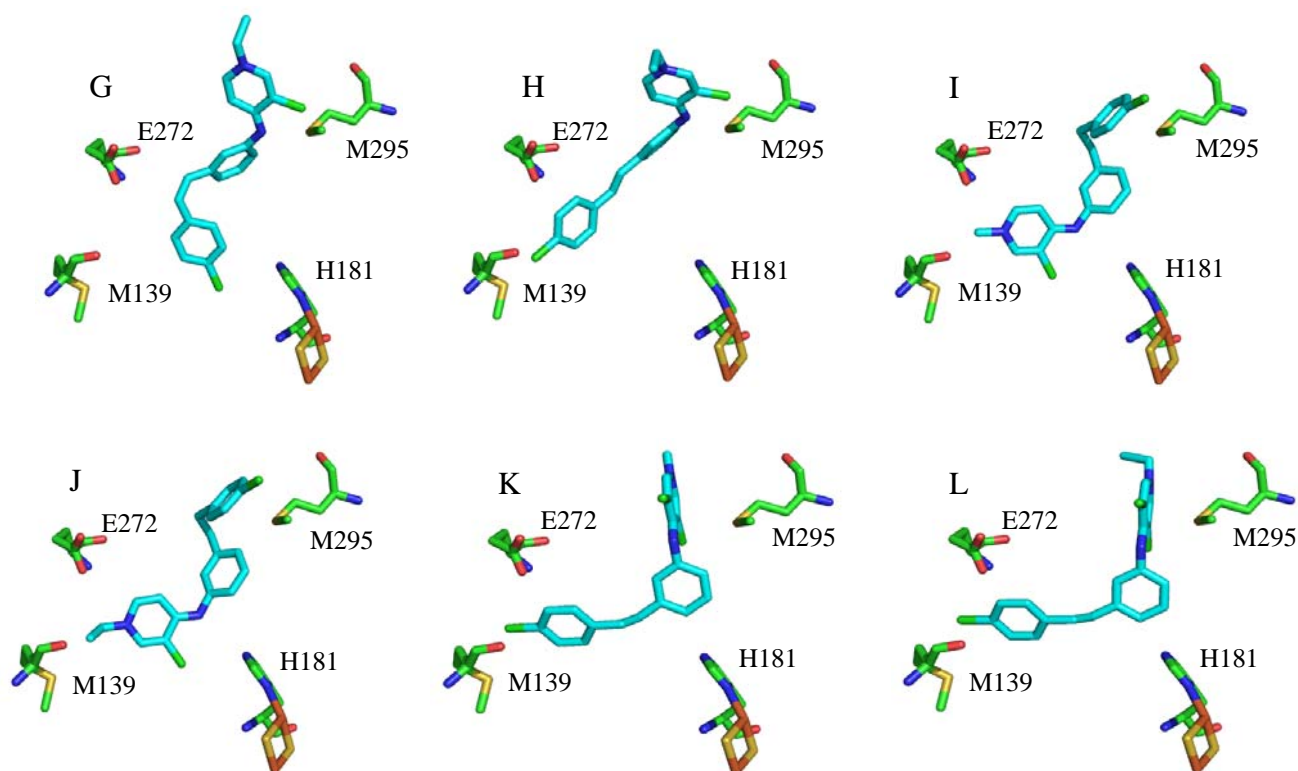


Figure 2.10 (cont.) Docking poses of (A) **2.29**; (B) **2.30**; (C) **2.31**; (D) **2.32**; (E) **2.33**; (F) **2.34**; (G) **2.35**; (H) **2.36**; (I) **2.37**; (J) **2.38**; (K) **2.39**; (L) **2.40**.

Finally, a subset of biphenyl compounds was tested, and the lower GoldScores showed the importance of a spacer between the two aryl moieties, e.g. **2.33** vs. **2.45**, Table 2.6. The best-fit poses are superimposed in Figure 2.11. The GoldScores can be explained on the basis of a lower hydrophobic contact with the binding site, and the higher steric clash with the protein that results from the lack of flexibility in the absence of a spacer.

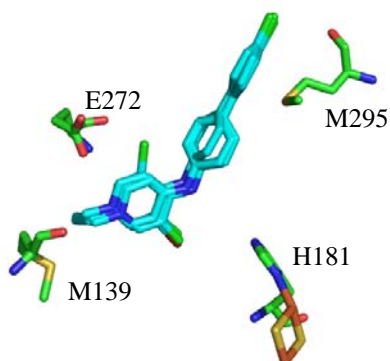
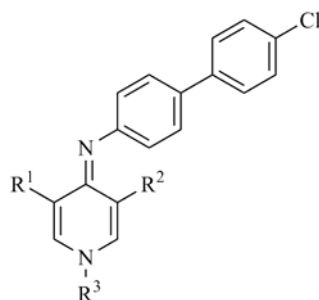


Figure 2.11 Docking poses for compounds **2.41-45**.

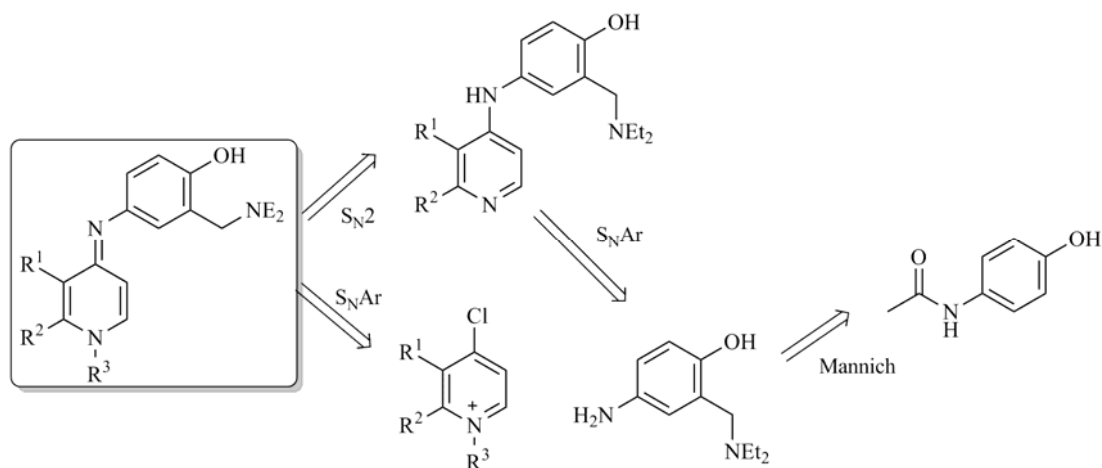
Table 2.6 Structures and GoldScores of compounds **2.41-45**.

Compound	R ¹	R ²	R ³	GoldScore
2.41	H	H	Me	52.31
2.42	H	H	Et	53.17
2.43	Cl	H	Et	57.98
2.44	Cl	Cl	Et	49.37
2.45	Br	H	Et	59.39

2.3 Synthesis

2.3.1 Rationale for Mannich-base 4-pyridonimines

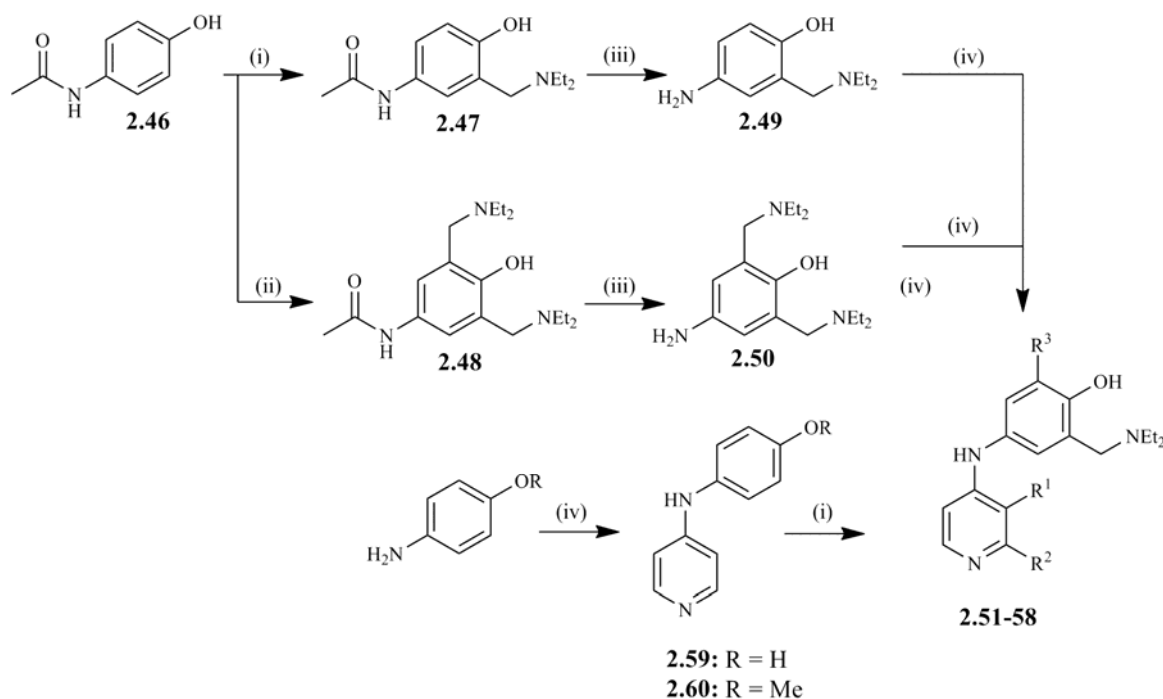
As hypothesized in chapter 1, compounds of substructure **1.169** would present antiplasmodial activity. The inception of such compounds derived from a previous study on amodiaquine-like molecules with potent antiplasmodial activity ^[172]. Therefore, in a first approach, the synthesized compounds would also include the diethylaminophenol side chain. By conserving this side chain it would be possible to assess the applicability of the 4-pyridonimine scaffold as antimalarial leads. It would also allow concluding which substituents on the core scaffold would suit best against *P. falciparum*. The retrosynthetic analysis for Mannich-base derivatives is given in Scheme 2.1.

**Scheme 2.1** Retrosynthetic analysis for Mannich-base derivatives.

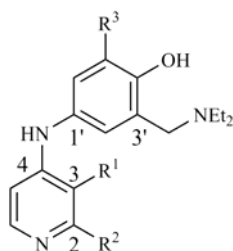
2.3.2 4-Pyridinamines

The synthetic pathway used for the obtention of the first series of compounds was already described in the literature ^[201]. First, the Mannich-base formation was achieved from reaction of paracetamol, **2.46**, with excess *N,N*-diethylamine and aqueous formaldehyde in ethanol, to give acetanilides **2.47** and **2.48**, Scheme 2.2. The desired product **2.47** was isolated in higher yield when the mixture was refluxed for 48 hours. Though, extending the reaction time from 24 to 48 hours resulted in the formation of small amounts of the bis-Mannich side-product, **2.48**. Moreover, the yield of **2.47** decreased as the reaction was further extended from 48 to 72 hours. In contrast, the bis-Mannich product **2.48** was the only product isolated with a reaction time of 72 hours.

The acid hydrolysis of **2.47** and **2.48** afforded the corresponding anilines **2.49** and **2.50** in near quantitative yields, which were used for the synthesis of compounds **2.51-58**, Table 2.7 and Scheme 2.2. Compounds **2.51-58** were obtained with yields, ranging from 11-89%. Compound **2.56** was obtained with 89% of theoretical mass, which can be explained with the electron withdrawing nature of the sulfonamide, favouring the aromatic nucleophilic substitution (S_NAr).



Scheme 2.2 Synthesis of pyridin-4-amines **2.51-58**. Reagents and conditions: (i) DEA, CH_2O , EtOH, reflux 24h (ii) DEA, CH_2O , EtOH, reflux 48-72h (iii) HCl 6N, reflux overnight (iv) 4-chloropyridine, EtOH, reflux.

Table 2.7 Synthesis of key intermediates **2.51-58**.

Compound	R ¹	R ²	R ³	Yield (%)
2.51	H	H	H	41
2.52	Me	H	H	54
2.53	NH ₂	H	H	76
2.54	NO ₂	H	H	0
2.55	H	Me	H	77
2.56	SO ₂ NH ₂	H	H	89
2.57	H	H	CH ₂ NEt ₂	16
2.58	Me	H	CH ₂ NEt ₂	11

With the aim of optimizing the S_NAr step, several reactions were carried out between 4-chloropyridine and 4-aminophenol, at different molar ratios, to synthesize **2.59**. This resulted in an increase of yield from 41% to 80%, Scheme 2.2 and Table 2.8. As can be seen from Table 2.8, increasing the aminophenol / chloropyridine molar ratio from 1 to 3 led to a significant increase in yield and reduction in the reaction time.

Table 2.8 Reaction conditions for the S_NAr reactions and synthesis of **2.59**.

Method	Aminophenol mol. eq.	Pyridine mol. eq.	Reaction time	Flash Chromatography	Yield (%)
A	1.4	1	reflux/16 h	CH ₂ Cl ₂ :MeOH (4:1)	41
B	3	1	reflux/2 h	CH ₂ Cl ₂ :MeOH (4:1)	54
C	3	1	reflux/4.5 h	CH ₂ Cl ₂ :MeOH (9:1)	80

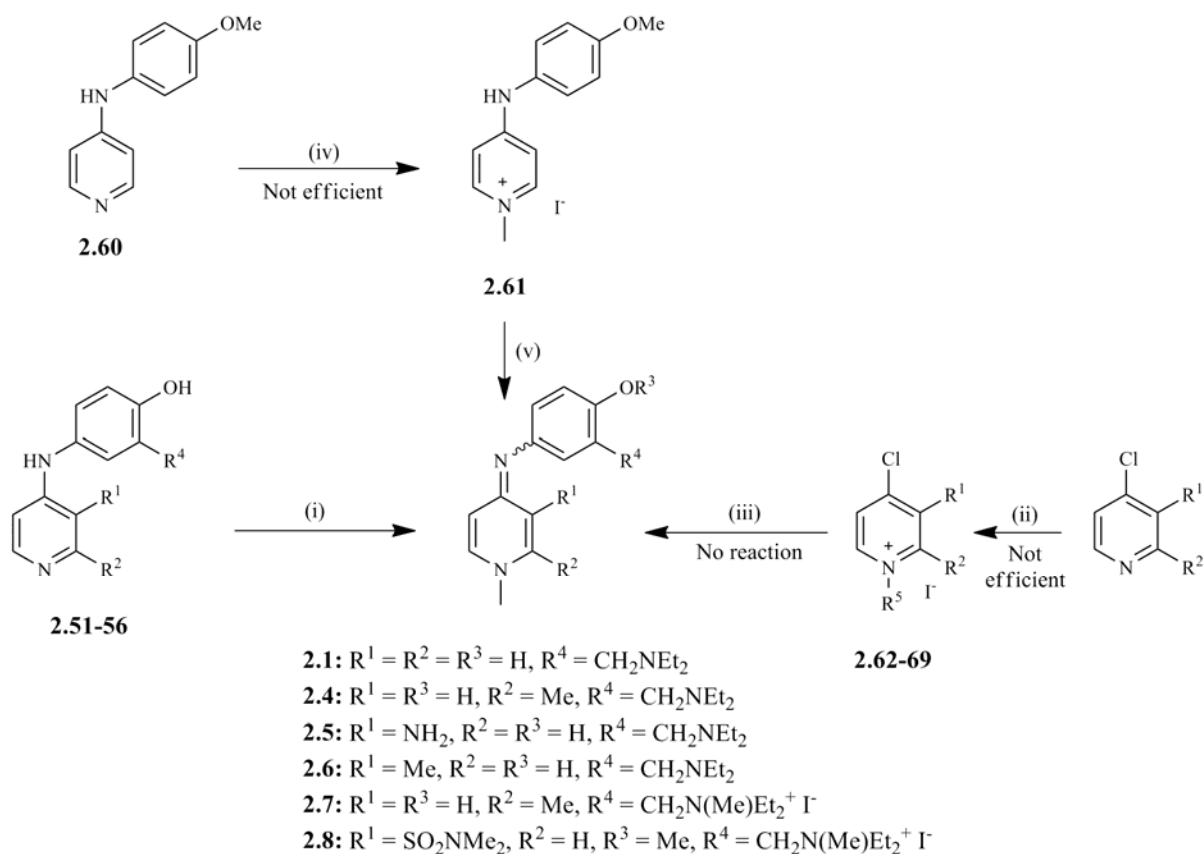
Compound **2.59** was also subjected to Mannich reaction and **2.51** was obtained in 65% yield. Despite the better overall yield and a shorter synthetic pathway, this was not the general approach followed because **2.47** and **2.49** could be synthesized in a very large scale, reducing the overall time consumed.

All 4-pyridinamines were characterized through common spectroscopic methods, including 1D and 2D NMR techniques, mass spectrometry and infra-red spectroscopy (IR). From inspection of the ^1H -NMR spectrum of **2.51**, it is possible to see that protons at C2 are the most deshielded protons, $\delta = 8.23$ ppm, and appear as a doublet, $^3J = 4.8$ Hz. This is a common coupling constant between C2-*H* and C3-*H* for pyridines, and results from the sp^2 hybridization of the nitrogen atom. On the other hand, the proton at C3 is comparatively less deshielded, $\delta = 6.63$ ppm. The remaining three protons, from the aromatic moiety, can be found between $\delta 6.81$ and $\delta 7.03$ ppm, whereas the amine proton is located at $\delta 5.83$ ppm, as a broad singlet. Further inspection of the spectrum reveals the aliphatic protons at higher field. Regarding the ^{13}C -NMR spectrum, nine aromatic carbons were found, five of which are CH, from DEPT analysis. HMQC was also performed and the CH carbons assigned on the basis of this spectrum.

2.3.3 4-Pyridonimines

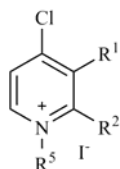
For the synthesis of compounds **2.1** and **2.4-8**, distinct pathways were followed, taking into account methods already described in the literature by Lopes *et al.* and Schock^[172, 202]. These are schematized in Scheme 2.3.

One of the pathways consisted of synthesizing a quaternary ammonium salt, **2.62-69**, from the starting material, and proceed afterwards to the aromatic nucleophilic substitution reaction with 4-amino-2-(diethylaminomethyl)phenol. This is a logical pathway, since the C4 at the pyridinium salt is activated towards nucleophilic substitution. Several methods to synthesize compounds **2.62-69** were attempted, but the chloro atom at C4 appears to deactivate *N*-alkylation because of its electron withdrawing nature. Hence, the poor nucleophilic pyridinic nitrogen made the methylation of both 4-chloro-3-pyridinesulfonamide and 4-chloro-3-nitropyridine impossible, which were further deactivated by their C3 substituents. Another reason for the low reactivity was the poor solubility of the starting materials. The only two pyridines that were efficiently alkylated through this pathway were the ones that gave **2.62**, **2.64** and **2.67**, Table 2.9. The structural identification of pyridinium salts was based on ^1H -NMR, which showed a characteristic singlet at $\delta 4.2$ ppm, assigned to *N-CH*₃. Given the difficulty of *N*-alkylation for this set of 4-chloropyridines, and the unanticipated failed reaction of **2.62**, **2.64**, **2.67** with **2.49**, to give any of compounds **2.1** and **2.4-8**, only the *N*-alkylation of 4-pyridinamines **2.51-56** was pursued, Scheme 2.3.



Scheme 2.3 Synthetic pathway to compounds **2.1** and **2.4-8**. Reagents and conditions: (i) a) dry THF or DMF, NaH, rt b) MeI; (ii) dry THF, alkyl iodide, rt or reflux; (iii) EtOH, **2.49**, reflux; (iv) DMF, MeI; (v) NaOH, rt.

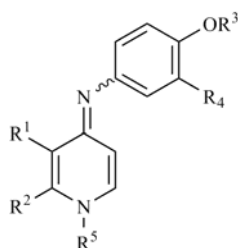
Table 2.9 Synthesis of compounds **2.62-69**.



Compound	R ¹	R ²	R ⁵	Yield (%)
2.62	H	H	Me	59
2.63	SO ₂ NMe ₂	H	Me	0
2.64	NH ₂	H	Me	68
2.65	H	Me	Me	0
2.66	NO ₂	H	Me	0
2.67	NH ₂	H	Et	44
2.68	H	H	Et	0
2.69	H	Me	Et	0

This pathway was a successful route to the required 4-pyridonimines, which were obtained with moderate to good yields, Table 2.10. This had already been described by Lopes *et al.* [172], who had made use of a strong base to deprotonate the substrate and increase the nucleophilicity of the pyridinic nitrogen. In the present case, the resulting anion was then reacted with methyl iodide at room temperature in a S_N2 type reaction. The pK_a values of the relevant functional groups within **2.51-56** range between 18.7 and 20.2 for the aniline and is *ca.* 10.5 for the phenol [181, 203-208] which made it difficult to predict the anion that formed first, while using NaH as a base. However, the absence of reaction at the phenol reflects either (i) the steric hindrance exerted by the diethylaminomethyl neighbouring group or, (ii) the preservation of an intramolecular hydrogen bond between the phenol and the dimethoxyaminomethyl moiety. The only exception was **2.56**, which might be the result of a competing hydrogen bond between the phenol and the sulfonamide with the nitrogen from the diethylaminomethyl group. It was also noted that changing the solvent from THF to DMF was crucial to obtain the required compounds in acceptable yields (Experimental Section for a full list of method variations).

Table 2.10 Synthesis of compounds **2.1** and **2.4-8**.



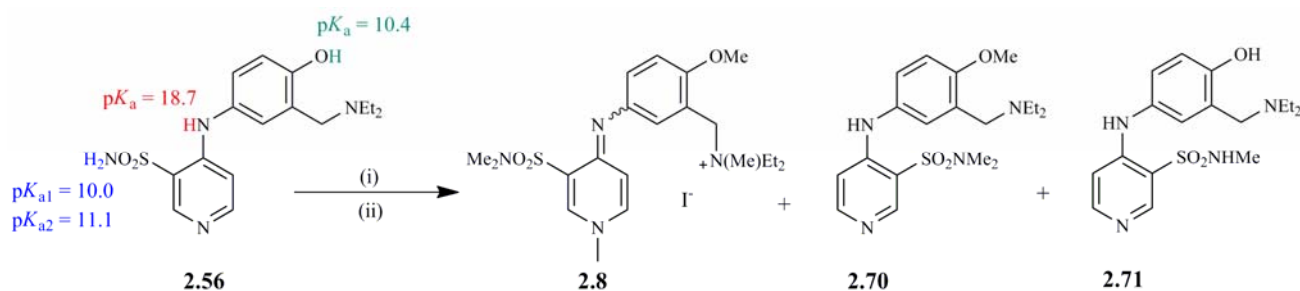
Compound	R ¹	R ²	R ³	R ⁴	R ⁵	Yield (%)
2.1	H	H	H	CH ₂ NEt ₂	Me	59
2.4	H	Me	H	CH ₂ NEt ₂	Me	66
2.5	NH ₂	H	H	CH ₂ NEt ₂	Me	0
2.6	Me	H	H	CH ₂ NEt ₂	Me	73
2.7	H	Me	H	CH ₂ N(Me)Et ₂ ⁺ I ⁻	Me	25
2.8	SO ₂ NMe ₂	H	Me	CH ₂ N(Me)Et ₂ ⁺ I ⁻	Me	36

In an attempt to make a sole methylation of **2.56** and understand its reactivity, the synthesis was repeated varying the molar equivalents of both sodium hydride and methyl iodide. Given the high pK_a value of the NaH, and the inexistence of regioselectivity in the methylation reaction, several products were formed and an untractable mixture resulted, in reactions with less than three molar

equivalents of both reagents, Table 2.11. The most acidic hydrogen appeared to be either the phenolic or the sulfonamide's, since **2.70** and **2.71** were isolated, depending on the reaction conditions. This observation reinforced the possibility of a hydrogen bond competition, and is also in agreement with the predicted pK_a values for the ionizable functions within **2.56** [181].

As the molar equivalents were increased, more of compound **2.8** formed, and this was the only compound isolated, from these starting materials, with the required 4-pyridonimine scaffold, Table 2.11. It was also possible to observe that DMF is the solvent best suited for this reaction, due to a better dissolution of the **2.56** starting material. This set of reactions also showed that compound **2.8** can be obtained in a clean reaction, when the base and alkylating agent are employed in great excess. Also, a significant difference can be observed between the methods that use 6 and 6.7 molar equivalents of the reagents. Whereas in the first case **2.8** can only be obtained in 6% yield, in the second, its value is 6-fold higher.

Table 2.11 Yields of the several species isolated from the alkylation of **2.56**.



Reaction Conditions	2.8	2.70	2.71
(i) NaH, THF (1.2 mol eq.)	N.I.	N.I.	N.I.
(ii) MeI (2 mol eq.)			
(i) NaH, DMF (3 mol eq.)	N.I.	N.I.	2%
(ii) MeI (3 mol eq.)			
(i) NaH, THF (3 mol eq.)	N.I.	N.I.	N.I.
(ii) MeI (6 mol eq.)			
(i) NaH, DMF (4 mol eq.)	4%	10%	N.I.
(ii) MeI (4 mol eq.)			
(i) NaH, DMF (6 mol eq.)	6%	4%	N.I.
(ii) MeI (6 mol eq.)			
(i) NaH, DMF (6.7 mol eq.)	36%	N.I.	N.I.
(ii) MeI (6.7 mol eq.)			

N.I. – Not isolated

Compounds **2.1** and **2.4-8** were identified on the basis of spectroscopic data, including 1D and 2D NMR techniques, mass spectrometry, IR and elemental analysis. Compound **2.8** was also characterized through X-Ray crystallography.

The $^1\text{H-NMR}$ spectra of these compounds feature a common singlet at *ca* δ 3.9-4.1 ppm assigned to *N-CH*₃. Further confirmation comes from the different coupling constants seen for the 4-pyridinamine and the 4-pyridonimine moieties. In these compounds, the coupling constant increases dramatically; $^3J = 7.2$ Hz for *Ar-H2* in **2.1**, whereas the **2.51** precursor has $^3J = 4.8$ Hz for *Ar-H2*. This was already observed by Lopes *et al* [172] and reflects the change in the nitrogen hybridization [209]. Also, 2D NOESY confirmed the correlation between the *Ar-H2* and the methyl group at the pyridyl nitrogen.

For the quaternary ammonium salts **2.7** and **2.8**, structural confirmation arrived from both COSY and NOESY spectra. Coupling of the δ 1.45 ppm signal to the multiplet at δ 3.34-3.56 ppm, and the presence of a singlet at δ 3.00 ppm for **2.8** confirmed the existence of a pro-chiral centre. Therefore, the protons from the diethylamino methylene group are non-equivalent. Each of these protons presents a doublet of quadruplets, due to geminal coupling ($^2J = 14.2$ Hz) and vicinal coupling ($^3J = 7.2$ Hz). The singlet at δ 3.04 ppm corresponds to the two methyl groups of the sulfonamide, whereas the singlet at δ 4.59 ppm is assigned to the methylene between the aromatic ring and the quaternary ammonium salt. These two protons are highly deshielded, because of the positive charge of the neighbouring amine, and the anisotropic effect exerted by the anisole ring. On the other hand, 2D NOESY confirmed the correlation between the *Ar-H2* and the methyl group at the pyridyl nitrogen (δ 4.10 ppm).

This series of compounds underwent very extensive fragmentation when electronic impact (EI) was used to obtain the spectra. Thus, fast atom bombardment (FAB) was preferred, as it is a “softer” ionization technique. Typically, the molecular ion itself is usually not seen, but an adduct ion, such as $[\text{M}+\text{H}]^+$, is prominent. The fragmentation pattern for the 4-pyridonimines is identical to the one that was observed for the 4-pyridinamines. The fragment that results from breaking the bond between the isolated methylene group and the nitrogen from the diethylamino moiety yields the most abundant ion, after the base peak, which is observed at $m/z = [\text{M}+\text{H}]^+$.

As for the IR spectrum, a broad stretching vibration at *ca.* 3300 cm^{-1} is informative of the presence of a phenol group, just like in its precursors. In addition, the C=N linkage results in absorption at *ca.* 1650 cm^{-1} , as a consequence of stretching vibrations.

Up to this point, there was spectroscopy data revealing the linkage of the methyl group to the pyridinic nitrogen. However, since there was a step in the reaction that involved the formation of an

anion, it was not known whether the final reaction product consisted of a sole isomer, i.e. (*Z*) or (*E*), or a mixture of diastereomers. To assess the outcome of the reactions, compound **2.8** was slowly crystallized from a mixture of water and acetone, affording crystals suitable for X-Ray analysis, which were analysed at the University of Santiago Compostela.

From this study it was possible to see that only the (*E*) isomer of **2.8** was obtained, Appendix 1.3. The same observation had been made in a study with amodiaquine analogues by Lopes *et al.* [172]. Also, there were two symmetry independent molecules, in the asymmetric unit, with no significant differences in bond lengths and angles. The observed imine bond distances C4-N14 and C44-N54 were longer than expected by *ca.* 0.035 Å, as a consequence of the imine group being protonated. This is consistent with imminium salts described elsewhere [210, 211]. The aromatic rings were also not coplanar with the 4-pyridonimine groups, as was indicated by the C4-N14-C15-C16 and C44-N54-C55-C56 dihedral angles of 47.7(7)° and 132.6(5)° respectively. The molecules were hydrogen-bonded through the imine nitrogen atoms at N14 and N54, acting as donors towards the sulfonyl oxygen atoms O9 and O19 of their respective sulfonamide moieties. Furthermore, the 4-pyridonimine scaffold was nearly planar, and the C5-C4-N14-C15 dihedral angle was 7.9(7)° for one of the molecules, whereas the C43-C44-N54-C55 dihedral angle on the other molecule was -14.1(7)°, Figure 2.12.

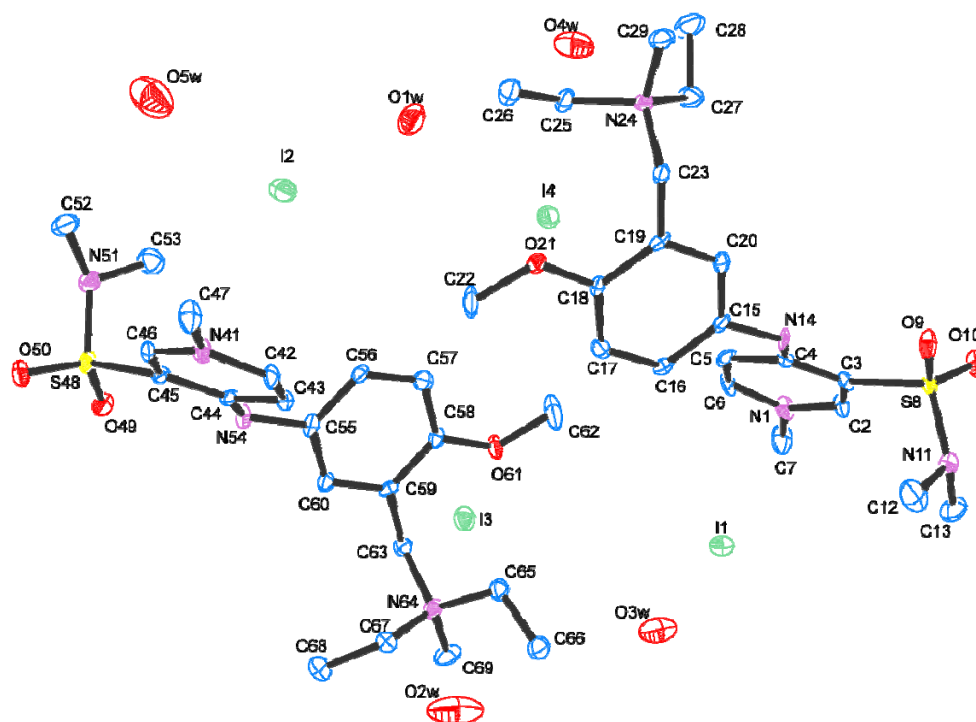


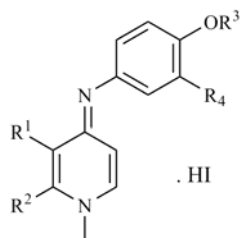
Figure 2.12 ORTEP view of the molecular structure of **2.8**, showing the labelling of all non-hydrogen atoms. Displacement ellipsoids for non-hydrogen atoms are shown at the 50% probability level. Hydrogen atoms have been omitted for clarity.

Antiplasmodial activity

All compounds **2.1**, **2.4** and **2.6-8** were tested *in vitro* against the chloroquine-resistant W2 and atovaquone-resistant FCR3 *P. falciparum* strains. These studies were carried out at the University of California, San Francisco. All figures are the mean of at least three measurements, and the experiments were carried out as described by Semenov *et al.* [212]. For this series, all compounds were in its hydroiodide salt form, and were tested as such, Table 2.12. The following trends on the SAR were observed:

- Derivative **2.1** presented IC₅₀ values of 8.6 and 7.9 μM against the W2 and FCR3 strains, respectively, that are close to those of clopidol, 9.7 and 3.4 μM, respectively;
- Incorporation of a methyl group at C3 of the 4-pyridonimine moiety, i.e. **2.6**, led to a significant decrease in antiplasmodial activity when compared to the parent **2.1**. However, a methyl group at C2, i.e. **2.4**, led to a decrease in activity against the W2 strain, but not against the FCR3 strain;
- Compounds with cationic side chains, i.e. **2.7** and **2.8**, were inactive against the W2 strain, but were more active against the FCR3 strain.

Table 2.12 Antiplasmodial activity of 4-pyridonimines containing a Mannich-base side chain, **2.1**, **2.4** and **2.6-8**.



Compd	R ¹	R ²	R ³	R ⁴	IC ₅₀ (μM)	
					W2	FCR3
2.1	H	H	H	CH ₂ NEt ₂	8.61 ± 0.41	7.90 ± 0.24
2.4	H	Me	H	CH ₂ NEt ₂	20.7 ± 1.7	8.09 ± 0.44
2.6	Me	H	H	CH ₂ NEt ₂	33.0 ± 0.7	> 10
2.7	H	Me	H	CH ₂ N(Me)Et ₂ ⁺ I ⁻	> 50	9.86 ± 0.28
2.8	SO ₂ NMe ₂	H	Me	CH ₂ N(Me)Et ₂ ⁺ I ⁻	> 50	> 10
Clopidol					9.73 ± 0.07	3.37 ± 0.19
Atovaquone					0.0012	1.89 ± 0.10
Cloroquine					0.052	0.051
GW844520					0.030 ^a	

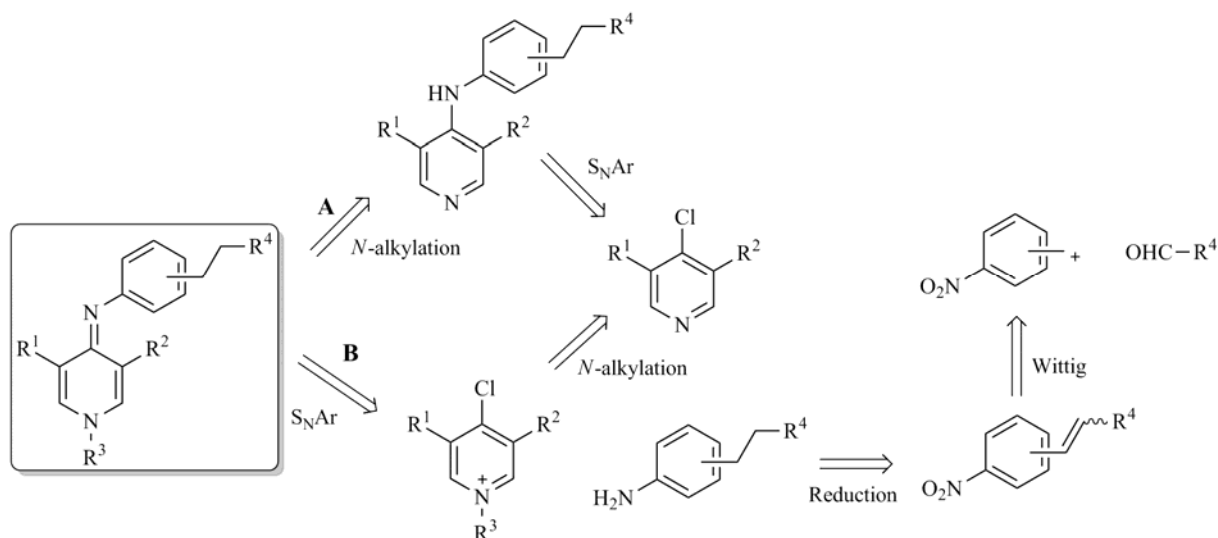
^aT9-96 strain [19].

It is also noteworthy that the antiplasmodial activity might be related, at least in part, to the inhibition of heme polymerization, since these compounds are associated to amodiaquine [213].

These compounds were also tested against the *Pf*NDH2 complex at the Liverpool School of Tropical Medicine, but showed no inhibitory activity.

2.3.4 Rationale for structure-based 4-pyridonimines

The docking studies that were presented revealed that the best potential antiplasmodial compounds would feature two aryl moieties spaced by two methylene groups, with the terminal phenyl harbouring an electron-withdrawing group. In Scheme 2.4 the retrosynthetic analysis of those 4-pyridonimines is presented. These compounds can be obtained through alkylation of the corresponding 4-pyridinamines, as was presented for the Mannich-base series (A). Alternatively, *N*-alkylation of 4-chloropyridines can precede and activate S_NAr (B). In both cases anilines can be obtained from the reduction of nitrostilbenes, which are in turn synthesized through Wittig chemistry.



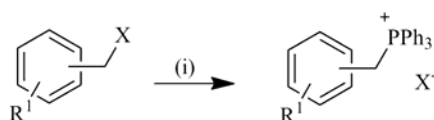
Scheme 2.4 Retrosynthetic analysis of target 4-pyridonimines.

2.3.5 Intermediates for structure-base 4-pyridonimines

Nitrostilbenes

Nitrostilbenes were synthesized via Wittig chemistry, using appropriate aldehydes and phosphonium salts. Phosphonium salts were obtained as referred in the literature [214] from several

benzyl halides, Scheme 2.5. The yields ranged from moderate to excellent, when chlorine and bromine were the leaving groups, respectively, after reacting for the same period of time, Table 2.13. These intermediates were easily identified by $^1\text{H-NMR}$ spectroscopy as a characteristic doublet at *ca.* δ 5.5-6.0 ppm with a high coupling constant, *ca.* $^2J = 14\text{-}15$ Hz was identified. This shows the presence of a C-P bond. The $^{31}\text{P-NMR}$ spectrum showed a singlet at *ca.* δ 20 ppm.



2.72-80

Scheme 2.5 Synthetic pathway to compounds **2.72-80**. Reagents and conditions: (i) dry benzene or toluene, PPh_3 , reflux.

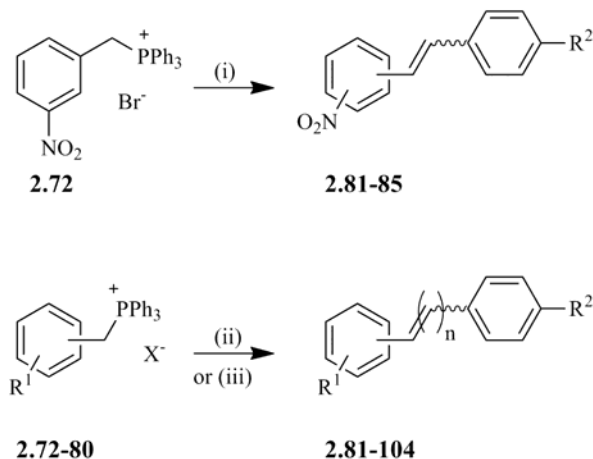
Table 2.13 Phosponium salts synthesized.

Compound	R^1	X	Yield (%)
2.72	3- NO_2	Br	99
2.73	H	Cl	54
2.74	4-Cl	Cl	55
2.75	4- CF_3	Br	96
2.76	4- OCF_3	Br	100
2.77	4-OMe	Br	91
2.78	3,5- NO_2	Cl	58
2.79	2,4- NO_2	Cl	60
2.80	2- NO_2	Br	99

The Wittig reactions were carried out under standard anhydrous conditions, using *n*-BuLi as a base (method A), and under phase transfer catalysis (PTC) at room temperature or with microwaves (MW), Scheme 2.6.

First, it was studied whether method A would be efficient for the desired synthesis, but it only provided compound **2.81** in good yield after refluxing for 7 hours, Table 2.14 entry 3. Additionally, a mixture of (*E*) and (*Z*) isomers was formed with predominance on the (*E*) isomer, which is consistent with what had already been described ^[215, 216]. In fact, as the reaction time increased, from 3 to 7 refluxing hours, more (*E*) isomer was formed, entry 5 *vs.* 3. Moreover, no influence on the yield was observed when 1.0 molar equivalents of benzaldehyde was used instead of 1.25, entry

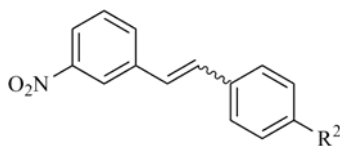
3 vs. 4, respectively. The synthesis of **2.82** through method A yielded a higher percentage of the (*Z*) isomer, entry 9, which was not expected ^[214], whereas **2.83** was only obtained using milder conditions but with a *Z/E* ratio of 0.5, entry 14.



Scheme 2.6 Synthetic pathway of compounds **2.81-104**. Reagents and conditions: (i) a) dry benzene, *n*-BuLi, N₂, b) aldehyde, rt or reflux; (ii) NaOH, CH₂Cl₂, aldehyde, rt; (iii) NaOH, CH₂Cl₂, aldehyde, MW.

As method A was not an efficient pathway to synthesize all the required stilbenes, the efforts were turned onto the phase transfer catalysis procedure, which made use of NaOH and CH₂Cl₂ as solvents, and the phosphonium salt as a ‘catalyst’ (methods B and B’). PTC Wittig reactions proved to be more efficient, given that higher yields were achieved in all cases, under milder conditions and lower reaction times.

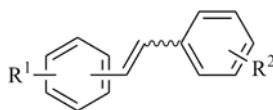
Using **2.72** as a starting material (method B), compound **2.81** was synthesized in excellent yield, and a high *Z/E* ratio was observed, entry 6. For compounds **2.82** and **2.83**, this procedure yielded them in 98%, entry 11, and 93%, entry 15, respectively, underpinning that the reaction is equally efficient with electron-withdrawing and donating groups on the aldehyde starting material. The *Z/E* ratios were also over 2.30 in both cases and showed no dependence on the substitution pattern of the aldehyde moiety. Though, when the benzyltriphenylphosphonium salt was left reacting with 3-nitrobenzaldehyde (method B’) for approximately 2 hours, not only **2.81** was obtained in a lower yield, but the *Z/E* ratio increased, entry 8 vs. 6. This was expected, as the interchange of substituents between the phosphonium salt and the aldehyde, especially nitro groups, has been connected with somewhat drastic changes in both the yield and *Z/E* ratio of the reaction ^[217]. For **2.83**, this phosphonium salt inversion gave nearly the same outcome when allowed to react for 2 hours, both in terms of yield and product ratio, entry 15 vs. 17.

Table 2.14 Comparison of Wittig reaction methods, to acquire **2.81-83**.

Entry	Compd	R ²	Method ^a	Time (h)	Yield (%)	Z:E (ratio) ^b
1	2.81	H	A	4, rt	0	-
2	2.81	H	A	25, rt	31	42:58 (0.72)
3	2.81	H	A	7, reflux	67	34:66 (0.52)
4	2.81	H	A	7, reflux	68	40:60 (0.67)
5	2.81	H	A	3, reflux	56	42:58 (0.72)
6	2.81	H	B	2, rt	92	84:16 (5.25)
7	2.81	H	B'	0.7, rt	74	75:25 (3.00)
8	2.81	H	B'	2, rt	89	85:15 (5.67)
9	2.82	OMe	A	6, reflux	20	62:38 (1.63)
10	2.82	OMe	B	0.5, rt	89	71:29 (2.45)
11	2.82	OMe	B	2, rt	98	77:23 (3.35)
12	2.82	OMe	B'	2, rt	92	67:33 (2.00)
13	2.83	Cl	A	7, reflux	0	-
14	2.83	Cl	A	7, rt	24	33:67 (0.50)
15	2.83	Cl	B	2, rt	93	70:30 (2.33)
16	2.83	Cl	B'	0.5, rt	92	69:31 (2.22)
17	2.83	Cl	B'	2, rt	94	71:29 (2.45)

^a Method A uses anhydrous conditions. Methods B and B' use PTC: B with nitrophosphonium salt, and B' with nitrobenzaldehyde; ^b Based on ¹H-NMR.

To assess the effect of the nitro group of the phosphonium salt in the reaction stereocontrol, and the scope of this reaction, compounds **2.84-94** were prepared. It can be seen that the stereoselectivity depends significantly on the position of the nitro group in the phosphonium halide, Table 2.15. A high (*Z*) stereoselectivity was observed for the reaction of 3- and 3,5-dinitrobenzylphosphonium salts with benzaldehyde, entries 1 and 7. In contrast, placement of the nitro group in the *ortho* or *para* positions of the phosphonium salt led to a significant increase in the proportion of the (*E*) alkene and loss of stereoselectivity, entries 4, 5 and 6. The diastereomeric ratio obtained for **2.85** is identical to the one reported for the synthesis of 2-nitro-2',5'-dimethylstilbene, Z:E = 1.4 ^[217], which was obtained through the same benzyltriphenyl phosphonium salt and identical conditions. Finally, the reaction of 2,4-dinitrobenzylphosphonium chloride with benzaldehyde shifted the stereoselectivity towards the formation of the (*E*)-**2.84**, entry 4.

Table 2.15 Reaction of nitro-substituted benzyltriphenyl phosphonium salts with aldehydes under standard PTC conditions at room temperature (Method B) and microwave-assisted synthesis (Method C).

Cpd	R ¹	R ²	Method B			Method C		
			Entry	Yield (%) ^a	Z:E (ratio) ^b	Entry	Yield (%) ^a	Z:E (ratio) ^b
2.81	3-NO ₂	H	1	92	84:16 (5.25)	1'	84	73:27 (2.70)
2.82	3-NO ₂	4-OMe	2	98	77:23 (3.35)	2'	79	77:23 (3.33)
2.83	3-NO ₂	4-Cl	3	93	70:30 (2.33)	3'	96	70:30 (2.38)
2.84	2,4-diNO ₂	H	4	34	17:83 (0.20)	4'	N.D. ^c	N.D. ^c
2.85	2-NO ₂	H	5	95	57:43 (1.33)	5'	24	69:31 (2.22)
2.86	4-NO ₂	H	6	88	58:42 (1.38)	6'	93	34:66 (0.52)
2.87	3,5-diNO ₂	H	7	76	88:12 (7.33)	7'	67	71:29 (2.45)
2.88	3-NO ₂	2-F	8	96	91:9 (10.11)	8'	49	86:14 (6.14)
2.89	3-NO ₂	2-Cl	9	100	85:15 (5.67)	9'	46	83:17 (4.88)
2.90	2-NO ₂	2-F	10	90	83:17 (4.88)	10'	88	76:24 (3.17)
2.91^d	2-NO ₂	2-CO ₂ Me	11	47	78:22 (3.54)	11'	39	63:37 (1.70)
2.92	4-NO ₂	2-F	12	100	58:42 (1.37)	12'	77	74:26 (2.85)
2.93	4-NO ₂	2-Cl	13	92	67:33 (2.00)	13'	96	80:20 (4.00)
2.94	3-NO ₂	4-NO ₂	14	61	100:0	14'	N.D.	N.D.

^a Yield is given for the isolated isomer mixture. ^b Z/E ratios were determined by ¹H NMR. ^c Untractable mixture. N.D. - Not Determined. ^d Aldehyde **2.95** obtained from the corresponding acid with methyl iodide.

The observed shift from (*Z*) to (*E*) stereoselectivity can be ascribed, at least in part, to the direct conjugation of the negative charge of the phosphonium ylide with the nitro groups in *ortho* or *para* positions and is consistent with the suggestion that the dominant structure of phosphonium ylides is the dipolar P⁺-C⁻ zwitterion rather than the P=C double bond [218]. Indeed, the equilibrium acidities, p*K*_{HA} in DMSO, of 4-substituted ArCH₂PPh₃⁺ cations correlate with the Hammett σ⁻ constants of the substituents in the aryl moiety with a slope of -4.78, reflecting the direct conjugation of the negative in the conjugate base, the ylide, with electron withdrawing groups such as NO₂ [218]. The similar Z:E ratios for **2.85** and **2.86**, Table 2.15 entries 5 and 6, suggest that stereoselectivity is not affected by sterical hindrance in the ylide moiety.

Stilbenes **2.88-94** were obtained in good yields, entries 8-14. Although diastereoselection was variable, the (*Z*) isomer was predominant in all cases. Interestingly the reaction diastereoselectivity

decreased with the introduction of both moderate electron withdrawing and donating groups in the aldehyde, i.e. **2.82** and **2.83**, in comparison to the non-substituted counterpart, but the introduction of 4-NO₂ resulted in the (*Z*) isomer, exclusively, under these reaction conditions, entry 14. For reactions with 2-halobenzaldehydes, the expected (*Z*) diastereoselectivity was observed even for the stabilized 2-nitro ylide. The cooperative *ortho* halo effect ^[219, 220] may be responsible for these results and overrides the stabilizing effect of resonance to the nitro group.

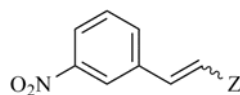
With these results in hand, it was studied the effect of the microwaves in the synthesis of **2.81**, at different temperatures, Table 2.16. Interestingly, the conversion rate decreased with higher temperatures, methods C-F. Also, the stereocontrol was poorer when compared to the reaction without microwaves. Since the microwave-assisted protocol was most successful at 30 °C, the reactions to acquire the remaining stilbenes were carried out at this temperature.

Table 2.16 Comparative study, rt vs. MW, for the synthesis of **2.81**.

Method	Temperature	Time	Yield (%)	Z:E (ratio)
B: PTC	rt	2 h	92	84:16 (5.25)
C: PTC/MW/100W	30	3 min	84	73:27 (2.70)
D: PTC/MW/100W	50	3 min	88	71:29 (2.45)
E: PTC/MW/100W	70	3 min	70	69:31 (2.23)
F: PTC/MW/100W	90	3 min	64	68:32 (2.13)

As for the microwave-assisted reactions, the yields were less consistent and resulted in a decrease of the (*Z*) stereoselectivity, e.g. Table 2.15 entries 7 vs. 7'. With the stabilized 4-nitrophosphorane the reaction rate increased and inversion on the stereoselectivity was observed, entries 6 vs. 6', whereas with 2,4-dinitrophosphorane an untractable mixture was obtained, entry 4'.

Variation of the substitution pattern in the aldehyde did not affect significantly the PTC reaction yield, except for **2.85**, **2.88** and **2.89**, entries 5/5', 8/8' and 9/9', and although diastereoselection was variable, the (*Z*) isomer was generally predominant. For reactions with 2-halobenzaldehydes, the expected (*Z*) diastereoselectivity was observed, but the co-operative *ortho* halo effect was not as pronounced when compared to method A of PTC reactions. Interestingly, reactions under microwaves with 4-nitrophosphorane afforded a greater (*Z*) selectivity than the standard PTC procedure, entries 12/12' and 13/13'. However, despite the lower yields and poorer diastereoselection, this procedure greatly reduces the reaction time.

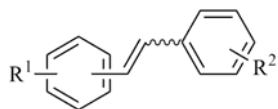
Table 2.17 Synthesis of alkenes **2.96-99** through Wittig chemistry.

Cpd	Z	Method B			Method C		
		Entry	Yield (%) ^a	Z:E (ratio) ^b	Entry	Yield (%) ^a	Z:E (ratio) ^b
2.96		1	45	80:20 (4.00)	1'	55	79:21 (3.76)
2.97		2	N.D. ^c	N.D. ^c	2'	N.D. ^c	N.D. ^c
2.98		3	N.D. ^c	N.D. ^c	3'	N.D. ^c	N.D. ^c
2.99^d		4	84	17:83 (0.20)	4'	N.D.	N.D.

^a Yield is given for the isolated isomer mixture. ^b Z/E ratios were determined by ¹H NMR. ^c Untractable mixture. N.D. - Not Determined. ^d Phosphonate **2.100** obtained from oxidation of the thioether.

The PTC and MW-assisted reactions carried out with phenylacetaldehyde gave only a moderate yield of the corresponding stilbene, Table 2.17 entries 1 and 1', and an increased rate of hydrolysis of the phosphorane into the 3-nitrotoluene was observed. Moreover, 3-nitrotoluene was the main product when the reactions were carried out with aliphatic aldehydes, and the main cause of lower yields for MW-assisted reactions. Instability of stabilized phosphoranes has already been reported whilst using microwave assisted synthesis ^[221] and the hydrolysis of phosphonium salts correlates with the Hammett σ values of 3-NO₂ and 4-NO₂. The rate limiting step in the mechanism is variable, but involves the attack of a hydroxide to the phosphorous, and formation of phosphine oxide. This step also results in expulsion of the benzylic carbanion, which in aqueous solution affords the corresponding toluene ^[222]. Finally, compounds **2.101** and **2.102** were obtained via method B', Table 2.18.

These intermediates were isolated in Z:E mixtures and identified by ¹H-NMR spectroscopy. The two CH doublets for the (Z) diastereomers usually appear at higher field. For **2.82** those protons can be found at δ 6.52 and 6.72 ppm, while the protons from its (E) counterpart are found at δ 7.01 and 7.21 ppm. Those protons in (Z) isomers also present a coupling constant of *ca.* ³J = 12 Hz, whereas their counterparts display a constant of *ca.* ³J = 16 Hz.

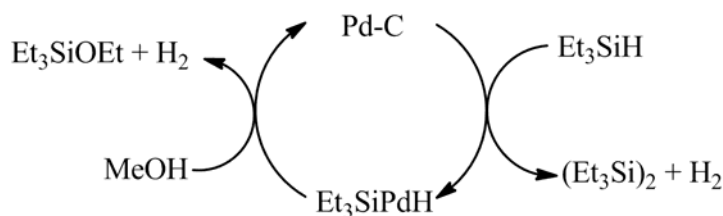
Table 2.18 Structure of compounds **2.101** and **2.102**.

Compound	R ¹	R ²	Yield (%) ^a	Z:E (ratio) ^b
2.101	3-NO ₂	4-CF ₃	98	75:25 (3.00)
2.102	3-NO ₂	4-OCF ₃	100	72:28 (2.57)

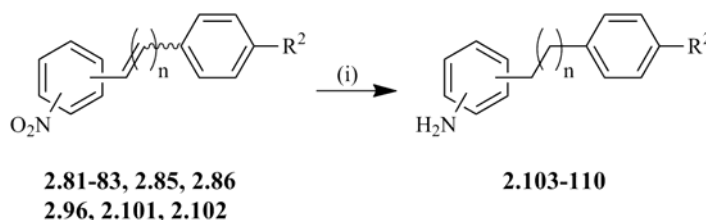
^a Yield is given for the isolated isomer mixture. ^b Z/E ratios were determined by ¹H NMR.

Anilines

The nitrostilbenes were reduced to the corresponding anilines through a method described by Mandal *et al.* [223]. Catalytic transfer of hydrogen (CTH) is a widely accepted alternative method that does not require the use of potentially dangerous hydrogen gas, and Et₃SiH (or TES)/Pd-C is a very convenient reagent that generates H₂ *in situ*, Scheme 2.7. The reactions were carried out using excess TES with 10-20% Pd-C (by weight) in MeOH, and simultaneous reduction at the C=C and nitro group was observed, Scheme 2.8. Generally, very good yields were obtained, Table 2.19.

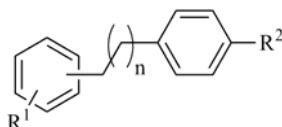


Scheme 2.7 Mechanism for *in situ* generation of H₂.



Scheme 2.8 Synthetic pathway to compounds **2.103-110**. Reagents and conditions: (i) CH₂Cl₂, MeOH, TES, Pd-C 10%, rt.

Table 2.19 Structure of compounds 2.103-110.



Compound	R ¹	R ²	n	Yield (%)
2.103	3-NH ₂	H	1	95
2.104	3-NH ₂	OMe	1	99
2.105	3-NH ₂	Cl	1	78
2.106	2-NH ₂	H	1	94
2.107	4-NH ₂	H	1	87
2.108	3-NH ₂	H	2	95
2.109	3-NH ₂	CF ₃	1	100
2.110	3-NH ₂	OCF ₃	1	98

All reactions were carried out swiftly at room temperature, and strong bubbling and heating was noted in all cases. Typically, the reactions were completed after 15-30 minutes (TLC). The reduction of **2.83** at room temperature afforded only *ca.* 1/3 of **2.105** and *ca.* 2/3 of **2.103**. This was already expected as there is halogen removal reported when using TES as an *in situ* H₂ generator [224]. Thus, the synthesis of **2.105** was attempted below room temperature. At -10 °C an equal amount of **2.105** and **2.103** was obtained, but at -65 °C only the desired product was formed. In this case, the reaction was allowed to develop for 3 hours before quenching, to avoid halogen substitution; hence the lower yield, comparing to other reactions.

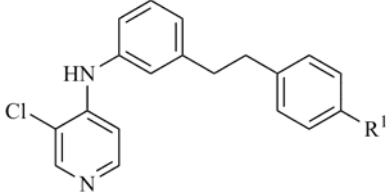
These intermediates were identified by 1D and 2D NMR spectroscopy. These series of intermediates is readily identified from the characteristic symmetric multiplet at *ca.* δ 2.7-3.0 ppm that corresponds to the two methylene groups spacing the aryl moieties. A simple triplet pattern for each methylene would be expected, but a closer inspection of the signal allows one to see seven peaks, which is only consistent with *ddd* coupling, i.e. all protons are non-equivalent. This would yield eight distinct peaks, but the rather low resolution of the spectrum does not permit the determination of the coupling constants.

Pyridinamines

With the synthesized anilines, S_NAr was carried out with 3,4-dichloropyridine in order to afford 4-pyridinamines, Scheme 2.4 A. Only two compounds were synthesized, **2.111** and **2.112**, from

reflux of the two starting materials in ethanol, as was done for the series of Mannich-base 4-pyridinamines, Table 2.20.

Table 2.20 Structure of compounds **2.111** and **2.112**.

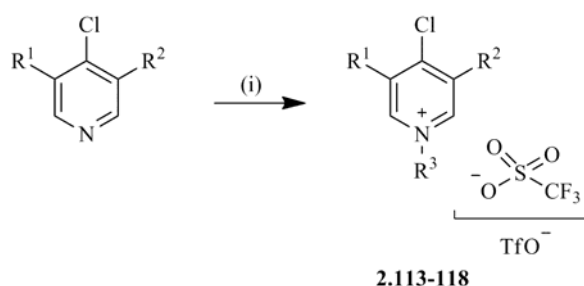


Compound	R ¹	Yield (%)
2.111	H	20
2.112	OMe	80

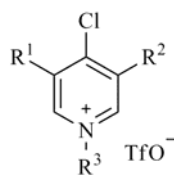
Both compounds were characterized by ¹H and ¹³C-NMR, and were used in the next step. Interestingly, the two methylene groups which appeared as a symmetric multiplet in the phenethylamines precursors now showed as a completely superimposed multiplet.

Pyridinium salts

The pyridinium salts were obtained through a S_N2 reaction, according to the procedure described by Bierer *et al.* [225]. *N*-alkylation with methyl and ethyl iodide upon deactivated pyridines had previously failed, and thus, a stronger alkylating agent was employed, i.e. methyl or ethyl triflate, Scheme 2.9. All compounds precipitated from the reaction mixture, and were obtained in excellent yields. The exception was observed for the 3-nitropyridine which did not react in these conditions, Table 2.21. The compounds were identified by ¹H-NMR spectroscopy and presented a characteristic peak at *ca.* δ 4.5 ppm, assigned to the methyl or methylene protons linked to pyridine.



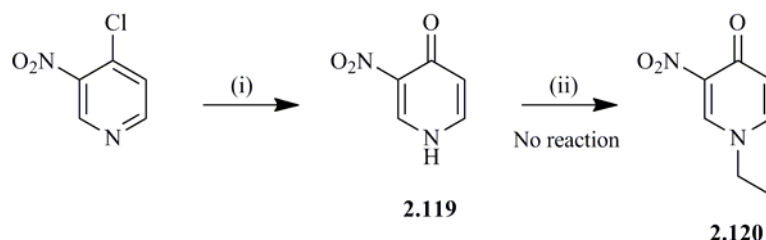
Scheme 2.9 Synthetic pathway to compounds **2.113-118**. Reagents and conditions: (i) dry toluene, TfOMe or TfOEt, rt.

Table 2.21 Structure and obtained yields for compounds **2.113-118**.

Compound	R ¹	R ²	R ³	Yield (%)
2.113	Cl	H	Me	95
2.114	NO ₂	H	Me	0
2.115	Cl	H	Et	100
2.116	Cl	Cl	Et	97
2.117	NO ₂	H	Et	0
2.118	NH ₂	H	Et	95

Since the synthesis of the unsubstituted and 3-nitro pyridinium salts was not successful, a different approach was taken. The 4-chloropyridines were transformed into the corresponding 4(1*H*)-pyridones, before undertaking the alkylation step. 3-Nitropyridone was prepared from a simple reaction with NaOH, under reflux, affording **2.119** in quantitative yield, Scheme 2.10.

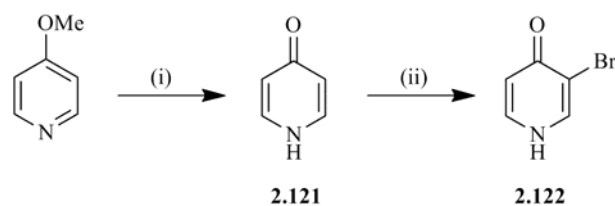
However, the attempted synthesis of the *N*-ethyl derivative of **2.119**, i.e. **2.120**, was also not successful.



Scheme 2.10 Synthetic pathway to compound **2.119**. Reagents and conditions: (i) NaOH, reflux; (ii) toluene, EtOTf, TEA, rt.

On the other hand, compound **2.121** was obtained in quantitative yield from deprotection of 4-methoxypyridine with trimethylsilyl iodide (TMSI), Scheme 2.11 ^[226]. This pyridone gave access to the introduction of bromine at C3, **2.122**, from reaction with NBS, which would be a key intermediate to synthesize the compounds with the highest docking scores. Though, the low yield of the bromination step (19%) made it unsuitable to progress further with the synthesis of its 4-chloro

derivative with POCl_3 . The synthesis of **2.122** has been reported as troublesome. The 3,5-dibromo compound is often formed in higher yields ^[227].

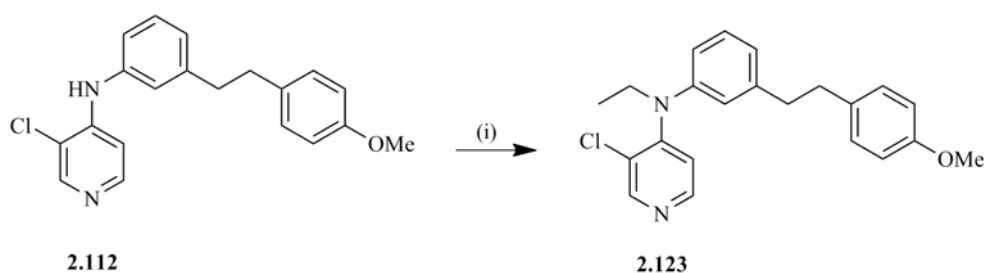


Scheme 2.11 Synthetic pathway for compound **2.121** and **2.122**. Reagents and conditions: (i) CH_3CN , TMSI, N_2 , reflux; (ii) CH_2Cl_2 , MeOH, NBS, rt, light

2.3.6 4-Pyridonimines

Via 4-pyridinamines

The synthesis of the second series of 4-pyridonimines was first carried out as described for the Mannich-base series of compounds, i.e. addition of sodium hydride in anhydrous DMF, followed by reaction with an alkyl iodide. It was noted that for the Mannich-base derivatives, alkylation occurred only at the pyridinic nitrogen, but for this series, alkylation occurred, remarkably, only at the amine nitrogen, Scheme 2.12.



Scheme 2.12 Synthetic pathway for compound **2.123**. Reagents and conditions: (i) a) DMF, NaH b) EtI.

The structure of **2.123** was confirmed by NMR techniques and the signal given by CH_2CH_3 was significantly different from what had been observed for the first series. Whereas the $N\text{-CH}_3$ protons of **2.1**, **2.4** and **2.6-8** appear at *ca.* δ 4.0 ppm, for this synthesis the $N\text{-CH}_2$ protons were obtained at a higher field, δ 3.83 ppm. Furthermore, the coupling constant of Ar- H_2 and Ar- H_3 remained at *ca.* $^3J = 4.5$ Hz, which is not consistent with the 4-pyridonimine core. The final confirmation came

from 2D NOESY spectrum, in which no correlation of the methylene with Ar-H2 was seen, Figure 2.13. For this reason, this pathway was abandoned for the remaining synthesis.

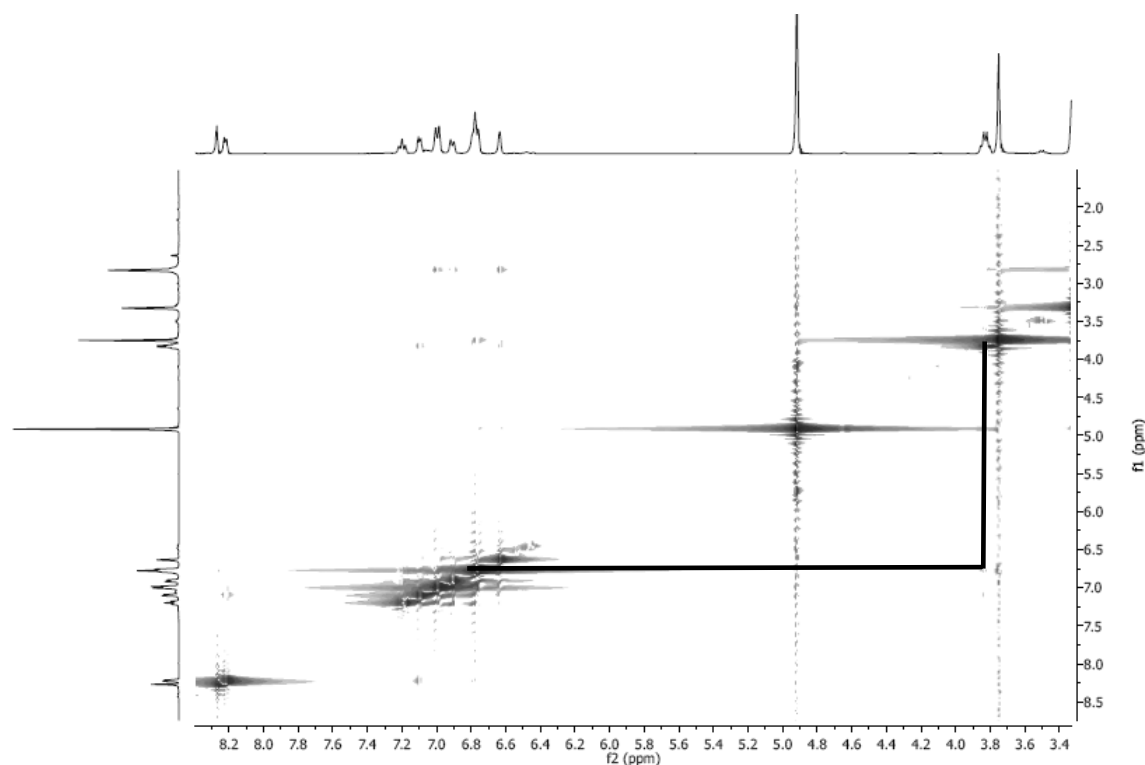
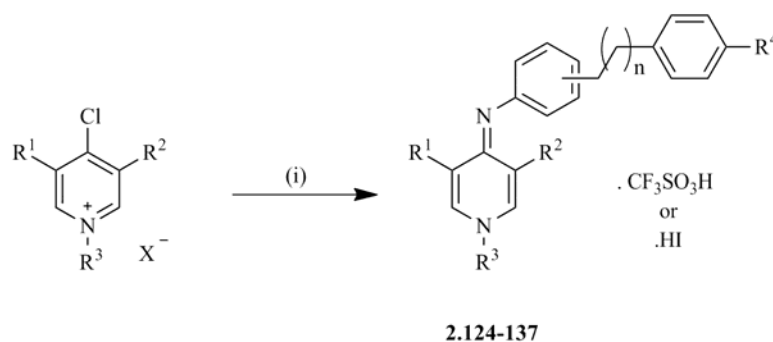


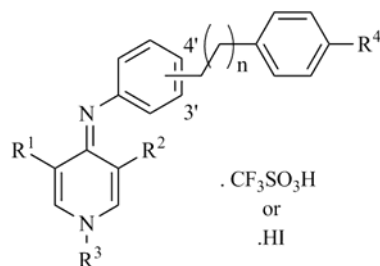
Figure 2.13 2D NOESY spectrum of **2.123**.

Via pyridinium salts

The S_NAr was carried out for 20-24 hours under reflux in the presence of triethylamine and in ethanol. The 4-pyridonimine derivatives **2.124-137** were obtained through an addition-elimination mechanism^[228], in good yields, and isolated as trifluoromethanesulfonates or hydroiodides, depending on the counterion of the pyridinium starting material, Scheme 2.13 and Table 2.22.



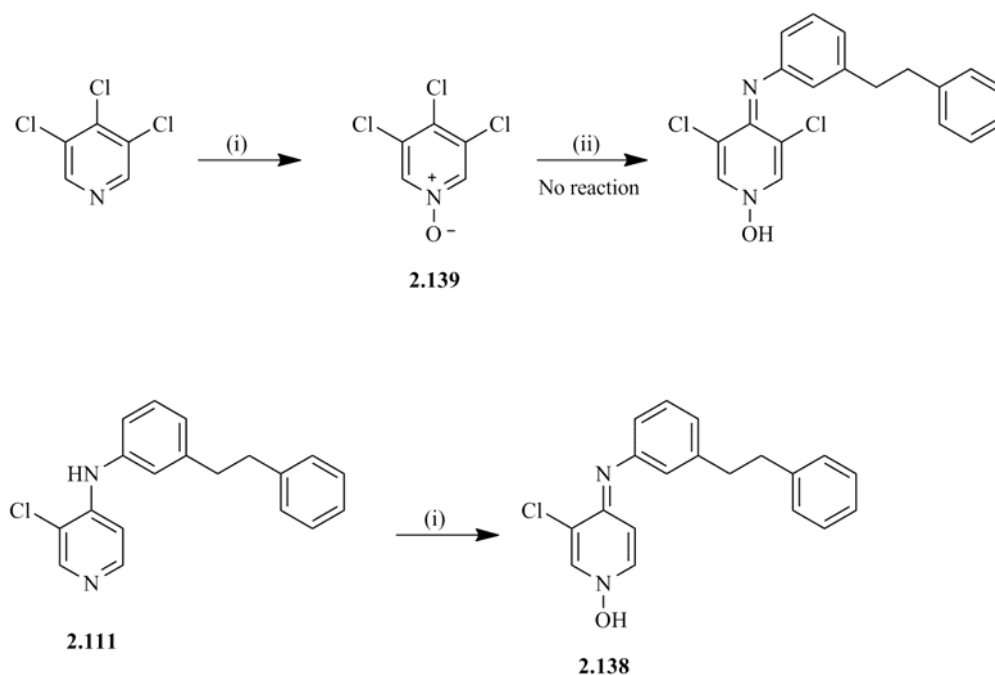
Scheme 2.13 Synthetic pathway to compound **2.124-137**. Reagents and conditions: (i) EtOH, TEA, aniline, reflux.

Table 2.22 Structure of 4-pyridonimines and yields.

Compound	R ¹	R ²	R ³	R ⁴	Isomer	n	Yield (%)
2.124	Cl	H	Et	OMe	3'	1	57
2.125	Cl	H	Me	OMe	3'	1	87
2.126	Cl	H	Et	H	3'	1	82
2.127	Cl	H	Me	H	3'	1	59
2.128	Cl	H	Et	Cl	3'	1	11
2.129	Cl	H	Et	CF ₃	3'	1	76
2.130	Cl	H	Et	OCF ₃	3'	1	76
2.131	Cl	Cl	Et	OCF ₃	3'	1	74
2.132	NH ₂	H	Et	H	3'	1	97
2.133	NH ₂	H	Me	H	3'	1	50
2.134	NH ₂	H	Et	OCF ₃	3'	1	70
2.135	Cl	H	Et	H	2'	1	59
2.136	Cl	H	Et	H	4'	1	53
2.137	Cl	H	Et	H	3'	2	33

Since *N*-hydroxides reduce the antiparasitic activity of 4(*1H*)-pyridones^[19], the *N*-hydroxide pyridonimine **2.138** was also synthesized, in order to confirm if the same trend was observed. Two different pathways were experimented, Scheme 2.14. First, *N*-oxidation of pyridine was carried out with *m*CPBA affording the desired *N*-oxide **2.139** in good yield (73%). An attempted S_NAr with the *N*-oxide followed, but no reaction was observed, probably due to the higher electron density at C4, as a consequence of the electron-donor effect from *N*-O⁻. This was also confirmed from the ¹H-NMR spectrum of **2.139**. The C2 protons are more shielded than in the starting material as a result of the resonance of the oxygen atom with the aromatic moiety. Greater difficulty to perform S_NAr reactions with *N*-oxides than with *N*-alkyl salts had been reported^[228].

Alternatively, *N*-oxidation of the previously synthesized 4-pyridinamine **2.111** was carried out with success, affording **2.138** in 31% yield.



Scheme 2.14 Synthetic pathway to compound **2.138**. Reagents and conditions: (i) CHCl_3 , *m*CPBA, reflux (ii) EtOH, TEA, aniline, reflux.

The compounds were characterized with several spectroscopic techniques, including 1D and 2D NMR and only the (*E*) isomer was formed. A characteristic feature of these compounds is the resonance of the *N-CH_x* group at *ca.* δ 4.0-4.3 ppm, presenting an upfield shift compared to the salt precursor. Additionally, the Ar-*H2* and Ar-*H3* resonances and their vicinal coupling constants provide further evidence of contrasting electronic features to those of the starting material: (i) Ar-*H2* resonance appears dramatically more shielded, *ca.* δ 8.0-8.8 ppm (3J of 7.2 to 7.6 Hz), than the pyridinium salt which appears at *ca.* δ 9.0-9.5 ppm (3J = 6.8 Hz); (ii) higher coupling constants indicate the shift in nitrogen hybridation from sp^2 to sp^3 as was also observed for the first series. As an example, the $^1\text{H-NMR}$ spectrum of **2.129** presents Ar-*H2* at δ = 8.74 ppm, and Ar-*H6* at δ = 8.18 ppm, whereas Ar-*H5* is found at δ = 6.88 ppm, the most shielded proton in the aromatic region. The spectrum also shows an AA' BB' system, δ = 7.38 and 7.56 ppm, corresponding to the terminal aryl moiety. At higher fields, one finds the chemical shifts of the ethyl group, and the methylene spacer as a broad singlet-like multiplet, δ 3.07 ppm.

Mass spectroscopy was carried out on electrospray ionization, positive mode. The base peak was obtained for $[\text{M}+\text{H}]^+$, for this series of compounds. Furthermore, the peak with m/z = 246 at a relative abundance of *ca.* 80% results from the fragmentation at the methylene linker. This was the

most common breaking point among the synthesized compounds, and was identical to the Mannich-base series, Figure 2.14.

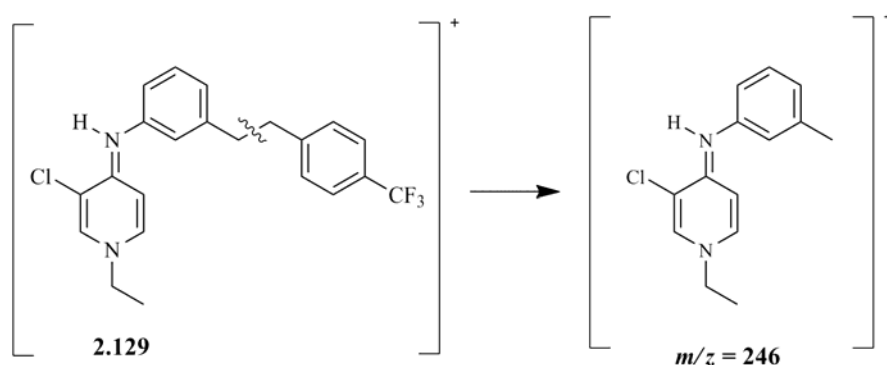


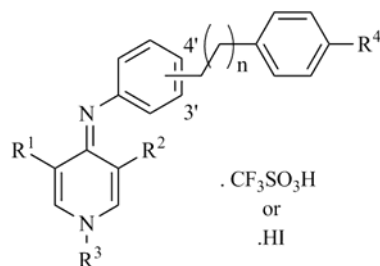
Figure 2.14 Fragmentation pattern for 4-pyridonimines, exemplified by **2.129**.

Antiplasmodial activity and cytotoxicity

With the introduction of a second aryl moiety, a lipophilic spacer in the structure-base designed 4-pyridonimines, and a chlorine atom at C3, it was expected that the antiplasmodial activities would improve, compared to the Mannich-base series. In fact, the IC_{50} s against the W2 strain dropped, at least, 1.5-fold, pinpointing the successful use of the docking model to design new inhibitors. Analysis of Table 2.23 allows the following observations on SAR:

- Introduction of a lipophilic side chain improved the antiplasmodial activity to a maximum of 9-fold, i.e. **2.1** vs. **2.131**;
- Exchange of the *N*-methyl for a *N*-ethyl group at R³ generally resulted in little effect on the antiplasmodial activity against the W2 and FCR3 strains, i.e. **2.126** vs. **2.127**, and **2.132** vs. **2.133**;
- For the 3-Cl series, the 4-OCF₃ substituent at the terminal aromatic ring increased activity against the W2 and FCR3 strains, when compared to the unsubstituted counterpart, i.e. **2.126** vs. **2.130**;
- The substituent effect on both strains was 4-OCF₃ (**2.130**) > 4-CF₃ (**2.129**) > 4-Cl (**2.128**) > H (**2.126**) ~ 4-OMe (**2.124**), which is similar to what had been reported for 4(1*H*)-pyridones^[19];
- For the 3-NH₂ subset, the 4-OCF₄ substituent at R⁴ had a detrimental effect on the antiplasmodial activity, for the W2 strain, which is also consistent with the drop of activity for 4(1*H*)-pyridones with electron-donating groups at C3^[19].

- f) Introduction of a second chlorine atom at C5 does not have a significant impact on activity, against the W2 strain, i.e. **2.130** vs. **2.131**;
- g) The *N*-hydroxy derivative **2.138** was inactive against both tested strains, in line with the SAR described for clopidol analogues ^[19];
- h) The position of the phenethyl side chain also had effect on the antiplasmodial activity, with the 2' and 4' isomers being less active than their 3' counterpart, against the W2 strain, i.e. **2.135** and **2.136** vs. **2.126**;
- i) The 3-phenylpropyl side chain resulted in increased activity, which is indicative of the importance of a lipophilic side chain, i.e. **2.126** vs. **2.137**;
- j) The antiplasmodial activities against the W2 and FCR3 strains are comparable, given the same point mutation on the gene that confers chloroquine resistance. The compound **2.136** is at least 3-fold more active against the FCR3 strain.

Table 2.23 Antiplasmodial activity against *P. falciparum* W2 and FCR3 strains.

Compound	R ¹	R ²	R ³	R ⁴	Isomer	n	IC ₅₀ (μM) ± SD	
							W2	FCR3
2.1							8.61 ± 0.41	7.90 ± 0.24
2.124	Cl	H	Et	OMe	3'	1	3.44 ± 0.08	3.95 ± 0.93
2.125	Cl	H	Me	OMe	3'	1	5.24 ± 0.68	5.12 ± 1.61
2.126	Cl	H	Et	H	3'	1	3.46 ± 0.28	3.53 ± 0.29
2.127	Cl	H	Me	H	3'	1	4.75 ± 0.78	2.89 ± 0.89
2.128	Cl	H	Et	Cl	3'	1	3.24 ± 0.24	2.17 ± 0.33
2.129	Cl	H	Et	CF ₃	3'	1	1.60 ± 0.15	1.87 ± 0.33
2.130	Cl	H	Et	OCF ₃	3'	1	1.07 ± 0.07	1.70 ± 0.20
2.131	Cl	Cl	Et	OCF ₃	3'	1	0.94 ± 0.12	2.80 ± 0.03
2.132	NH ₂	H	Et	H	3'	1	1.67 ± 0.15	2.08 ± 0.95
2.133	NH ₂	H	Me	H	3'	1	1.47 ± 0.10	2.21 ± 0.22
2.134	NH ₂	H	Et	OCF ₃	3'	1	3.91 ± 0.03	1.83 ± 1.27
2.135	Cl	H	Et	H	2'	1	6.67 ± 0.38	3.19 ± 0.90
2.136	Cl	H	Et	H	4'	1	> 10	3.74 ± 0.12
2.137	Cl	H	Et	H	3'	2	2.43 ± 0.10	2.25 ± 1.12
2.138^a	Cl	H	OH	H	3'	1	> 8.9	> 8.9
Clopidol							9.73 ± 0.07	3.37 ± 0.19
Atovaquone							0.0012	1.89 ± 0.10
Chloroquine							0.052	0.051

^a Compound **2.138** was obtained in the neutral form.

Molecular docking

Finally, to understand how the two most active compounds would interact with the predicted binding site, a docking study was carried out in their iminium form, since they had been tested as triflates. Compound **2.130**, Figure 2.15 B, presents the side chain occupying the hydrophobic channel leading to the Q₀ centre, and interacts with aliphatic and aromatic side chains of L150, F151, L275, F278, M295, I299 which is similar to GW844520, Figure 2.15 A. Interestingly, the iminium hydrogen atom of **2.130** is close to the nitrogen atom of H181 (2.8 Å) which is compatible

with a hydrogen bond. On the other hand, **2.131** presents an identical docking pose to **2.130**, where the side chain is occupying the hydrophobic channel. The iminium hydrogen atom of **2.131** is 4.2 Å away from the oxygen atom of E272, which is compatible with a water-mediated hydrogen bond. These results support the hypothesis that 4-pyridonimines can bind to the Q_o site in cytochrome *b*, promoting interactions with the residues that define the hydrophobic channel in a similar way to GW844520.

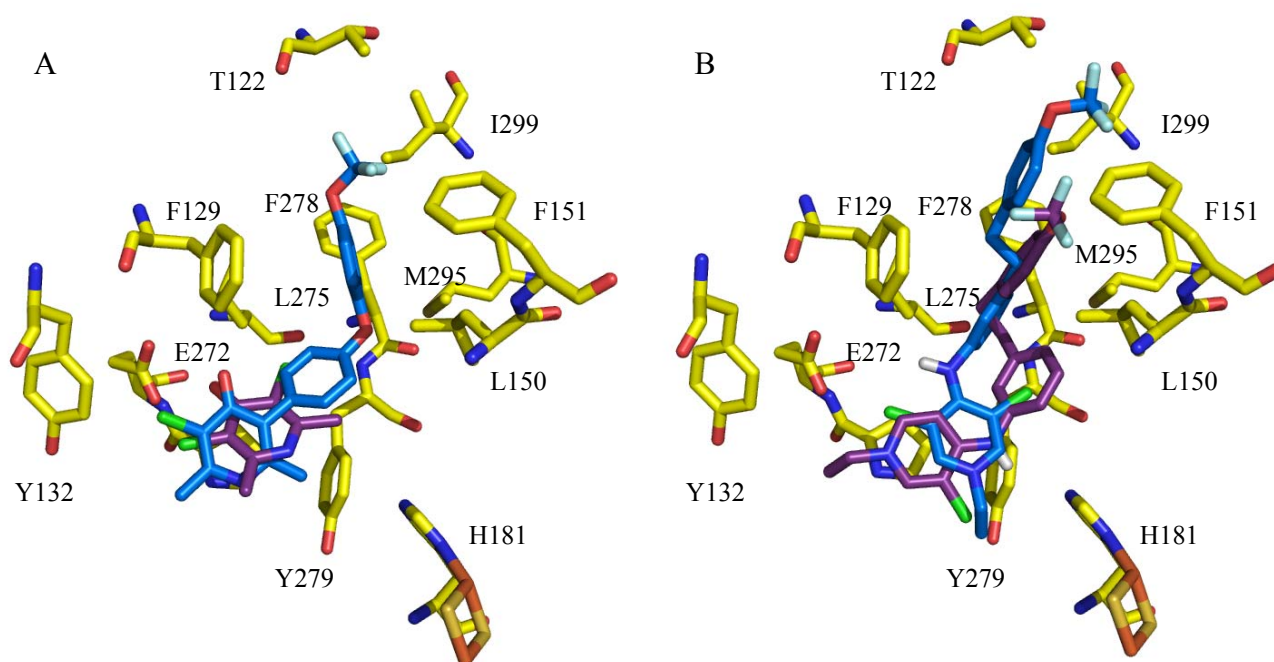


Figure 2.15 Docking poses of (A) clopidol (purple), and GW844520 (blue); (B) **2.130** (purple), and **2.131** (blue).

Anti-liver activity and cytotoxicity

Compounds **2.124-138** were also tested for their activity against the liver stages of *P. berghei* in human hepatoma cells. Primaquine and atovaquone are known to act at this point of the life cycle. However, it is an under-exploited target, and the dormant hypnozoites are responsible for malaria relapses^[229, 230]. In short, the method is based on the measurement of luminescence of Huh-7 cells, a human hepatoma cell line, following infection with *PbGFP-Luc_{con}*-expressing *P. berghei* sporozoites. At a given time after infection, the percentage of parasitized cells is given by the percentage of luminescence. Because this gene is under the control of the constitutive *eef1aα* promoter, the extent of intracellular development is proportional to the number of luciferase copies in the cell, measured as the intensity of luminescence.

The compounds were assayed three times at 10 μM and 2 μM , and compared with primaquine at 5 μM , Figure 2.16.

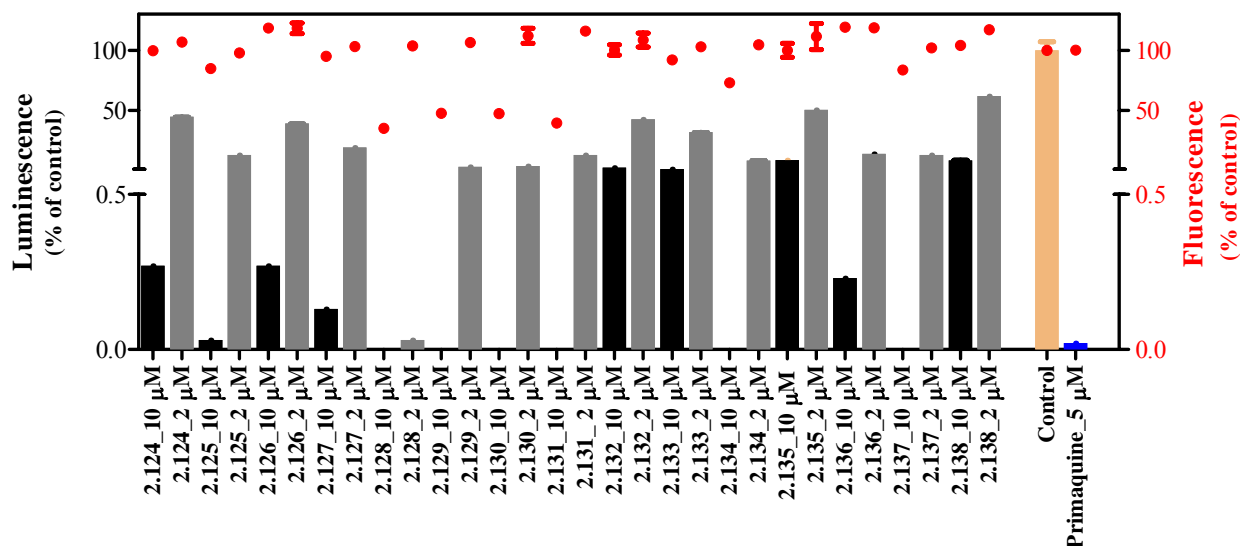


Figure 2.16 Antiplasmodial activity of compounds **2.124-138** at 10 μM (black bars) and 2 μM (grey bars) against liver stage *P. berghei*. The luminescence (bars) is given as percentage of control (MeOH) inhibition. The cytotoxicity was measured in fluorescence (dots) from the Alamar Blue test and is also given as percentage of control. Primaquine was tested at 5 μM . All concentrations were tested and missing bars account for the total suppression of parasite load.

From observation of the plot, it is possible to conclude that:

- The antiplasmodial activity is dose-dependent, i.e. the compounds are more active at 10 μM than at 2 μM ;
- At 10 μM compounds **2.132**, **3.133**, **2.135** and **2.138** are the least potent; the remaining compounds are considerably more potent, i.e. at least over 2-fold;
- Similar SAR to that of the blood stage can be found: electron-withdrawing groups on the terminal aryl moiety still afford more potent compounds, e.g. **2.128** vs. **2.126** and **2.124**; the introduction of a second chlorine atom does not improve activity, i.e. **2.130** vs. **2.131**; compounds **2.135** and **2.138** are among the least active, as against the W2 strain;
- In this case, *N*-ethyl substitution appears to be detrimental when compared to *N*-methyl, i.e. **2.124** vs. **2.125** and **2.126** vs. **2.127**, in opposition to what was observed against the W2 strain;
- In the 3-NH₂ subset, the terminal OCF₃ group also appears to be favourable for activity;
- At 2 μM , compound **2.128** is as active as primaquine at 5 μM .

The toxicity of those compounds was then assayed using the Alamar Blue test. The active ingredient, resazurin, is a non-toxic, cell permeable compound that is blue in colour and virtually non-fluorescent. Upon entering cells, it is reduced to resorufin, which produces red fluorescence. Viable cells continuously produce the fluorescent compound, thereby measuring viability / cytotoxicity.

The following observations can be made:

- a) The compounds that are most active against the liver stage, are also the most toxic;
- b) At 10 μM , compound **2.126** shows comparable toxicity to primaquine;
- c) All compounds present similar toxicity at 2 μM ; which in turn is similar to primaquine at 5 μM and the control.

2.4 Conclusions

The 4-pyridonimines present similar electronic properties to the 4(1*H*)-pyridones. The structure-based approach to optimize the scaffold was successful, i.e. while the most active Mannich-base compound **2.1** displayed an IC_{50} of *ca.* 8.5 μM , the most active pyridonimine from the second series was **2.131**, with an IC_{50} of 0.94 μM . The introduction of an extended and lipophilic side chain was probably key, and the docking poses of the compounds also give a possible explanation for the IC_{50} s, on a molecular basis. These compounds also displayed interesting anti-liver activity and can be used as leads for further optimizations.

CHAPTER 3

QUINOLONIMINE SCAFFOLD

3. QUINOLONIMINE SCAFFOLD

3.1 Rationale

After studying the 4-pyridonimine scaffold the attention was drawn to 4-quinolonimines. Since that all synthesized compounds from the previous series were obtained as triflate or iodide salts, it was hypothesized that the positive charge would be detrimental for the molecule to reach the drug target. Moreover, since those molecules had been designed to inhibit a highly hydrophobic binding site, this charge could be responsible for less efficient interactions with the binding pocket. Thus, in order to eliminate this problem, it was decided to include an extra aromatic ring into the 4-pyridonimine scaffold to decrease the basicity of the imine nitrogen and, consequently, increase the lipophilicity of the molecules. In fact, the inclusion of a second aryl increases the predicted logP in 1.30 units in test scaffolds, Figure 3.1 ^[231].

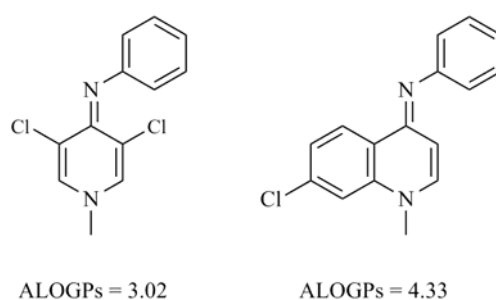
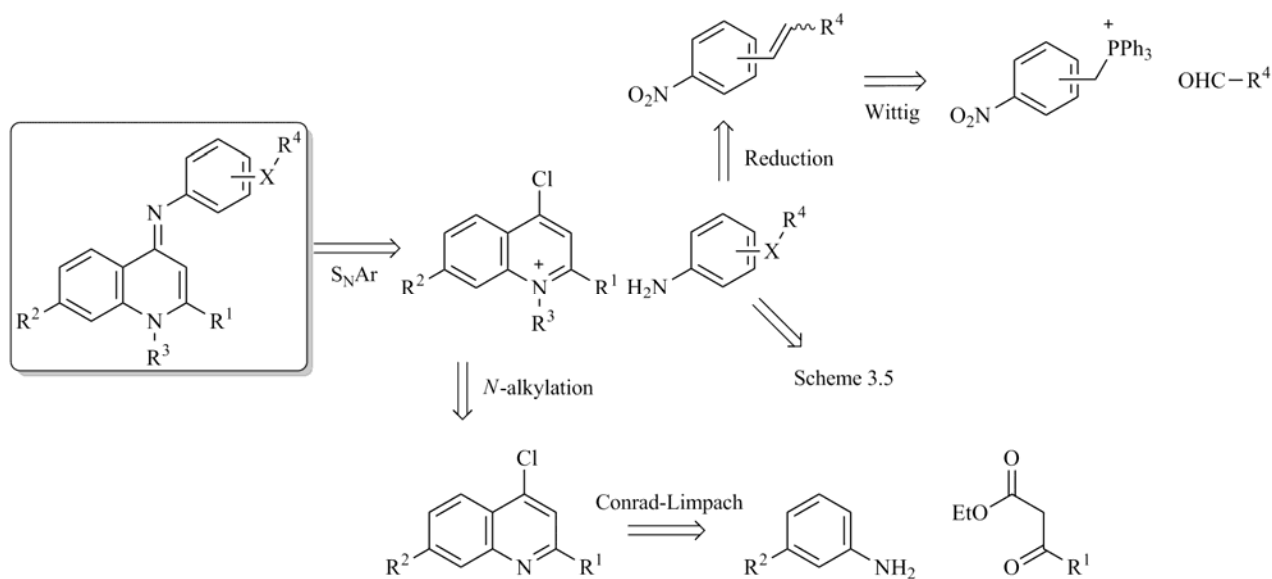


Figure 3.1 Predicted LogP for the 4-pyridonimine and 4-quinolonimine scaffolds.

In this series, quinolines that are used to obtain known antimalarials were employed as starting materials, to enhance the eventual antiplasmodial activity of 4-quinolonimines. Since the 7-chloroquinoline core would be used, it was expected that the resulting compounds could also present a mechanism of action similar to chloroquine. Additionally, the side chains described by Yeates *et al.* ^[19] and those derived from the 4-pyridonimine study were used, to obtain some insight into the SAR. Furthermore, it was desired to introduce a methyl group at C2, since it had been reported the importance of this group for the activity of 4(1*H*)-pyridones, i.e. its withdrawal results in significant loss of antiplasmodial activity ^[19].

The retrosynthetic analysis for the target molecules is shown in Scheme 3.1. Most of the chemical reactions were identical to ones that had been used for the 4-pyridonimines, and the required quinoline could be obtained via a Conrad-Limpach cyclization.



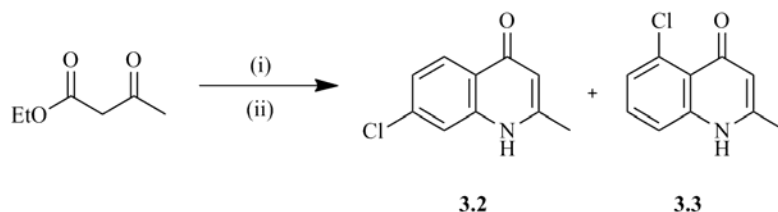
Scheme 3.1 Retrosynthetic analysis of target 4-quinolonimines.

3.2 Synthesis

The synthetic pathway was identical to the one employed for the structure-based design series of 4-pyridonimines, i.e. *N*-alkylation of a given quinoline, followed by S_NAr reaction with a commercial or synthesized primary amine in ethanol, and TEA as a base.

3.2.1 4,7-Dichloro-2-methylquinoline

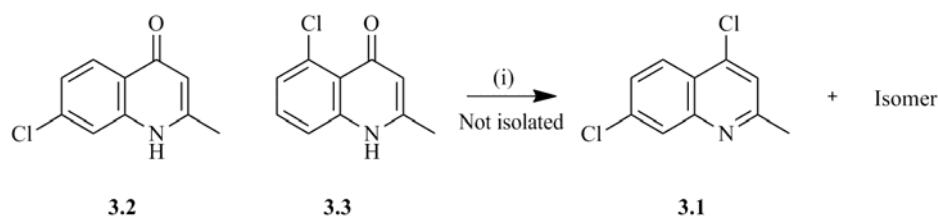
In order to study the effect of the substitution pattern of the quinoline moiety on the antiplasmodial activity, the synthesis of 4,7-dichloro-2-methylquinoline, **3.1**, was tried. This would present a key intermediate for a quinolonimine with a methyl group inserted at C2. The synthetic route for this intermediate included the synthesis of the required 4(1*H*)-quinolone, **3.2**, from the corresponding aniline and ketoester in a Conrad-Limpach procedure, i.e. formation of an imine in the first step, followed by an intra-molecular Friedel-Crafts acylation, Scheme 3.2.



Scheme 3.2 Synthetic pathway for compound **3.2**. Reagents and conditions: (i) PPA, 3-chloroaniline, 110 °C (ii) 150 °C.

However the cyclization step afforded two distinct isomers in equal amounts, **3.2** and **3.3**. Those were isolated in 87% yield and were not separated at this point. It is also noteworthy that this procedure can afford the respective 2(*1H*)-quinolones, but being the thermodynamic product, higher temperatures would be needed, since the imine formation is faster than the formation of the required amide. The two isomers were identified by a characteristic singlet at *ca.* δ 6.15 ppm in the $^1\text{H-NMR}$ spectrum, which accounts for the proton at C3. Moreover, the protons of the ethyl group were not present, which gave evidence of the cyclization step.

Once **3.2** and **3.3** were obtained the synthesis of **3.1** was attempted with POCl_3 under reflux, but a complex mixture was obtained, Scheme 3.3. It appeared that the starting material had decomposed, from TLC analysis, and no further attempts were made.

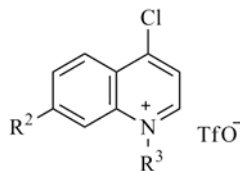


Scheme 3.3 Synthetic pathway to compound **3.1**. Reagents and conditions: (i) POCl_3 , reflux.

3.2.2 Quinolinium salt intermediates

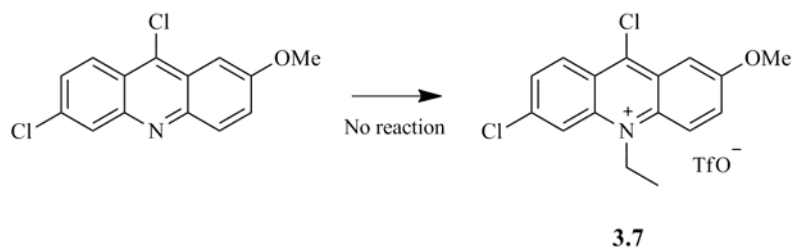
The quinolinium salts **3.4-6** were obtained in good yields from an identical procedure to the pyridinium salts, Table 3.1. Compound **3.6** was obtained in lower yield due to the methanesulfonate starting material being already partially hydrolyzed. All three compounds were easily identified by $^1\text{H-NMR}$ spectroscopy, with the key peak at δ 4.5-5.2 ppm corresponding to the *N-CH_x* protons.

Table 3.1 Structure and yields of **3.4-6**.



Compound	R ²	R ³	Yield (%)
3.4	Cl	Et	92
3.5	CF ₃	Et	95
3.6	Cl	Me	65

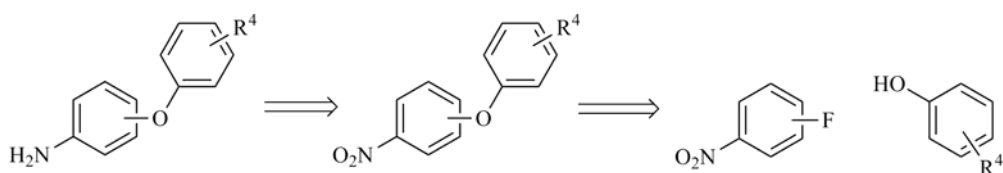
In regard to the reports of potent antiplasmodial activity of acridone derivatives^[100] it was also intended to obtain an acridonimine, but the *N*-alkylation of 6,9-dichloro-2-methoxyacridine with ethyl triflate was not successful due to the very poor dissolution of the starting material in toluene, even at reflux temperature, Scheme 3.4.



Scheme 3.4 Attempted synthesis of 3.7.

3.2.3 1-Nitro-4-phenoxybenzene intermediates

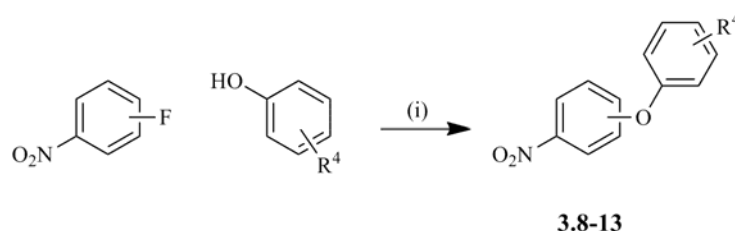
Anilines were selected from previous studies on SAR for cytochrome *bc*₁ inhibitors, either 4(1*H*)-pyridones^[19] or the 4-pyridonimines described in chapter 2. The selection was made in order to incorporate a suitable and extended lipophilic side chain, which has been shown to improve the *bc*₁ complex blocking^[100]. The retrosynthetic analysis for the desired side chains is presented in Scheme 3.5. These can be derived from simple starting materials as phenols and fluoronitrobenzenes. Because the side chains require an aromatic C-O coupling, care had to be taken with the needs of a *S_NAr* reaction. A nitro group, as a precursor of the amino group, had to be present. The electron withdrawing nature of the nitro function facilitates the nucleophilic attack. Additionally, a fluoro atom, instead of another halogen, had also to be present. Fluoride is a very poor leaving group for *S_N2* reactions, but the best leaving group for *S_NAr*, due to the small size and high electronegativity, which favours the characteristic *ipso* attack by the nucleophile, in this type of reactions.



Scheme 3.5 Retrosynthetic analysis for the phenoxyanilines

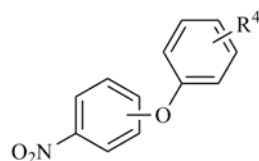
The conversion of nitro intermediates to their aniline counterparts could then be attained in identical fashion to the reduction of the nitrostilbenes, which was reported in the previous chapter.

Compounds **3.8-12** were synthesized in good yields from the reaction of the corresponding starting materials in presence of a base (Na_2CO_3) and a coupling catalyst (CuI), i.e. an Ullmann condensation, Table 3.2 and Scheme 3.6.



Scheme 3.6 Synthetic pathway to compounds **3.8-13**. Reagents and conditions: (i) DMF, Na_2CO_3 , CuI , reflux.

Table 3.2 Structure and yields of **3.8-13**.



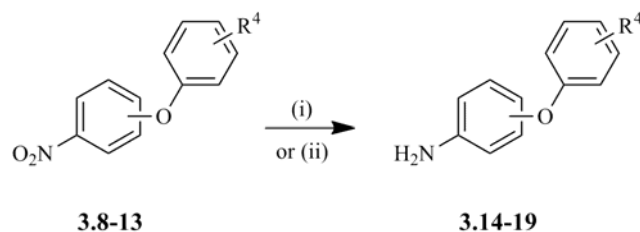
Compound	Isomer	R ⁴	Yield (%)
3.8	4	4-OCF ₃	73
3.9	4	H	65
3.10	4	3-OCF ₃	81
3.11	4	4-CF ₃	71
3.12	4	4-Cl	75
3.13	3	4-OCF ₃	30

As for compound **3.13**, a lower yield was observed, probably due to the *meta* substitution of the fluorine atom, where no conjugated resonance with NO_2 is possible after the *ipso* attack. Therefore, the electron withdrawing nature of the nitro group is not enough to drive the reaction in this case.

The compounds were identified by $^1\text{H-NMR}$ spectroscopy. **3.8**, **3.11** and **3.12** present AA' BB' or AA' XX' systems in the spectrum, as a result of the *para* substitution pattern in both aromatic rings, whereas **3.10** and **3.13** present a more complex spectrum due to the non-equivalence of several protons.

3.2.4 4-Phenoxyanilines intermediates

Reduction of the nitro group in **3.8-11** and **3.13** to their respective amines **3.14-17** and **3.19** was obtained, in good yields, through CTH reaction with TES, as described for the phenethylamines intermediates. Alternatively, for the 4-Cl intermediate, i.e. **3.12**, the nitro reduction was achieved via Sn, HCl reaction, to circumvent dehalogenation of the aromatic ring that took place under catalytic hydrogenation, Scheme 3.7. The yields can be found in Table 3.3.



Scheme 3.7 Synthetic pathway to compounds **3.14-19**. Reagents and conditions: (i) CH₂Cl₂, MeOH, TES, Pd-C 10%, rt; (ii) Sn, HCl, reflux.

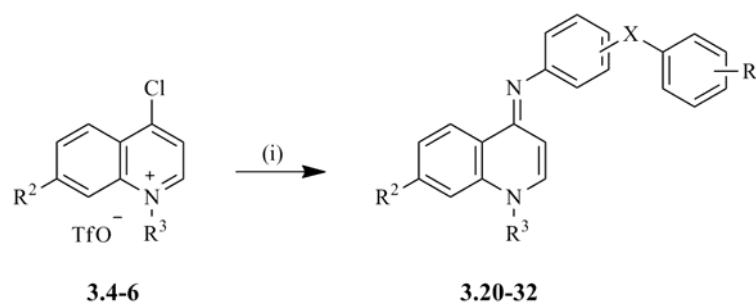
Table 3.3 Structure and yields for compounds **3.14-19**.

Compound	Isomer	R ³	Yield (%)
3.14	4	4-OCF ₃	68
3.15	4	H	75
3.16	4	3-OCF ₃	85
3.17	4	4-CF ₃	93
3.18	4	4-Cl	85
3.19	3	4-OCF ₃	85

This set of anilines was identified from ¹H-NMR spectroscopy, by comparison with the spectrum of its precursors. Despite presenting an identical coupling pattern and the same integration for each set of peaks, the chemical shifts are significantly different. Compounds **3.8-13** present a peak at *ca.* δ 8.5 ppm which is assigned to the the protons nearer to the nitro group, whereas for compounds **3.14-19** the most deshielded protons are seen at *ca.* δ 7.5 ppm. The NH₂ protons could also be found at *ca.* δ 3.5 ppm.

3.2.5 4-Quinolonimines

The synthesis of 4-quinolonimines was carried out via their quinolinium triflates in an identical procedure to what was described for 4-pyridonimines, Scheme 3.8. Besides the synthesized anilines, two other commercial building blocks, 4-benzylaniline and 4-biphenylamine, were used to add further variation to the SAR analysis that would follow. These compounds were obtained in excellent yields and their structures are given in Table 3.4. Compound **3.32** was not isolated. In this case, only degradation products from the aniline side chain were recovered. All other compounds were isolated as triflate salts.

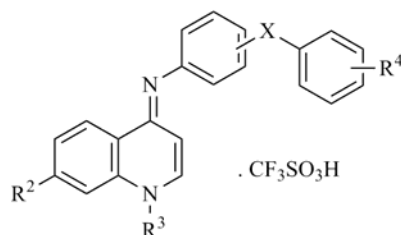


Scheme 3.8 Synthetic pathway to compounds **3.20-32**. Reagents and conditions: (i) EtOH, TEA, aniline, reflux.

The compounds were characterized with several spectroscopic techniques, including 1D and 2D NMR, IR and mass spectrometry. X-Ray crystallography studies were also performed for **3.22**. Considering all spectral data it was possible to conclude that only the (*E*) isomer of each compound was formed.

The $^1\text{H-NMR}$ spectra of **3.20-31** presented the same general features as the ones exhibited by the 4-pyridonimine series. For example, the Ar-*H3* resonance in **3.22** appears as a doublet at *ca.* δ 6.95 ppm ($^3J = 7.6$ Hz), which represents a dramatic upfield shift compared to the value of δ 8.33 ppm for the Ar-*H3* in **3.4** ($^3J = 6.4$ Hz). Furthermore, the Ar-*H2* doublet can be identified at δ 8.47 ppm, whilst protons Ar-*H6* (δ 7.87 ppm), and Ar-*H8* (δ 8.31 ppm), are given as doublets. From the $^1\text{H-}^1\text{H}$ COSY experiment it was also possible to see association between Ar-*H6* and Ar-*H5* (δ 8.64 ppm). The Ar-*H5* proton is superimposed to two protons from the AA' XX' system, and the other two are found at δ 7.55 ppm. The remaining five protons in the spectrum correspond to the terminal aryl moiety. The *N-CH*₂ peak is found at *ca.* δ 4.6 ppm which is a common feature for all 4-quinolonimines. For the remaining compounds, the $^1\text{H-NMR}$ spectrum differed mainly at the chemical shifts and couplings from the terminal aryl, due to the substitution pattern.

Table 3.4 Structure and yields of compounds 3.20-32.



Compound	R ²	R ³	Isomer	X	R ⁴	Yield (%)
3.20	Cl	Et	3'	CH ₂ CH ₂	4-OCF ₃	76
3.21	CF ₃	Et	3'	CH ₂ CH ₂	4-OCF ₃	81
3.22	Cl	Et	4'	-	H	100
3.23	CF ₃	Et	4'	-	H	98
3.24	Cl	Et	4'	CH ₂	H	86
3.25	Cl	Et	4'	O	H	92
3.26	Cl	Et	4'	O	4-Cl	83
3.27	Cl	Et	4'	O	4-OCF ₃	75
3.28	Cl	Et	4'	O	4-CF ₃	99
3.29	Cl	Me	4'	O	4-CF ₃	73
3.30	Cl	Et	4'	O	3-OCF ₃	85
3.31	CF ₃	Et	4'	O	3-OCF ₃	97
3.32	Cl	Et	3'	O	4-OCF ₃	-

The fragmentation of compounds **3.20** and **3.21** presents similar features to the 4-pyridonimines, i. e. break at CH₂-CH₂ bond. For the remaining compounds, the base peak is accounted to the [M+H]⁺ adduct, or a peak resulting from loss of the ethyl group. In opposition to the 4-pyridonimine series, the N-C bond is the most labile. Analysis of daughter fragments, allowed to see that fragmentation at the linker between the two aryl moieties occurs subsequently, as in **3.28**. However, in opposition to its *N*-ethyl counterpart, compound **3.29** breaks in the linker connection prior to other fragmentations. This presented the only exception among the studied compounds. The fragmentation patterns are shown in Figure 3.2.

In the infra-red spectrum, the imine linkage resulted in absorption at *ca.* 1600 cm⁻¹, as a consequence of stretching vibrations. This is a marginally lower wave number than that of the 4-pyridonimines, as a consequence of the additional aromatic ring, i. e. conjugation.

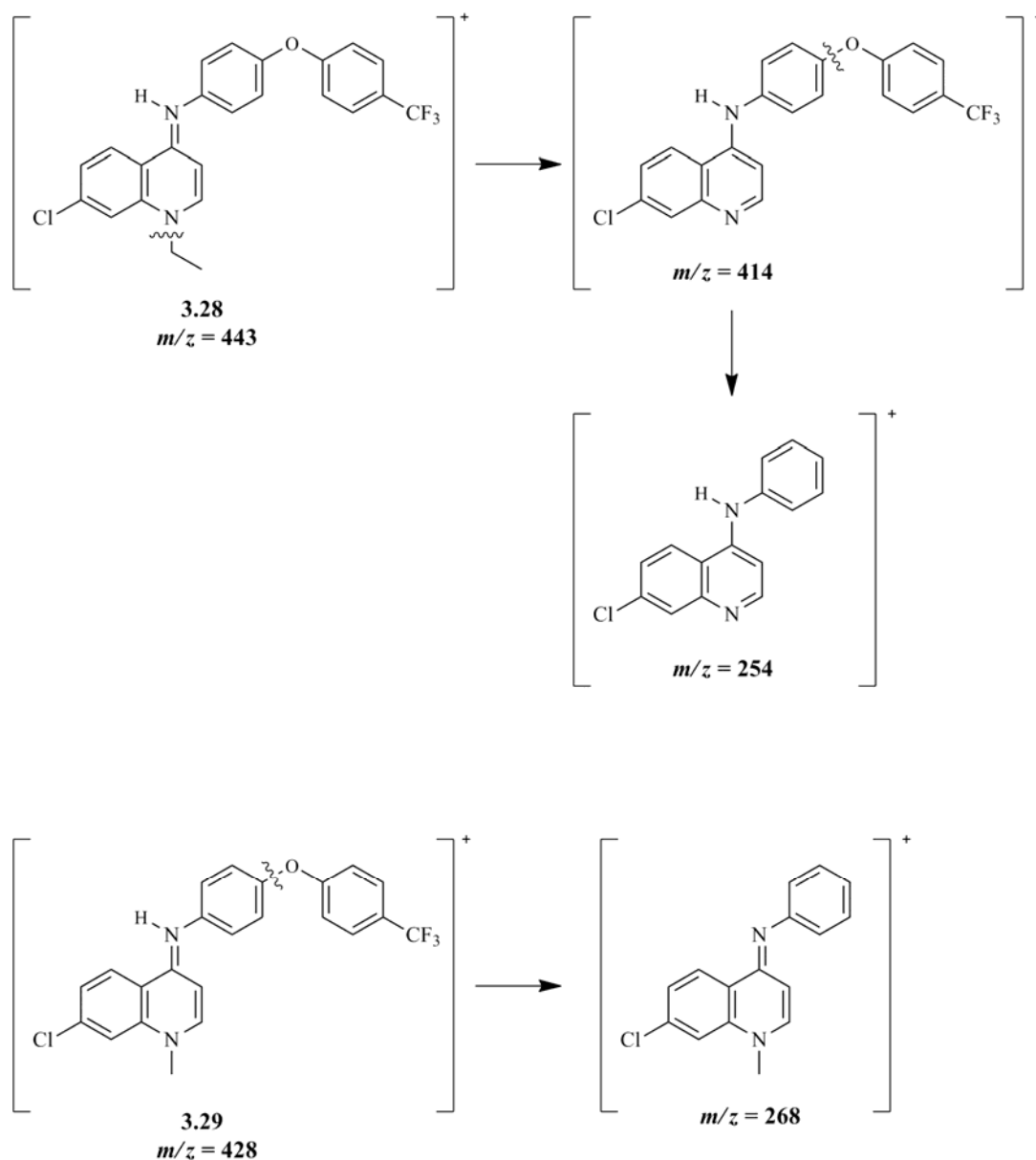


Figure 3.2 Fragmentation pattern for 4-quinolonimines, exemplified by **3.28** and **3.29**.

In order to confirm also the (*E*) configuration for this series of 4-quinolonimines, compound **3.22** was slowly crystallized from water and acetone, affording colourless prisms suitable for analysis. As opposed to **2.8**, only one geometry independent molecule was obtained, and the crystals corresponded to the neutral form of **3.22**, Figure 3.3.

The obtained imine bond distance of 1.2999(18) Å in **3.22** differed significantly (~0.04 Å) from what had been observed for **2.8**. This was expected and consistent with previous reports, since the imine is not protonated in this case. The aromatic rings of the biphenyl side chain were also not coplanar, as given by the C19-C18-C21-C26 dihedral angle of -26.7(2)°. These were also not

coplanar with the 4-quinolonimine group, with a C5-C4-N14-C15 dihedral angle of $-178.98(12)^\circ$, i.e. the rings are almost perpendicular to one another. Finally, the 4-quinolonimine ring is almost planar, as shown by the C2-C3-C4-C5 dihedral angle of $4.4(2)^\circ$. Further details of the crystal structure can be found in Appendix 2.1.

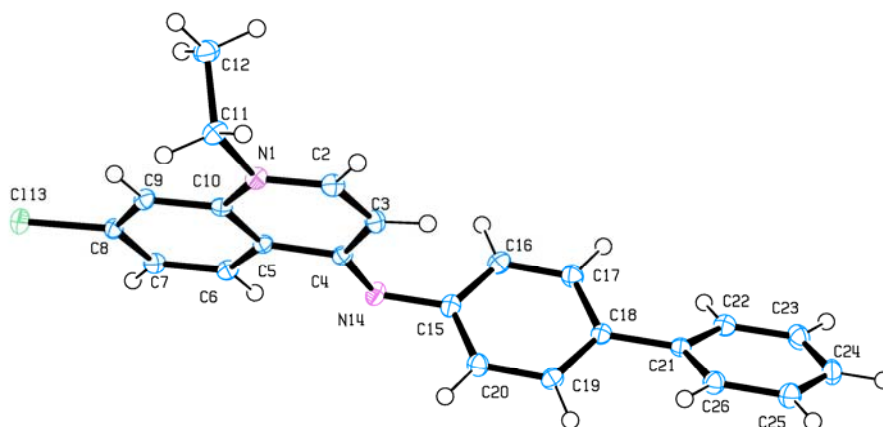


Figure 3.3 ORTEP view of the molecular structure of **3.22**, showing the labelling of all non-hydrogen atoms. Displacement ellipsoids for non-hydrogen atoms are shown at the 50% probability level.

Antiplasmodial activity and toxicity

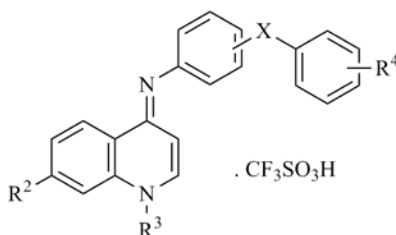
Polycyclic compounds with the same substructure have been reported to present antiproliferative activity, namely by selective quadruplex DNA binding. Those have shown to efficiently target telomere ends, blocking telomerases^[232, 233]. Some 4-quinolonimines have also been described for the treatment of memory disfunctions^[234], Src kinase inhibitors^[235], potassium ion channel inhibitors^[236] and topoisomerase II inhibitors^[237], but no antiplasmodial activity has been reported. The synthesized compounds were tested against the *P. falciparum* W2 strain, Table 3.5. They showed improved activity when compared to their 4-pyridonimine counterparts and clopidol. The additional aromatic ring should be responsible for an increased lipophilicity, and the consequent drop in the IC_{50} values, as was initially hypothesized. Inspection of the data in Table 3.5 allows the following observations regarding the SAR of **3.20-31**:

- Biaryl compounds, i.e. **3.22** and **3.23**, were the most active against the W2 strain of *P. falciparum*, presenting activities of *ca.* $0.55 \mu\text{M}$;
- Introduction of spacers between aromatic systems is detrimental for the antiplasmodial activity, i.e. no spacer (**3.22**, $0.54 \mu\text{M}$) > O (**3.25**, $0.89 \mu\text{M}$) > CH_2 (**3.24**, $1.69 \mu\text{M}$);
- Regarding the 4-phenoxy derivatives, the substituent effect on the antiplasmodial activity against the W2 strain was 4-CF_3 (**3.28**, $1.26 \mu\text{M}$) < 4-Cl (**3.26**, $1.09 \mu\text{M}$) < 4-OCF_3 (**3.27**,

0.96 μM) < H (**3.25**, 0.89 μM) in opposition to what had been reported for 4(1*H*)-pyridones and 4-pyridonimines. Isomerization of 4-OCF₃, **3.27**, to 3-OCF₃, **3.30**, led to a small drop of activity;

- d) Substitution of *N*-ethyl, **3.28**, to *N*-methyl, **3.29**, led to the increase of antiplasmodial activity, again in opposition to what had been observed in the previous studies;
- e) Substitution of Cl for CF₃ at C7 resulted in a 2-fold increase of antiplasmodial activity for the phenylethyl derivatives, **3.20** vs. **3.21**. However, the trend was not observed for the 4-phenoxy compounds, resulting in an increase of IC₅₀ from 1.18 μM for the 7-Cl compound, **3.30**, to 1.56 μM for the 7-CF₃ counterpart, **3.31**. For the biaryl compounds, no significant change of IC₅₀ was observed, **3.22** vs. **3.23**.

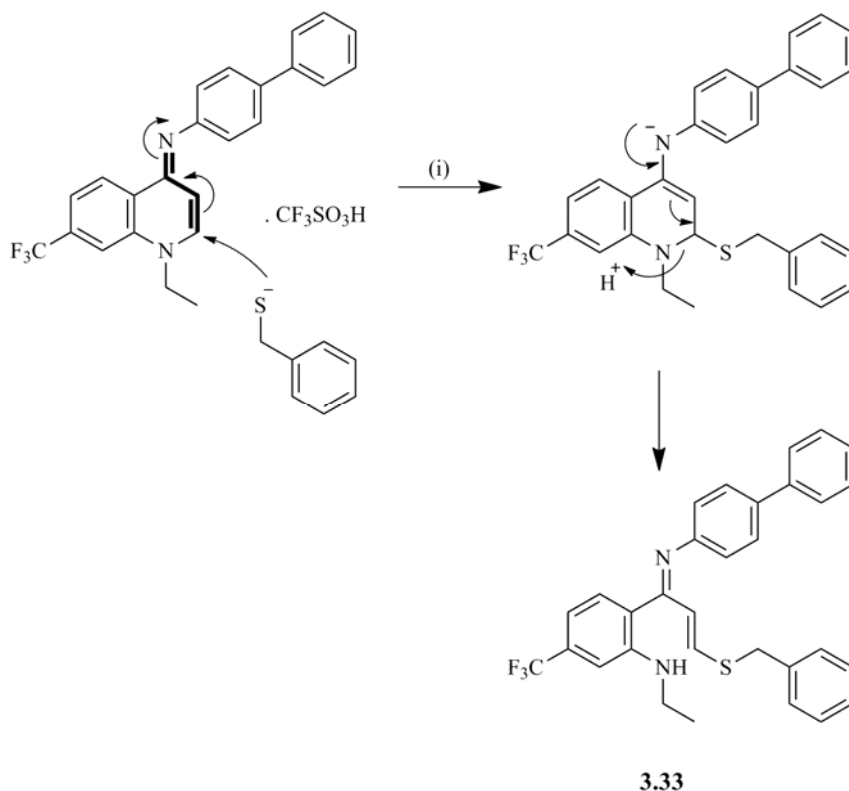
Table 3.5 Effect of R²-R⁴ and X substitutions in compounds **3.20-31** on the antiplasmodial activity against *P. falciparum* W2 strain and association constants (binding to FPIX in 1:1 stoichiometry).



Compound	R ²	R ³	Isomer	X	R ⁴	IC ₅₀ ± SD (μM)	log(<i>K</i> _{ass} / μM^{-1})	<i>K</i> _{ass} / M^{-1}
3.20	Cl	Et	3'	CH ₂ CH ₂	4-OCF ₃	3.11 ± 0.18	5.2	1.7 × 10 ⁻⁷
3.21	CF ₃	Et	3'	CH ₂ CH ₂	4-OCF ₃	1.67 ± 0.03	4.9	7.5 × 10 ⁻⁸
3.22	Cl	Et	4'	-	H	0.54 ± 0.02	5.6	3.6 × 10 ⁻⁷
3.23	CF ₃	Et	4'	-	H	0.59 ± 0.01	5.7	5.3 × 10 ⁻⁷
3.24	Cl	Et	4'	CH ₂	H	1.69 ± 0.11	5.0	9.7 × 10 ⁻⁸
3.25	Cl	Et	4'	O	H	0.89 ± 0.08	5.4	2.6 × 10 ⁻⁷
3.26	Cl	Et	4'	O	4-Cl	1.09 ± 0.15	5.1	1.4 × 10 ⁻⁷
3.27	Cl	Et	4'	O	4-OCF ₃	0.96 ± 0.01	4.9	8.2 × 10 ⁻⁸
3.28	Cl	Et	4'	O	4-CF ₃	1.26 ± 0.07	4.7	4.9 × 10 ⁻⁸
3.29	Cl	Me	4'	O	4-CF ₃	1.08 ± 0.04	4.9	7.6 × 10 ⁻⁸
3.30	Cl	Et	4'	O	3-OCF ₃	1.18 ± 0.01	5.1	1.2 × 10 ⁻⁷
3.31	CF ₃	Et	4'	O	3-OCF ₃	1.56 ± 0.08	3.9	7.2 × 10 ⁻⁹
Clopidol						9.73 ± 0.07	4.7	4.8 × 10 ⁻⁸
Atovaquone						0.0012	N.D.	N.D.
Chloroquine							4.8	5.9 × 10 ⁻⁸

N.D. - Not Determined

Given the presence of an α,β -unsaturated imine for these compounds, it was investigated whether they were prone to Michael additions. If so, this would present a major problem, because of the potential depletion of host's glutathione, resulting in acute toxicity. Therefore, the glutathione attack was mimicked by reaction of **3.23** with excess TEA and benzylthiol in methanol, for 24 hours at room temperature, Scheme 3.9. After flash chromatography, 97% of the starting material was recovered and thus, no toxicity from addition of sulfur-containing proteins is expected.



Scheme 3.9 Simulated glutathione attack to afford **3.33**. Reagents and conditions: (i) TEA, MeOH, rt.

Molecular docking

To clarify the possible binding mode of **3.20**, **3.22** and **3.27**, a docking study was carried out at the bc_1 complex. At first glance, it is possible to see that **3.20**, Figure 3.4 A, binds in a complete different pose, and presents a different shape to that of **3.22**, Figure 3.4 B, and **3.27**, Figure 3.4 C. Although no hydrogen bonds with glutamate 272 and histidine 181 can be formed, it appears that the side chain is better located in the binding channel, i.e. **3.22** and **3.27**, instead of the 4-quinolonimine moiety, i.e. **3.20**, as the conjunction of activity and docking results suggest. Thus, this side chain interacts through strong hydrophobic interactions with the active site residues.

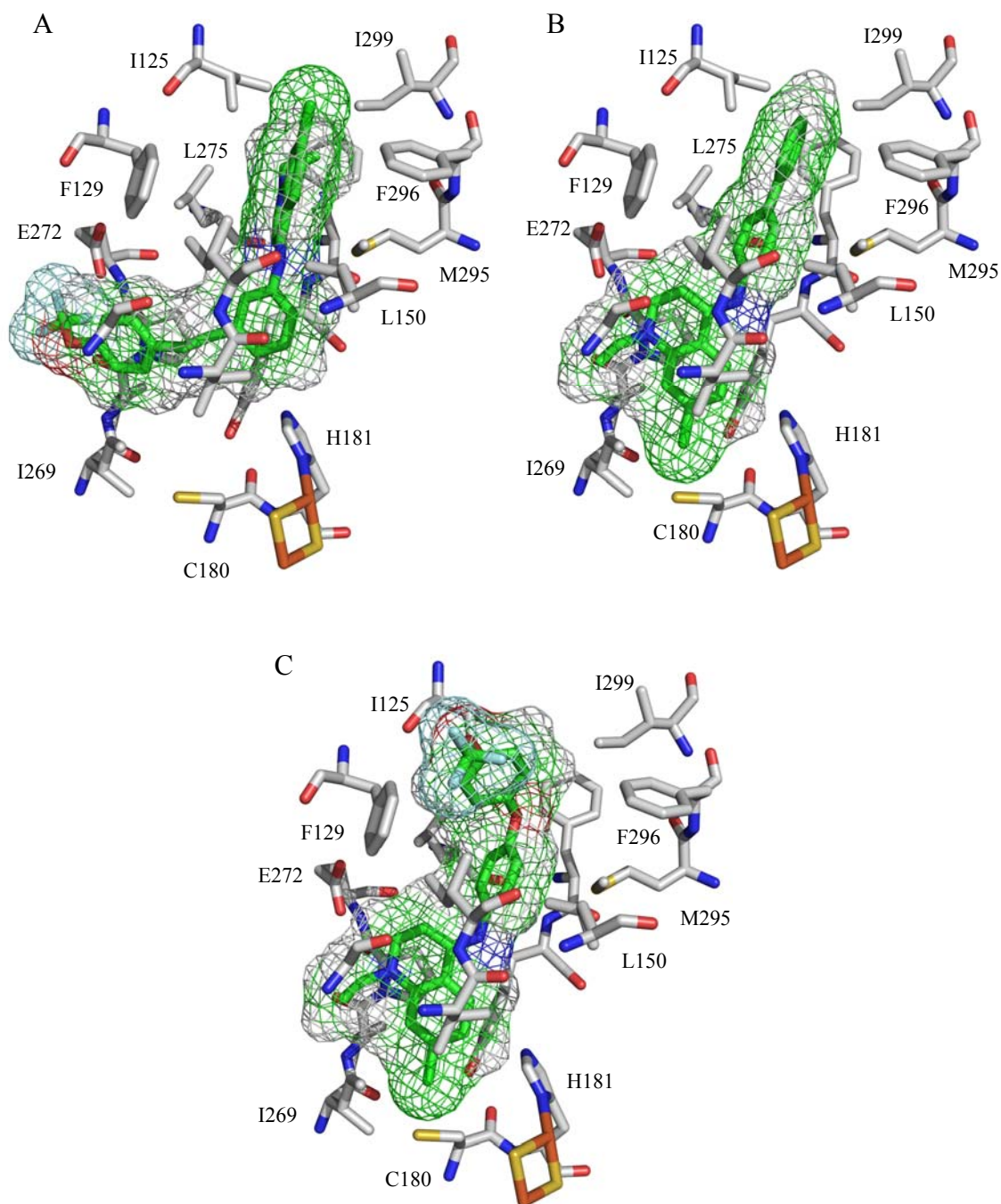


Figure 3.4 Docking poses of **3.20**, **3.22** and **3.27**, with mesh highlighting the volume and shape of the ligands inside the Q_o binding site of cytochrome *bc*₁.

Anti-liver activity and cytotoxicity

Regarding the liver stage, all compounds showed excellent activity, Figure 3.5, and the following observations can be made:

- The anti-liver activity is dose-dependent for most cases;

- b) All compounds at 10 μM present comparable or better activity than primaquine at 5 μM ;
- c) The nature of the linker does not have a significant effect on the activity, but all other SAR that are seen for the blood stage apply in a qualitative manner at 10 μM ;
- d) At 2 μM most of the compounds still display a comparable or better activity than primaquine. Compounds **3.21-23** and **3.25** are the exceptions;
- e) Compounds **3.26** and **3.27** are the most active at 2 μM , and are, approximately, 2-fold more active than primaquine at 5 μM ;
- f) Compounds **3.22**, **3.23** and **3.25** are among the least active compounds, in opposition to the activity against *P. falciparum* W2 strain. Therefore, the mechanism of action of these compounds in each stage can be different, i.e. the main target in the blood stage may not be present or accessible in the liver stage of the life cycle.

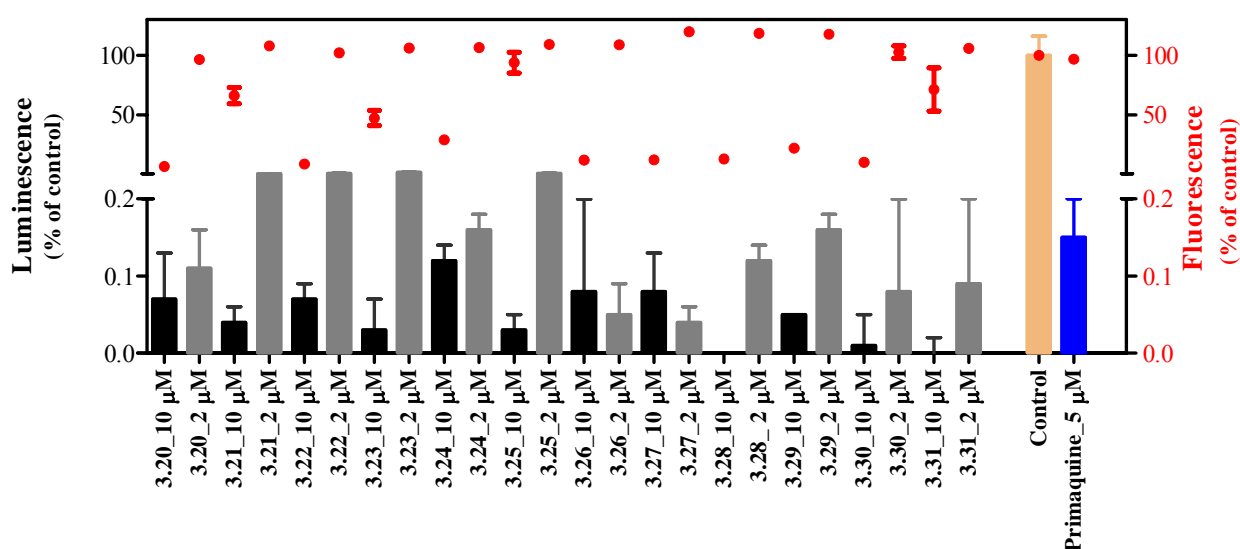


Figure 3.5 Antiplasmodial activity of compounds **3.20-31** at 10 μM (black bars) and 2 μM (grey bars) against liver stage *P. berghei*. The luminescence (bars) is given as percentage of control (MeOH) inhibition. The cytotoxicity was measured in fluorescence (dots) from the Alamar Blue test and is also given as percentage of control. Primaquine was tested at 5 μM . All concentrations were tested and missing bars account for the total suppression of parasite load.

Also, despite the high toxicity that the compounds presented at 10 μM , at 2 μM these were, in the worst case, as toxic as primaquine at 5 μM . As a result, this series of compounds represent good leads for further studies, in particular, against the liver stages of *P. falciparum* and *P. vivax*.

Hematin binding

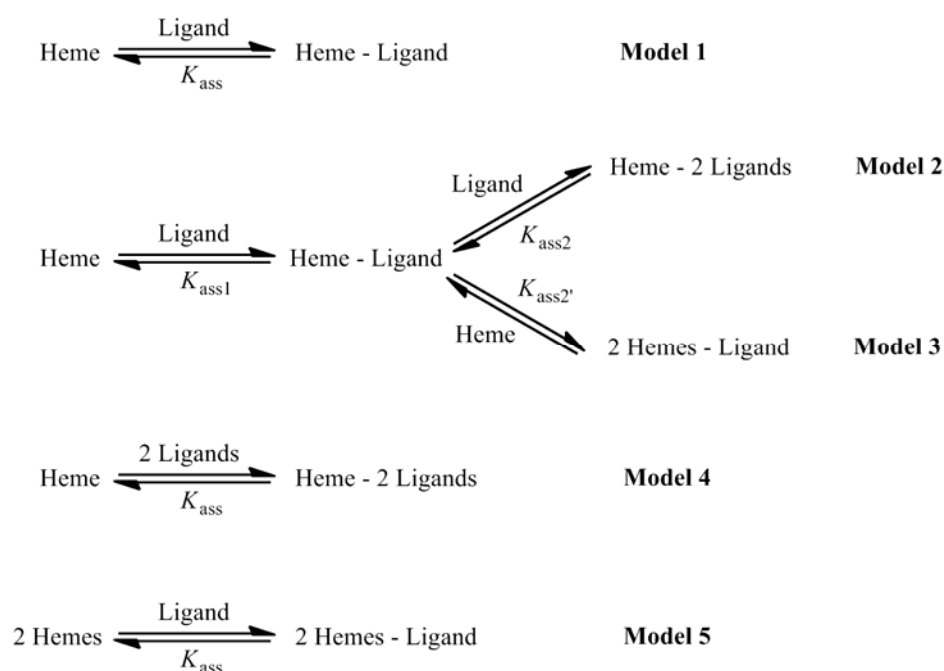
Since compounds **3.20-31** presented the quinoline scaffold, it was also investigated whether they would bind to hematin, in resemblance to other antimalarial drugs. Clopidol was also incorporated in the study and chloroquine was used as a positive control.

Degradation of the host's hemoglobin takes place in the food vacuole and results in free heme, containing Fe^{3+} , which is very toxic because it can generate reactive oxygen species. To overcome its toxicity, the parasite polymerizes free heme into hemozoin, β -hematin. Thus, by corrupting this pathway, accumulation of toxic by-products occur, leading to the parasite death. It is known that several compounds presenting structurally diverse scaffolds exert antiplasmodial activity by enhancing the toxicity of free heme. Aminoquinolines are one of the most relevant classes that are known to inhibit hemozoin formation, but azoles, isonitriles, xanthenes, methylene blue and derivatives, among others can be also counted in [238, 239]. Despite the distinct mode of binding and stoichiometry of the complexes with hematin, the inhibition results from intercalation, i.e. non-covalent association between drugs and ferriprotoporphyrin IX (FPIX). Therefore, the electrostatic interactions of ionizable chemical functions and π - π stacking of aromatic moieties are responsible for the tight binding [240-243].

To study the interaction of all compounds with FPIX, an UV-visible spectroscopic method was applied to determine accurately the binding or dissociation equilibrium constant, K_{ass} or K_{d} , respectively. The titrations were carried out in a mixed aqueous-organic solvent to minimize the porphyrin aggregation effect, which results in a sizeable hypochromic effect at the Soret band. Therefore, a buffered 40% (v/v) DMSO was used to provide a strictly monomeric heme species in solution, in accordance with Egan *et al.* [244, 245]. Additionally, all experiments were carried out at 20 °C and at apparent pH 5.5, to mimic the pH inside the food vacuole of the parasite.

The Soret band of FPIX at 400 nm is the net effect of several closely spaced bands, which also overlaps with the porphyrin N-band [244]. Upon titration with the query compound it was possible to see a considerable hypochromic effect, dependent on the concentration of the added ligand. Hence, this quenching was used to determine the association constants. The absorbances were corrected for dilution and a blank titration of the compounds was performed when those exhibited strong absorbance at 400 nm. Alternatively, the reference cell, containing only the buffer, was supplied with an equal amount of compound as the one added to the titration cell. The experimental data curves were fitted into common models to describe ligand binding, and were statistically analyzed with χ^2 parameters. Model 1, Scheme 3.10, consists of a 1:1 complexation of drug to FPIX, as a function of free ligand concentration. In model 2 there is a stepwise bonding of two equivalents of

the ligand to one equivalent of heme, whereas in model 3 the inverse of model 2 is considered. Models 4 and 5 consist of a simultaneous binding of two equivalents of ligand or heme to one equivalent of heme or ligand, respectively. The mathematical equations of the models were described in detail by Wang *et al.* [246] and Egan *et al.* [245].



Scheme 3.10 Models fitted to the experimental curves.

Chloroquine fitted best to model 1, i.e. 1:1 binding stoichiometry. It presented a $\log K_{\text{ass}}$ of 4.8, under these experimental conditions, a value in accordance with what is reported in the literature [245]. Despite the different experimental conditions, it has been shown that the $\log K_{\text{ass}}$ value is not affected significantly by either pH or ionic strength [247]. However, it is also noteworthy that literature regarding the chloroquine association constant and stoichiometry of binding is very diverse. While Egan *et al.* report a 1:1 stoichiometry with $\log K_{\text{ass}}$ 5.52 [245], O'Neill *et al.* report a stepwise addition of 2 equivalents of chloroquine and $\log K_{\text{ass1}}$ 5.30, $\log K_{\text{ass2}}$ 6.20 [248]. Furthermore, Surolia and co-workers reported a two-site model with $\log K_{\text{ass}}$ 8.1 and 5.1 for high and low affinity sites, respectively, and impressive pH-dependent stoichiometries [249]. The attempt to mathematically fit the chloroquine data, into more complex models was unsuccessful. Since model 3 afforded a poor fit, it is excluded the possibility of FPIX dimerization upon chloroquine

complexation or simultaneous bonding of a second FPIX to the opposite face of the drug, after bonding of the first FPIX. The spectroscopic changes in the Soret band when hematin is titrated with increasing concentrations of chloroquine can be seen in Figure 3.6 A. Also, chloroquine showed no absorbance at 400 nm, Figure 3.6 B, and the decay of absorbance of FPIX at 400 nm, for chloroquine, can be found in Figure 3.6 C.

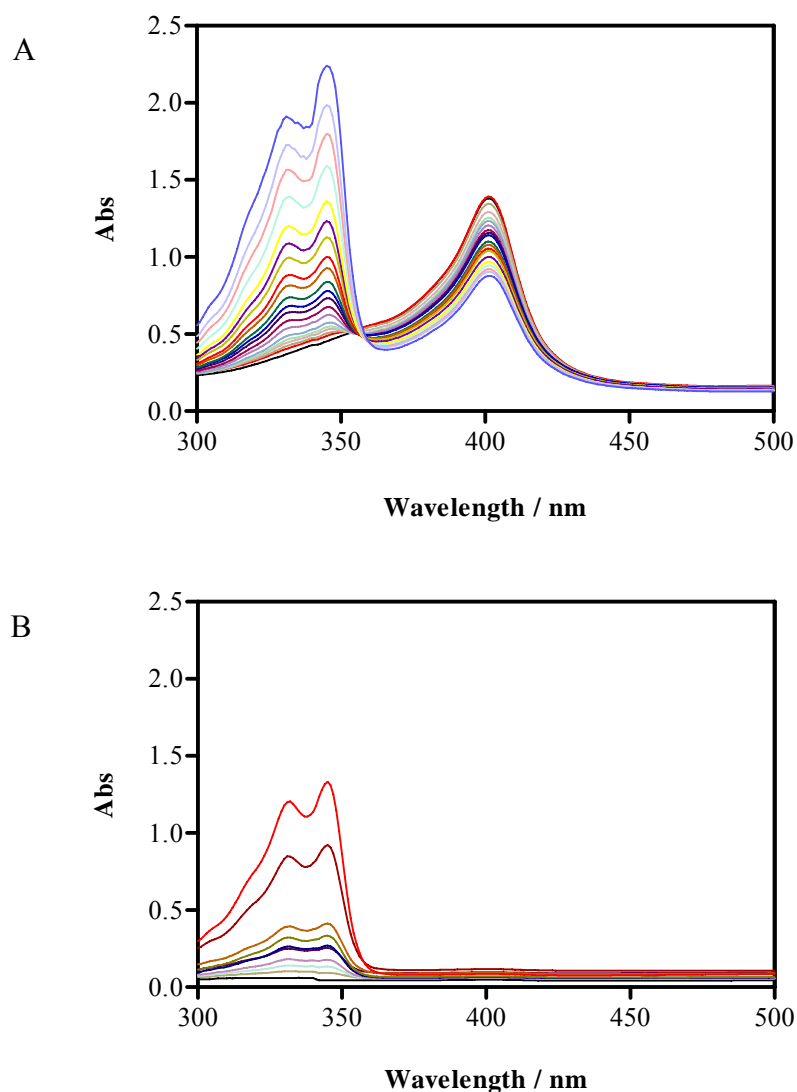


Figure 3.6 (A) Spectroscopic changes in the Soret band (400 nm) when hematin is titrated with increasing concentrations of chloroquine (20 °C, apparent pH 5.5, HEPES buffer with 40% DMSO); (B) Absorbance of chloroquine under the same experimental conditions as (A).

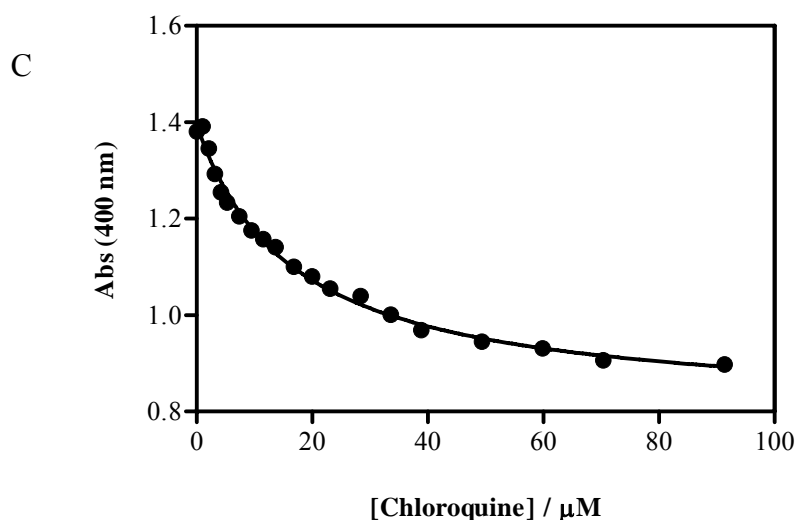
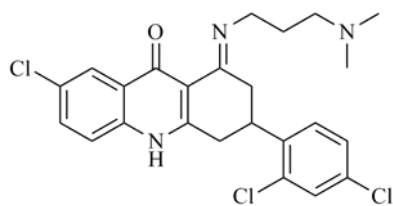


Figure 3.7 (cont.) (C) Variation of absorbance of hematin at 400 nm as a function of chloroquine concentration. The solid line represents the best fit curve for the 1:1 stoichiometry model. The curve was corrected for dilution and absorbance of the ligand.

Clopidol is a known bc_1 complex inhibitor and was tested in order to predict the binding affinity of 4(1*H*)-pyridones to hematin. Interestingly, in this incubation assay, the $\log K_{\text{ass}}$ was identical to chloroquine with a value of 4.7 and the 1:1 stoichiometry was the best fit model ($r^2 = 0.9906$). This was not an expected result, and binding of clopidol to hematin must be governed by different determinants to those of chloroquine. However, it is important to stress that, despite the strong association, care must be taken in concluding that this might be a secondary mechanism of action, from off-target binding. Clopidol does not present the requested features to accumulate in the acidic food vacuole, i.e. it has no ionizable functions and, therefore, it is not expected to accumulate up to values equivalent to the IC_{50} . The same observation had been made for 9-epiquinine. At a $\log K_a$ of 4.04, it binds to heme but it is known that it does not inhibit hematin polymerization into hemozoin [245]. Therefore, binding to hematin appears to be necessary, but not sufficient to safely conclude the mechanism of action of a given molecule. On a similar note to clopidol, floxacrine binds to hematin, despite being a potent bc_1 complex inhibitor. Also, its WR 243251 imino analogue, **3.34**, showed identical heme binding to chloroquine, despite being more active against the chloroquine sensitive (NF54), and chloroquine resistant (K1) strains, which underlies the existence of another mechanism of action [106, 250].



3.34

Finally, primaquine which is thought to wield antimalarial activity from inhibition of the mitochondrial function is reported to not show detectable binding to heme [245].

Clopidol did not absorb in the 300-500 nm range and the decay of absorbance of FPIX at 400 nm can be seen in Figure 3.7 A, as well as the spectroscopic changes in the Soret band, Figure 3.7 B. The data was untractable to other models, except model 2 (2 ligands : 1 heme) which also gave a satisfactory compliance to the experimental data ($\log K_{\text{ass}} = 3.4$, $r^2 = 0.9813$). No Fisher's test was needed in this case as the degrees of freedom are the same for both models, i.e. the model with higher r^2 applies.

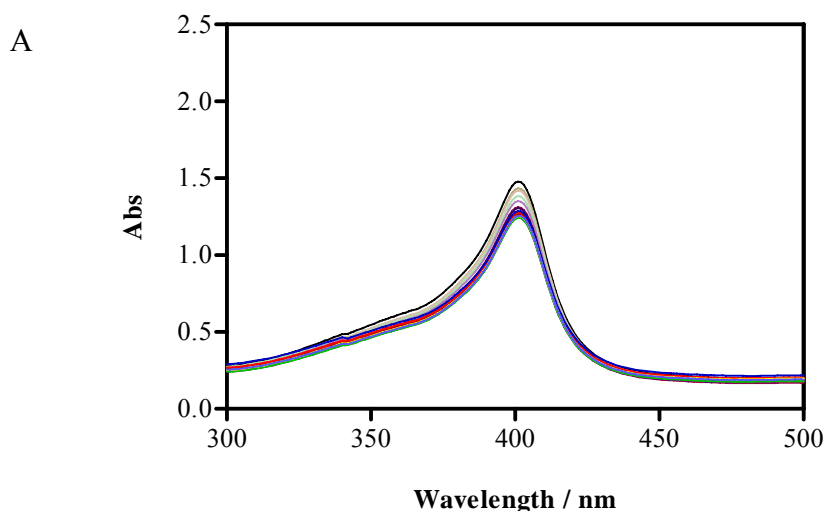


Figure 3.8 A) Spectroscopic changes in the Soret band (400 nm) when hematin is titrated with increasing concentrations of clopidol (20 °C, apparent pH 5.5, HEPES buffer with 40% DMSO).

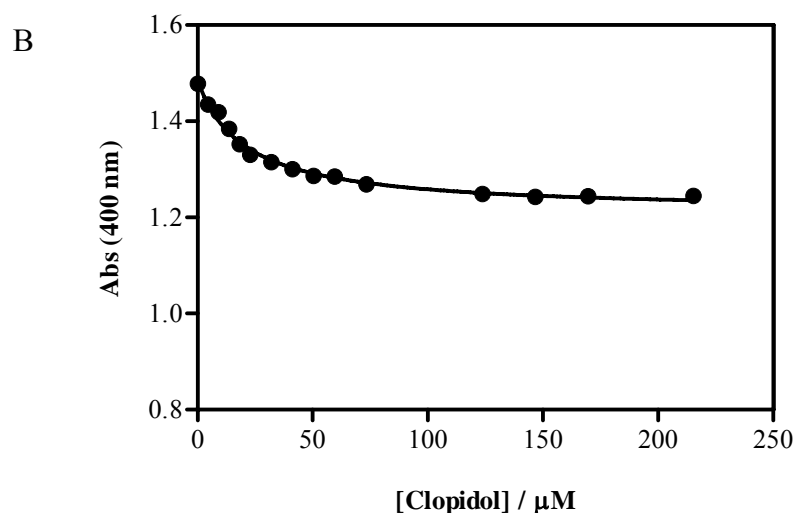


Figure 3.9 (cont.) (B) Variation of absorbance of hematin at 400 nm as a function of clopidol concentration. The solid line represents the best fit curve for the 1:1 stoichiometry model. The curve was corrected for dilution and absorbance of the ligand.

All the other studied compounds, **3.20-31**, showed an excellent agreement to the 1:1 binding stoichiometry with no plausible fitting to other models, and needed correction for their absorbance at 400 nm. Compound **3.28** is given as an example for the curves obtained for this series, Figure 3.8 (Appendix 2.2 for the remaining compounds).

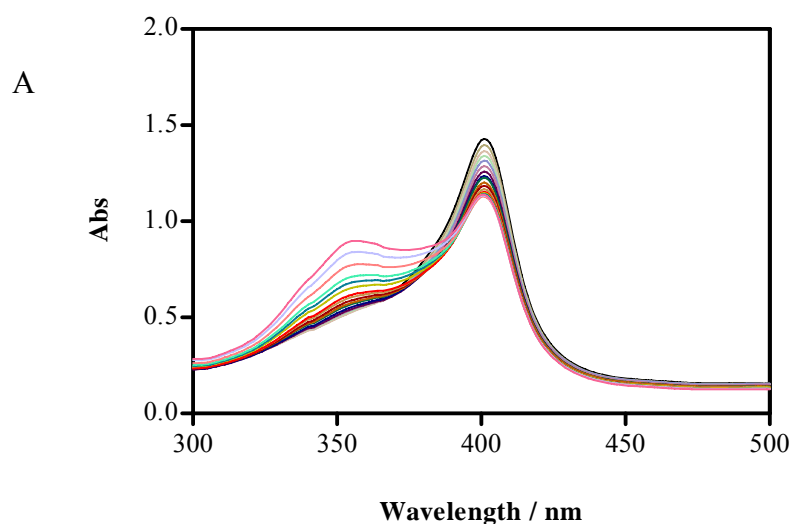


Figure 3.10 (A) Spectroscopic changes in the Soret band (400 nm) when hematin is titrated with increasing concentrations of **3.28** (20 °C, apparent pH 5.5, HEPES buffer with 40% DMSO).

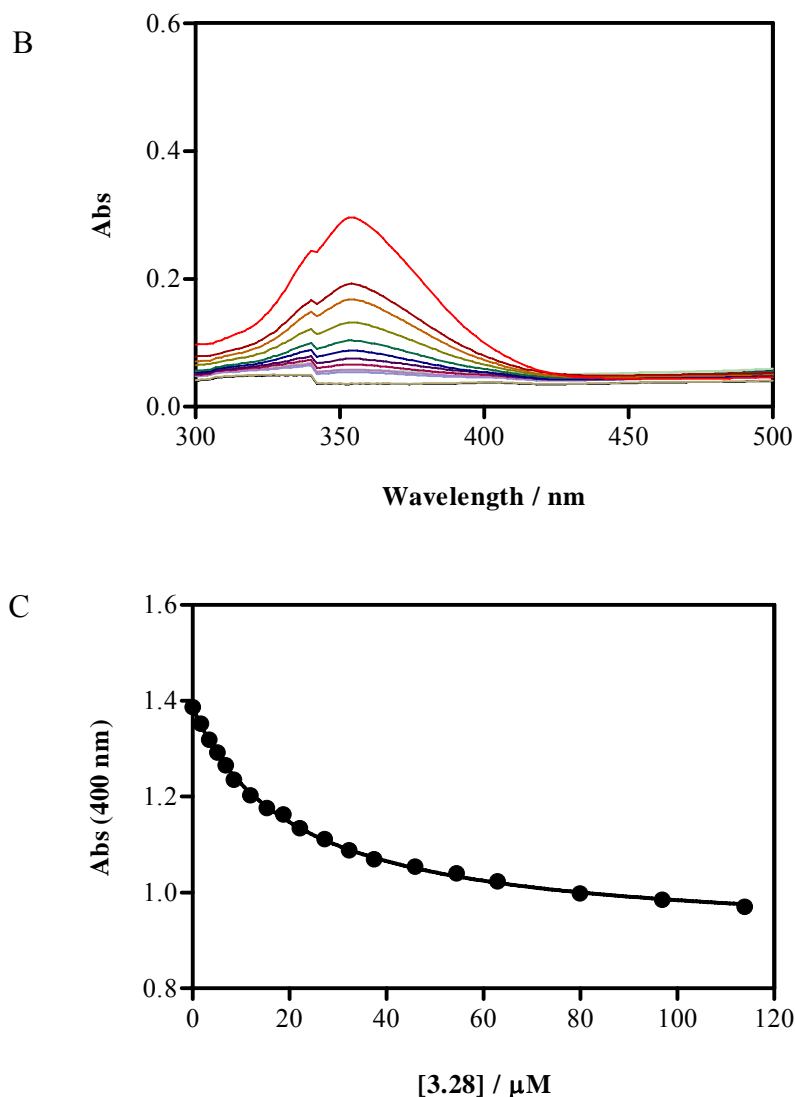


Figure 3.11 (cont.) (B) Absorbance of **3.28** under the same experimental conditions as (A); (C) Variation of absorbance of hematin at 400 nm as a function of **3.28** concentration. The solid line represents the best fit curve for the 1:1 stoichiometry model. The curve was corrected for dilution and absorbance of the ligand.

Inspection of Table 3.5 allows the following observations, regarding FPIX binding:

- a) All compounds bound to hematin at least as tightly as chloroquine, with exception of **3.31**, whose $\log K_{\text{ass}}$ is 3.9. The CF_3 group at C7 must be responsible for the weaker binding as its 7-Cl counterpart, **3.30**, displayed a $\log K_{\text{ass}}$ of 5.1. Interestingly, such variation on C7 did not have the same effect on the biphenyl compounds **3.22** and **3.23**. Both presented the same $\log K_{\text{ass}}$, which was the highest among the studied compounds. Given that those two compounds were the most active against the W2 strain, it is possible that blocking of hematin polymerization plays a role in the mode of action;

- b) The oxygen linker favours binding to FPIX compared to the methylene group, i. e. **3.25** vs. **3.24**, again in line with their antiplasmodial activities;
- c) Introduction of an electron withdrawing group in the terminal aryl moiety reduces binding to FPIX in the order, H (**3.25**) > 4-Cl (**3.26**) = 3-OCF₃ (**3.30**) > 4-OCF₃ (**3.27**) > 4-CF₃ (**3.28**), in similar trend as the antiplasmodial activity;
- d) Substitution of *N*-methyl to *N*-ethyl, **3.29** vs. **3.28**, did not result in significant changes regarding FPIX binding.

3.3 Conclusions

These 4-quinolonimines showed improved antiplasmodial and anti-liver activity in comparison with the 4-pyridonimines. Furthermore, they are likely unreactive towards the 1,4-addition of proteins containing sulfur, such as glutathione, and displayed low toxicity at 2 μM. Given the compliance with the rule of 5, with the exception of the predicted logP (ranging from 6 to 8 for the neutral form), these compounds can find an interesting application in the development of new antimalarial agents. The studies regarding the inhibition of the *bc*₁ complex are ongoing for the most active compounds.

CHAPTER 4

CHROMONE SCAFFOLD

4. CHROMONE SCAFFOLD

4.1 Rationale

Chromones are a class of structurally diverse compounds. Applications of compounds from this class, and from the closely related flavones and isoflavones, can be found in the literature, in a vast number of fields. Some have shown potent anticoronavirus activity^[251], anticholinesterase activity^[252], antiproliferative activity^[253-257], anti-inflammatory^[258], human steroid sulfatase inhibitory activity^[259], and have even been used as radioligands for imaging^[260-262], among others^[263-266]. Additionally, there have been recent reports of modest to potent antiplasmodial activity related to flavones^[200, 267-270].

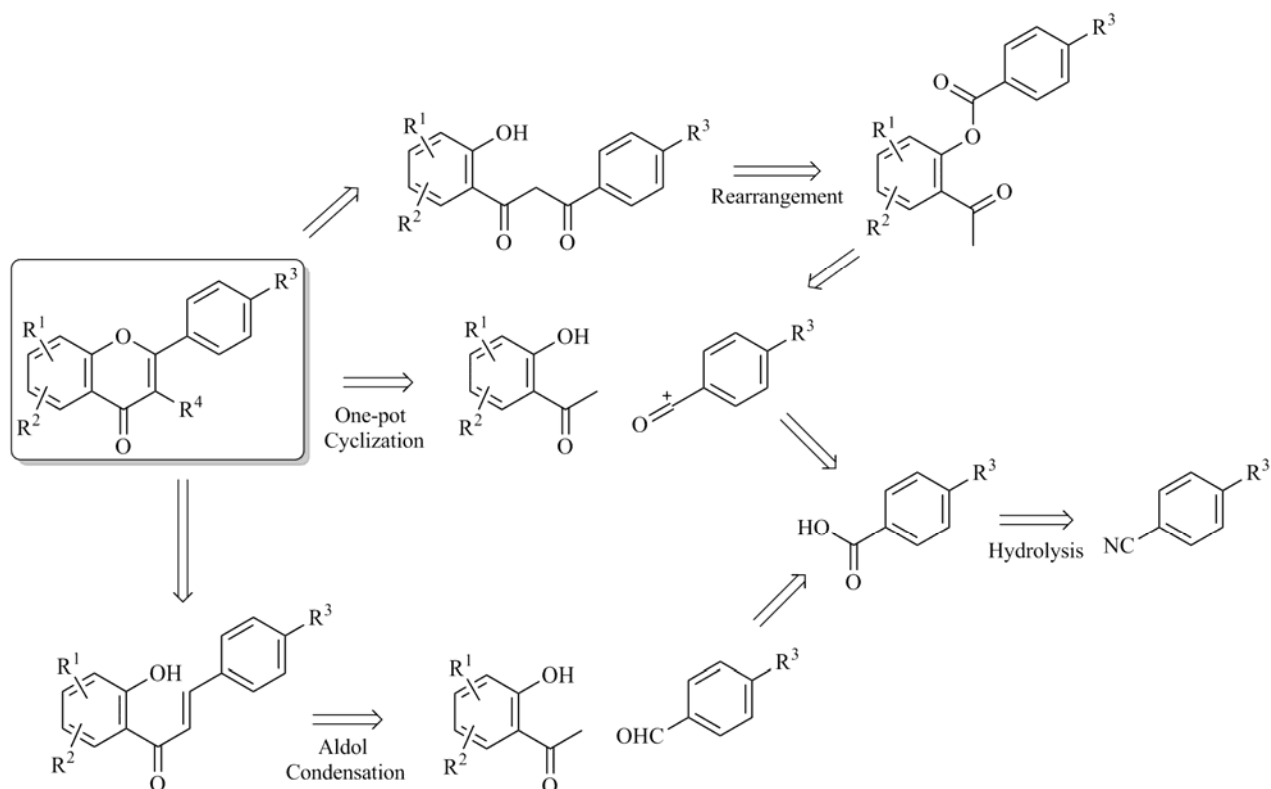
Stigmatellin is a natural, chromone-based compound with potent anti-*bc*₁ complex activity and an IC₅₀ of 2 μM in whole cell cultures^[62, 159]. With the results from the previous series of compounds it was, therefore, necessary to insert the side chains that resulted in better antiplasmodial activity for the 4-quinolonimine series, into diverse chromone rings, in order to improve the activity against *P. falciparum*. Since the antiplasmodial mode of action for stigmatellin is through the inhibition of cytochrome *bc*₁, all synthesized compounds would be expected to block this vital pathway. Also, isoflavones have shown to possess an interesting antiplasmodial activity, which might also be related to inhibition of the mitochondrial function, at the *bc*₁ complex level^[271, 272].

4.2 Synthesis

4.2.1 Retrosynthetic analysis of flavones

A quick search in the literature revealed a wide range of synthetic procedures to obtain flavones from simple starting materials. The Sonogashira carbonylative annulation is a common procedure, where an iodophenol is reacted with an alkyne in presence of carbon monoxide^[273-275]. Flavones can also be obtained following the Baker-Venkataraman reaction at room temperature, conventional heating or MW^[276-281]. In short, a 2-hydroxyacetophenone is esterified with a suitable acylating agent, which rearranges to the 1,3-diketone compound under basic conditions. This key intermediate is then cyclized into the corresponding flavone. Alternatively, flavones can be obtained from cyclization of the corresponding chalcones^[282-285].

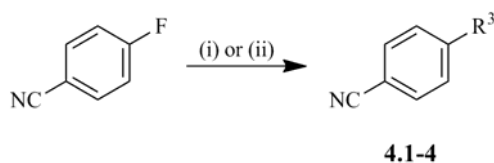
The retrosynthetic analysis in Scheme 4.1 shows the general strategy that was employed to obtain the target compounds. Whereas the 2-hydroxyacetophenones were commercially available, most of the required acid chlorides or anhydrides (represented as a synthon) had to be synthesized. These chemical entities can be easily derived from carboxylic acids and those can be obtained from nitriles, which are sufficiently strong electron withdrawing groups to favour S_NAr reactions. Some of these reactions can be carried out as a one-pot procedure or in multi-stage synthesis.



Scheme 4.1 Retrosynthetic analysis of target flavones.

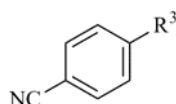
4.2.2 4-Phenoxybenzotrile and 4-phenoxybenzoic acid intermediates

The synthesis of 4-phenoxybenzotrile intermediates was initially carried out using the same Ullmann condensation procedure (method A) described in chapter 3. As an alternative, the reactions were conducted under identical conditions, but without the copper catalyst (method B), Scheme 4.2. These afforded matching yields over a full day of reflux, when compared to the 5 hours that were needed in method A, Table 4.1. However, in method B the purification was simpler, i.e. without the need to handle copper salts, which resulted in a less demanding work-up.



Scheme 4.2 Synthetic pathway to compounds **4.1-4**. Reagents and conditions: (i) DMF, Na₂CO₃, CuI, nucleophile, reflux; (ii) DMF, Na₂CO₃, nucleophile, reflux.

Table 4.1 Structure and yields of compounds **4.1-4**.



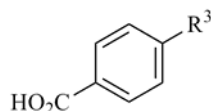
Compound	Method	R ³	Yield (%)
4.1	A	4-OPh-4-Cl	95
4.1	B	4-OPh-4-Cl	100
4.2	B	4-OPh-4-OCF ₃	100
4.3	B	4-O(CH ₂) ₃ CF ₃	94
4.4	B	4-OPh-3-OCF ₃	100

All compounds were identified by NMR spectroscopy. Compound **4.3** presented the most complex spectrum. While the OCH₂ protons are given as a simple triplet at δ 4.09 ppm, the other methylenes display very complex patterns, given the coupling with fluorine. Proton-fluorine coupling constants are typically large, and long distance coupling is also possible, resulting in multiplets.

The hydrolysis of compound **4.1** was tested under various conditions. Initially, an acid hydrolysis with HCl 6N was attempted. This had been the procedure used for the acetamides in chapter 1, but in this case no reaction was seen over 24 hours of reflux. A more drastic method was tried, employing concentrated H₂SO₄ under reflux. Although the reaction occurred, only *ca.* 1/3 of the starting material was consumed to the respective amide. In a third attempt, basic hydrolysis with NaOH 10% was assayed with a similar result to the hydrolysis with H₂SO₄. Finally, the reaction was achieved by using the basic hydrolysis method described by Sawyer *et al.* [286]. This involves the hydroperoxide anion generated through the abstraction of a proton from H₂O₂. The nucleophilic attack to the nitrile, described as the rate-limiting step, is followed by a swift reaction of the peroxyimidic acid with hydrogen peroxide to originate the corresponding amide. The attack of the hydroperoxide ion to benzonitrile was shown to be over four orders of magnitude faster than that of

the hydroxyl ion^[287]. These hydrolysis reactions were usually complete in 4 hours. The isolation of the required products consisted only in acidifying the reaction mixture and extracting with dichloromethane, to afford **4.5-8** in excellent yields, Table 4.2.

Table 4.2 Structure and yields of compounds **4.5-8**.



Compound	R ³	Yield (%)
4.5	4-OPh-4-Cl	100
4.6	4-OPh-4-OCF ₃	98
4.7	4-O(CH ₂) ₃ CF ₃	95
4.8	4-OPh-3-OCF ₃	96

The benzoic acids were identified by NMR. The spectra are identical to their precursors, except the protons nearer to the acid function which are more deshielded than in the nitriles. For example, in **4.5** the most deshielded protons are located at δ 8.11 ppm, while in its nitrile precursor **4.1** the corresponding protons are at δ 7.64 ppm.

Regarding the IR spectrum, a strong band at 1675 cm^{-1} can be found, and is characteristic of the C=O stretching vibrations for aromatic carboxylic acids. Furthermore, the 3400 cm^{-1} band provides evidence of the O-H stretch, whereas those in the 1400 cm^{-1} area result from C-O-H in-plane bending.

4.2.3 Flavones

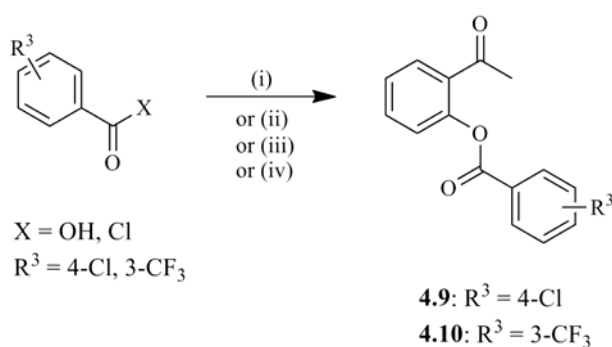
Via Baker-Venkataraman-like synthesis

In parallel with the benzoic acid intermediates, the method for the synthesis of flavones was optimized. Initially the reaction of 2-hydroxyacetophenone with 4-chlorobenzoic acid was attempted as described by Furuta *et al.*^[258]. The reaction consists of a DMAP-catalyzed acylation at the hydroxyl group of 2-hydroxyacetophenone, with a DCC-activated carboxylic acid which is the source of the acyl moiety. DMAP plays an important function as it prevents the 1,3-rearrangement of the intermediate ester to the *N*-acylurea, which would halt further reactions. Also, the

introduction of a 4-Cl in the terminal aryl would give access to the desired compounds through reaction with different phenols. However, no reaction was observed.

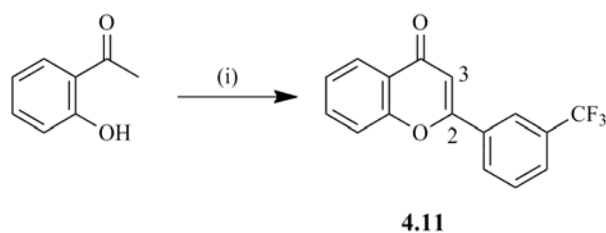
In the second attempt it was decided to transform the 4-chlorobenzoic acid to the corresponding acid chloride with thionyl chloride. This would provide an intermediate with a better leaving group for the subsequent reaction, but likewise, no reaction was observed.

In the third method, the esterification was attempted via a carbonic anhydride. This was synthesized from reaction of 4-chlorobenzoic acid with ethylchloroformate, followed by coupling with 2-hydroxyacetophenone. Once again, no ester was formed, Scheme 4.3.



Scheme 4.3 Synthetic pathway to compounds **4.9**. Reagents and conditions: (i) 2-hydroxyacetophenone, DCC, CH_2Cl_2 , DMAP, rt (ii) a) SOCl_2 , reflux; b) 2-hydroxyacetophenone, CH_2Cl_2 , DMAP, rt; (iii) a) CH_2Cl_2 , TEA, rt; b) ClCO_2Et , rt; c) 2-hydroxyacetophenone, DMAP, rt; (iv) 2-hydroxyacetophenone, dry pyridine, rt.

Analyzing the procedures that had been tried, it was noted that a base in excess could be missing in the esterification process. Furthermore, there is the possibility of an intra-molecular hydrogen bond in 2-hydroxyacetophenones, which can make the reaction more difficult without the use of a base in greater amount. Taking these points into consideration it was attempted the procedure described by Ono *et al.*, consisting of an acylation in pyridine medium^[261]. Despite acquiring compound **4.10** from this pathway, Scheme 4.3, it was obtained in only 30% yield, and with two more steps left to reach the flavone, this pathway was deemed unsuitable. Next, the synthesis was performed as described by Riva *et al.*^[288]. In this study, a one-pot cyclization was achieved using DBU and benzoyl halides, in a simple and mild procedure. Compound **4.11** was obtained in good yield, 32% for a combined of 3 steps, over 6 hours of reflux, and after adequate work-up and flash chromatography, Scheme 4.4.



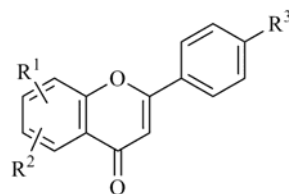
Scheme 4.4 Synthetic pathway for compounds **4.11**. Reagents and conditions: (i) Dry pyridine, 3-(trifluoromethyl)benzoyl chloride, DBU, reflux.

Therefore, the synthesis of the remaining compounds was pursued with minor changes to this procedure. Compound **4.12** was initially synthesized as described for **4.11**, but remarkably, a mixture of **4.12** and its C3-acylated analogue was obtained in 1:0.7 ratio, which was not separable due to the same R_f . Although such side product had not been reported by Riva *et al.*, C3 acylation has been accounted elsewhere, but while using a greater excess of benzoyl chloride^[277, 289]. This side product likely forms from acylation of the ester or the diketone intermediates, rather than from the flavone, as proposed in the literature^[277].

To circumvent this side product, the acetophenone was used in excess (1.5 molar equivalents) instead of the acid chloride (1 molar equivalent), but despite obtaining a much higher percentage of **4.12**, the C3-acyl side product still formed. The synthesis of flavones without the formation of the C3-acyl side product was only achieved when an excess of two molar equivalents of acetophenone was employed. The structures and yields of the synthesized compounds can be found in Table 4.3.

In the attempt to obtain **4.19** several other variations were performed in the procedure. Reflux under 22 hours still afforded no reaction. In the next variation, microwaves were introduced as the heating source. When the reaction was carried out for 40 minutes at 150W, up to a maximum of 200 °C, no reaction was observed, but remarkably, **4.19** was synthesized under milder conditions, i.e. 40 minutes at 100W and 150 °C. Even though, it was not possible to isolate the compound as a result of a superimposed R_f with that of the exceeding reagent. Nevertheless, the reaction yield, based on ¹H-NMR spectroscopy, was 27%. Compound **4.18** was also prepared under the same conditions, as a standard to compare with the procedure employing reflux. This compound was obtained in a higher yield, 37%, showing the effectiveness of the microwave-assisted synthesis of flavones.

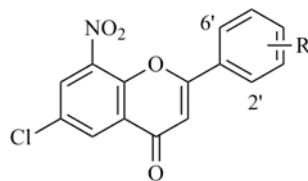
Also, in accordance with what was found with the reactions under reflux, the C3-acyl side product of **4.18** was obtained in 9% and 10% yield, when the MW-assisted reaction was carried out with 1 and 1.2 molar eq. of acid chloride, respectively. In both cases the yield of **4.18** was *ca.* 35%.

Table 4.3 Structure and yields (over 4 steps) of compounds **4.12-21** under standard heating conditions and MW-assisted synthesis.

Compound	R ¹	R ²	R ³	Yield (%)	
				reflux ^a	MW ^b
4.12	H	H	4-OPh-4-Cl	30	N.D.
4.13	H	6-Cl	4-OPh-4-Cl	15	N.D.
4.14	7-Cl	H	4-OPh-4-Cl	32	N.D.
4.15	7-Me	H	4-OPh-4-Cl	11	N.D.
4.16	7-Me	6-Cl	4-OPh-4-Cl	21	N.D.
4.17^c	7-Me	6-Cl	4-OPh-4-OCF ₃	40	N.D.
4.18^c	7-Me	6-Cl	4-Ph	27	37
4.19	8-NO ₂	6-Cl	4-Ph	-	27
4.20	7-Me	6-Cl	4-O(CH ₂) ₂ CF ₃	15	N.D.
4.21	H	H	4-OPh-3-OCF ₃	37	N.D.

^a Conditions: 2 molar eq. of acetophenone, reflux 6-8h. ^b Conditions: 2 molar eq. of acetophenone, 100W, 40 min., 150 °C. ^c Three steps. N.D. - Not Done.

The scope of this procedure towards the synthesis of 8-nitroflavones was studied from the reaction of nitroacetophenone with a range of acid chlorides containing both electron withdrawing and donating groups. Though, the synthesis of compounds **4.22-25** was not achieved, underlining the lack of reactivity of the nitroacetophenone.



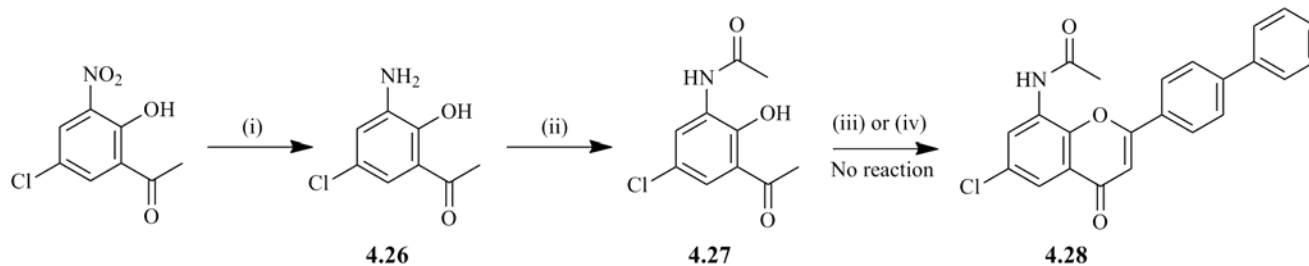
4.22: R = 3'-CF₃

4.23: R = 4'-OMe

4.24: R = 3',5'-NO₂

4.25: R = 3',5'-Cl

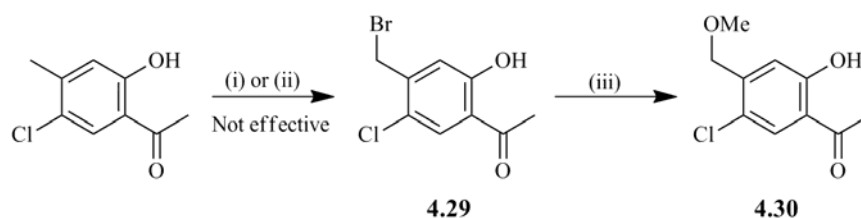
Due to the lack of reactivity of the nitroacetophenone it was investigated if the aminoacetophenone derivative **4.27** would cyclize to the required flavone. The synthetic procedure is shown in Scheme 4.5. Reduction of the nitro group was achieved in excellent yield, 94%.



Scheme 4.5 Synthetic pathway to compound **4.28**. Reagents and conditions: (i) Sn, HCl, EtOH, reflux; (ii) dry pyridine, acetic anhydride, reflux; (iii) dry pyridine, DBU, [1,1'-biphenyl]-4-carbonyl chloride, reflux (iv) Similar to (iii), MW.

However, no cyclization was seen in both thermal heating and microwaves. As a result, no further attempts from this pathway were made, to synthesize the nitro and aminoflavone derivatives, despite the great interest that these compounds would present for the antiplasmodial activity. Stigmatellin makes a hydrogen bond with H181 from the ISP, through the carbonyl group of the chromone, and participates in hydrogen bonding with E272 from cytochrome *b*, through a methoxy group located at C8. Therefore, the 8-NO₂, 8-NH₂ and 8-NHCOCH₃ groups would represent replacements of the 8-OMe in stigmatellin, and would likely contribute to the antiplasmodial activity of such derivatives.

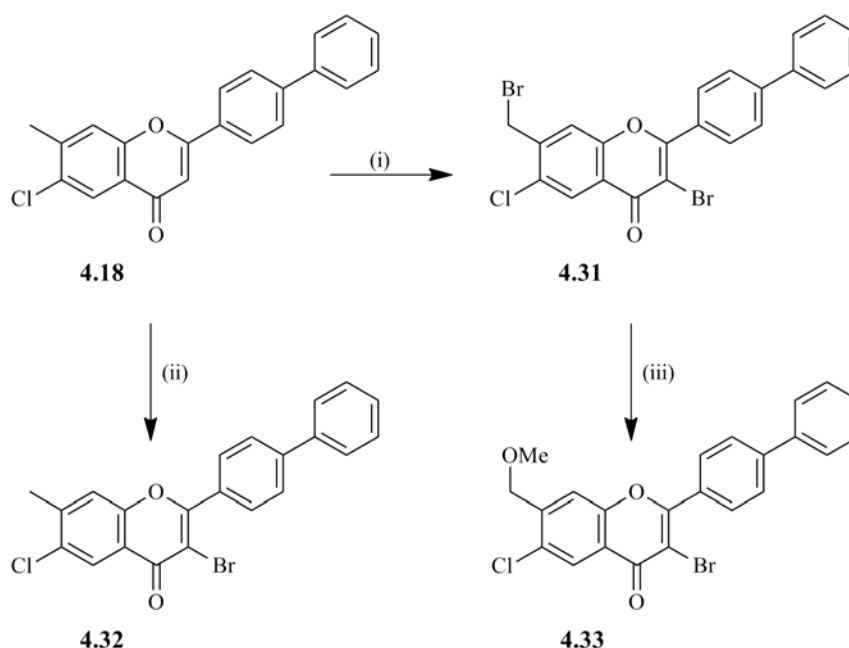
The introduction of a hydrogen bond acceptor or donor, in this series of compounds, was then attempted from the benzyl bromination of 4-methylacetophenone, Scheme 4.6.



Scheme 4.6 Synthetic pathway to compounds **4.29** and **4.30**. Reagents and conditions: (i) NBS, AIBN, benzene, reflux 2 h; (ii) NBS, AIBN, benzene, reflux 24 h; (iii) MeOH, MeONa, reflux.

The synthesis of **4.29** was not effective in both methods. When a small excess of NBS was used, as in (i), only 50% of conversion was seen through ¹H-NMR, but when the bromine source was

used in greater excess, and the reflux prolonged for 24 hours, (ii), several side products were formed. Therefore the synthesis of **4.30** was not pursued. Alternatively, direct bromination of **4.18** was assayed with interesting results, Scheme 4.7. When the bromination procedure was attempted with NBS (1.2 molar eq.), using benzoyl peroxide as an initiator, only **4.31** was isolated, 27%. This reaction had been designed for a sole bromination, which might explain the modest yield. Probably if NBS had been used in a larger amount the yield would have been higher. Since only a small amount of **4.31** was isolated, the synthesis of **4.33** was also not attempted.



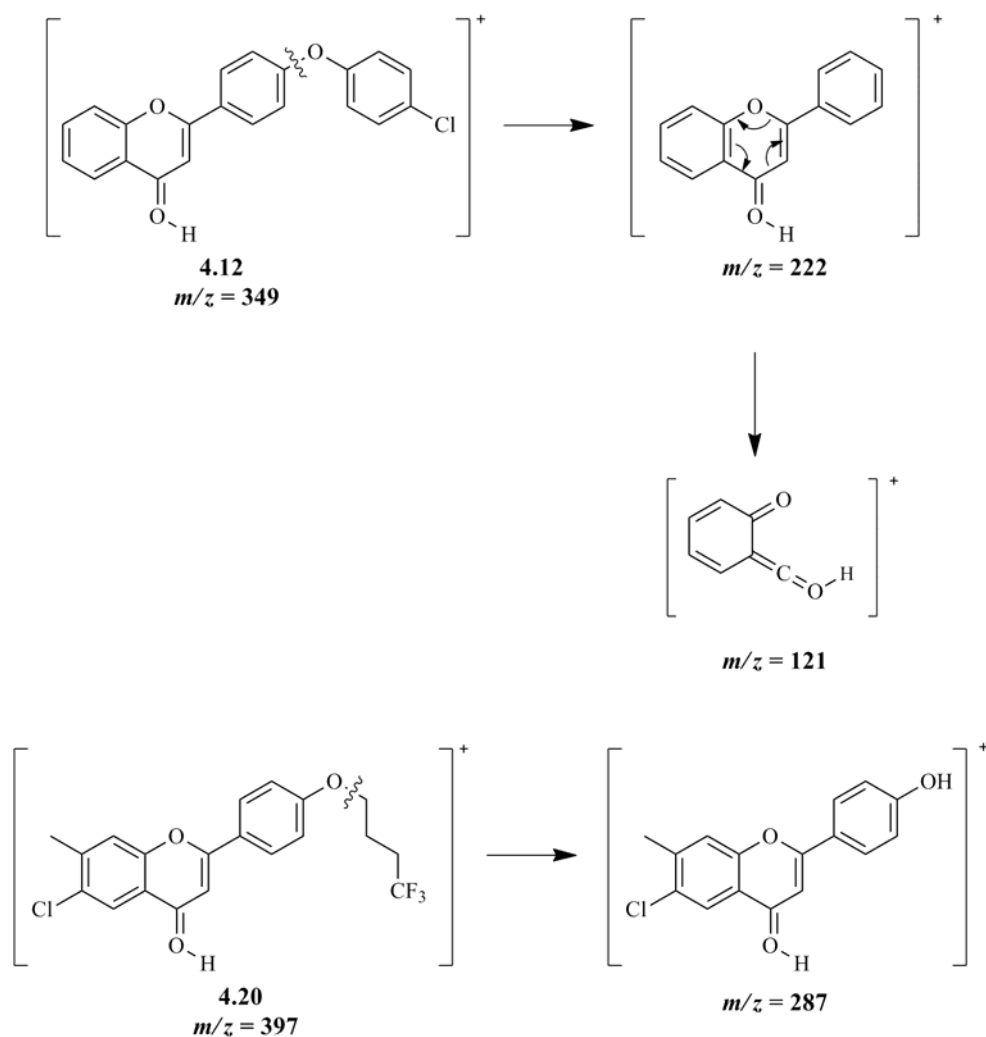
Scheme 4.7 Synthetic pathway to compounds **4.31-33**. Reagents and conditions: (i) NBS, benzoyl peroxide, CCl_4 , reflux; (ii) NBS, ZrCl_4 , CCl_4 , rt; (iii) MeOH, MeONa, reflux.

As this method proved to be inefficient for the benzylic bromination of flavones, the procedure described by Shibatomi *et al.* ^[290] was tested. In that paper, the authors report that the ZrCl_4 / NBS system promotes benzylic bromination of toluene derivatives without bromination on the aromatic ring. Interestingly, in this case, only bromination at C3 was achieved, resulting in **4.32**, which was isolated in 10% yield.

The compounds were characterized with several spectroscopic techniques, including 1D and 2D NMR, IR and mass spectrometry. The NMR spectra of **3.12-21** presented the same general features among them. Flavones were promptly identified for the success of the reaction by the characteristic singlet at δ 6.7-6.9 ppm. This peak corresponds to the proton at C3 and, therefore, no correspondent signal is present in the starting materials. The AA' XX' systems of the side chain can be found with

their typical symmetric doublet-like pattern, while the proton at C5 is the most deshielded at δ 8.21 ppm. The proton at C8 is also given as a doublet at δ 7.54 ppm ($^3J = 8.8$ Hz). The remaining proton at C7 is given as a skewed doublet of doublets, as a result of coupling with the protons at C8 and C5.

The compounds were also identified by their mass spectra, and the base peak results from the $[M+H]^+$ adduct. Further investigation into the fragmentation patterns led to the identification of a peak corresponding to the flavone core, i.e. loss of the phenol group. In turn, this prominent peak gives rise to another that originates from retro Diels-Alder fission of the heterocyclic ring, the quinonoid ion. These have already been reported by Itagaki *et al.* [291] and in Scheme 4.8 an example of the fragmentation is given. For compound **4.20**, however, only fragmentation of the O-CH₂ bond was seen.



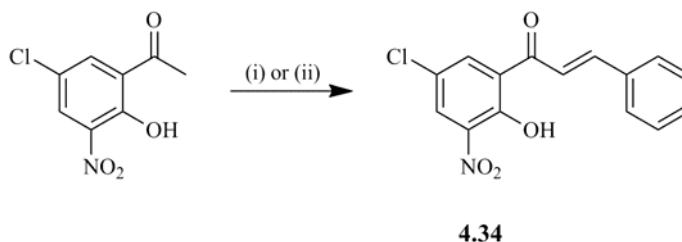
Scheme 4.8 Fragmentation pattern of **4.12** and **4.20** as examples for the flavone series.

The IR spectrum for the flavone series of compounds is characterized by the existence of few bands. Stretching vibrations for the C=O bond are found at *ca.* 1650 cm⁻¹ which is coherent with the expected wave number for six-membered cyclic ketones.

Via chalcones

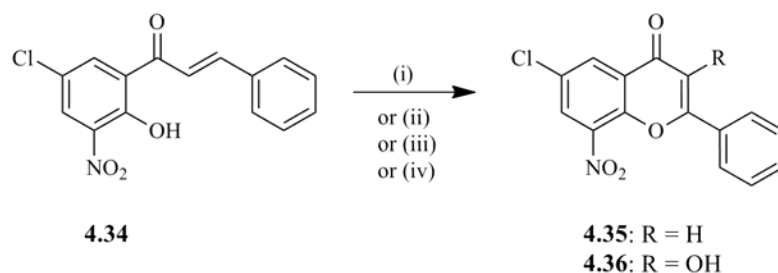
Chalcones are structurally similar to flavones and also display antiplasmodial activity, possibly from *bc*₁ complex inhibition [139, 144]. These are readily accessible chemical entities from a crossed aldol condensation between acetophenones and aldehydes. Furthermore, if 2-hydroxyacetophenones are used, the resulting chalcone can be employed as an intermediate for the synthesis of flavones, as supported by a broad spectrum of literature [251, 284, 285, 292, 293].

To tune up the synthetic procedures, an aldol condensation between nitroacetophenone, and freshly distilled benzaldehyde was performed, Scheme 4.9. When refluxing the mixture, no evolution through TLC was seen after 40 minutes. In this case the **4.34** was isolated in 51% yield. However, when the reactants were left at room temperature with a greater excess of base, for 24 hours, the chalcone was isolated in quantitative yield.



Scheme 4.9 Synthetic pathway to compounds **4.34**. Reagents and conditions: (i) Benzaldehyde, NaOH, reflux; (ii) Benzaldehyde, NaOH, rt.

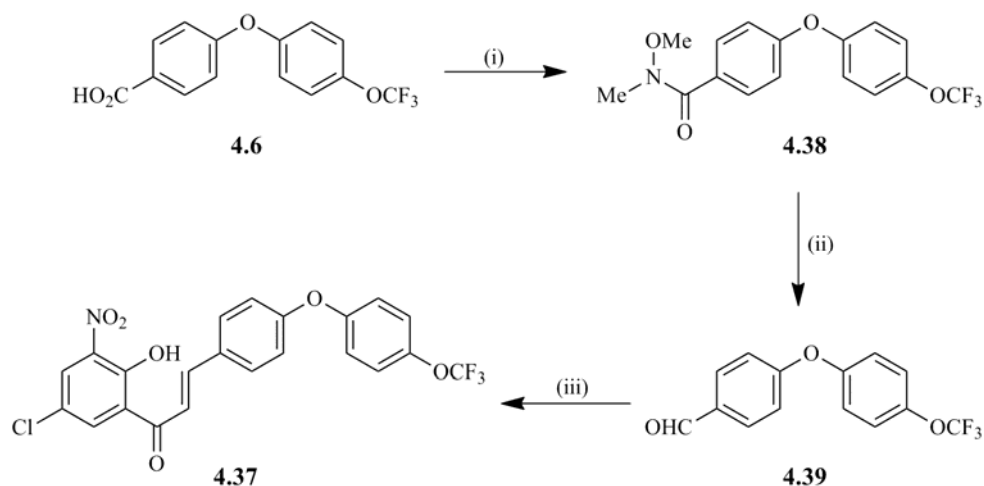
After acquiring the chalcone, four cyclization methods were tested from procedures described in the literature, Scheme 4.10 [284, 285, 294]. Methods (i)-(iii) would result in **4.35**, from a iodine-catalyzed reaction, or from a Pd(II) catalyst. In method (iv), **4.36** would result from a H₂O₂ promoted reaction. However, no cyclization was observed in any case, and only degradation products were recovered.



Scheme 4.10 Synthetic pathway to compounds **4.35** and **4.36**. Reagents and conditions: (i) DMSO, I₂, MW; (ii) DMSO, I₂, reflux; (iii) PdCl₂, AcONa, AcOH, AIBN; (iv) H₂O₂ 30%, NaOH, EtOH.

Since it was not possible, again, to obtain an 8-nitroflavone derivative, it was decided to assess the influence of the nitro substituent in the chalcone that would serve as a precursor to the desired flavone, in order to gain some insight on the substituent effect. Chalcones are typically more active than their flavone counterparts in IC₅₀ assays against *P. falciparum* strains. Therefore, the IC₅₀ value of **4.37** would serve as an indicator on whether to invest further or not in the synthesis of the flavone derivative.

Compound **4.38** was obtained in quantitative yield from its **4.6** precursor, using TBTU as a coupling reagent. TBTU is a widely known reagent and the mechanism of the reaction has been depicted by Movassagh *et al.* [295]. Compound **4.39** was acquired afterwards, from simple LiAlH₄ reduction under anhydrous conditions, and subjected to an aldol condensation, to afford **4.37** in excellent yield, Scheme 4.11.

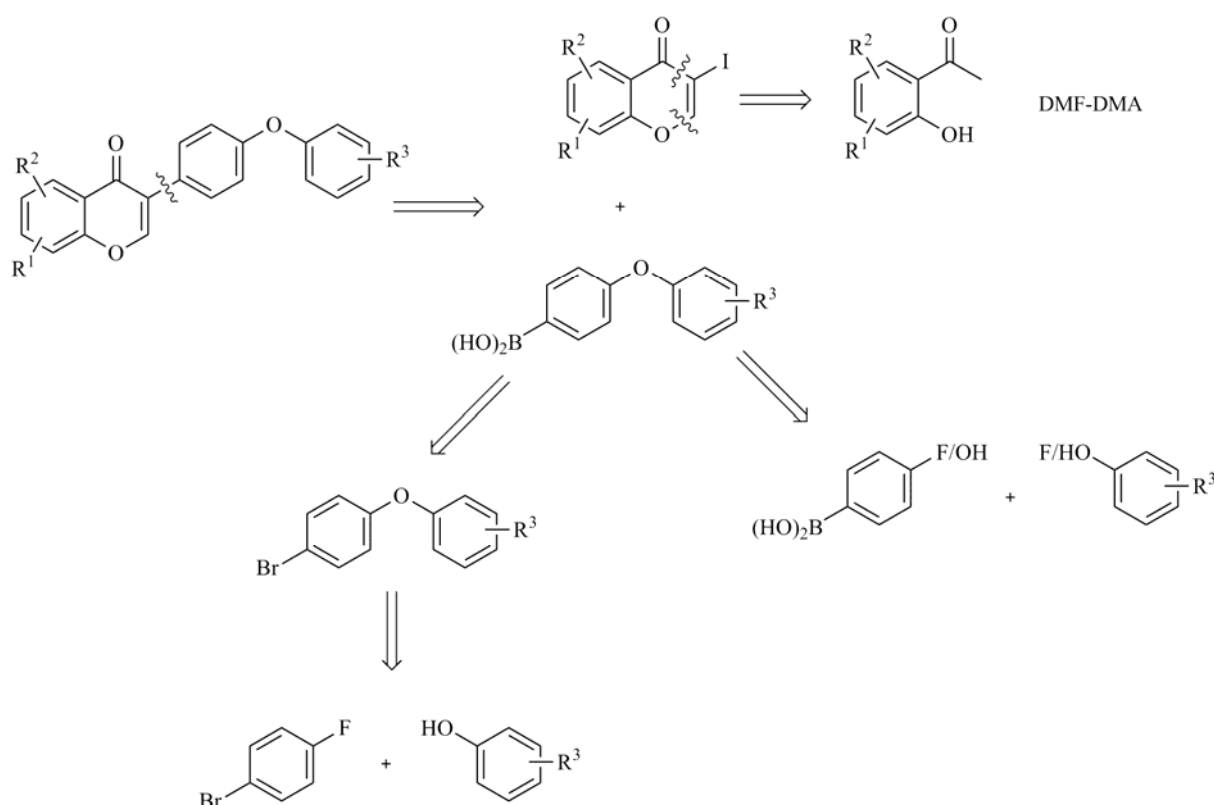


Scheme 4.11 Synthetic pathway to compound **4.37**. Reagents and conditions: (i) TEA, TBTU, NH(Me)OMe, rt; (ii) dry THF, LiAlH₄, -5 °C; (iii) EtOH, NaOH, acetophenone, rt.

Chalcone **4.37** was identified by NMR spectroscopy, with the most characteristic protons being located at δ 7.46 and 7.97 ppm. Those correspond to the alkene function, and a $^3J = 15.4$ Hz allows to conclude that only the (*E*) isomer was formed from the aldol condensation. Further inspection of the spectrum permits the identification of the AA' XX' systems as well as the proton from the hydroxyl function at δ 13.33 ppm.

4.2.4 Retrosynthetic analysis of isoflavones

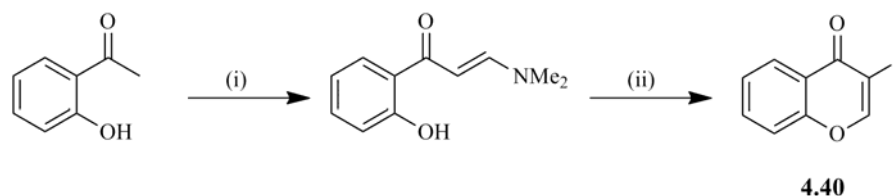
A search in the available literature revealed that isoflavones are commonly accessible through Suzuki-Miyaura cross coupling. Bearing in mind the side chains that were intended to be introduced into the scaffold, it was deduced that the required boronic acids would have to be synthesized. These can be obtained from Grignard chemistry. Alternatively, the cross coupling could be achieved with a commercial boronic acid, prior to executing the needed S_NAr , Scheme 4.12.



Scheme 4.12 Retrosynthetic analysis of isoflavones.

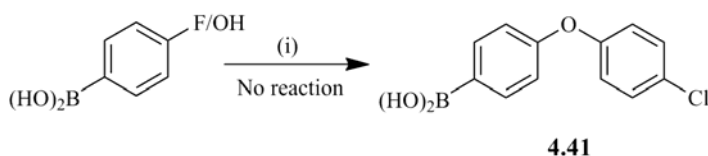
4.2.5 Attempted synthesis of isoflavones

As a first step towards the synthesis of isoflavones, compound **4.40** was synthesized as described by Felpin *et al.* [296]. In short, reaction of the acetophenone with DMF-DMA results in a propenone which is cyclized into 3-iodochromone **4.40** in the following step, Scheme 4.13.



Scheme 4.13 Synthetic procedure for **4.40**. Reagents and conditions: (i) DMF-DMA, 95 °C; (ii) CHCl₃, pyridine, I₂, rt.

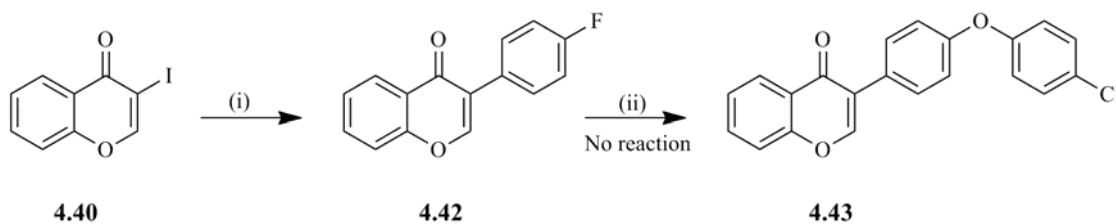
With this key intermediate in hand, it was possible to attempt the synthesis of several isoflavones from a Pd-C mediated cross coupling with boronic acids. As a first approach, synthesis of **4.41** was tested, for this would provide directly the boronic acid of the planned side chain. However, the S_NAr did not occur with either 4-(fluorophenyl)boronic acid or 4-(hydroxyphenyl)boronic acid, despite prolonging reflux for 24 hours, Scheme 4.14.



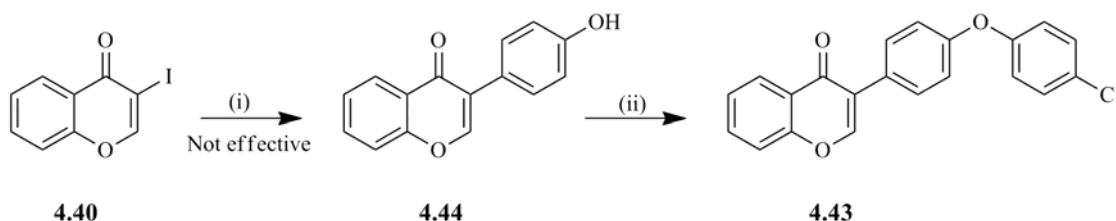
Scheme 4.14 Synthetic procedure for **4.41**. Reagents and conditions: (i) DMF, CuI, 4-chlorophenol or 4-fluorophenol, Na₂CO₃, reflux.

Consequently, the Suzuki-Miyaura coupling was first performed with 4-(fluorophenyl)boronic acid and **4.40**, resulting **4.42** in excellent yield, 93%. Unfortunately, this was also not reactive towards the formation of **4.43**, Scheme 4.15.

The synthesis of **4.43** was also attempted via intermediate **4.44**, but the cross coupling reaction in this case gave an untractable mixture, Scheme 4.16.

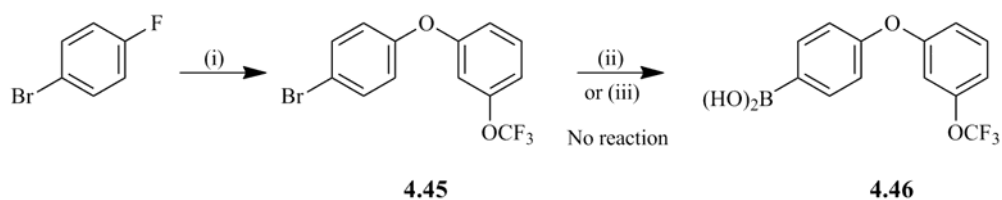


Scheme 4.15 Synthetic procedure for compounds **4.42** and **4.43**. Reagents and conditions: (i) 4-(fluorophenyl)boronic acid, DME, H₂O, Na₂CO₃, Pd-C, 45 °C; (ii) 4-chlorophenol, CuI, Na₂CO₃, DMF, reflux.



Scheme 4.16 Alternative pathway to **4.43**, using the same reactions as in Scheme 4.15.

In a final attempt, the boronic acid was synthesized from small building blocks. Compound **4.45** was obtained in moderate yield, 38%, from two days of reflux, Scheme 4.17. This reaction was expectedly more demanding than the others that had been performed, containing a nitro or cyano groups in the *para* position, because of the much poorer electron withdrawing nature of bromine. However, since the reaction was carried out in a large scale, enough compound was obtained to proceed with the following reactions. The synthesis of the boronic acid **4.46** was attempted via the organolithium species, as described by Yeates *et al.* [19], and through *in situ* generated Grignard reagent, adapting the procedure from Wong *et al.* [297]. Triisopropyl borate was used as a boron source because, being sterically hindered, it would avoid bisalkylation to the corresponding borinic acid. Moreover, a catalytic amount of iodine was added to the mixture, and it was also sonicated in order to initiate the Grignard reaction. Though, no reaction was observed in either reaction conditions.

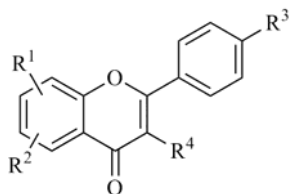


Scheme 4.17 Synthetic procedure for compounds **4.45** and **4.46**. Reagents and conditions: (i) DMF, Na₂CO₃, CuI, 3-(trifluoromethoxy)phenol, reflux; (ii) a) dry THF, *n*-BuLi, borate triisopropyl, -78 °C b) HCl 6N, rt; (iii) a) dry THF, Mg, N₂, I₂, reflux b) triisopropyl borate, -78 °C c) HCl 6N, rt.

4.2.6 Antiplasmodial activity and molecular docking

The antiplasmodial activity of compounds **4.12-21**, **4.31**, **4.32** and **4.37** was tested against the W2 strain. All available data show that this series of compounds present only modest activity, Table 4.4. Nevertheless, those values are in line with analogous flavones reported by Lim *et al.* and Auffret *et al.* [267, 268], displaying IC₅₀s around 10 μM. Since most of the compounds were tested only up to 10 μM it is not possible to withdraw the SAR for this series. However, the presence of the bromomethyl group at C7 appears to be important for the antiplasmodial activity, i.e. **4.31** vs. **4.32**.

Table 4.4 Substituent effect on the antiplasmodial activity, against the W2 strain, of compounds **4.12-21**, **4.31**, **4.32**.



Compound	R ¹	R ²	R ³	R ⁴	IC ₅₀ ± SD (μM)	GoldScore
4.12	H	H	4-OPh-4-Cl	H	21.0 ± 0.37	57.15
4.13	H	6-Cl	4-OPh-4-Cl	H	> 25.0	58.69
4.14	7-Cl	H	4-OPh-4-Cl	H	> 10.0	58.57
4.15	7-Me	H	4-OPh-4-Cl	H	19.7 ± 2.98	58.27
4.16	7-Me	6-Cl	4-OPh-4-Cl	H	> 10.0	61.43
4.17	7-Me	6-Cl	4-OPh-4-OCF ₃	H	> 10.0	61.60
4.18	7-Me	6-Cl	4-Ph	H	> 10.0	53.12
4.20	7-Me	6-Cl	4-O(CH ₂) ₂ CF ₃	H	> 10.0	55.18
4.21	H	H	4-OPh-3-OCF ₃	H	> 10.0	58.53
4.31	7-CH ₂ Br	6-Cl	4-Ph	Br	5.96 ± 0.07	63.27
4.32	7-Me	6-Cl	4-Ph	Br	> 10.0	52.42

The synthesized compounds were also docked into the Q_o site of the bc₁ complex and compared with the docking pose of stigmatellin. Two different poses were obtained within this set, Figure 4.1. For compounds **4.12**, **4.13**, **4.15**, **4.16** and **4.31** the chromone is located inside the binding pocket and the side chain in the channel, as in stigmatellin, Figure 4.1 A and B. Stigmatellin interacts through hydrogen bonds with both cytochrome *b* and the ISP. For the synthesized compounds, the carbonyl group is at *ca.* 2.0 Å from H181, and the sp³ oxygen of the chromone ring at *ca.* 5.5 Å of

E272, which is consistent with a possible water-mediated hydrogen bond. The longer distances, i.e. weaker interactions, compared to stigmatellin might justify the modest IC_{50} values for the synthesized compounds. However, in these molecules, the chlorine and bromine atoms at the chromone ring are at *ca.* 3.0 Å from a carbonyl of the protein backbone. These halogen bonds are strong interactions and have been described by Bissantz *et al.* and Lu *et al.* [298, 299]. Taking these interactions in consideration, compound **4.31** was predicted to be the best binder, which was confirmed from *in vitro* studies. For the remaining compounds, the docking pose is inverted, i.e. with the side chain inside the binding pocket and the chromone ring in the channel, Figure 4. C. Interestingly, all compounds containing the trifluoromethoxy group in the terminal aryl display this pose, probably as a consequence of multipolar interactions with the active residues. Furthermore, the shift of 6-Cl in **4.13**, to 7-Cl in **4.14** also resulted in an inverted pose. Also, a bromomethyl group at C7 appears to be beneficial for the desired docking pose, **4.31** vs. **4.32**.

The chalcone **4.37** was tested against the W2 strain, but no antiplasmodial activity was seen up to 10 μ M, probably making the 8-nitroflavone not a very good lead for further drug development.

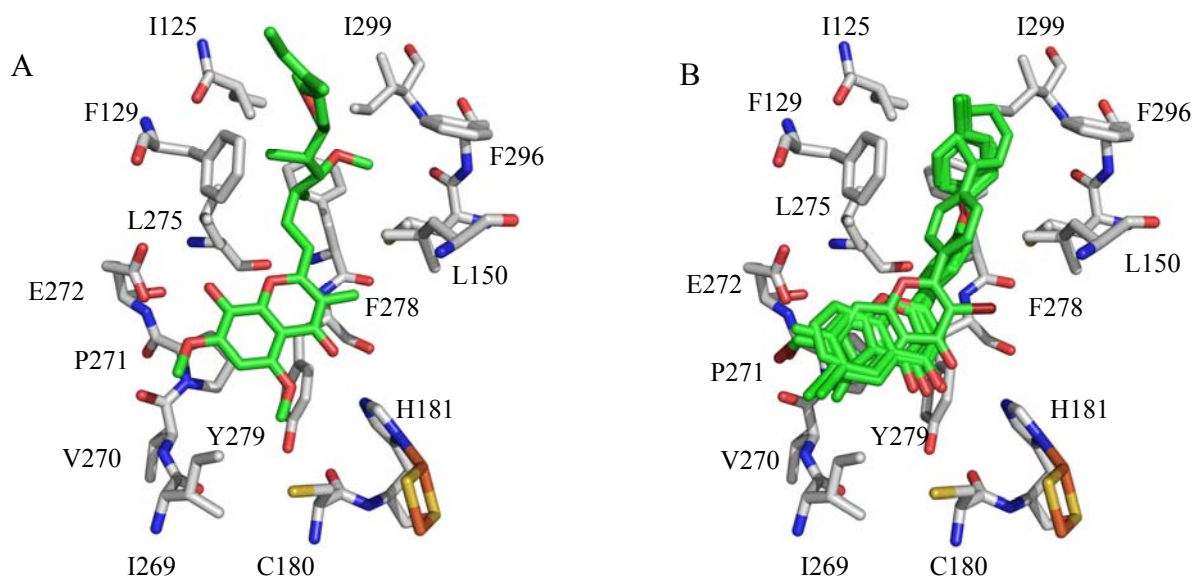


Figure 4.1 Docking poses of (A) stigmatellin; (B) **4.12**, **4.13**, **4.15**, **4.16** and **4.31**.

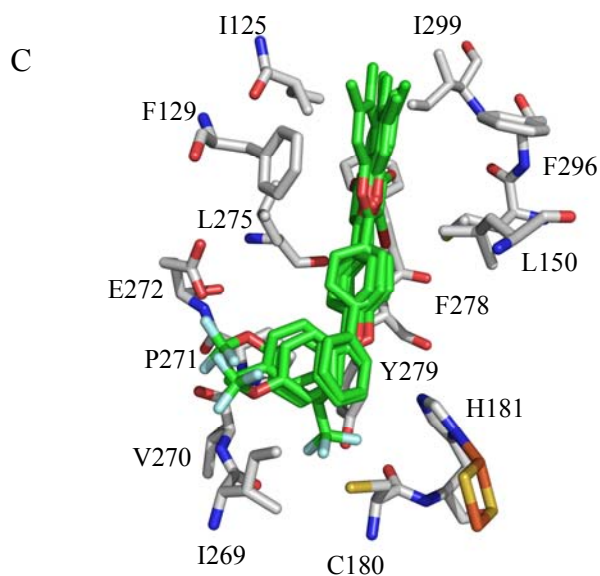


Figure 4.1 (cont.) Docking poses of (C) **4.14**, **4.17**, **4.18**, **4.20**, **4.21** and **4.32**.

4.2.7 Anti-liver activity and cytotoxicity

Given the tissue-schizonticidal activity of the isoflavone genistein ($IC_{50} \sim 20 \mu\text{M}$)^[300] and the structural similarities, it was predicted that this series of flavones would be similarly active against the liver forms of *Plasmodia*. The synthesized compounds are able to decrease the infection load of Huh-7 cells to different extents, when compared to the control, and displayed a dose-dependent effect on the development of the parasite, Figure 4.2. At $10 \mu\text{M}$, compounds **4.12** and **4.21** were able to decrease infection in the same order of magnitude of primaquine at $5 \mu\text{M}$, albeit being less active than the latter (*ca.* 3.5- and 3-fold less active, respectively). Also, **4.12** and **4.15** displayed moderate antiplasmodial activity in the blood stage, but were more active in the liver-stage. **4.32** was essentially non-active against the liver stage, while displaying the lowest IC_{50} in *P. falciparum* W2 strain.

The IC_{50} values were determined for compounds **4.12**, **4.15** and **4.21**, since they showed a stronger drop in infection between 10 and $2 \mu\text{M}$. While flavone **4.21** presented an IC_{50} of $8.5 \mu\text{M}$, compounds **4.12** and **4.15** showed more potent inhibition with IC_{50} s of $6.2 \mu\text{M}$ and $4.1 \mu\text{M}$, respectively, Figure 4.3. These results highlight the higher potency of this series against liver stages, rather than against blood stages of *Plasmodia*. Also, these molecules are over 2-fold more potent than the related isoflavone genistein. Therefore, it is hypothesized that the introduction of an extended side chain into the chromone moiety is responsible for the observed results, and the following SAR observations can be drawn:

- Introduction of 6-Cl or 7-Cl in the chromone ring is detrimental for anti-liver activity, i.e. **4.12** vs. **4.13** and **4.14**;
- Simple substitution of 7-Me in the chromone ring is desirable, among the assayed compounds, i.e. **4.15**;
- Introduction of 7-Me does not restore significantly the anti-liver activity of compounds containing a chlorine in the core scaffold, i.e. **4.13** vs. **4.16**;
- 4-Cl substitution in the terminal aryl moiety is preferred over 4-OCF₃, i.e. **4.16** vs. **4.17**;
- Introduction of a spacer between the aryl moieties that confers flexibility to the side chain also appears to be critical, as compounds **4.18**, **4.31** and **4.32** are amongst the least active flavones.

Also, none of the molecules presented significant cytotoxicity at any concentration in the Alamar Blue test.

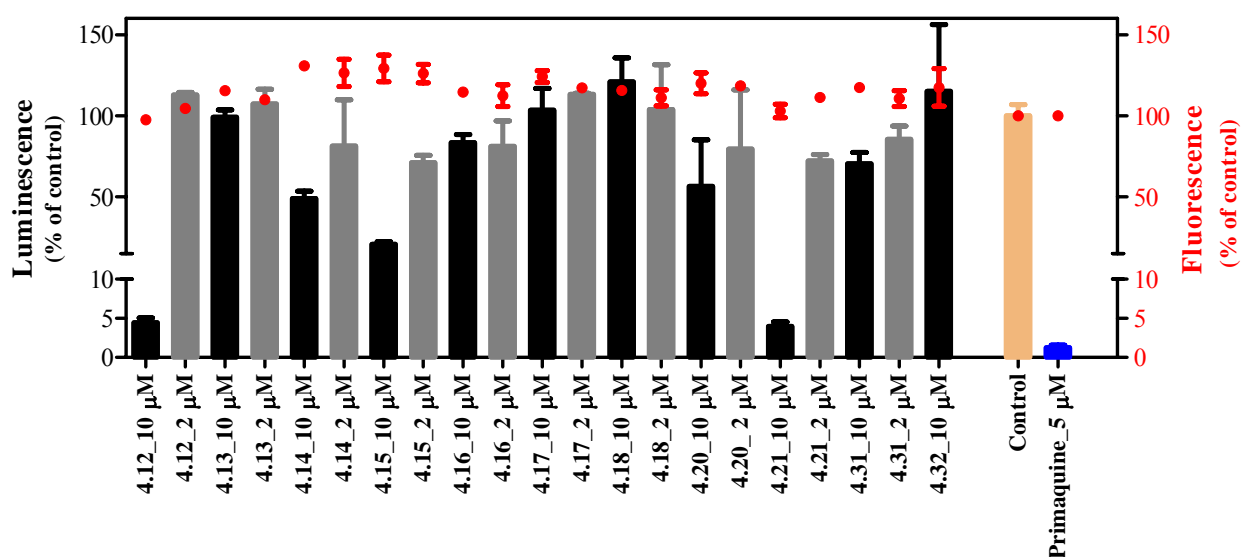


Figure 4.2 Antiplasmodial activity of compounds **4.12-21** and **4.31-32** against the liver stage of *P. berghei*. The luminescence (bars) is given as percentage of control (DMSO) inhibition. The cytotoxicity was measured in fluorescence (dots) from the Alamar Blue test and is also given as percentage of control. The compounds were tested in two concentrations: 10 μM (black bars), 2 μM (grey bars) and primaquine was tested at 5 μM. Compound 4.34 was only tested at 10 μM.

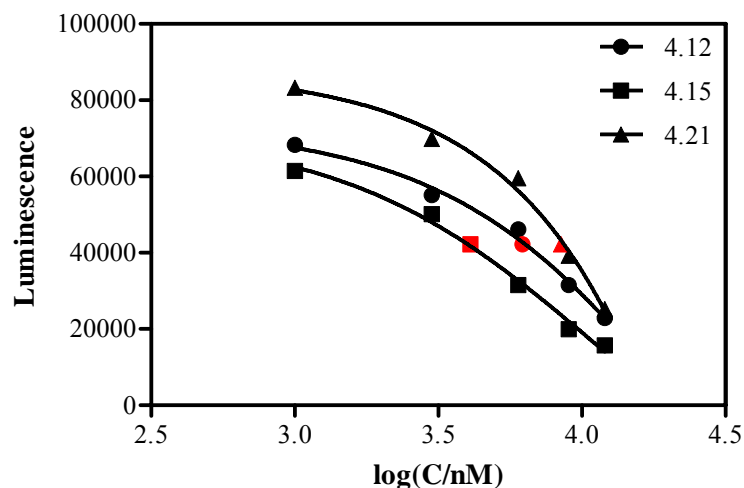


Figure 4.3 Dose-response curve of luminescence intensity, as a function of the logarithm of compound concentration. The red markers refer to logIC₅₀.

4.3 Conclusions

The flavone derivatives showed only modest antiplasmodial activity. However, these compounds were interestingly more potent against the liver stage and may find further applicability after the optimization of the substitution pattern around the chromone core. These have also shown to be considerably more active than genistein and are the most potent flavones reported thus far, for this stage of the life cycle.

CHAPTER 5

VIRTUAL SCREENING STUDIES

5. VIRTUAL SCREENING STUDIES

5.1 Brief overview on Virtual Screening

Virtual screening (VS) of chemically available ligand databases has become an useful tool to search the chemical space in recent years, given it accelerates the initial stages of drug development. It takes only a few hours or days to screen *in silico* a library of around one million compounds, while a few months are required to screen *in vitro* (high-throughput screening) the same number of chemical entities^[301]. Furthermore, it has proven to be effective in several projects, by applying a good set of filters. As primary constraints to the search, common approaches include:

- a) Receptor-based, also known as docking- or structure-based strategy, where all the characteristics of the binding site are determined;
- b) Ligand-based, or pharmacophore-based strategy, where due to the lack of knowledge of the binding site features, known ligands are taken into account.

Other constraints include, for example, ADMET properties^[302, 303].

However, receptor-based VS strategies generally face the problem of protein flexibility, because it is usually kept rigid to speed up the screening process. In this case, the docking program attempts to find complementarity between the receptor and the ligand, which is quantified by the search algorithm. In ligand-based VS, the program recognizes compounds from the library with the required features to bind to the target. To execute it, a pharmacophore model is built by defining the pharmacophoric features, and the user-defined tolerance zone. Its major advantage over the docking-based protocol stands in the throughputness which is considerably higher, making it adequate for filtering overly large databases^[301].

VS strategies are becoming increasingly popular and have been reasonably successful in the search of new antimalarial leads. While some studies have focused on finding novel leads for a known drug target such as hematin and dihydrofolate reductase^[304-306], others have delivered leads for the design of drug candidates for novel targets. Those include plasmodial kinases^[307], falcipains^[308-310] and enoyl-acyl carrier protein reductase^[311]. Despite some successful cases, VS is still not a fully matured technology. Few foundations of ligand-protein recognition are understood well enough to be deployed in large scale efforts. The role of water molecules, solvation, electrostatics and entropic changes are problems yet to be solved, which increase the tendency to detect false-positives^[312, 313].

5.2 3D-Pharmacophore model generation and screening

With the intention of filtering out the two chemical databases in an expedite way, a 3D pharmacophore model was generated using the MOE software, which is a highly regarded software for this purpose [314, 315].

This was modeled from the bioactive pose of GW844520, **1.113**, at the Q_o site of the *bc*₁ complex described in chapter 2, Figure 2.7 and Figure 5.1. Traditionally, several molecules with significant scaffold diversity are used for the generation of a 3D pharmacophore model, i.e. a consensus query. In the present case only GW844520 was used for the model generation, given that:

- Currently there is a lack of chemical diversity, regarding the inhibitors of cytochrome *bc*₁;
- The inhibitors of the *bc*₁ complex may present different binding modes, making it inappropriate for aligning features, i.e. the pharmacophores of the different classes of inhibitors bind distinctively to the active site;
- The aim of the study was to find novel leads with the binding characteristics of the 4(1*H*)-pyridones. By using only one molecule to generate the model redundancy was avoided, since the training set consisted of a different set of molecules.

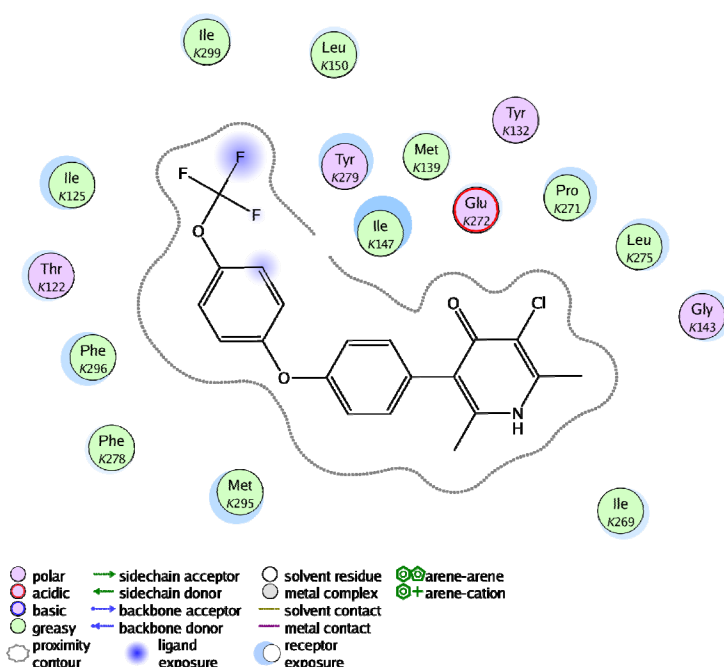


Figure 5.1 The ligand-receptor interactions for GW844520, **1.113**; strong hydrophobic interactions can be seen between the side chain and hydrophobic aminoacid residues. Water molecules have not been included in docking calculations, but are likely to intervene as hydrogen-bond mediators.

GW844520 is one of the most potent cytochrome bc_1 inhibitors known to date ($IC_{50} = 30$ nM)^[19] and to validate the generated model a training set of 14 4(1*H*)-pyridones with structurally different substituents at either C3 and / or C5 was assembled. These were then subjected to a conformational sampling with MOE, with a determined energy cut-off to avoid redundancy. Chen *et al.* had shown that the MOE performs at least as well as Catalyst in high-throughput library generation and conformational modeling^[316]. Finally, the generated conformers were treated as rigid entities for the validation screening. The chemical structures and their IC_{50} values against the *P. falciparum* T9-96 strain^[19] are given in Figure 5.2.

In MOE, a pharmacophore model consists of spheres depicting the tolerance of location allowed for each feature. The pharmacophore model used for the ZINC drug-like database^[317] consisted of seven features, Figure 5.3 A. Features F1 through F5 represent alternate hydrophobic and aromatic regions, with hydrophobic represented in green, i.e. F1, F3 and F5, and aromatic regions given in orange, i.e. F2 and F4. The spheres radius was manually adjusted in order to optimize the model. Hence, F1 had a sphere of radius equal to 1.5 Å, F3 a radius of 1.6 Å and F5 with 1.9 Å. The aromatic region F2 had a radius of 1.9 Å and F4 a radius of 1.5 Å. Both hydrogen bond acceptor, F6, and donor, F7, had a radius of 1.0 Å.

The pharmacophore models proved to be efficient in excluding compounds with an IC_{50} higher than 2,200 nM and compound **1.126**, with an IC_{50} of 2,200 nM, presented the highest RMSD value amongst the 4(1*H*)-pyridones, Appendix 3.1. Atovaquone, despite the low IC_{50} against the T9-96 strain, presented the highest RMSD value of all hit molecules within the training set. Thus, the model is expected to be restrictive towards compounds presenting features other than those of the 4(1*H*)-pyridones, regardless of their bc_1 complex inhibitory potency.

Prior to executing the pharmacophore-based VS, the ZINC database was filtered with the Lipinski's rule of five^[318, 319]. This predicts that the poor oral absorption and / or distribution are more likely to occur when a molecule has two of the following features:

- a) Five hydrogen bond donors;
- b) Ten hydrogen bond acceptors;
- c) A molecular weight over 500 Da;
- d) The calculated logP greater than 5.

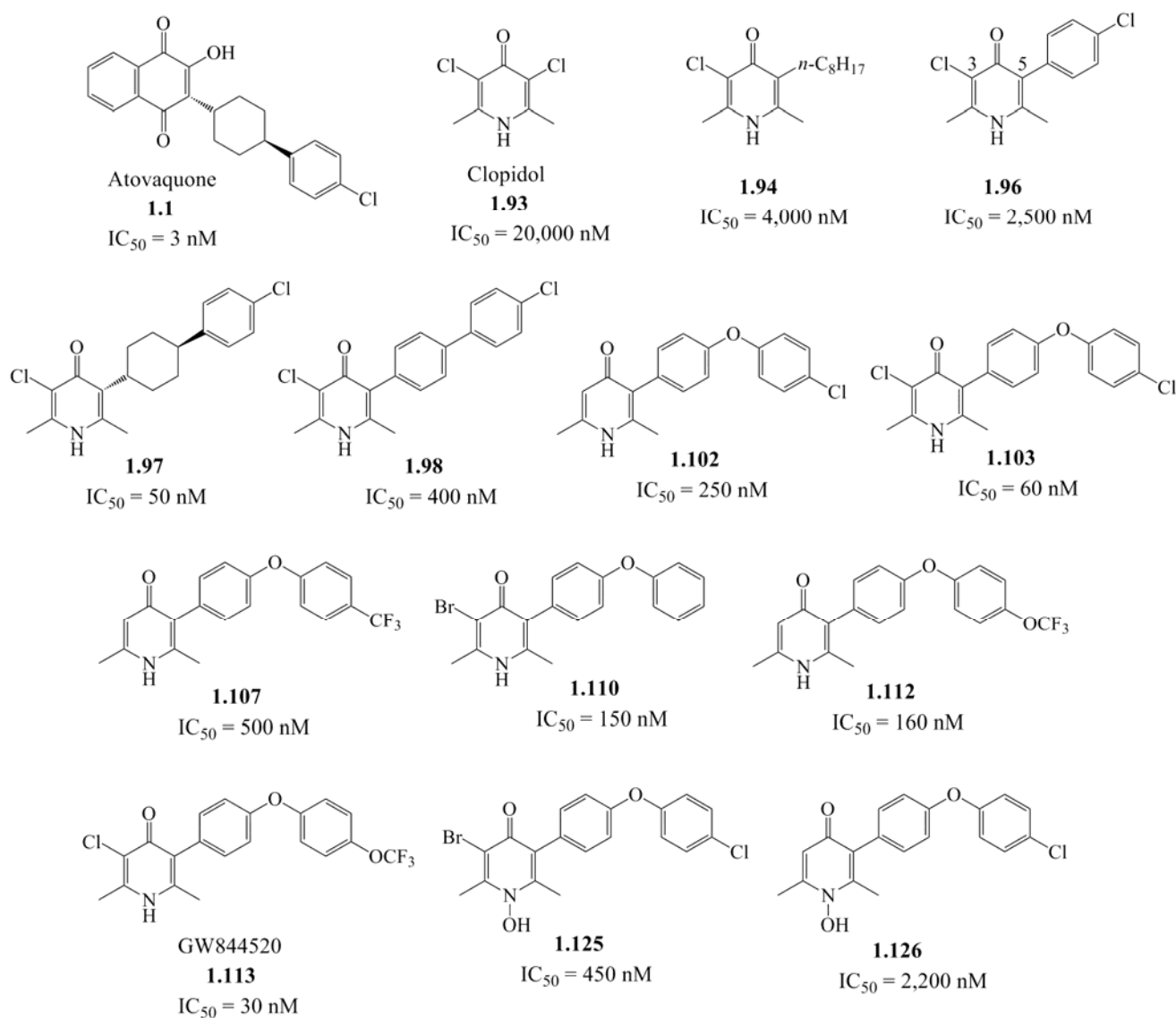


Figure 5.2 Chemical structures of the training set selected for the pharmacophore modeling.

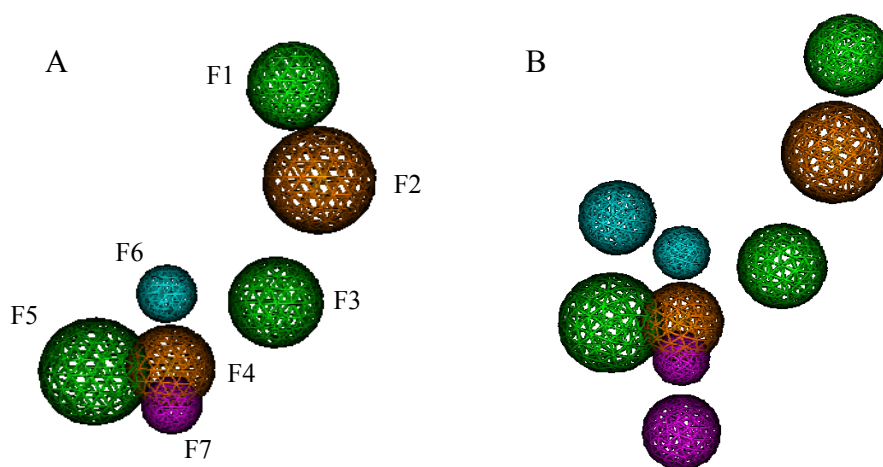


Figure 5.3 (A) shows the pharmacophore model used to screen the ZINC database; (B) shows the model used for the MOE database. Green spheres represent hydrophobic regions, orange represents aromatic regions, blue is a hydrogen-bond acceptor and its projection and purple represents hydrogen-bond donor and its projection.

Therefore, from roughly 8.5 million molecules, the database was reduced to *ca.* 0.5 million drug-like compounds. However, given that this was still a huge number of compounds to perform a conformational search in an acceptable timing, a second filter was applied. Database clustering was achieved by analyzing similarities between the compounds, and was carried out with the algorithm of Bienfait, which incrementally selects compounds that differ from all previous. The downloaded database consisted of a 136,996 compound set for which the conformational search was performed.

For the MOE drug-like database, over 600,000 compounds were supplied with the conformational library already constructed. Therefore, no other filters were applied before the VS.

In the *in silico* screen of the ZINC database with the pharmacophore model, F1-F5 were deemed essential for a compound to be considered a hit and a partial match of six out of the seven features was allowed, by marking that option in the software window. This permitted to drastically reduce the database size, without being excessively restrictive. Around 1000 positive hits were obtained, according to this methodology, as indicated in Figure 5.4.

For the MOE database screen, projections of both hydrogen bond acceptors and donors with a 1.4 Å radius were added, Figure 5.3 B, and retrieved only those compounds that matched every feature. This was due to the high number of hits for the MOE database when the first model was used (over 7,000), which would be unsuitable for the second stage of VS, i.e. receptor-based VS. Thus, employing this methodology the size of the database was reduced to approximately 700 compounds which were selected for further refinement, Figure 5.4.

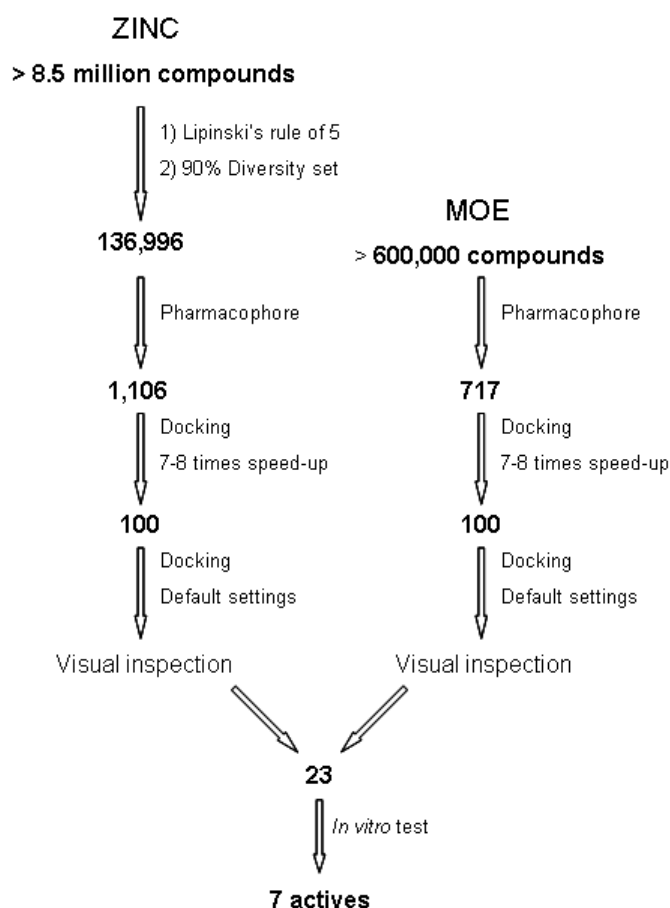


Figure 5.4 Virtual screening protocol breakdown.

5.3 Receptor-based virtual screening

The hits were docked with GOLD^[192] into the cytochrome *bc*₁ model that had been validated in previous studies. VS involving docking of large databases can be computationally very expensive. Therefore it is needed to find an approach that optimizes the balance between the precision of docking and the time required for the process. The initial stages of receptor-based virtual screening are generally executed to discard many compounds quickly, retaining only those which fit the receptor. Exhaustive docking for the retained compounds can subsequently be carried out to estimate their binding pose, and interactions with the target receptor. Thus, in the present study, the docking processes were performed in three consecutive stages, employing different settings in GOLD.

At first, VS was performed with 7-8 times speed-up settings. This is an optimized setting for VS protocols, since a lower number of genetic operations are done. As a result, a higher throughput is obtained with acceptable accuracy rates in the prediction^[192]. The best 100 ligands of each

database, Appendices 3.2 and 3.3, were subjected to further docking refinement, this time with standard settings, i.e. a higher number of genetic operations, but a relatively low number of runs. The final GoldScores were ordered, and each ligand was visually inspected for hydrogen bonding with histidine 181 and glutamate 272, since these two residues are involved in physiological electron transfer across the *bc*₁ complex^[58]. Favourable hydrophobic interactions were also sought, as well as plausible docking poses, based on my experience.

5.3 Antiplasmodial activity

From the 200 molecules visually inspected, 23 compounds were purchased, Figure 5.5, and shifted to *in vitro* antiplasmodial testing against the *P. falciparum* W2 and 3D7 (chloroquine-sensitive) strains. Out of the 23 compounds submitted for *in vitro* assays, 7 of them were found to present antiplasmodial activity in the micromolar range against the W2 strain, Table 5.1. While one of the compounds, **5.10**, exhibited activity with an IC₅₀ value of 12 μM against the W2 strain, and 10 μM against the 3D7 strain, most of the other active compounds presented IC₅₀ values around 30 μM, i.e. compounds **5.6**, **5.11** and **5.12**. Compound **5.7** showed an IC₅₀ of around 50 μM for *P. falciparum* W2. Finally, compounds **5.21** and **5.23** demonstrated activity below 10 μM, with the former displaying an IC₅₀ of 2 μM. All other compounds did not present noticeable activity up to the tested concentrations.

These results are very encouraging and partly validate the virtual screening protocol, as it proved to be efficient in identifying active compounds. The expected success rate for a good pharmacophore ranges from 0.5 to 20%, according to Soichet *et al.*^[320]. In this case, the overall success rate was at least 30% (7 out of 23), since some of the compounds were tested only up to 10 μM. From those, 6 of the active compounds were from MOE (44% success rate), and only 1 was from ZINC (14% success rate).

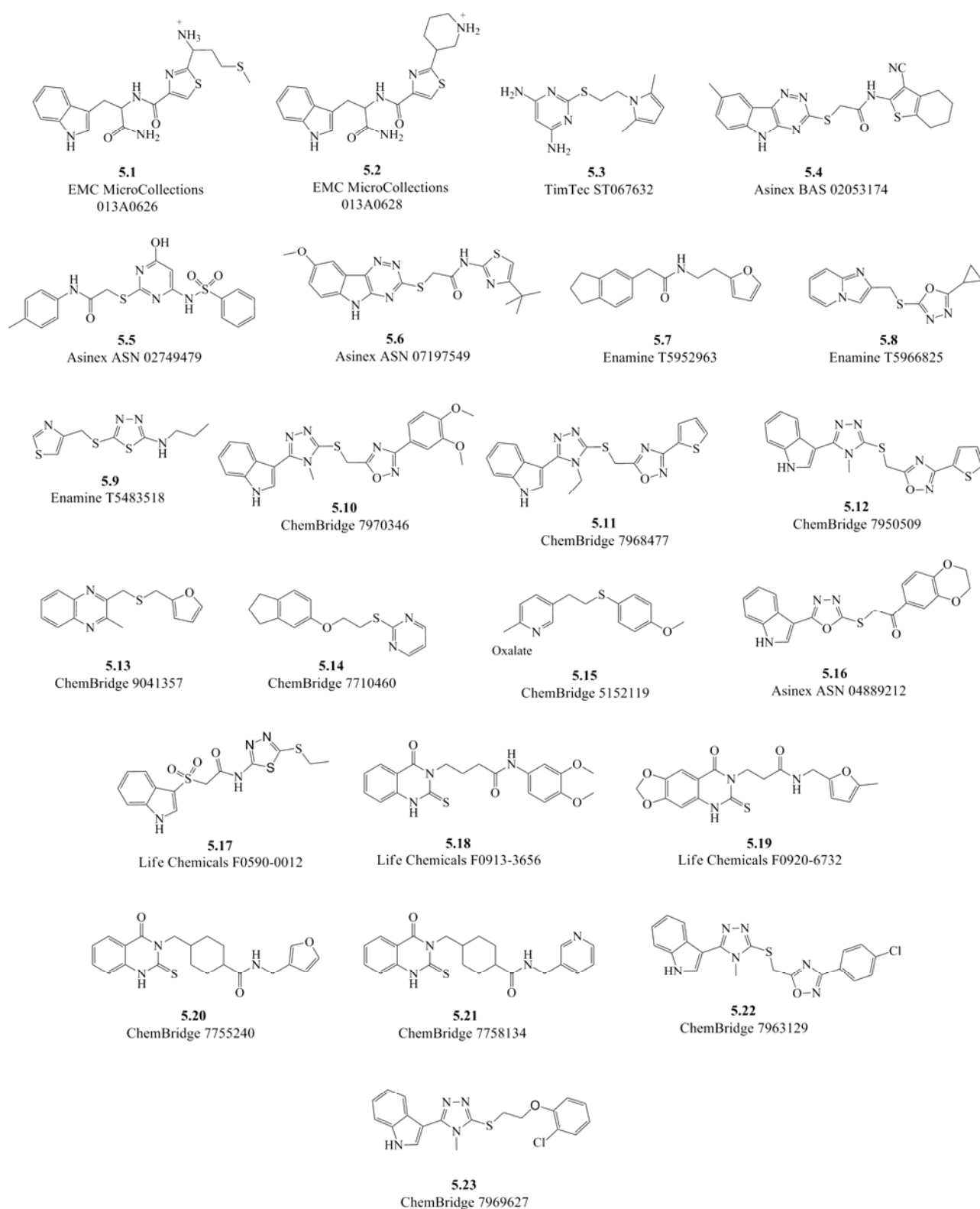


Figure 5.5 Structures of compounds selected from the virtual screening protocol.

Table 5.1 Biological data for compounds selected from virtual screening.

Compound	IC ₅₀ ± SD (μM)	
	W2 strain	3D7 strain
5.1	N.D.	> 10
5.2	N.D.	> 10
5.3	> 25	> 10
5.4	> 50	> 10
5.5	> 50	> 10
5.6	27.1 ± 2.0	> 10
5.7	49.8 ± 1.9	> 10
5.8	> 50	> 10
5.9	> 50	> 10
5.10	12.1 ± 0.2	10.2
5.11	28.5 ± 0.3	> 10
5.12	29.5 ± 2.7	> 10
5.13	> 50	> 10
5.14	> 50	> 10
5.15	> 50	> 10
5.16	> 10	N.A.
5.17	N.D.	N.A.
5.18	> 10	N.A.
5.19	> 10	N.A.
5.20	> 10	N.A.
5.21	1.97 ± 0.9	N.A.
5.22	> 10	N.A.
5.23	6.69 ± 2.1	N.A.

N.D. - Not Determined; N.A. - Not Available

The third round of docking studies was performed to better predict the binding pose of the active compounds in the Q_o site. Taken the antiplasmodial activities and the docking poses together one can observe the following:

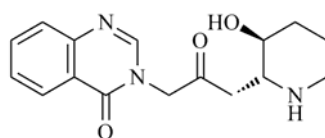
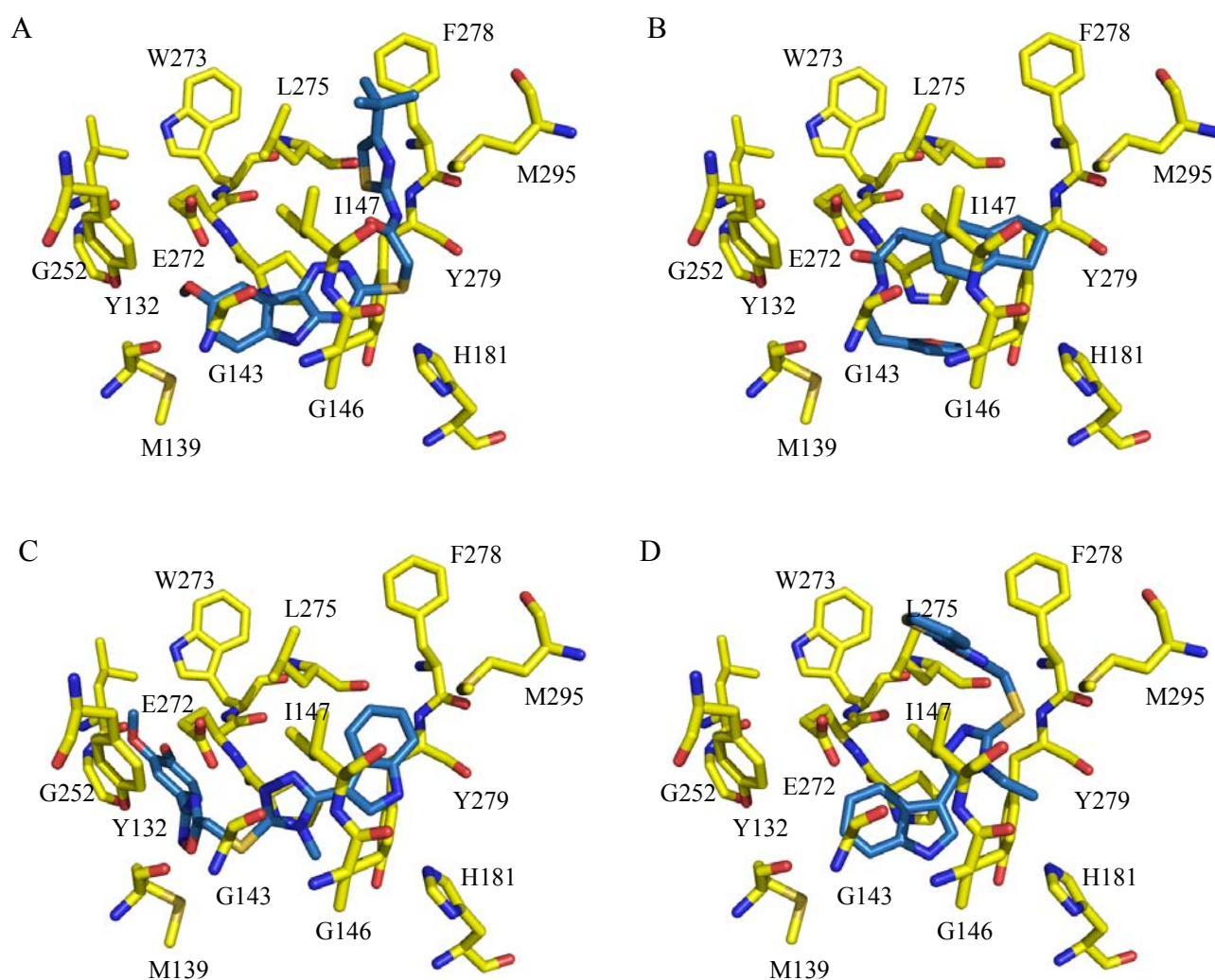
- a) All compounds fit well in the active site and show mainly hydrophobic interactions with the aminoacid residues, which may be insufficient for an effective blocking of cytochrome *bc*₁, Figure 5.6. Compound **5.6**, is one exception, presenting an interaction with the critical histidine 181; the nitrogen of the triazino group distances 2.42 Å from the protonated imidazole group of the protein. The sulfur atom is also at 1.77 Å from the same proton. Despite all compounds complying with the Lipinski's rule of five, deficient

cell permeability is still possible, which might be one possible factor for the modest antiplasmodial activity^[318], namely for compound **5.6**;

- b) The presence of a dimethoxyphenyl group in **5.10** is responsible for a 2-fold increase in activity when compared to its thiophene counterpart, i.e. compound **5.12**. Moreover, the docking study reveals a different docking pose for **5.10**, Figure 5.6 C, when compared to its related indole compounds **5.11-12**, Figure 5.6 D and E. This may help explain the different IC₅₀ values, based on a stronger van der Waals interaction with the receptor. While in **5.10** the side chain is docked deep into protein, for **5.11** and **5.12** it is directed to the outer side of the binding pocket;
- c) The insertion of an ethyl or methyl groups in the triazole moiety appears to be insignificant for the antiplasmodial activity, i.e. **5.11** vs. **5.12**;
- d) Compound **5.23** displays an analogous docking pose to **5.10** which is consistent with the higher activity, for the triazolylindole subset of compounds. In this case, it appears that the oxadiazole ring present in **5.10-12** is also detrimental for the antiplasmodial activity, as a shorter linker to the terminal aryl moiety, e.g. **5.23**, leaves this better accommodated in the binding pocket;
- e) Compound **5.21** displays excellent antiplasmodial activity and a docking pose consistent with the *in vitro* tests. The carbonyl group from the 2-thioxoquinazolinone scaffold is placed at 5.00 Å of E272 and possibly lodges a water molecule between to mediate a hydrogen bond. The thioxo group is also at 3.83 Å of H181, which is a documented distance for interaction with aromatic moieties^[298]. Taken together, these strong interactions possibly account for the low IC₅₀ against the W2 strain;
- f) Compound **5.20**, which differs only in the terminal aryl moiety from **5.21**, does not present antiplasmodial activity up to 10 µM. Also, **5.20** exhibits a very similar docking pose to the one seen by **5.21** and, as a consequence, an IC₅₀ in the same order of magnitude would be expected. Compound **5.20** has a logS_w of -5.06, whereas its **5.21** analogue is considerably more soluble in water, logS_w = -3.36 (data from the supplier). Therefore, the observed difference in activity can be related to the better solubility of the compound in the assay;
- g) For the 2-thioxoquinazolinone subset of compounds it is possible to see that a cyclohexyl group in the side chain is probably important for the antiplasmodial potency, **5.21** vs. **5.18**.

In summary, this VS study allowed the identification of new scaffolds with potential for lead optimization. β-Carbolines are known to present antiplasmodial activity in the low micromolar or

nanomolar range [321, 322]. For the related [1,2,4]triazino[5,6*b*]indole scaffold, only one study by Kgekong *et al.* can be found, and all compounds presented antiplasmodial activities around 20 μM [323], which is very similar to **5.6**. However, compounds with this scaffold have shown great value in inhibiting human papiloma virus infections [324]. Regarding the 3-(1,2,4-triazol-3-yl)indole and 2-thioxo-2,3-dihydroquinazolin-4(1*H*)-one scaffolds, no reports on antiplasmodial activity can be found. Still, a vast number of papers have been published on the related alkaloid febrifugine, **5.24**, and analogues, reporting antiplasmodial activities in the low nanomolar range [325-328].

**5.24****Figure 5.6** Docking poses for selected compounds: (A) **5.6**; (B) **5.7**; (C) **5.10**; (D) **5.11**.

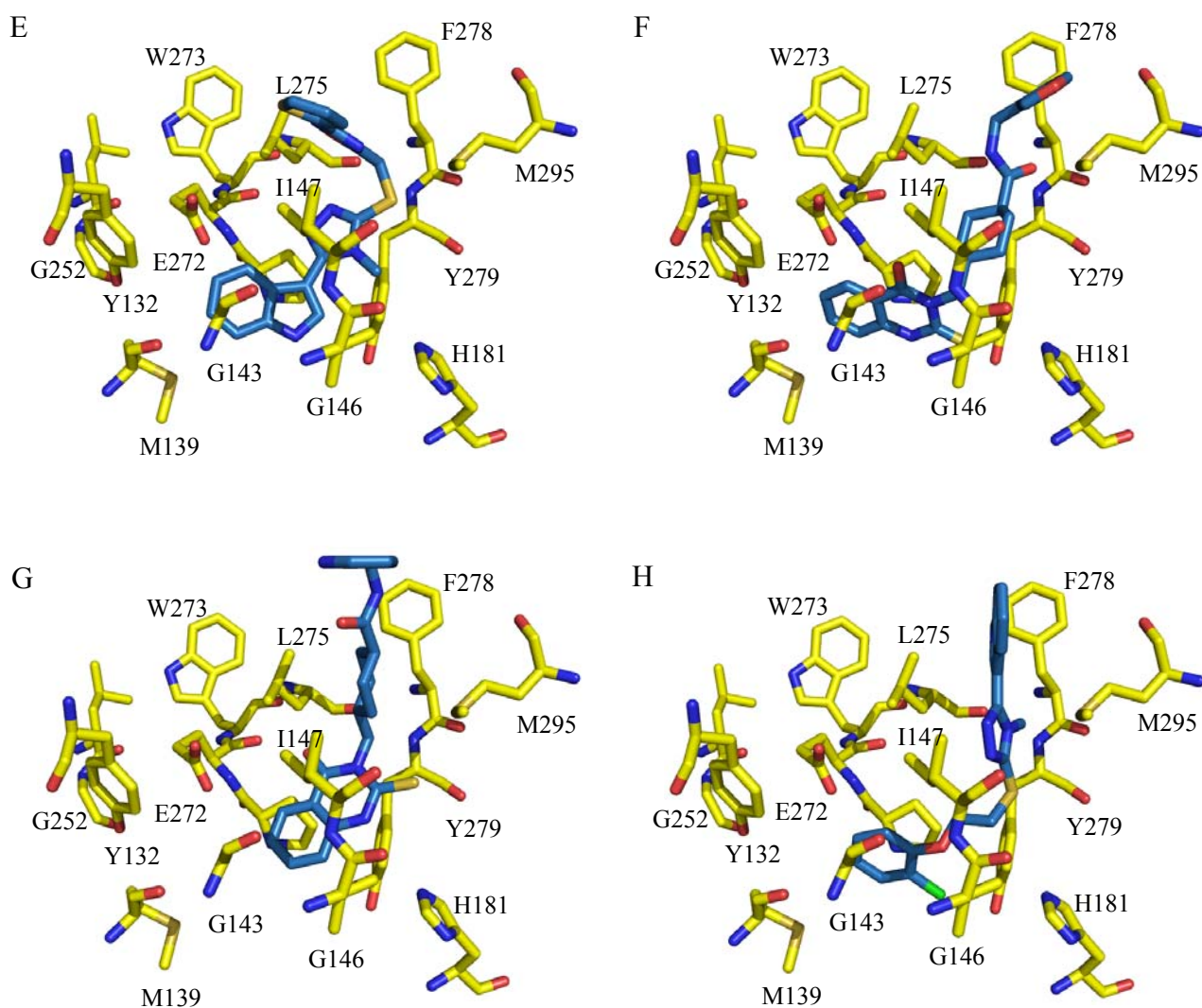


Figure 5.7 (cont.) Docking poses for selected compounds: (E) 5.12; (F) 5.20; (G) 5.21; (H) 5.23.

5.4 Conclusions

Scaffold hopping is one of the major goals in VS studies, particularly in ligand-based approaches. This strategy allowed the discovery of novel scaffolds with potential for optimization, which partly validates the protocol. The *in vitro* screening of the active compounds in whole cell assays is now ongoing against the bc_1 complex.

CHAPTER 6

CONCLUSIONS AND PERSPECTIVES

6. CONCLUSIONS AND PERSPECTIVES

This doctoral work set out to identify novel inhibitors of the bc_1 complex, supported on the bioisosteric replacement of the carbonyl group of 4(1*H*)-pyridones and quinolones by an imine bond. This would allow probing unexplored chemical space, while seeking the obtention of compounds with useful antiplasmodial activity.

Regarding the 4-pyridonimine scaffold, the quantum mechanical studies allowed to validate such compounds as isosteres of the related 4(1*H*)-pyridones. The similarity of their frontier orbitals and the MEPs pattern, with those of 4(1*H*)-pyridones provided proof-of-concept on a theoretical basis. Also, for the Mannich-base compounds that were selected for this study, the antiplasmodial activity correlated well with the complementarity of the electrostatic potential between the binding site and the ligands.

The structure-based design approach that was taken for the scaffold optimization was also very successful. Starting from lead compounds with an IC_{50} of *ca.* 10 μ M, it was possible to design inhibitors with IC_{50} s around 1 μ M against the W2 strain of *P. falciparum*. Concerning the blood stage of the plasmodial infection, the SAR that was found is similar to that of the GSK's 4(1*H*)-pyridones. For the liver stage, some of the compounds showed very potent activity at 10 μ M, but were also cytotoxic.

For the 4-quinolonimines, the antiplasmodial activity improved further, possibly from the introduction of a second aromatic ring. The most active compounds presented a biphenyl side chain, i. e. **3.22** and **3.23**, and IC_{50} s of *ca.* 0.5 μ M. Against the liver stage, most of the compounds at 2 μ M were at least as active as primaquine at 5 μ M, and were not significantly cytotoxic. Also, these have shown not to suffer Michael additions at C2. Therefore, these 4-quinolonimines are interesting compounds for further studies. Structures to be studied include different substituents at quinolonimine core and eventually other aromatic rings in the side chain, **6.1**.

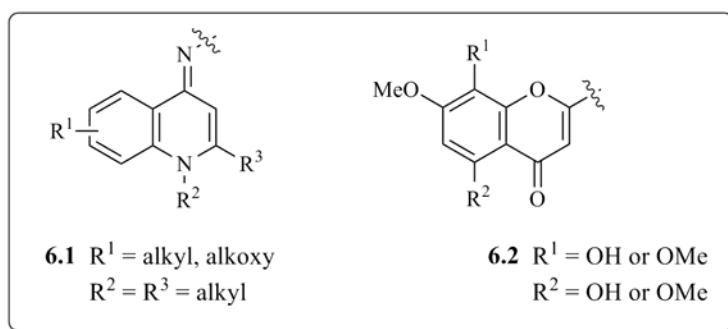
In relation to their mechanism of action it is necessary to stress that it might be composited by inhibition of more than one target:

- a) The docking studies into the bc_1 complex provided a rationale for its inhibition;
- b) The compounds present a 7-chloro or 7-(trifluoromethyl)quinoline moiety which is similar to known inhibitors of hemozoin polymerization;
- c) The compounds bind to hemozoin as tightly as chloroquine, and the $\log K_{\text{ass}}$ follows the same trend as the antiplasmodial activity;

- d) The compounds are very active against the liver stage, where no haemoglobin degradation occurs. Thereby the mechanism of action must be other than the inhibition of hemozoin polymerization;
- e) The SAR for these compounds in both blood and liver stages is different. Bearing in mind that the tests were carried out in different species, it is difficult to draw conclusions. The most active compounds against the W2 strain, i.e. **3.22** and **3.23**, were also the ones that bound more tightly to hemozoin. However, **3.22** and **3.23** were among the least active compounds at 2 μM in the liver stage studies. It is possible that, for at least these two compounds, more than one mechanism of action exists.

Hence, further studies on the mechanism of action are required in the future, namely the inhibition of the cytochrome bc_1 complex. This will also provide the proof-of-concept for the rationale behind the development of these compounds.

For the flavone series, only modest antiplasmodial activity against the blood and liver stages was obtained, but there are still some chemical modifications in the chromone moiety that may improve the IC_{50} . Among those, compounds with the scaffold **6.2** deserve some attention. The substituent at R^1 would interact with E272, whereas the substituent at R^2 would interact with H181. Also, the resemblance to ubiquinol can improve the antiplasmodial activity.



Regarding the virtual screening studies a 3D-pharmacophore model was built and successfully sieved two databases into a workable number of compounds for the structure-based VS. From 23 compounds tested *in vitro*, 7 displayed antiplasmodial activity. From those, 3 had an IC_{50} of 10 μM or better, with the most active at an IC_{50} of 2 μM , **5.21**. More importantly, three novel scaffolds for drug development were discovered: triazolyloindoles, triazinoindoles and 2-thioxoquinazolinones. Besides, this is the first VS study targeting the bc_1 complex, to the best of my knowledge.

Finally, this work has enabled the understanding of the required features that an effective bc_1 complex inhibitor must have. It also contributed to the discovery of interesting leads for further drug development in the context of malaria.

CHAPTER 7

EXPERIMENTAL SECTION

7. EXPERIMENTAL SECTION

7.1 Reagents and solvents

Reagent grade chemicals were bought from Sigma-Aldrich, Alfa-Aesar or Matrix Scientific. MeOH and CHCl₃ were dried from calcium chloride and distilled at atmospheric pressure. THF was distilled from sodium-benzophenone as a humidity indicator and stored with molecular sieves 4A. Pyridine was distilled from NaOH at room pressure while liquid aldehydes were distilled under reduced pressure. Toluene was dried with sodium and distilled at room pressure. The remaining solvents and reagents were used without further purification.

7.2 Chromatography

Column chromatography was performed with silica gel (Merck, 230-400 mesh ASTM). TLC was performed on pre-coated silica gel 60 F254 (Merck) and visualized under UV light or by exposure to iodine vapour. All the reactions were monitored by TLC unless otherwise stated.

7.3 Equipment

Melting points were determined using a Kofler camera Bock Monoscope M and are uncorrected. The IR spectra were determined using thin films between NaCl plates on a Nicolet Impact 400 FTIR spectrophotometer, and only the most significant absorption bands are reported. Low-resolution mass spectra were recorded using a VG Quattro LCMS instruments. Elemental analyses were performed using an EA 1110 CE Instruments automatic analyser. HR-ESI-MS were recorded on an ESI-TOF spectrometer (Biotof II Model, Bruker). NMR spectra were recorded on a Bruker Avance 400 NMR spectrometer (¹H 400 MHz; ¹³C 100.61 MHz; ³¹P 161.98 MHz) and a Jeol JNM-60 (¹H 60 MHz). ¹H and ¹³C chemical shifts (δ) are expressed in ppm (parts per million) and are relative to the corresponding resonance of tetramethylsilane. Coupling constants (*J*) are reported in hertz (Hz). X-ray crystallography was carried out on a Bruker Kappa APEX II. Microwave-assisted synthesis was performed in a CEM Corporation Discover[®] Labmate[™], and hematin titrations were carried out at a Shimadzu UV-visible spectrophotometer.

7.4 Synthesis

7.4.1 Mannich-base side chain

2-(Diethylaminomethyl)paracetamol, 2.47

The compound was obtained from a previously described method ^[201]. Generally the Mannich reaction was performed with paracetamol (1 molar eq.), *N,N*-diethylamine (2 molar eq.) and liquid formaldehyde 37% (2 molar eq.) in absolute ethanol (3.3 mL/mmol). The mixture was refluxed for variable periods of time, after which the solvent was removed under reduced pressure and the residue dissolved in dichloromethane (10 mL). The organic solution was extracted with hydrochloric acid. This solution was then basified (pH 9-10) and extracted with dichloromethane (3×50 mL). The combined extracts were washed with water (20 mL) and dried over MgSO₄. Recrystallization was achieved using toluene / petroleum ether (40-60 °C) (20:80 v/v).

Table 7.1 Conditions for the synthesis of 2-(diethylaminomethyl)paracetamol.

Method	Reaction time	[HCl] (M)	Yield (%)
A	reflux/48 h	0.1	76
B	reflux/24 h	1.5	70

Pale yellow solid; mp 128-130 °C; ¹H-NMR (CDCl₃, 400.13 MHz) δ 1.07 (6H, t, *J* = 7.2 Hz, CH₃); 2.11 (3H, s, CH₃); 2.58 (4H, q, *J* = 7.2 Hz, CH₂); 3.75 (2H, s, CH₂); 6.71 (1H, d, *J* = 9.0 Hz, Ar-*H*); 7.01 (1H, dd, *J* = 2.7 and 8.7 Hz, Ar-*H*); 7.09 (1H, br.s, NH); 7.29 (1H, d, *J* = 2.4 Hz, Ar-*H*); ¹³C-NMR (CDCl₃, 100.61 MHz) δ 11.21; 24.36; 46.31; 56.91; 116.09; 120.77; 121.17; 122.34; 129.28; 155.28; 168.14; IR (film): ν_{max} 3267; 1651; 1561; 1491; 1255 cm⁻¹.

Bis[2,6-(diethylaminomethyl)]paracetamol, 2.48

Paracetamol (1 molar eq.), diethylamine (2 molar eq.), liquid formaldehyde 37% (2 molar eq.) and absolute ethanol (3.3 mL/mmol) was refluxed for 48-72 hours and the mixture treated as described for **2.47**. A white solid was obtained; 18%; mp 33-35 °C; ¹H-NMR (CD₃OD, 400.13 MHz) δ 1.13 (12H, t, *J* = 7.2 Hz, CH₃); 2.10 (3H, s, CH₃); 2.64 (8H, q, *J* = 7.2 Hz, CH₂); 3.73 (4H, s, CH₂); 7.25 (2H, s, Ar-*H*).

4-Amino-2-(diethylaminomethyl)phenol, 2.49

2.47 (1 molar eq.) was heated overnight in hydrochloric acid 6N (5 mL/mmol) at reflux temperature. This solution was concentrated under reduced pressure and then coevaporated with ethanol. Flash chromatography of the crude product on silica gel with CH₂Cl₂ : MeOH (8:2) gave **2.49** as an amorphous brown gum; 100%; ¹H-NMR (DMSO-*d*₆, 400.13 MHz) δ 1.24 (6H, t, *J* = 7.2 Hz, CH₃); 3.05 (4H, q, *J* = 7.2 Hz, CH₂); 4.20 (2H, s, CH₂); 7.09 (1H, d, *J* = 8.4 Hz, Ar-*H*); 7.27 (1H, dd, *J* = 2.4 and 8.7 Hz, Ar-*H*); 7.47 (1H, d, *J* = 2.4 Hz, Ar-*H*); 9.85 (1H, br.s, OH).

4-Amino-2,6-bis((diethylamino)methyl)phenol, 2.50

Amorphous brown gum; 100%; ¹H-NMR (DMSO-*d*₆, 400.13 MHz) δ 1.16 (12H, t, *J* = 7.2 Hz, CH₃); 3.11 (8H, q, *J* = 7.2 Hz, CH₂); 4.24 (4H, s, CH₂); 7.34 (2H, s, Ar-*H*); 10.10 (1H, br.s, OH).

7.4.2 4-(Pyridin-4-ylamino)phenols

2.49 or **2.50** was added to 4-chloropyridine in absolute ethanol (5 mL/mmol). The mixture was heated under reflux temperature and the reaction followed by TLC. Several methods were employed and are summarized in Table 7.2.

Table 7.2 Conditions for the synthesis of 4-(pyridin-4-ylamino)phenols.

Method	2.49 mol eq.	Py mol eq.	Work-up	Purification	Eluent
A ^[201]	1	1	NH ₄ OH, CH ₂ Cl ₂	Column chromatograph.	CH ₂ Cl ₂ :MeOH (4:1)
B	2	1	NH ₄ OH, CH ₂ Cl ₂	Column chromatograph.	CH ₂ Cl ₂ :MeOH (4:1)
C	1	1	-	Column chromatograph.	CH ₂ Cl ₂ :MeOH:TEA 1%
D	3	1	-	Flash chromatography	CH ₂ Cl ₂ :MeOH (4:1)

2-Diethylaminomethyl-4-(pyridin-4-ylamino)phenol, 2.51

Method B - **2.49** and 4-chloropyridine hydrochloride were dissolved in absolute ethanol. The mixture was heated under reflux temperature for 4 hours and a dark brown solid was obtained; 41%; mp 120-123 °C; ¹H-NMR (CDCl₃, 400.13 MHz) δ 1.13 (6H, t, *J* = 7.2 Hz, CH₃); 2.66 (4H, q, *J* = 7.2 Hz, CH₂); 3.77 (2H, s, CH₂); 5.83 (1H, s, NH); 6.63 (2H, d, *J* = 4.8 Hz, Ar-*H*3); 6.82 (1H, d, *J* = 8.8 Hz, Ar-*H*); 6.85 (1H, d, *J* = 1.6 Hz, Ar-*H*); 7.02 (1H, dd, *J* = 2.0 and 8.4 Hz, Ar-*H*); 8.23 (2H, d, *J* = 4.8 Hz, Ar-*H*2); ¹³C-NMR (CDCl₃, 100.61 MHz) δ 11.22; 46.38; 56.83; 108.51; 116.91;

123.07; 124.53; 124.76; 130.14; 150.09; 152.32; 156.14; IE-MS m/z (abund.): 271.15 $[M]^+$ (45); 198.00 (100); Anal. Calcd. ($C_{16}H_{21}N_3O \cdot 0.15 CH_2Cl_2 \cdot 0.3 H_2O$): C, 67.00; H, 7.42; N, 14.51. Found: C, 68.18; H, 7.49; N, 14.43.

Method E - **2.59** (1 molar eq.) was added to liquid formaldehyde 37% (2 molar eq.), diethylamine (2 molar eq.) and absolute ethanol (3.3 mL/mmol). The mixture was heated under reflux temperature for 18 hours, the solvent evaporated under reduced pressure and the resulting crude product purified by flash chromatography CH_2Cl_2 : MeOH : TEA (4:1:0.01). A dark brown oil was obtained (65%) and identified as **2.51**.

2-Diethylaminomethyl-4-(3-methylpyridin-4-ylamino)phenol, 2.52

Method A - The mixture was heated under reflux temperature for 27 hours and a brown solid was obtained; 17%; mp 96-98 °C; 1H -NMR ($CDCl_3$, 400.13 MHz) δ 1.15 (6H, t, $J = 7.2$ Hz, CH_3); 2.21 (3H, s, CH_3); 2.66 (4H, q, $J = 7.2$ Hz, CH_2); 3.78 (2H, s, CH_2); 5.58 (1H, s, NH); 6.65 (1H, d, $J = 5.6$ Hz, Ar-*H5*); 6.84 (1H, d, $J = 8.4$ Hz, Ar-*H*); 6.86 (1H, d, $J = 2.0$ Hz, Ar-*H*); 7.02 (1H, dd, $J = 2.0$ and 8.6 Hz, Ar-*H*); 8.11 (1H, d, $J = 5.2$ Hz, Ar-*H6*); 8.16 (1H, s, Ar-*H2*); ^{13}C -NMR ($CDCl_3$, 100.61 MHz) δ 11.22; 14.28; 46.37; 56.81; 105.92; 116.93; 123.10; 125.03; 125.24; 126.99; 130.35; 148.47; 150.17; 150.77; 156.15; IR (film): ν_{max} 3164; 1593; 1498 cm^{-1} ; IE-MS m/z (abund.): 285.15 $[M]^+$ (78); 212.10 (100); Anal. Calcd. ($C_{17}H_{23}N_3O \cdot 0.15 CH_2Cl_2 \cdot 0.45 H_2O$): C, 67.26; H, 7.97; N, 13.72. Found: C, 67.29; H, 7.98; N, 13.66.

On the other hand, method D was used and afforded a brown solid (54%), identified as **2.52**.

2-Diethylaminomethyl-4-(3-aminopyridin-4-ylamino)phenol, 2.53

Several methods were used for the synthesis of **2.53**, as summarized in Table 7.3.

Table 7.3 Conditions for the synthesis of **2.53**.

Method	2.49 mol eq.	Py mol eq.	Reaction time	Flash Chromatograph	Yield (%)
C	1	1	reflux/24 h	-	17
D	3	1	reflux/24 h	CH_2Cl_2 :MeOH (4:1)	76
F	2.5	1	reflux/2 h	CH_2Cl_2 :MeOH (4:1)	43
G	2.5	1	reflux/20 h	CH_2Cl_2 :MeOH (4:1)	65

A dark brown solid was obtained; 76%; mp 130-132 °C; ¹H-NMR (CD₃OD, 400.13 MHz) δ 1.41 (6H, t, *J* = 7.2 Hz, CH₃); 3.28 (4H, q, *J* = 7.2 Hz, CH₂); 3.37 (2H, s, NH₂); 4.38 (2H, s, CH₂); 5.71 (1H, s, NH); 6.92 (1H, d, *J* = 6.6 Hz, Ar-*H*5); 7.09 (1H, d, *J* = 8.6 Hz, Ar-*H*); 7.35 (1H, dd, *J* = 2.6 and 8.6 Hz, Ar-*H*); 7.46 (1H, d, *J* = 2.8 Hz, Ar-*H*); 7.75 (1H, d, *J* = 6.6 Hz, Ar-*H*6); 7.79 (1H, s, Ar-*H*2); ¹³C-NMR (CD₃OD, 100.61 MHz) δ 7.78; 46.66; 50.95; 104.70; 116.41; 117.77; 121.90; 128.37; 129.11; 129.46; 131.62; 133.25; 146.95; 155.39; IE-MS *m/z* (abund.): 286.15 [M]⁺ (62); 184.05 (100); Anal. Calcd. (C₁₆H₂₂N₄O • 0.5 CH₂Cl₂ • 0.40 H₂O): C, 58.97; H, 7.14; N, 16.67. Found: C, 59.16; H, 7.11; N, 16.76.

2-Diethylaminometil-4-(2-methylpyridin-4-ylamino)phenol, 2.55

Method C - The mixture was heated under reflux temperature for 28 hours. A brown solid was obtained; 17%; mp 202-204 °C; ¹H-NMR (CD₃OD, 400.13 MHz) δ 1.38 (6H, t, *J* = 7.2 Hz, CH₃); 2.51 (3H, s, CH₃); 3.20 (4H, q, *J* = 7.2 Hz, CH₂); 4.31 (2H, s, CH₂); 6.84 (1H, br.s, Ar-*H*3); 6.90 (1H, dd, *J* = 7.2 and 2.2 Hz, Ar-*H*5); 7.05 (1H, d, *J* = 8.8 Hz, Ar-*H*); 7.28 (1H, dd, *J* = 8.8 and 2.8 Hz, Ar-*H*); 7.37 (1H, d, *J* = 2.8 Hz, Ar-*H*); 8.03 (1H, d, *J* = 7.2 Hz, Ar-*H*6); ¹³C-NMR (CD₃OD, 100.61 MHz) δ 7.87; 17.09; 47.44; 50.48; 108.00; 109.72; 116.42; 117.66; 122.99; 127.72; 128.55; 128.92; 139.90; 156.63; 157.68; IE-MS *m/z* (abund.): 285.15 [M]⁺ (35); 212.10 (100); Anal. Calcd. (C₁₇H₂₃N₃O • 1.1 CH₂Cl₂ • 1.7 H₂O): C, 53.10; H, 7.04; N, 10.26. Found: C, 52.89; H, 7.01; N, 10.33.

Method G - The mixture was heated under reflux temperature for 4 hours and the crude product purified by flash chromatography CH₂Cl₂ : MeOH : TEA in several proportions. A black solid was obtained (53%), corresponding to **2.55**.

Method D - The mixture heated under reflux temperature for 21 hours. The crude product was purified by flash chromatography CH₂Cl₂ : MeOH : TEA in several proportions. A black solid was obtained (77%), also corresponding to **2.55**.

4-(3-((Diethylamino)methyl)-4-hydroxyphenylamino)pyridine-3-sulfonamide, 2.56

Method C - The mixture was heated under reflux temperature for 30 hours. A pale yellow solid was obtained after purification; 15%; mp 72-75 °C (EtOH/CH₂Cl₂); ¹H-NMR (CD₃OD, 400.13 MHz) δ 1.38 (6H, t, *J* = 7.2 Hz, CH₃); 3.22 (4H, q, *J* = 7.2 Hz, CH₂); 4.32 (2H, s, CH₂); 6.82 (1H, d, *J* = 5.6 Hz, Ar-*H*5); 7.05 (1H, d, *J* = 8.4 Hz, Ar-*H*); 7.29 (1H, d, *J* = 8.4 Hz, Ar-*H*); 7.37 (1H, s, Ar-*H*); 8.16 (1H, d, *J* = 5.6 Hz, Ar-*H*6); 8.68 (1H, s, Ar-*H*2); ¹³C-NMR (CD₃OD, 100.61 MHz) δ 7.95; 47.28; 51.44; 107.77; 116.32; 118.14; 122.52; 128.71; 129.28; 129.70; 148.48; 149.88; 151.29;

155.38; IR (film): ν_{\max} 3370; 3125; 1587; 1498; 1415; 1262; 1146 cm^{-1} ; IE-MS m/z (abund.): 350.15 $[\text{M}]^+$ (38); 58.00 (100); Anal. Calcd. ($\text{C}_{16}\text{H}_{22}\text{N}_4\text{O}_3\text{S} \cdot 2.7 \text{CH}_2\text{Cl}_2$): C, 38.74; H, 4.76; N, 9.66; S, 5.53. Found: C, 37.51; H, 4.68; N, 9.68; S, 5.49.

Method D - The mixture heated under reflux temperature for 20 hours. The crude product was purified by flash chromatography CH_2Cl_2 : MeOH (4:1) and TEA (500 μL /200 mL) after evaporating the solvent. The product was recrystallized from EtOH/ CH_2Cl_2 , yielding a pale yellow solid (89%) corresponding to **2.56**.

2,6-Bis[diethylaminomethyl]-4-(pyridin-4-ylamino)phenol, 2.57

After acidic hydrolysis of **2.50**, the corresponding aniline (1 molar eq.) was added to 4-chloropyridine hydrochloride (1.5 molar eq.) and absolute ethanol (3.3 mL/mmol). The mixture was heated under reflux temperature for 23 hours, after which the solvent was evaporated and the crude product subjected to column chromatography CH_2Cl_2 : MeOH : TEA (2:7.9:0.1). A light brown solid was obtained; 16%; mp 108-110 $^\circ\text{C}$; $^1\text{H-NMR}$ (CDCl_3 , 400.13 MHz) δ 1.09 (12H, t, $J = 7.0$ Hz, CH_3); 2.61 (8H, q, $J = 7.0$ Hz, CH_2); 3.68 (4H, s, CH_2); 6.40 (1H, s, NH); 6.63 (2H, d, $J = 5.0$ Hz, Ar- H_3); 6.98 (2H, s, Ar- H); 8.17 (2H, d, $J = 5.0$ Hz, Ar- H_2); $^{13}\text{C-NMR}$ (CD_3OD , 100.61 MHz) δ 10.10; 46.21; 53.10; 108.08; 123.81; 123.99; 130.42; 148.45; 153.39; 154.04; IE-MS m/z (abund.): 356.25 $[\text{M}]^+$ (7); 212.05 (100); Anal. Calcd. ($\text{C}_{22}\text{H}_{33}\text{N}_3\text{O} \cdot 0.5 \text{H}_2\text{O}$): C, 69.01; H, 9.10; N, 15.33. Found: C, 69.06; H, 8.97; N, 15.22.

2,6-Bis[diethylaminomethyl]-4-(3-methylpyridin-4-ylamino)phenol, 2.58

After acidic hydrolysis of **2.50**, the corresponding aniline (1 molar eq.) was added to 4-chloro-3-methylpyridine hydrochloride (1.5 molar eq.) and absolute ethanol (3.3 mL/mmol). The mixture was heated under reflux temperature for 41 hours. The solvent was evaporated and the crude product purified by column chromatography CH_2Cl_2 : MeOH : TEA (2:7.9:0.1). A greyish-brown solid was obtained; 11%; mp 104-105 $^\circ\text{C}$; $^1\text{H-NMR}$ (CD_3OD , 400.13 MHz) δ 1.15 (12H, t, $J = 7.2$ Hz, CH_3); 2.23 (3H, s, CH_3); 2.68 (8H, q, $J = 7.2$ Hz, CH_2); 3.77 (4H, s, CH_2); 6.66 (1H, d, $J = 5.6$ Hz, Ar- H_5); 7.01 (2H, s, Ar- H); 7.90 (1H, d, $J = 5.6$ Hz, Ar- H_6); 7.98 (1H, s, Ar- H_2); $^{13}\text{C-NMR}$ (CD_3OD , 100.61 MHz) δ 10.05; 13.36; 46.21; 53.07; 105.57; 118.01; 123.70; 125.57; 130.50; 146.47; 148.14; 152.23; 154.49; IE-MS m/z (abund.): 37.25 $[\text{M}]^+$ (10); 226.05 (100); Anal. Calcd. ($\text{C}_{23}\text{H}_{35}\text{N}_3\text{O} \cdot 0.5 \text{CH}_2\text{Cl}_2$): C, 65.43; H, 8.54; N, 13.57. Found: C, 65.79; H, 8.60; N, 13.63.

4-(Pyridin-4-ylamino)phenol, 2.59

Several methods were used for the synthesis of **2.59**, as summarized in Table 7.4.

Table 7.4 Conditions for the synthesis of **2.59**.

Method	Aminophenol mol eq.	Pyridine mol eq.	Reaction time	Flash Chromatography	Yield (%)
A	1.4	1	reflux/16 h	CH ₂ Cl ₂ :MeOH (4:1)	41
B	3	1	reflux/2 h	CH ₂ Cl ₂ :MeOH (4:1)	54
C	3	1	reflux/4.5 h	CH ₂ Cl ₂ :MeOH (9:1)	80

A light purple solid was obtained; mp 185-187 °C; ¹H-NMR (CD₃OD, 400.13 MHz) δ 6.91 (2H, d, *J* = 8.8 Hz, Ar-*H*); 6.94 (2H, d, *J* = 7.2 Hz, Ar-*H*3); 7.14 (2H, d, *J* = 8.8 Hz, Ar-*H*); 8.09 (2H, d, *J* = 7.2 Hz, Ar-*H*2).

***N*-(4-Methoxyphenyl)pyridin-4-amine, 2.60**

4-Chloropyridine hydrochloride (1 molar eq.) was added to *p*-anisidine (3 molar eq.) and absolute ethanol (5 mL/mmol). The mixture was heated under reflux temperature for 3.5 hours, after which it was completed. The solvent was evaporated under reduced pressure and the crude product purified by flash chromatography CH₂Cl₂ : MeOH (8.5:1.5). An amorphous light blue gum was obtained; 95%; ¹H-NMR (CD₃OD, 400.13 MHz) δ 3.37 (1H, br.s, *NH*); 3.84 (3H, s, *CH*₃); 7.00 (2H, d, *J* = 6.8 Hz, Ar-*H*3); 7.04 (2H, d, *J* = 10.0 Hz, Ar-*H*); 7.25 (2H, d, *J* = 10.0 Hz, Ar-*H*); 8.13 (2H, d, *J* = 6.8 Hz, Ar-*H*2).

7.4.3 4-Chloro-*N*-alkylpyridinium iodides**4-Chloro-*N*-methylpyridinium iodide, 2.62**

Method A - NaH oil dispersion 80% (2 molar eq.) and 4-chloropyridine hydrochloride (1 molar eq. neutral 4-chloropyridine) were kept stirring in anhydrous DMF (20 mL/mmol) at room temperature for approximately 1 hour. Methyl iodide (2.5 molar eq.) was added and the mixture stirred for another 17 hours. The reaction was followed by TLC, CH₂Cl₂ : MeOH : TEA (2:7.9:0.1). The precipitate was filtered off and the filtrate evaporated under reduced pressure. The resulting

crude product from the filtrate was washed with dichloromethane and a light brown solid was recovered, which did not correspond to the desired product.

Method B - 4-Chloropyridine hydrochloride (1 molar eq. of neutral 4-chloropyridine) was neutralized in aqueous solution with Na_2CO_3 until pH 10. The neutral 4-chloropyridine was extracted with diethyl ether (5 and 10 mL) and methyl iodide (4 molar eq.) was added to the ethereal solution. This was left stirring at room temperature for 24 hours, after which the solvent was evaporated, yielding a brown solid; 3%; mp 150-153 °C; $^1\text{H-NMR}$ (CD_3OD , 400.13 MHz) δ 4.40 (3H, s, CH_3); 8.23 (2H, d, $J = 6.4$ Hz, Ar- $H3$); 8.92 (2H, d, $J = 6.8$ Hz, Ar- $H2$).

Method C - 4-Chloropyridine hydrochloride (1 molar eq.) and distilled TEA (6 molar eq.) were added to dry THF (30 mL/mmol). The mixture was left stirring at room temperature for 15 hours and methyl iodide (8 molar eq.) was added afterwards. The solution was stirred for 3 hours and the precipitate was filtered. Only methylated and protonated TEA was recovered.

Method D - 4-Chloropyridine hydrochloride (1 molar eq. of neutral 4-chloropyridine) was neutralized in aqueous solution with Na_2CO_3 until pH 10. The neutral 4-chloropyridine was extracted with dichloromethane (3×10 mL) and the solvent evaporated under reduced pressure. The residue was dissolved in dry THF (1 mL) and methyl iodide (5 molar eq.) was added to the organic solution, which was stirred for 5 days. The precipitate was filtered off as a dark green solid, corresponding to **2.62** (59%).

3-Amino-4-chloro-*N*-methylpyridinium iodide, 2.64

3-Amino-4-chloropyridine (1 molar eq.) was dissolved in dry THF (5 mL/mmol) and methyl iodide (1.5 molar eq.) was added. The solution was left stirring at room temperature for 14 hours. The reaction was then recharged with methyl iodide (1 molar eq.) and left under agitation for 10.5 hours. The precipitate was filtered off and a light brown solid was recovered; 68%; mp 137-139 °C; $^1\text{H-NMR}$ ($\text{DMSO-}d_6$, 400.13 MHz) δ 4.18 (3H, s, CH_3); 6.94 (2H, s, NH_2); 8.02 (1H, d, $J = 6.4$ Hz, Ar- $H5$); 8.09 (1H, d, $J = 6.4$ Hz, Ar- $H6$); 8.14 (1H, s, Ar- $H2$).

3-Amino-4-chloro-*N*-ethylpyridinium iodide, 2.67

3-Amino-4-chloropyridine (1 molar eq.) was dissolved in THF (16 mL/mmol) and ethyl iodide (1 molar eq.) was added. The mixture was heated under reflux temperature for 2 hours. The precipitate was filtered and a dark brown solid was recovered; 44%; mp > 320 °C; $^1\text{H-NMR}$ (CD_3OD , 400.13 MHz) δ 1.63 (3H, t, $J = 7.6$ Hz, CH_3); 4.50 (2H, q., CH_2); 7.79 (1H, d, $J = 6.0$ Hz, Ar- $H5$); 7.91 (1H, d, $J = 6.0$ Hz, Ar- $H6$); 8.15 (1H, s, Ar- $H2$).

7.4.4 Mannich-base 4(1*H*)-pyridonimines

2-(Diethylaminomethyl)-4-(1-methylpyridin-4(1*H*)-ylideneamino)phenol dihydro iodide, **2.1**

Method A - **2.49** (1.1 molar eq.) was added to **2.62** (1 molar eq.) and absolute ethanol (22 mL/mmol). The mixture was heated under reflux temperature for 27 hours and followed by TLC, CH₂Cl₂ : MeOH : TEA (7.9:2:0.1). The solvent was evaporated under reduced pressure, and the crude product purified by column chromatography. No **2.1** was isolated.

Method B - **2.51** (1 molar eq.) was suspended in dry THF (27 mL/mmol) and NaH oil dispersion 80% (1.3 molar eq.) was added. The mixture was stirred at room temperature for 1 hour and methyl iodide (1.8 molar eq.) was added. The suspension was recharged with methyl iodide (1.8 molar eq.) after 5 hours of reaction and then it was left stirring at room temperature for another 20 hours. The precipitate was filtered off, and the filtrate was purified by flash chromatography CH₂Cl₂ : MeOH (4:1). A dark yellow gum was obtained; 59%; ¹H-NMR (CD₃OD, 400.13 MHz) δ 1.34 (6H, t, *J* = 7.2 Hz, CH₃); 3.12 (4H, q, *J* = 7.2 Hz, CH₂); 4.01 (3H, s, CH₃); 4.27 (2H, s, CH₂); 7.02 (1H, d, *J* = 8.8 Hz, Ar-*H*); 7.04 (2H, d, *J* = 7.2 Hz, Ar-*H*3); 7.26 (1H, d, *J* = 8.8 Hz, Ar-*H*); 7.36 (1H, s, Ar-*H*); 8.16 (2H, d, *J* = 7.2 Hz, Ar-*H*2); ¹³C-NMR (CD₃OD, 100.61 MHz) δ 8.56 (CH₂CH₃); 44.18 (CH₂); 47.17 (CH₂CH₃); 52.48 (NCH₃); 106.66 (CH); 116.53 (CH); 119.52 (Cq); 121.50 (Cq); 126.90 (CH); 127.43 (CH); 128.38 (Cq); 143.50 (CH); 156.33 (Cq); IR (film): ν_{max} 3368; 1641; 1402; 1034 cm⁻¹; FAB-MS *m/z* (abund.): 286.25 [M+H]⁺ (100); 285.24 [M]⁺ (10); 213.16 (49); Anal. Calcd. (C₁₇H₂₃N₃O • 2 HI • 1.6 CH₂Cl₂): C, 32.99; H, 4.20; N, 6.21%. Found: C, 32.84; H, 4.15; N, 6.55%.

2-(Diethylaminomethyl)-4-(3-amino-1-methylpyridin-4(1*H*)-ylideneamino) phenol, **2.5**

Method A - **2.49** (1.2 molar eq.) was added to **2.64** (1 molar eq.) and absolute ethanol (20 mL/mmol). The mixture was heated under reflux temperature for 18 hours and followed by TLC, CH₂Cl₂ : MeOH : TEA (7.9:2:0.1). The solvent was evaporated under reduced pressure, and the crude product purified by column chromatography using the same eluent as in the TLC. **2.5** was not recovered.

Method B - **2.53** (1 molar eq.) was added to dry THF (35 mL/mmol) and NaH oil dispersion 80% (2 molar eq.). The mixture stirred at room temperature for 1 hour and methyl iodide (2 molar eq.) was added. The mixture stirred for an additional 3.5 hours. The precipitate was filtered off and the filtrate was purified by flash chromatography CH₂Cl₂ : MeOH (9:1). No product was recovered.

Method C - **2.53** (1 molar eq.) and NaH oil dispersion 80% (3 molar eq.) were suspended in dry DMF (6 mL/mmol). The suspension was stirred at room temperature for 2 hours. Methyl iodide (3.5 molar eq.) was added and recharged (3 molar eq.) 30 minutes after the first addition. The mixture stirred at room temperature for 23 hours, the solvent was evaporated under reduced pressure, and the crude product purified by flash chromatography CH₂Cl₂ : MeOH (9.25:0.75). **2.5** was not isolated.

2-(Diethylaminomethyl)-4-(1,3-dimethylpyridin-4(1H)-ylideneamino)phenol dihydroiodide, 2.6

Method C - **2.52** (1 molar eq.) was dissolved in anhydrous DMF (5 mL/mmol) and NaH oil dispersion 80% (1.5 molar eq.) added. The solution stirred at room temperature for 2 hour and then methyl iodide (1.6 molar eq.) added to the mixture. The mixture was stirred for 23 hours, the solvent evaporated under reduced pressure. The crude product was purified by flash chromatography, CH₂Cl₂ : MeOH (9:1). A yellow oil was obtained; 73%; ¹H-NMR (CD₃OD, 400.13 MHz) δ 1.24 (6H, t, *J* = 7.2 Hz, CH₃); 2.35 (3H, s, CH₃); 2.87 (4H, q, *J* = 7.2 Hz, CH₂); 3.99 (3H, s, CH₃); 4.02 (2H, s; CH₂); 6.81 (1H, d, *J* = 7.2 Hz, Ar-*H5*); 6.91 (1H, d, *J* = 8.4 Hz, Ar-*H*); 7.18 (2H, m, Ar-*H*); 8.04 (1H, d, *J* = 7.2 Hz, Ar-*H6*); 8.16 (1H, s, Ar-*H2*); ¹³C-NMR (CD₃OD, 100.61 MHz) δ 9.53 (CH₂CH₃); 13.61 (CH₃); 44.02 (CH₂); 46.58 (CH₂CH₃); 54.47 (NCH₃); 106.07 (CH); 116.66 (CH); 120.16 (Cq); 122.07 (Cq); 126.92 (CH); 127.31 (CH); 128.06 (Cq); 141.86 (Cq); 142.32 (CH); 156.00 (CH); 157.54 (Cq); IR (film): ν_{max} 3437; 2915; 1641; 1467; 1368; 1218 cm⁻¹; FAB⁺-MS *m/z* (abund.): 300.17 [M+H]⁺ (100); Anal. Calcd. (C₁₈H₂₅N₃O • 2 HI): C, 38.94; H, 4.90; N, 7.57%. Found: C, 39.29; H, 4.41; N, 7.59%.

2-(Diethylaminomethyl)-4-(1,2-dimethylpyridin-4(1H)-ylideneamino)phenol, 2.4

Method D - **2.55** (1 molar eq.) was dissolved in anhydrous DMF (5 mL/mmol) and NaH oil dispersion 80% (1.5 molar eq.) was added. The solution stirred at room temperature for 2 hours after which methyl iodide (1.5 molar eq.) was added. The reaction was recharged with methyl iodide (1.5 molar eq.) after stirring for 5 hours and then left reacting for another 18 hours. The solvent was evaporated and the crude product purified by flash chromatography, CH₂Cl₂ : MeOH (4:1). A green-brown very hygroscopic gum was obtained, corresponding to **2.4** (66%). Another green solid was obtained, and identified as **2.7** (25%).

2-(Diethylaminomethyl)-4-(1,2-dimethylpyridin-4(1H)-ylideneamino)phenol dihydroiodide, 2.4

¹H-NMR (CD₃OD, 400.13 MHz) δ 1.37 (6H, t, *J* = 7.2 Hz, CH₃); 2.59 (3H, s, CH₃); 3.20 (4H, q, *J* = 7.2 Hz, CH₂); 3.93 (3H, s, CH₃); 4.34 (2H, s, CH₂); 6.93 (2H, m, Ar-*H*3 and Ar-*H*5); 7.03 (1H, d, *J* = 8.8 Hz, Ar-*H*); 7.28 (1H, dd, *J* = 2.6 and 8.8 Hz, Ar-*H*); 7.42 (1H, d, *J* = 2.6 Hz, Ar-*H*); 8.16 (1H, d, *J* = 7.6 Hz, Ar-*H*6); ¹³C-NMR (CD₃OD, 100.61 MHz) δ 8.10 (CH₂CH₃); 19.33 (CH₃); 41.91 (CH₂); 51.39 (CH₂CH₃); 55.78 (NCH₃); 105.44 (CH); 109.03 (CH); 116.45 (CH); 117.99 (Cq); 127.70 (CH); 128.35 (CH); 128.89 (Cq); 128.92 (Cq); 155.58 (Cq); 156.53 (Cq); 164.81 (CH); IR (film): ν_{max} 3354; 1641; 1395; 1047 cm⁻¹; FAB⁺-MS *m/z* (abund.): 300.24 [M+H]⁺ (100); Anal. Calcd. (C₁₈H₂₅N₃O • 2 HI): C, 38.94; H, 4.90; N, 7.57%. Found: C, 39.29; H, 4.41; N, 7.59%.

(E)-N-[5-(1,2-Dimethylpyridin-4(1H)-ylideneamino)-2-hydroxybenzyl]-N-ethyl-N-methylethanaminium iodide hydroiodide, 2.7

Mp 204-206 °C; ¹H-NMR (CD₃OD, 400.13 MHz) δ 1.45 (6H, m, CH₃); 2.59 (3H, s, CH₃); 3.02 (3H, s, CH₃); 3.43 (2H, dq, *J* = 7.4 and 14.8 Hz, CH₂); 3.52 (2H, dq, *J* = 7.4 and 14.8 Hz, CH₂); 3.92 (3H, s, CH₃); 4.57 (2H, s, CH₂); 6.94 (2H, m, Ar-*H*3 and Ar-*H*5); 7.10 (1H, d, *J* = 8.8 Hz, Ar-*H*); 7.35 (1H, dd, *J* = 2.6 and 8.8 Hz, Ar-*H*); 7.48 (1H, d, *J* = 2.6 Hz, Ar-*H*); 8.15 (1H, d, *J* = 7.6 Hz, Ar-*H*6); ¹³C-NMR (CD₃OD, 100.61 MHz) δ 7.40 (CH₂CH₃); 19.31 (CH₃); 42.00 (CH₂CH₃); 46.23 (CH₂); 55.97 (NCH₃); 59.31 (CH₃); 109.56 (CH); 113.38 (Cq); 115.29 (Cq); 116.49 (CH); 117.18 (CH); 128.64 (CH); 128.90 (CH); 130.67 (Cq); 142.61 (CH); 156.52 (Cq); 156.58 (Cq); IR (film): ν_{max} 3409; 2928; 1647; 1402; 1109 cm⁻¹; FAB⁺-MS *m/z* (abund.): 442.23 [M+H]⁺ (5); 176.10 (100); Anal. Calcd. (C₁₉H₂₈N₃OI • HI): C, 40.09; H, 5.13; N, 7.38%. Found: C, 40.12; H, 5.24; N, 7.37%.

(E)-N-[5-(3-(N,N-Dimethylsulfamoyl)-1-methylpyridin-4(1H)-ylideneamino)-2-methoxybenzyl]-N-ethyl-N-methylethanaminium iodide hydroiodide, 2.8

Several synthetic methods were used with variation of reagent equivalents between them. The general procedure was as follows: **2.56** was either suspended or dissolved in dry THF or anhydrous DMF, respectively, and NaH oil dispersion 80% was added. The mixture was left stirring at room temperature for approximately 1 hour and then methyl iodide poured into the solution. The solution stirred for 1 day at room temperature and the crude product purified by flash chromatography, unless stated on the text.

Method A - **2.56** (1 molar eq.) was suspended in dry THF (60 mL/mmol) and NaH 80% (1.2 molar eq.) added. The suspension stirred for 1 hour. Methyl iodide (2 molar eq.) was added and the

mixture stirred for 22 hours. The crude product was purified by flash chromatography, CH₂Cl₂ : MeOH (9:1). No pure product was isolated in any fraction.

Method B - **2.56** (1 molar eq.) was suspended in dry THF (15 mL/mmol) and NaH 80% (3 molar eq.) was added. The suspension was stirred for 1 hour. Methyl iodide (3 molar eq.) was added and after 5 hours the mixture was recharged with methyl iodide (3 molar eq.). The suspension was stirred for 20 hours and crude product was purified by flash chromatography, CH₂Cl₂ : MeOH (9:1). No pure product was isolated in any fraction.

Method C - **2.56** (1 molar eq.) was dissolved in anhydrous DMF (5 mL/mmol) and NaH 80% (4 molar eq.) added. The solution was stirred for 1 hour. Methyl iodide (4 molar eq.) was added and the mixture stirred for 25,5 hours. The precipitate was filtered off, and the filtrate purified by flash chromatography, CH₂Cl₂ : MeOH (9.5:0.5) and (9:1), sequentially. Two products were isolated, corresponding to **2.70** and **2.8**. The compound with *R_f* 0.40, on CH₂Cl₂ : MeOH (4:1) eluent, was isolated as an orange-brown oil (10%) and identified as **2.70**. The compound with *R_f* 0.24 in the same eluent was isolated as a reddish solid upon crystallization from EtOH (4%, mp 177-180 °C), and identified as **2.8**.

4-((3-((Diethylamino)methyl)-4-methoxyphenyl)amino)-N,N-dimethylpyridine-3-sulfonamide, 2.70

¹H-NMR (CD₃OD, 400.13 MHz) δ 1.31 (6H, t, *J* = 7.2 Hz, CH₃); 2.87 (6H, s, SO₂NMe₂); 3.07 (4H, q, CH₂); 3.98 (3H, s, OCH₃); 4.17 (2H, s, CH₂); 6.83 (1H, d, *J* = 6.0 Hz, Ar-H₅); 7.21 (1H, d, *J* = 8.4 Hz, Ar-H); 7.37-7.41 (2H, m, Ar-H); 8.20 (1H, d, *J* = 6.0 Hz, Ar-H₆); 8.55 (1H, s, Ar-H₂); ¹³C-NMR (CD₃OD, 100.61 MHz) δ 8.44; 36.27; 36.72; 50.67; 55.20; 108.35; 112.03; 115.00; 123.73; 128.05; 129.27; 130.36; 150.34; 151.28; 152.13; 156.85.

(E)-N-[5-(3-(N,N-Dimethylsulfamoyl)-1-methylpyridin-4(1H)-ylideneamino)-2-methoxy-benzyl]-N-ethyl-N-methylethanaminium hydroiodide, 2.8

¹H-NMR (CD₃OD, 400.13 MHz) δ 1.45 (6H, m, CH₃); 3.00 (3H, s, CH₃); 3.04 (6H, s, SO₂NMe₂); 3.40 (2H, dq, *J* = 7.2 and 14.2 Hz, CH₂); 3.51 (2H, dq, *J* = 7.2 and 14.2 Hz, CH₂); 4.02 (3H, s, OCH₃); 4.10 (3H, s, CH₃); 4.59 (2H, s, CH₂); 7.17 (1H, d, *J* = 7.2 Hz, Ar-H₅); 7.36 (1H, d, *J* = 9.0 Hz, Ar-H); 7.58 (1H, dd, *J* = 9.0 and 2.4 Hz, Ar-H); 7.75 (1H, d, *J* = 2.4 Hz, Ar-H); 8.26 (1H, d, *J* = 7.2 Hz, Ar-H₆); 8.83 (1H, s, Ar-H₂); ¹³C-NMR (CD₃OD, 100.61 MHz) δ 7.51 (CH₂CH₃); 37.34 (CH₃); 45.38 (CH₂CH₃); 46.49 (CH₂); 55.73 (SO₂N(CH₃)CH₃); 56.20 (SO₂N(CH₃)CH₃); 58.94 (NCH₃); 111.63 (CH); 113.51 (Cq); 117.46 (CH); 117.70 (Cq); 128.61 (CH); 130.84 (Cq); 133.06 (CH); 146.15 (CH); 146.22 (CH); 154.01 (Cq); 159.18 (Cq); IR (film): ν_{max} 3422; 2914;

1627; 1457; 1361; 1266; 1130; 1013 cm^{-1} ; FAB⁺-MS m/z (abund.): 549.25 $[\text{M}+\text{H}]^+$ (4); 176.10 (100); Anal. Calcd. ($\text{C}_{21}\text{H}_{33}\text{N}_4\text{O}_3\text{SI} \cdot 1.2 \text{ HI}$): C, 35.93; H, 4.91; N, 7.98; S, 4.57. Found: C, 36.24; H, 4.60; N, 7.87; S, 4.71.

Method D - **2.56** (1 molar eq.) was dissolved in anhydrous DMF (7 mL/mmol) and NaH 80% (6 molar eq.) added. The solution was stirred for 1 hour. Methyl iodide (6 molar eq.) was added, and the mixture kept stirring for 23 hours. The crude product was purified by flash chromatography, CH_2Cl_2 : MeOH (9.5:0.5) and (9:1). **2.70** (4%) and **2.8** (6%, mp 214-215 °C) were isolated.

Method E - **2.56** (1 molar eq.) was dissolved in anhydrous DMF (7 mL/mmol) and NaH 80% (6.7 molar eq.) added. The solution was stirred for 2 hours. Methyl iodide (6.7 molar eq.) was added and the mixture stirred for another 24 hours. The precipitate was filtered off, and the filtrate purified by flash chromatography CH_2Cl_2 : MeOH (9.5:0.5) and (9:1). Only **2.8** was recovered (36%).

Method F - **2.56** (1 molar eq.) was dissolved in anhydrous DMF (6 mL/mmol) and NaH 80% (3 molar eq.) added. The solution was stirred for 1 hour. Methyl iodide (3 molar eq.) was added and the mixture stirred for another 23 hours. The crude product was purified by flash chromatography, CH_2Cl_2 : MeOH (9.5:0.5) and (9:1). Further purification was achieved from preparative layer chromatography on silicagel 60. Only a translucent oil was recovered pure, corresponding to **2.71** (2%).

4-((3-((Diethylamino)methyl)-4-hydroxyphenyl)amino)-N-methylpyridine-3-sulfonamide, 2.71

¹H-NMR (CD_3OD , 400.13 MHz) δ 1.17 (6H, t, $J = 7.2$ Hz, CH_3); 2.63 (3H, s, CH_3); 2.71 (4H, q, $J = 7.2$ Hz, CH_2); 3.87 (2H, s, CH_2); 6.79 (1H, d, $J = 6.0$ Hz, Ar-*H*₅); 6.83 (1H, d, $J = 8.4$ Hz, Ar-*H*); 7.01 (1H, d, $J = 2.4$ Hz, Ar-*H*); 7.08 (1H, dd, $J = 8.4$ and 2.4 Hz, Ar-*H*); 8.14 (1H, d, $J = 6.0$ Hz, Ar-*H*₆); 8.58 (1H, s, Ar-*H*₂); ¹³C-NMR (CD_3OD , 100.61 MHz) δ 10.06; 27.42; 46.18; 55.57; 107.63; 116.57; 117.40; 123.45; 125.92; 126.17; 128.43; 149.74; 150.78; 151.61; 157.18.

Procedure for the synthesis of 4-(4-methoxyaniline)-N-methylpyridinium iodide, 2.61

2.60 (1 molar eq.) was added to anhydrous DMF (1 mL/mmol) and methyl iodide (2 molar eq.). The mixture stirred at room temperature for 8.5 days and a yellow solid was recrystallized from DMF; 15%; mp 228-230 °C; ¹H-NMR (CD_3OD , 400.13 MHz) δ 3.86 (3H, s, OCH_3); 3.98 (3H, s, CH_3); 6.97 (2H, d, $J = 7.0$ Hz, Ar-*H*₃); 7.07 (2H, d, $J = 8.6$ Hz, Ar-*H*); 7.26 (2H, d, $J = 8.6$ Hz, Ar-*H*); 8.12 (2H, d, $J = 7.0$ Hz, Ar-*H*₂); ¹³C-NMR (CD_3OD , 100.61 MHz) δ 44.02; 54.67; 98.93;

114.91; 125.60; 129.36; 156.54; 158.98; 163.46; FAB⁺-MS *m/z* (abund.): 216.10 [M]⁺ (16); 215.09 [M-H]⁺ (100).

7.4.5 Intermediates of structure-base designed 4(1*H*)-pyridonimines

General procedure for phosphonium salts ^[214]

Triphenylphosphine (1 molar eq.) and substituted benzylhalide (1 molar eq.) were dissolved in benzene (0.5 mL/mmol) and refluxed for 2-9 hours. After cooling, the white precipitate was filtered off and washed with benzene. If needed the solid was crystallized from chloroform-petroleum ether.

(3-Nitrobenzyl)triphenylphosphonium bromide, 2.72

White powder; 99%; mp > 300 °C; ¹H-NMR (CDCl₃, 400.13 MHz) δ 5.74 (2H, d, *J* = 14.8 Hz, CH₂); 7.43 (1H, t, *J* = 8.0 Hz, Ar-*H*); 7.53 (1H, br.s., Ar-*H*); 7.71 (6H, m, Ar-*H*); 7.84 (9H, m, Ar-*H*); 8.10 (2H, m, Ar-*H*); ³¹P-NMR (CDCl₃, 161.98 MHz) δ 23.85.

Benzyltriphenylphosphonium chloride, 2.73

White powder; 54%; mp > 270 °C; ¹H-NMR (CDCl₃, 400.13 MHz) δ 5.49 (2H, d, *J* = 14.4 Hz, CH₂); 7.12 (4H, m, Ar-*H*); 7.23 (1H, m, Ar-*H*); 7.64 (6H, m, Ar-*H*); 7.76 (9H, m, Ar-*H*); ³¹P-NMR (CDCl₃, 161.98 MHz) δ 23.43.

(4-Chlorobenzyl)triphenylphosphonium chloride, 2.74

White powder; 55%; mp 295-297 °C; ¹H-NMR (CDCl₃, 400.13 MHz) δ 5.67 (2H, d, *J* = 14.8 Hz, CH₂); 7.06 (2H, d, *J* = 8.4 Hz, Ar-*H*); 7.13 (2H, d, *J* = 8.4 Hz, Ar-*H*); 7.63 (6H, m, Ar-*H*); 7.77 (9H, m, Ar-*H*); ³¹P-NMR (CDCl₃, 161.98 MHz) δ 23.59.

(4-Trifluoromethylbenzyl)triphenylphosphonium bromide, 2.75

White powder; 96%; mp 247-249 °C; ¹H-NMR (CDCl₃, 400.13 MHz) δ 5.72 (2H, d, *J* = 15.2 Hz, CH₂); 7.36 (4H, m, Ar-*H*); 7.65 (6H, m, Ar-*H*); 7.80 (9H, m, Ar-*H*); ³¹P-NMR (CDCl₃, 161.98 MHz) δ 23.90.

(4-Trifluoromethoxybenzyl)triphenylphosphonium bromide, 2.76

White powder; 100%; mp 233-235 °C; $^1\text{H-NMR}$ (CDCl_3 , 400.13 MHz) δ 5.71 (2H, d, $J = 14.4$ Hz, CH_2); 6.97 (2H, d, $J = 8.8$ Hz, Ar- H); 7.26 (2H, d, $J = 8.8$ Hz, Ar- H); 7.64 (6H, m, Ar- H); 7.79 (9H, m, Ar- H); $^{31}\text{P-NMR}$ (CDCl_3 , 161.98 MHz) δ 23.82.

(4-Methoxybenzyl)triphenylphosphonium bromide, 2.77

White powder; 91%; mp 242-245 °C; $^1\text{H-NMR}$ (CDCl_3 , 400.13 MHz) δ 5.34 (2H, d, $J = 13.6$ Hz, CH_2); 6.70 (2H, d, $J = 8.4$ Hz, Ar- H); 7.04 (2H, d, $J = 8.4$ Hz, Ar- H); 7.66 (6H, m, Ar- H); 7.75 (9H, m, Ar- H); $^{31}\text{P-NMR}$ (CDCl_3 , 161.98 MHz) δ 22.37.

(3,5-Dinitrobenzyl)triphenylphosphonium chloride, 2.78

Dark brown solid; 58%; mp 254-257 °C; $^1\text{H-NMR}$ (CD_3OD , 400.13 MHz) δ 5.31 (2H, d, $J = 15.2$ Hz, CH_2); 7.77-7.83 (12H, m, Ar- H); 7.96 (3H, t, $J = 7.2$ Hz, Ar- H); 8.24 (2H, s, Ar- H); 8.95 (1H, s, Ar- H); $^{31}\text{P-NMR}$ (CD_3OD , 161.98 MHz) δ 23.81.

(2,4-Dinitrobenzyl)triphenylphosphonium chloride, 2.79

Dark brown gum; 60%; $^1\text{H-NMR}$ (CD_3OD , 400.13 MHz) δ 5.38 (2H, d, $J = 15.0$ Hz, CH_2); 7.76-7.78 (13H, m, Ar- H); 7.95 (3H, t, $J = 7.2$ Hz, Ar- H); 8.50 (1H, dd, $J = 8.6$ and 2.0 Hz, Ar- H); 8.84 (1H, d, $J = 2.0$ Hz, Ar- H); $^{31}\text{P-NMR}$ (CD_3OD , 161.98 MHz) δ 24.13.

(2-Nitrobenzyl)triphenylphosphonium chloride, 2.80

Yellowish solid; 99%; mp 242-244 °C; $^1\text{H-NMR}$ (CDCl_3 , 400.13 MHz) δ 6.11 (2H, d, $J = 14.8$ Hz, CH_2); 7.50 (1H, tt, $J = 7.6$ and 2.0 Hz, Ar- H); 7.61-7.73 (13H, m, Ar- H); 7.79-7.83 (3H, m, Ar- H); 7.95 (1H, d, $J = 8.0$ Hz, Ar- H); 8.11 (1H, dq, $J = 7.2$ and 1.2 Hz, Ar- H); $^{31}\text{P-NMR}$ (CDCl_3 , 161.98 MHz) δ 24.05.

Procedure for the synthesis of methyl 2-formylbenzoate, 2.95 ^[329]

2-Formylbenzoic acid (1 molar eq.) was dissolved in acetonitrile (2 mL/mmol). Methyl iodide (1 molar eq.) and DBU (1 molar eq.) were added and the solution stirred in an ice bath for 2 hours, after which it was left reacting for 24 hours at room temperature. The solvent was evaporated under reduced pressure and the crude product dissolved in chloroform (5 mL/mmol). It was sequentially washed with Na_2CO_3 30% (3×15 mL) and HCl 10% (3×15 mL). The organic layer was dried over

Na₂SO₄ and the solvent evaporated under reduced pressure to afford a yellow oil; 68%; ¹H-NMR (CDCl₃, 60 MHz) δ 4.1 (3H, s, CH₃); 7.7-8.4 (4H, m, Ar-H); 10.9 (1H, s, CHO).

Procedure for the synthesis of diethylphenylsulfonomethyl phosphonate, 2.100

Diethyl phenylthiomethyl phosphonate (1 molar eq.) was dissolved in acetic acid (1 mL/mmol). The solution was heated to 50 °C and then hydrogen peroxide 30% (0.33 mL/mmol) was added dropwise. The resulting mixture was heated until 95 °C and left reacting for 3 hours. After cooling down to room temperature, ice cold water (4 mL/mmol) was added, and the pH set to 8-9 with NaOH 10 N. The crude product was extracted with dichloromethane (5×10 mL). The organic layer was washed with sodium bisulfite (3×2 mL) and dried over Na₂SO₄. The solvent was evaporated under reduced pressure to afford a pale yellow oil; 85%; ¹H-NMR (CDCl₃, 400.13 MHz) δ 1.26 (6H, t, *J* = 7.2 Hz, CH₃); 3.76 (2H, d, *J* = 16.8 Hz, PCH₂); 4.13 (4H, m, CH₃CH₂); 7.55 (2H, t, *J* = 6.8 Hz, Ar-H); 7.65 (1H, t, *J* = 6.8 Hz, Ar-H); 7.97 (2H, d, *J* = 7.2 Hz, Ar-H); IR (film): ν_{max} 3052; 1613; 1525; 1348; 1307; 1143; 856; 808 cm⁻¹.

General procedure for nitrostilbenes and vinylsulfones

Method A ^[214, 216] - To a stirred suspension of phosphonium salt (1 molar eq.) in dry benzene (5 mL/mL) under nitrogen, *n*-BuLi (1.25 molar eq.) was added. After stirring for 1-2 hours at room temperature, distilled or crystallized aldehyde (1.0-1.2 molar eq.) was added. The reaction was run at room temperature (4-25 hours) or refluxed (3-7 hours). The resulting precipitate was filtered off and the filtrate concentrated under reduced pressure. The crude product was purified by column chromatography, hexane : diethyl ether (3:2).

Method B and B' ^[217] - To a stirred suspension of phosphonium salt (1 molar eq.) and distilled or crystallized aldehyde (1 molar eq.) in dichloromethane (3 mL/mL), an aqueous solution of NaOH 0.1-0.5 N (1.2 molar eq.) was added. The biphasic mixture was stirred (1600 rpm) at room temperature for 0.5-2 hours, after which the organic phase was separated, concentrated under reduced pressure and the crude product purified by column chromatography, hexane : diethyl ether (3:2 or 4:1).

Method C-F - The same proportions as method B were stirred under microwaves (100W) for 3 minutes, at 30, 50, 70 or 90 °C. Purifications were carried out as previously indicated.

1-Nitro-3-styrylbenzene, 2.81

Yellowish gum corresponding to an *E/Z* mixture; 92%. *Z* isomer: $^1\text{H-NMR}$ (CDCl_3 , 400.13 MHz) δ 6.63 (1H, d, $J = 12.0$ Hz, *CH*); 6.81 (1H, d, $J = 12.0$ Hz, *CH*); 7.18-7.24 (2H, m, *Ar-H*); 7.27-7.30 (3H, m, *Ar-H*); 7.39 (1H, t, $J = 8.0$ Hz, *Ar-H*); 7.56 (1H, br.d, $J = 7.6$ Hz, *Ar-H*); 8.06 (1H, dd, $J = 8.4$ and 1.6 Hz, *Ar-H*); 8.12 (1H, dd, $J = 1.6$ Hz, *Ar-H*). *E* isomer: mp 92-95 °C. $^1\text{H-NMR}$ (CDCl_3 , 400.13 MHz) δ 7.16 (1H, d, $J = 16.4$ Hz, *CH*); 7.27 (1H, d, $J = 16.4$ Hz, *CH*); 7.35 (1H, d, $J = 6.4$ Hz, *Ar-H*); 7.42 (2H, t, $J = 7.2$ Hz, *Ar-H*); 7.55 (3H, m, *Ar-H*); 7.83 (1H, d, $J = 8.0$ Hz, *Ar-H*); 8.13 (1H, d, $J = 8.4$ Hz, *Ar-H*); 8.13 (1H, br.s, *Ar-H*); IR (film): ν_{max} 3093; 1532; 1348; 846 cm^{-1} .

1-(4-Methoxystyryl)-3-nitrobenzene, 2.82

Yellowish gum corresponding to an *E/Z* mixture; 98%. *Z* isomer: $^1\text{H-NMR}$ (CDCl_3 , 400.13 MHz) δ 3.79 (1H, s, OCH_3); 6.51 (1H, d, $J = 12.0$ Hz, *CH*); 6.70 (1H, d, $J = 12.0$ Hz, *CH*); 6.79 (2H, d, $J = 8.4$ Hz, *Ar-H*); 7.15 (2H, d, $J = 8.4$ Hz, *Ar-H*); 7.37 (1H, t, $J = 8.0$ Hz, *Ar-H*); 7.58 (1H, t, $J = 8.0$ Hz, *Ar-H*); 8.03 (1H, m, *Ar-H*); 8.13 (1H, s, *Ar-H*). *E* isomer: $^1\text{H-NMR}$ (CDCl_3 , 400.13 MHz) δ 3.85 (1H, s, OCH_3); 6.93 (2H, d, $J = 8.4$ Hz, *Ar-H*); 6.98 (1H, d, $J = 16.0$ Hz, *CH*); 7.02 (1H, m, *Ar-H*); 7.50 (3H, m, 2 *Ar-H* and *CH*); 7.76 (1H, d, $J = 7.6$ Hz, *Ar-H*); 8.03 (1H, m, *Ar-H*); 8.32 (1H, s, *Ar-H*); IR (film): ν_{max} 3416; 1603; 1528; 811 cm^{-1} .

1-(4-Chlorostyryl)-3-nitrobenzene, 2.83

Yellowish gum corresponding to an *E/Z* mixture; 94%. *Z* isomer: $^1\text{H-NMR}$ (CDCl_3 , 400.13 MHz) δ 6.65 (1H, d, $J = 12.0$ Hz, *CH*); 6.73 (1H, d, $J = 12.0$ Hz, *CH*); 7.10-7.59 (6H, m, *Ar-H*); 8.08 (1H, d, $J = 8.8$ Hz, *Ar-H*); 8.11 (1H, s, *Ar-H*). *E* isomer; mp 104-107°C; $^1\text{H-NMR}$ (CDCl_3 , 400.13 MHz) δ 7.12 (1H, d, $J = 16.0$ Hz, *CH*); 7.27 (1H, d, $J = 16.0$ Hz, *CH*); 7.10-7.59 (5H, m, *Ar-H*); 7.81 (1H, d, $J = 7.6$ Hz, *Ar-H*); 8.13 (1H, d, $J = 8.8$ Hz, *Ar-H*); 8.39 (1H, s, *Ar-H*); IR (film): ν_{max} 3079; 1586; 1525; 1341; 808 cm^{-1} .

2,4-Dinitro-1-styrylbenzene, 2.84

Yellow gum corresponding to an *E/Z* mixture; 34%. *Z* isomer: $^1\text{H-NMR}$ (CDCl_3 , 400.13 MHz) δ 6.90 (1H, d, $J = 12.0$ Hz, *CH*); 6.99 (1H, d, $J = 12.0$ Hz, *CH*); 7.06-7.12 (2H, m, *Ar-H*); 7.21-7.27 (3H, m, *Ar-H*); 7.38-7.51 (1H, m, *Ar-H*); 8.21 (1H, dd, $J = 8.6$ and 2.2 Hz, *Ar-H*); 8.96 (1H, d, $J = 2.2$ Hz, *Ar-H*). *E* isomer: $^1\text{H-NMR}$ (CDCl_3 , 400.13 MHz) δ 7.32 (1H, d, $J = 16.4$ Hz, *CH*); 7.38-

7.51 (3H, m, Ar-*H*); 7.61 (2H, d, $J = 8.0$ Hz, Ar-*H*); 7.66 (1H, d, $J = 16.4$ Hz, CH); 8.02 (1H, d, $J = 8.8$ Hz, Ar-*H*); 8.46 (1H, dd, $J = 8.8$ and 2.2 Hz, Ar-*H*); 8.86 (1H, d, $J = 2.2$ Hz, Ar-*H*).

1-Nitro-2-styrylbenzene, 2.85

Yellow gum corresponding to an *E/Z* mixture; 95%. *Z* isomer: $^1\text{H-NMR}$ (CDCl_3 , 400.13 MHz) δ 6.80 (1H, d, $J = 12.0$ Hz, CH); 6.93 (1H, d, $J = 12.0$ Hz, CH); 7.08 (2H, dd, $J = 7.0$ and 3.2 Hz, Ar-*H*); 7.30 (1H, d, $J = 7.6$ Hz, Ar-*H*); 7.38-7.48 (3H, m, Ar-*H*); 7.54-7.67 (2H, m, Ar-*H*); 8.07-8.15 (1H, m, Ar-*H*). *E* isomer: $^1\text{H-NMR}$ (CDCl_3 , 400.13 MHz) δ 7.12 (1H, d, $J = 16.4$ Hz, CH); 7.16-7.22 (3H, m, Ar-*H*); 7.26-7.34 (1H, m, Ar-*H*); 7.36 (1H, d, $J = 7.2$ Hz, Ar-*H*); 7.38-7.48 (2H, m, Ar-*H*); 7.63 (1H, d, $J = 16.4$ Hz, CH); 7.80 (1H, d, $J = 8.0$ Hz, Ar-*H*); 7.99 (1H, d, $J = 8.2$ Hz, Ar-*H*). IR (film): ν_{max} 3065; 1606; 1525; 1341; 856; 881 cm^{-1} .

1-Nitro-4-styrylbenzene, 2.86

Yellow gum corresponding to an *E/Z* mixture; 93%. *Z* isomer: $^1\text{H-NMR}$ (CDCl_3 , 400.13 MHz) δ 6.64 (1H, d, $J = 12.0$ Hz, CH); 6.84 (1H, d, $J = 12.0$ Hz, CH); 7.23-7.72 (7H, m, Ar-*H*); 8.09 (2H, d, $J = 8.4$ Hz, Ar-*H*). *E* isomer: $^1\text{H-NMR}$ (CDCl_3 , 400.13 MHz) δ 7.17 (1H, d, $J = 16.4$ Hz, CH); 7.38 (1H, m, CH); 7.23-7.72 (7H, m, Ar-*H*); 8.25 (2H, d, $J = 8.4$ Hz, Ar-*H*); IR (film): ν_{max} 3067; 1593; 1525; 1504; 1334; 829; 763 cm^{-1} .

3,5-Dinitro-1-styrylbenzene, 2.87

Yellow amorphous solid corresponding to an *E/Z* mixture; 76%; mp 101-105 °C. *Z* isomer: $^1\text{H-NMR}$ (CDCl_3 , 400.13 MHz) δ 6.67 (1H, d, $J = 12.0$ Hz, CH); 7.02 (1H, d, $J = 12.0$ Hz, CH) 7.18-7.25 (2H, m, Ar-*H*); 7.30-7.37 (3H, m, Ar-*H*); 8.38 (2H, d, $J = 1.8$ Hz, Ar-*H*); 8.85 (1H, t, $J = 1.8$ Hz, Ar-*H*). *E* isomer: $^1\text{H-NMR}$ (CDCl_3 , 400.13 MHz) δ 7.36-7.50 (5H, m, 2 CH and 3 Ar-*H*); 7.61 (2H, d, $J = 7.2$ Hz, Ar-*H*); 8.68 (2H, d, $J = 2.0$ Hz, Ar-*H*); 8.91 (1H, t, $J = 7.2$ Hz, Ar-*H*).

1-Fluoro-2-(3-nitrostyryl)benzene, 2.88

Yellow gum corresponding to an *E/Z* mixture; 96%. *Z* isomer: $^1\text{H-NMR}$ (CD_3OD , 400.13 MHz) δ 6.75 (1H, d, $J = 12.4$ Hz, CH); 6.81 (1H, d, $J = 12.4$ Hz, CH); 7.00 (1H, t, $J = 7.6$ Hz, Ar-*H*); 7.08 (1H, t, $J = 9.2$ Hz, Ar-*H*); 7.15 (1H, t, $J = 7.6$ Hz, Ar-*H*); 7.29 (1H, m, Ar-*H*); 7.39 (1H, m, Ar-*H*); 7.53 (1H, d, $J = 7.6$ Hz, Ar-*H*); 8.06 (1H, d, $J = 8.6$ Hz, Ar-*H*); 8.09 (1H, s, Ar-*H*). *E* isomer $^1\text{H-NMR}$ (CDCl_3 , 400.13 MHz) δ 7.15-7.30 (4H, m, CH + 3 Ar-*H*); 7.40 (1H, d, $J = 16.0$ Hz, CH);

7.56 (1H, d, $J = 8.2$ Hz, Ar-*H*); 7.63 (1H, t, $J = 7.6$ Hz, Ar-*H*); 7.85 (1H, d, $J = 7.6$ Hz, Ar-*H*); 8.13 (1H, d, $J = 8.0$ Hz, Ar-*H*); 8.39 (1H, s, Ar-*H*).

1-Chloro-2-(3-nitrostyryl)benzene, 2.89

Yellow solid corresponding to an *E/Z* mixture; 100%; mp 44-50 °C. *Z* isomer $^1\text{H-NMR}$ (CDCl_3 , 400.13 MHz) δ 6.76 (1H, d, $J = 12.4$ Hz, *CH*); 6.89 (1H, d, $J = 12.4$ Hz, *CH*); 7.08-7.16 (2H, m, Ar-*H*); 7.25 (1H, m, Ar-*H*); 7.36 (1H, t, $J = 8.0$ Hz, Ar-*H*); 7.44-7.47 (2H, m, Ar-*H*); 8.00-8.10 (2H, m, Ar-*H*). *E* isomer $^1\text{H-NMR}$ (CDCl_3 , 400.13 MHz) δ 7.12 (1H, m, *CH*); 7.25 (1H, m, Ar-*H*); 7.36 (1H, m, Ar-*H*); 7.45 (1H, m, Ar-*H*); 7.58 (1H, t, $J = 8.0$ Hz, Ar-*H*); 7.66 (1H, d, $J = 16.4$ Hz, *CH*); 7.72 (1H, d, $J = 7.6$ Hz, Ar-*H*); 7.89 (1H, d, $J = 8.0$ Hz, Ar-*H*); 8.16 (1H, d, $J = 8.0$ Hz, Ar-*H*); 8.43 (1H, s, Ar-*H*).

1-Fluoro-2-(2-nitrostyryl)benzene, 2.90

Yellow gum corresponding to an *E/Z* mixture; 90%. *Z* isomer: $^1\text{H-NMR}$ (CD_3OD , 400.13 MHz) δ 6.83 (1H, d, $J = 12.0$ Hz, *CH*); 6.79-6.96 (2H, m, Ar-*H*); 7.02 (1H, t, $J = 9.2$ Hz, Ar-*H*); 7.05 (1H, d, $J = 12.0$ Hz, *CH*); 7.15-7.26 (2H, m, Ar-*H*); 7.36-7.50 (2H, m, Ar-*H*); 8.13 (1H, m, Ar-*H*). *E* isomer: $^1\text{H-NMR}$ (CDCl_3 , 400.13 MHz) δ 7.04 (1H, m, Ar-*H*); 7.21 (1H, m, Ar-*H*); 7.27-7.35 (2H, m, *CH* + Ar-*H*); 7.44 (1H, m, Ar-*H*); 7.64 (1H, d, $J = 16.4$ Hz, *CH*); 7.62-7.72 (2H, m, Ar-*H*); 7.82 (1H, d, $J = 7.6$ Hz, Ar-*H*); 8.01 (1H, d, $J = 8.0$ Hz, Ar-*H*).

Methyl 2-(2-nitrostyryl)benzoate, 2.91

Yellowish oil corresponding to an *E/Z* mixture; 47%. The ratio was obtained from the OCH_3 peaks, but the aromatic protons could not be attributed with 1D and 2D NMR.

1-Fluoro-2-(4-nitrostyryl)benzene, 2.92

Yellow oil corresponding to an *E/Z* mixture; 77%. *Z* isomer: $^1\text{H-NMR}$ (CDCl_3 , 400.13 MHz) δ 6.67 (1H, d, $J = 12.0$ Hz, *CH*); 6.84 (1H, d, $J = 12.0$ Hz, *CH*); 7.00 (1H, t, $J = 7.6$ Hz, Ar-*H*); 7.04-7.32 (3H, m, Ar-*H*); 7.38 (2H, d, $J = 8.6$ Hz, Ar-*H*); 8.10 (2H, d, $J = 8.6$ Hz, Ar-*H*). *E* isomer: $^1\text{H-NMR}$ (CDCl_3 , 400.13 MHz) δ 7.04-7.32 (5H, m, *CH* + 4 Ar-*H*); 7.45 (1H, d, $J = 16.4$ Hz, *CH*); 8.68 (2H, d, $J = 8.6$ Hz, Ar-*H*); 8.25 (2H, d, $J = 8.6$ Hz, Ar-*H*).

1-Chloro-2-(4-nitrostyryl)benzene, 2.93

Yellow oil corresponding to an *E/Z* mixture; 96%. *Z* isomer: $^1\text{H-NMR}$ (CDCl_3 , 400.13 MHz) δ 6.67 (1H, d, $J = 12.0$ Hz, *CH*); 6.92 (1H, d, $J = 12.0$ Hz, *CH*); 7.05-7.13 (2H, m, *Ar-H*); 7.21-7.37 (3H, m, *Ar-H*); 7.46 (1H, d, $J = 8.2$ Hz, *Ar-H*); 8.07 (2H, d, $J = 8.6$ Hz, *Ar-H*). *E* isomer: $^1\text{H-NMR}$ (CDCl_3 , 400.13 MHz) δ 7.15 (1H, d, $J = 16.4$ Hz, *CH*); 7.21-7.37 (2H, m, *CH* + *Ar-H*); 7.45 (1H, d, $J = 8.0$ Hz, *Ar-H*); 7.66-7.76 (4H, m, *Ar-H*); 8.26 (2H, d, $J = 8.6$ Hz, *Ar-H*).

1-Nitro-3-(4-nitrostyryl)benzene, 2.94

Yellow solid corresponding to the *Z* isomer only; 61%, mp 71-72 °C; $^1\text{H-NMR}$ (CDCl_3 , 400.13 MHz) δ 6.84 (2H, br.d, $J = 13.4$ Hz, 2 *CH*); 7.37 (2H, dd, $J = 8.8$ and 2.4 Hz, *Ar-H*); 7.44 (1H, td, $J = 7.6$ and 2.8 Hz, *Ar-H*); 7.50 (1H, m, *Ar-H*); 8.12 (4H, m, *Ar-H*); IR (film): ν_{max} 3217; 1580; 1511; 1402; 1341 cm^{-1} .

1-Nitro-3-(3-phenylprop-1-enyl)benzene, 2.95

Yellow oil corresponding to an *E/Z* mixture; 55%. *Z* isomer: $^1\text{H-NMR}$ (CDCl_3 , 400.13 MHz) δ 3.69 (2H, d, $J = 7.4$ Hz, CH_2); 6.07 (1H, dt, $J = 11.4$ and 7.6 Hz, *CH*); 6.64 (1H, d, $J = 11.4$ Hz, *CH*); 7.23-7.67 (7H, m, 7 *Ar-H*); 8.14 (1H, d, $J = 8.0$ Hz, *Ar-H*); 8.21 (1H, s, *Ar-H*). *E* isomer: $^1\text{H-NMR}$ (CDCl_3 , 400.13 MHz) δ 3.62 (2H, d, $J = 5.5$ Hz, CH_2); 6.52 (1H, m, *CH*); 6.64 (1H, d, $J = 11.4$ Hz, *CH*); 7.23-7.67 (7H, m, *Ar-H*); 8.07 (1H, d, $J = 8.0$ Hz, *Ar-H*); 8.21 (1H, s, *Ar-H*); IR (film): ν_{max} 3065; 1600; 1531; 1348; 805; 729 cm^{-1} .

3-Nitrophenylvinylsulfone, 2.99

White amorphous solid corresponding to an *E/Z* mixture; 84%. *E* isomer, white needles, mp 129-131 °C; $^1\text{H-NMR}$ (CDCl_3 , 400.13 MHz) δ 7.04 (1H, d, $J = 15.4$ Hz, *CH*); 7.59-7.71 (4H, m, *Ar-H*); 7.76 (1H, d, $J = 15.4$ Hz, *CH*); 7.82 (1H, d, $J = 7.6$ Hz, *Ar-H*); 7.99 (2H, d, $J = 7.2$ Hz, *Ar-H*); 8.29 (1H, d, $J = 8.0$ Hz, *Ar-H*); 8.37 (1H, br.s, *Ar-H*); IR (film): ν_{max} 3093; 1620; 1532; 1443; 1348; 1313; 1143; 856; 805 cm^{-1} .

1-Nitro-3-(4-(trifluoromethyl)styryl)benzene, 2.101

Greenish gum corresponding to an *E/Z* mixture; 98%. *Z* isomer: $^1\text{H-NMR}$ (CDCl_3 , 400.13 MHz) δ 6.76 (1H, d, $J = 12.4$ Hz, *CH*); 6.83 (1H, d, $J = 12.4$ Hz, *CH*); 7.34 (2H, d, $J = 8.0$ Hz, *Ar-H*); 7.42 (1H, t, $J = 8.4$ Hz, *Ar-H*); 7.54 (2H, t, $J = 8.0$ Hz, *Ar-H*); 7.65 (1H, m, *Ar-H*); 8.05-8.13 (2H, m, *Ar-H*). *E* isomer: $^1\text{H-NMR}$ (CDCl_3 , 400.13 MHz) δ 6.97-7.05 (2H, m, *CH* and *Ar-H*); 7.27 (2H, m, *CH*

and Ar-*H*); 7.54 (2H, t, $J = 8.0$ Hz, Ar-*H*); 7.59 (1H, d, $J = 8.0$ Hz, Ar-*H*); 7.86 (1H, d, $J = 8.0$ Hz, Ar-*H*); 8.16 (1H, d, $J = 8.0$ Hz, Ar-*H*); 8.42 (1H, s, Ar-*H*); IR (film): ν_{\max} 3079; 1620; 1531; 1327; 1123; 821 cm^{-1} .

1-Nitro-3-(4-(trifluoromethyl)styryl)benzene, 2.102

Yellow gum corresponding to an *E/Z* mixture; 100%. *Z* isomer: $^1\text{H-NMR}$ (CDCl_3 , 400.13 MHz) δ 6.68 (1H, d, $J = 12.2$ Hz, *CH*); 6.77 (1H, d, $J = 12.2$ Hz, *CH*); 7.13 (2H, d, $J = 7.6$, Ar-*H*); 7.20-7.29 (3H, m, Ar-*H*); 7.41 (1H, t, $J = 8.0$ Hz, Ar-*H*); 8.04-8.15 (2H, m, Ar-*H*). *E* isomer: $^1\text{H-NMR}$ (CDCl_3 , 400.13 MHz) δ 6.96-7.04 (2H, m, Ar-*H* and *CH*); 7.13 (2H, d, $J = 7.6$, Ar-*H* and *CH*); 7.50-7.61 (3H, m, Ar-*H*); 7.82 (1H, t, $J = 7.6$ Hz, Ar-*H*); 8.11-8.15 (1H, m, Ar-*H*); 8.37 (1H, s, Ar-*H*); IR (film): ν_{\max} 3079; 1531; 1347; 805 cm^{-1} .

General procedure for the reduction of nitrostilbenes^[223]

Nitrostilbenes were dissolved in the minimum possible amount of dichloromethane (typically 1 mL). Neat TES (3-5 molar eq.) was added dropwise, from a pressure-equalizing dropping funnel, to the stirred solution of nitrostilbene (1 molar eq.), Pd-C 10% (15% by weight) and MeOH (5 molar eq.). When the reaction was complete (TLC), the mixture was filtered off and the solvent was removed under reduced pressure. Reactions were typically complete within 30 minutes. The product was purified through flash chromatography, hexane : diethyl ether (3:2 or 4:1).

3-(2-Phenylethyl)aniline, 2.103

White needles; 95%; mp 46-47 °C; $^1\text{H-NMR}$ (CDCl_3 , 400.13 MHz) δ 2.84-2.96 (4H, m, CH_2CH_2); 3.60 (2H, br.s, NH_2); 6.58 (2H, m, Ar-*H*); 6.64 (1H, d, $J = 7.6$ Hz, Ar-*H*); 6.87 (2H, d, $J = 8.4$ Hz, Ar-*H*); 7.10 (1H, d, $J = 7.6$ Hz, Ar-*H*); 7.14 (2H, d, $J = 8.4$ Hz, Ar-*H*); $^{13}\text{C-NMR}$ (CDCl_3 , 100.61 MHz) δ 37.85; 37.99; 112.99; 115.42; 119.01; 125.91; 128.36; 128.46; 129.31; 141.98; 143.16; 146.13; IR (film): ν_{\max} 3423; 3340; 1613; 1450; 1293; 1170; 1068 cm^{-1} .

3-(2-(4-Methoxyphenyl)ethyl)aniline, 2.104

White needles; 99%; mp 70-71 °C; $^1\text{H-NMR}$ (CDCl_3 , 400.13 MHz) δ 2.80-2.90 (4H, m, CH_2CH_2); 3.64 (2H, br.s, NH_2); 3.83 (3H, s, CH_3); 6.56-6.59 (2H, m, Ar-*H*); 6.66 (1H, d, $J = 7.6$ Hz, Ar-*H*); 6.87 (2H, d, $J = 8.0$ Hz, Ar-*H*); 7.09 (1H, d, $J = 7.6$ Hz, Ar-*H*); 7.14 (2H, d, $J = 8.0$ Hz,

Ar-*H*); ^{13}C -NMR (CDCl_3 , 100.61 MHz) δ 36.92; 38.26; 55.28; 112.81; 113.74; 115.32; 118.85; 129.26; 129.34; 134.11; 143.20; 146.39; 157.80.

3-(2-(4-Chlorophenyl)ethyl)aniline, 2.105

The product was not isolated through the general procedure.

Method B - Under the same conditions as the general procedure, except it was carried out at -10 °C. The product was formed, but a 1:1 mixture of **2.105** and **2.103** was isolated.

Method C - Under the same conditions as the general procedure, except it was carried out at -65 °C. White gum; 78%; ^1H -NMR (CD_3OD , 400.13 MHz) δ 2.75-2.78 (2H, m, CH_2); 2.83-2.87 (2H, m, CH_2); 6.52 (1H, d, $J = 7.6$ Hz, Ar-*H*); 6.56-6.58 (2H, m, Ar-*H*); 7.00 (1H, t, $J = 8.0$ Hz, Ar-*H*); 7.12 (2H, d, $J = 8.4$ Hz, Ar-*H*); 7.22 (2H, d, $J = 8.4$ Hz, Ar-*H*).

2-(2-Phenylethyl)aniline, 2.106

Colourless oil; 94%; ^1H -NMR (CD_3OD , 400.13 MHz) δ 2.76-2.90 (4H, m, CH_2CH_2); 6.66 (1H, td, $J = 7.6$ and 1.2 Hz, Ar-*H*); 6.74 (1H, dd, $J = 7.6$ and 0.8 Hz, Ar-*H*); 6.93-7.00 (2H, m, Ar-*H*); 7.14-7.20 (5H, m, Ar-*H*).

4-(2-Phenylethyl)aniline, 2.107

Orange solid; 87%; mp 35-37 °C; ^1H -NMR (CD_3OD , 400.13 MHz) δ 2.75-2.86 (4H, m, CH_2CH_2); 6.67 (2H, d, $J = 8.4$ Hz, Ar-*H*); 6.92 (2H, d, $J = 8.4$ Hz, Ar-*H*); 7.12-7.16 (3H, m, Ar-*H*); 7.23 (2H, t, $J = 7.2$ Hz, Ar-*H*).

3-(3-Phenylpropyl)aniline, 2.108

Yellow oil; 95%; ^1H -NMR (CDCl_3 , 400.13 MHz) δ 2.04-2.12 (2H, m, CH_2); 2.70 (2H, t, $J = 8.0$ Hz, CH_2); 2.79 (2H, t, $J = 8.0$ Hz, CH_2); 6.60-6.64 (3H, m, Ar-*H*); 6.72-6.75 (1H, m, Ar-*H*); 7.06-7.16 (1H, m, Ar-*H*); 7.20-7.26 (2H, m, Ar-*H*); 7.32 (2H, t, $J = 6.4$ Hz, Ar-*H*).

3-(2-(4-Trifluoromethylphenyl)ethyl)aniline, 2.109

White needles; 100%; mp 66-68 °C; ^1H -NMR (CD_3OD , 400.13 MHz) δ 2.84 (2H, t, $J = 8.0$ Hz, CH_2); 2.99 (2H, t, $J = 7.6$ Hz, CH_2); 3.83 (3H, s, CH_3); 6.54-6.60 (3H, m, Ar-*H*); 7.01 (1H, t, $J = 7.6$ Hz, Ar-*H*); 7.35 (2H, d, $J = 8.0$ Hz, Ar-*H*); 7.54 (2H, d, $J = 8.0$ Hz, Ar-*H*).

3-[2-(4-Trifluoromethoxyphenyl)ethyl]aniline, 2.110

Yellow oil; 98%; ¹H-NMR (CD₃OD, 400.13 MHz) δ 2.75-2.90 (4H, m, CH₂CH₂); 3.83 (3H, s, CH₃); 6.53 (1H, d, *J* = 7.6 Hz, Ar-*H*); 6.56-6.59 (2H, m, Ar-*H*); 7.01 (1H, t, *J* = 7.2 Hz, Ar-*H*); 7.15 (2H, d, *J* = 8.0 Hz, Ar-*H*); 7.20 (2H, d, *J* = 8.0 Hz, Ar-*H*); ¹³C-NMR (CD₃OD, 100.61 MHz) δ 36.76; 37.53; 113.18; 115.52; 118.36; 120.44; 125.64; 128.69; 129.66; 137.39; 141.11; 142.16; 147.10.

General procedure for pyridin-4-amines

Corresponding anilines (2 molar eq.) and 4-chloropyridines (1 molar eq.) were dissolved in ethanol absolute (3.5 mL/mmol). The mixture was heated at reflux temperature for 20-24 hours, after which the solvent was evaporated and the crude product purified by flash chromatography.

3-Chloro-*N*-(3-(2-phenylethyl)phenyl)pyridin-4-amine, 2.111

Flash chromatography with hexane : ethyl ether (3:2). Yellow oil; 20%; ¹H-NMR (CDCl₃, 400.13 MHz) δ 2.98 (4H, br.s, CH₂CH₂); 6.52 (1H, br.s, NH); 6.78 (1H, d, *J* = 5.6 Hz, Ar-*H*₅); 7.00 (1H, br.s, Ar-*H*); 7.08 (2H, t, *J* = 7.2 Hz, Ar-*H*); 7.19-7.37 (6H, m, Ar-*H*); 8.11 (1H, d, *J* = 5.6 Hz, Ar-*H*₆); 8.38 (1H, s, Ar-*H*₂); ¹³C-NMR (CDCl₃, 100.61 MHz) δ 37.68; 37.73; 107.35; 120.75; 123.39; 125.66; 126.04; 126.08; 128.44; 128.56; 128.69; 138.19; 141.19; 143.52; 147.07; 148.24; 148.73.

3-Chloro-*N*-3-(2-(4-methoxyphenyl)ethyl)phenylpyridin-4-amine, 2.112

Flash chromatography with CH₂Cl₂ : hexane (9:1). Brown oil; 80%; ¹H-NMR (CDCl₃, 400.13 MHz) δ 2.92 (4H, br.s, CH₂CH₂); 3.80 (3H, s, OCH₃); 6.53 (1H, br.s, NH); 6.77 (1H, d, *J* = 5.6 Hz, Ar-*H*₅); 6.85 (2H, d, *J* = 6.8 Hz, Ar-*H*); 6.98 (1H, br.s, Ar-*H*); 7.04-7.09 (4H, m, Ar-*H*); 7.34 (1H, t, *J* = 7.6 Hz, Ar-*H*); 8.11 (1H, d, *J* = 5.6 Hz, Ar-*H*₆); 8.37 (1H, s, Ar-*H*₂); ¹³C-NMR (CDCl₃, 100.61 MHz) δ 36.84; 37.94; 55.25; 107.41; 113.79; 117.45; 120.67; 123.40; 125.61; 129.47; 129.64; 133.24; 138.24; 143.57; 146.95; 148.41; 148.95; 157.93.

General procedure for pyridinium triflates ^[225]

Corresponding 4-chloropyridines (1 molar eq.) were dissolved or suspended in dry toluene (0.5 mL/mmol). Ethyl or methyl trifluoromethanesulfonate (1-5 molar eq.) was added and the mixture

left reacting at room temperature for 24 hours. The precipitate was filtered off and washed with diethyl ether to afford pure triflate salts.

3,4-Dichloro-*N*-methylpyridinium triflate, 2.113

Yellow amorphous gum; 95%; ¹H-NMR (CD₃OD, 400.13 MHz) δ 4.40 (3H, s, CH₃); 8.36 (1H, d, *J* = 6.4 Hz, Ar-*H*5); 8.87 (1H, d, *J* = 6.8 Hz, Ar-*H*6); 9.39 (1H, s, Ar-*H*2).

3,4-Dichloro-*N*-ethylpyridinium triflate, 2.115

Yellow gum; 100%; ¹H-NMR (CD₃OD, 400.13 MHz) δ 1.68 (3H, t, *J* = 7.2 Hz, CH₃); 4.40 (2H, q, *J* = 7.2 Hz, CH₂); 8.38 (1H, d, *J* = 6.8 Hz, Ar-*H*5); 8.97 (1H, d, *J* = 6.8 Hz, Ar-*H*6); 9.46 (1H, s, Ar-*H*2).

3,4,5-Trichloro-*N*-ethylpyridinium triflate, 2.116

White solid; 97%, mp 241-245 °C; ¹H-NMR (CD₃OD, 400.13 MHz) δ 1.69 (3H, t, *J* = 7.2 Hz, CH₃); 4.67 (2H, q, *J* = 7.2 Hz, CH₂); 9.49 (1H, s, Ar-*H*2).

3-Amino-4-chloro-*N*-ethylpyridinium triflate, 2.118

Brown solid; 95%; mp 56-58 °C; ¹H-NMR (DMSO-*d*₆, 400.13 MHz) δ 1.48 (3H, t, *J* = 7.2 Hz, CH₃); 4.46 (2H, q, *J* = 7.2 Hz, CH₂); 6.92 (2H, br.s, NH₂); 8.04 (1H, d, *J* = 6.4 Hz, Ar-*H*5); 8.20 (1H, d, *J* = 6.4 Hz, Ar-*H*6); 8.25 (1H, s, Ar-*H*2).

4(1*H*)-Pyridones

3-Nitro-4(1*H*)-pyridone, 2.110

4-Chloro-3-nitropyridine hydrochloride (1 molar eq.) was dissolved in NaOH (4 molar eq.). The solution stirred at room temperature for 2 hours and then heated at reflux temperature for another 4 hours. The solvent was evaporated and the sodium chloride crystallized from methanol and dichloromethane. The filtrate was evaporated to yield a yellow solid; 100%; mp > 300 °C; ¹H-NMR (CD₃OD, 400.13 MHz) δ 6.59 (1H, d, *J* = 6.4 Hz, Ar-*H*5); 7.87 (1H, d, *J* = 6.4 Hz, Ar-*H*6); 8.73 (1H, s, Ar-*H*2).

4(1H)-Pyridone, 2.121

4(1H)-Pyridone was synthesized according to a procedure described in the literature [226]. A mixture of 4-methoxypyridine (1 molar eq.) and trimethylsilyl iodide (1.1 molar eq.) was diluted in acetonitrile (11 mL/mmol). The solution was heated at reflux for 22 hours under nitrogen atmosphere to remove methyl iodide generated. The reaction was quenched by adding MeOH (15 mL), and the solvent evaporated under reduced pressure. The crude product was purified by flash chromatography, CH₂Cl₂ : MeOH (9:1). Brown amorphous solid; 100%; ¹H-NMR (CD₃OD, 400.13 MHz) δ 6.90 (2H, d, *J* = 6.8 Hz, Ar-*H*₃); 8.20 (2H, d, *J* = 6.8 Hz, Ar-*H*₂).

3-Bromo-4(1H)-pyridone, 2.122

3-Bromo-4(1H)-pyridone was synthesized adapting the procedure described in the literature [19]. Compound **2.121** (1 molar eq.) was dissolved in dichloromethane (7.6 mL/mmol) and MeOH (2 mL/mmol). NBS (1 molar eq.) was added slowly to the stirring solution and kept at room temperature for 6 hours. The precipitate was filtered off and recrystallized from water to afford a white solid; 19%; mp > 300 °C; ¹H-NMR (DMSO-*d*₆, 400.13 MHz) δ 8.30-8.39 (3H, m, Ar-*H*); 12.24 (1H, s, *NH*).

7.4.6 Structure-base designed 4(1H)-pyridonimines

Method A - Identical to the Mannich-base series of compounds. 4-Pyridinamine (1 molar eq.) was dissolved in anhydrous DMF (6.5 mL/mmol) and NaH 80% oil dispersion was added (2 molar eq.) The solution was kept stirring at room temperature for 1 hour and then alkyl iodide (2 molar eq.) was added. The mixture was left reacting at room temperature for 24 hours. The desired product was not isolated.

Method B - Pyridinium triflate (1 molar eq.) and the corresponding aniline (1.1 molar eq.) were dissolved in ethanol absolute (3.5 mL/mmol). TEA (1 molar eq.) was added to the solution that was kept under reflux for 20-24 hours. The solvent was evaporated under reduced pressure and the crude product was purified by flash chromatography, CH₂Cl₂ : MeOH (9.5:0.5).

3-Chloro-*N*-ethyl-*N*-(3-(4-methoxyphenethyl)phenyl)pyridine-4-amine, 2.123

Method A- Yellowish oil; 38%; ¹H-NMR (CD₃OD, 400.13 MHz) δ 1.17 (3H, t, *J* = 7.0 Hz, CH₂CH₃); 2.80-2.86 (4H, m, CH₂CH₂); 3.75 (3H, s, OCH₃); 3.83 (2H, q, *J* = 7.0 Hz, NCH₂); 6.63 (1H, s, Ar-*H*); 6.73-6.83 (3H, m, Ar-*H*); 6.91 (1H, d, *J* = 7.4 Hz, Ar-*H*); 7.00 (2H, d, *J* = 8.2 Hz, Ar-

H); 7.10 (1H, d, $J = 4.4$ Hz, Ar-*H5*); 7.20 (1H, t, $J = 7.8$ Hz, Ar-*H*); 8.22 (1H, $J = 4.4$ Hz, Ar-*H6*); 8.27 (1H, s, Ar-*H2*); ^{13}C -NMR (CD_3OD , 100.61 MHz) δ 11.76; 36.52; 37.57; 44.42; 54.20; 113.23; 117.26; 120.04; 123.16; 123.90; 124.15; 128.79; 129.20; 133.21; 142.97; 145.57; 147.50; 150.10; 152.39; 157.93.

(*E*)-*N*-(3-Chloro-1-ethylpyridin-4(1*H*)-ylidene)-3-(4-methoxyphenethyl)aniline trifluoromethanesulfonate, 2.124

Method B - Yellowish oil; 57%; ^1H -NMR (CD_3OD , 400.13 MHz) δ 1.55 (3H, t, $J = 7.2$, CH_3); 2.89-2.97 (4H, m, CH_2CH_2); 3.77 (3H, s, OCH_3); 4.30 (2H, q, $J = 7.2$ Hz, NCH_2); 6.70 (1H, d, $J = 7.2$ Hz, Ar-*H5*); 6.82 (2H, d, $J = 8.4$ Hz, Ar-*H*); 7.05-7.06 (3H, m, $J = 8.4$ Hz, Ar-*H*); 7.16 (1H, d, $J = 7.6$ Hz, Ar-*H*); 7.29 (1H, d, $J = 7.6$ Hz, Ar-*H*); 7.46 (1H, t, $J = 7.6$ Hz, Ar-*H*); 8.10 (1H, dd, $J = 7.2$ and 2.0 Hz, Ar-*H6*); 8.71 (1H, d, $J = 2.0$ Hz, Ar-*H2*); ^{13}C -NMR (CD_3OD , 100.61 MHz) δ 14.87 (CH_2CH_3); 36.37 (CH_2CH_2); 37.31 (CH_2CH_2); 53.93 (OCH_3); 54.32 (NCH_2); 107.50 (CH); 113.43 (CH); 117.26 (Cq); 122.78 (Cq); 125.62 (CH); 128.26 (CH); 129.30 (CH); 129.78 (CH); 133.11 (Cq); 135.97 (Cq); 141.42 (CH); 141.48 (CH); 144.14 (CH); 153.27 (Cq); 157.96 (Cq); IR (film): ν_{max} 1641; 1566; 1504; 1272; 1170; 1027 cm^{-1} ; ESI-MS m/z (abund.): 367.18 [$\text{M}+\text{H}$] $^+$ (100); Anal. calcd. ($\text{C}_{22}\text{H}_{23}\text{ClN}_2\text{O} \cdot \text{CF}_3\text{SO}_3\text{H}$): C, 53.44; H, 4.68; N, 5.42; S, 6.20%. Found: C, 52.62; H, 4.54; N, 5.27; S, 5.81%.

(*E*)-*N*-(3-Chloro-1-methylpyridin-4(1*H*)-ylidene)-3-(4-methoxyphenethyl)aniline trifluoromethanesulfonate, 2.125

Method B - Yellowish oil; 87%; ^1H -NMR (CD_3OD , 400.13 MHz) δ 2.90-2.99 (4H, m, CH_2CH_2); 3.77 (3H, s, OCH_3); 4.03 (3H, s, NCH_3); 6.69 (1H, d, $J = 7.2$ Hz, Ar-*H5*); 6.82 (2H, d, $J = 8.4$ Hz, Ar-*H*); 7.05-7.07 (3H, m, $J = 8.4$ Hz, 2 Ar-*H* and Ar-*H*); 7.15 (1H, d, $J = 7.6$ Hz, Ar-*H*); 7.28 (1H, d, $J = 8.0$ Hz, Ar-*H*); 7.45 (1H, dd, $J = 7.6$ and 8.0 Hz, Ar-*H*); 8.01 (1H, dd, $J = 7.2$ and 1.6 Hz, Ar-*H6*); 8.62 (1H, d, $J = 1.6$ Hz, Ar-*H2*); ^{13}C -NMR (CD_3OD , 100.61 MHz) δ 36.35 (CH_2CH_2); 37.30 (CH_2CH_2); 44.42 (OCH_3); 54.29 (NCH_3); 107.18 (CH); 113.41 (CH); 116.96 (Cq); 122.76 (Cq); 125.60 (CH); 128.25 (CH); 129.29 (CH); 129.77 (CH); 133.08 (Cq); 135.96 (Cq); 142.60 (CH); 143.69 (CH); 144.14 (CH); 153.09 (Cq); 157.96 (Cq); IR (film): ν_{max} 1647; 1245; 1150; 1027 cm^{-1} ; ESI-MS m/z (abund.): 353.14 [$\text{M}+\text{H}$] $^+$ (100); Anal. calcd. ($\text{C}_{21}\text{H}_{21}\text{ClN}_2\text{O} \cdot \text{CF}_3\text{SO}_3\text{H}$): C, 52.54; H, 4.41; N, 5.57; S, 6.38%. Found: C, 52.45; H, 4.46; N, 5.54; S, 6.11%.

(E)-N-(3-Chloro-1-ethylpyridin-4(1H)-ylidene)-3-phenethylaniline trifluoromethanesulfonate, 2.126

Method B - Yellowish oil; 82%; $^1\text{H-NMR}$ (CD_3OD , 400.13 MHz) δ 1.55 (3H, t, $J = 7.2$ Hz, CH_3); 2.97-3.04 (4H, m, CH_2CH_2); 4.30 (2H, q, $J = 7.2$ Hz, NCH_2); 6.74 (1H, d, $J = 7.2$ Hz, Ar-*H5*); 7.09 (1H, br.s, Ar-*H*); 7.15-7.32 (7H, m, Ar-*H*); 7.47 (1H, t, $J = 7.6$ Hz, Ar-*H*); 8.14 (1H, dd, $J = 7.2$ and 1.6 Hz, Ar-*H6*); 8.73 (1H, d, $J = 1.6$ Hz, Ar-*H2*); $^{13}\text{C-NMR}$ (CD_3OD , 100.61 MHz) δ 14.94 (CH_2CH_3); 37.10 (CH_2CH_2); 37.21 (CH_2CH_2); 54.01 (CH_2CH_3); 107.46 (CH); 117.27 (Cq); 122.82 (CH); 125.53 (CH); 125.64 (CH); 127.98 (CH); 128.25 (CH); 128.31 (CH); 129.79 (CH); 140.41 (Cq); 141.05 (CH); 141.45 (CH); 144.10 (Cq); 153.33 (Cq); 159.25 (Cq); IR (film): ν_{max} 1641; 1559; 1484; 1259; 1156; 1027 cm^{-1} ; ESI-MS m/z (abund.): 337.19 $[\text{M}+\text{H}]^+$ (100); Anal. calcd. ($\text{C}_{21}\text{H}_{21}\text{ClN}_2 \cdot \text{CF}_3\text{SO}_3\text{H}$): C, 54.27; H, 4.55; N, 5.75; S, 6.59%. Found: C, 54.38; H, 4.67; N, 5.77; S, 6.29%.

(E)-N-(3-Chloro-1-methylpyridin-4(1H)-ylidene)-3-phenethylaniline trifluoromethanesulfonate, 2.127

Method B - Yellowish oil; 59%; $^1\text{H-NMR}$ (CD_3OD , 400.13 MHz) δ 2.96-3.05 (4H, m, CH_2CH_2); 4.03 (3H, s, NCH_3); 6.70 (1H, d, $J = 7.2$ Hz, Ar-*H5*); 7.08 (1H, d, $J = 1.6$ Hz, Ar-*H*); 7.15-7.44 (7H, m, Ar-*H*); 7.46 (1H, t, $J = 7.6$ Hz, Ar-*H*); 8.05 (1H, dd, $J = 7.2$ and 1.6 Hz, Ar-*H6*); 8.63 (1H, d, $J = 1.6$ Hz, Ar-*H2*); $^{13}\text{C-NMR}$ (CD_3OD , 100.61 MHz) δ 37.10 (CH_2CH_2); 37.20 (CH_2CH_2); 44.35 (NCH_3); 107.13 (CH); 116.96 (Cq); 122.80 (CH); 125.51 (CH); 125.64 (CH); 127.98 (CH); 128.24 (CH); 128.33 (CH); 129.79 (CH); 136.01 (Cq); 141.05 (Cq); 142.62 (CH); 142.76 (CH); 144.07 (Cq); 153.09 (Cq); IR (film): ν_{max} 1647; 1566; 1491; 1259; 1150; 1027 cm^{-1} ; ESI-MS m/z (abund.): 323.18 $[\text{M}+\text{H}]^+$ (100); Anal. calcd. ($\text{C}_{20}\text{H}_{19}\text{ClN}_2 \cdot \text{CF}_3\text{SO}_3\text{H}$): C, 53.33; H, 4.26; N, 5.92; S, 6.78%. Found: C, 53.88; H, 3.98; N, 5.92; S, 6.49%.

(E)-N-(3-Chloro-1-ethylpyridin-4(1H)-ylidene)-3-(4-chlorophenethyl)aniline trifluoromethanesulfonate, 2.128

Method B - Yellow oil; 11%; $^1\text{H-NMR}$ (CD_3OD , 400.13 MHz) δ 1.55 (3H, t, $J = 7.2$ Hz, CH_3); 2.95-3.10 (4H, m, CH_2CH_2); 4.30 (2H, q, $J = 7.2$ Hz, NCH_2); 6.76 (1H, d, $J = 7.2$ Hz, Ar-*H5*); 7.08 (1H, s, Ar-*H*); 7.09-7.16 (3H, m, Ar-*H*); 7.26 (2H, d, $J = 7.2$ Hz, Ar-*H*); 7.30 (1H, d, $J = 7.6$ Hz, Ar-*H*); 7.47 (1H, t, $J = 7.6$ Hz, Ar-*H*); 8.16 (1H, d, $J = 7.2$ Hz, Ar-*H6*); 8.73 (1H, s, Ar-*H2*); $^{13}\text{C-NMR}$ (CD_3OD , 100.61 MHz) δ 14.90 (CH_2CH_3); 36.42 (CH_2CH_2); 36.81 (CH_2CH_2); 53.91 (NCH_2); 107.44 (CH); 117.26 (Cq); 123.02 (Cq); 125.70 (CH); 128.00 (CH); 128.33 (CH); 129.87 (CH);

129.99 (CH); 131.29 (CH); 136.09 (Cq); 139.89 (Cq); 141.46 (Cq); 141.53 (CH); 143.78 (CH); 153.37 (Cq); IR (film): ν_{\max} 1644; 1561; 1485; 1261; 1191; 1025; 737 cm^{-1} ; ESI-MS m/z (abund.): 370.0 $[\text{M}]^+$ (100), 371.0 $[\text{M}+\text{H}]^+$ (27), 371.0 $[\text{M}+2]^+$ (69); Anal. calcd. ($\text{C}_{21}\text{H}_{20}\text{Cl}_2\text{N}_2 \cdot \text{CF}_3\text{SO}_3\text{H}$): C, 50.68; H, 4.06; N, 5.37%. Found: C, 50.85; H, 4.35%; N, 5.64%.

(E)-N-(3-Chloro-1-ethylpyridin-4(1H)-ylidene)-3-(4-(trifluoromethyl)phenethyl)aniline trifluoromethanesulfonate, 2.129

Method B - Colourless oil; 76%; $^1\text{H-NMR}$ (CD_3OD , 400.13 MHz) δ 1.55 (3H, t, $J = 7.2$ Hz, CH_3); 3.07 (4H, br.s, CH_2CH_2); 4.30 (2H, q, $J = 7.2$ Hz, NCH_2); 6.88 (1H, d, $J = 7.2$ Hz, Ar-*H5*); 7.15 (1H, br.s, Ar-*H*); 7.20 (1H, d, $J = 7.6$ Hz, Ar-*H*); 7.31 (1H, d, $J = 7.6$ Hz, Ar-*H*); 7.38 (2H, d, $J = 8.0$ Hz, Ar-*H*); 7.47 (1H, t, $J = 7.6$ Hz, Ar-*H*); 7.57 (2H, d, $J = 8.0$ Hz, Ar-*H*); 8.16 (1H, dd, $J = 7.2$ and 1.6 Hz, Ar-*H6*); 8.74 (1H, d, $J = 1.6$ Hz, Ar-*H2*); $^{13}\text{C-NMR}$ (CD_3OD , 100.61 MHz) δ 14.88 (CH_2CH_3); 36.61 (CH_2CH_2); 36.84 (CH_2CH_2); 53.92 (NCH_2); 107.52 (CH); 117.29 (Cq); 123.10 (Cq); 124.75 (CH); 124.79 (CH); 124.83 (CH); 125.63 (CH); 128.28 (CH); 128.97 (CH); 129.86 (CH); 136.22 (Cq); 141.52 (CH); 141.55 (Cq); 143.67 (Cq); 145.84 (Cq); 153.38 (Cq); IR (film): ν_{\max} 1641; 1566; 1491; 1320; 1252; 1157; 1034 cm^{-1} ; ESI-MS m/z (abund.): 405.24 $[\text{M}]^+$ (100); Anal. calcd. ($\text{C}_{22}\text{H}_{20}\text{ClF}_3\text{N}_2 \cdot \text{CF}_3\text{SO}_3\text{H}$): C, 49.78; H, 3.81; N, 5.05; S, 5.78%. Found: C, 49.86; H, 3.57; N, 4.94; S, 5.50%.

(E)-N-(3-Chloro-1-ethylpyridin-4(1H)-ylidene)-3-(4-(trifluoromethoxy)phenethyl)-aniline trifluoromethanesulfonate, 2.130

Method B - Colourless oil; 76%; $^1\text{H-NMR}$ (CD_3OD , 400.13 MHz) δ 1.55 (3H, t, $J = 7.2$ Hz, CH_3); 3.02 (4H, br.s, CH_2CH_2); 4.30 (2H, q, $J = 7.2$ Hz, NCH_2); 6.87 (1H, d, $J = 7.6$ Hz, Ar-*H5*); 7.15-7.32 (7H, m, Ar-*H*); 7.47 (1H, t, $J = 8.0$ Hz, Ar-*H*); 8.17 (1H, dd, $J = 7.6$ and 1.6 Hz, Ar-*H6*); 8.74 (1H, d, $J = 1.6$ Hz, Ar-*H2*); $^{13}\text{C-NMR}$ (CD_3OD , 100.61 MHz) δ 14.88 (CH_2CH_3); 36.38 (CH_2CH_2); 36.90 (CH_2CH_2); 53.91 (NCH_2); 107.51 (CH); 117.29 (CH); 120.58 (Cq); 123.04 (CH); 125.63 (CH); 128.29 (CH); 129.86 (CH); 136.18 (Cq); 140.49 (Cq); 141.52 (CH); 143.83 (CH); 146.56 (Cq); 147.38 (CH); 150.73 (Cq); 153.38 (Cq); 155.44 (Cq); IR (film): ν_{\max} 1641; 1566; 1491; 1259; 1157; 1027 cm^{-1} ; ESI-MS m/z (abund.): 421.07 $[\text{M}]^+$ (100); Anal. calcd. ($\text{C}_{22}\text{H}_{20}\text{ClF}_3\text{N}_2\text{O} \cdot \text{CF}_3\text{SO}_3\text{H}$): C, 48.39; H, 3.71; N, 4.91; S, 5.62%. Found: C, 48.86; H, 3.70; N, 4.91; S, 5.29%.

***N*-(3,5-Dichloro-1-ethylpyridin-4(1*H*)-ylidene)-3-(4-(trifluoromethoxy)phenethyl)-aniline trifluoromethanesulfonate, 2.131**

Method B - Yellowish oil; 74%; ¹H-NMR (CD₃OD, 400.13 MHz) δ 1.57 (3H, t, *J* = 7.2 Hz, CH₃); 2.99 (4H, br.s, CH₂CH₂); 4.31 (2H, q, *J* = 7.2 Hz, NCH₂); 7.04-7.07 (2H, m, Ar-*H*); 7.14-7.17 (3H, m, Ar-*H*); 7.26-7.33 (3H, m, Ar-*H*); 8.63 (2H, s, Ar-*H*₂); ¹³C-NMR (CD₃OD, 100.61 MHz) δ 14.80 (CH₂CH₃); 36.36 (CH₂CH₂); 36.90 (CH₂CH₂); 54.25 (NCH₂); 118.77 (CH); 120.51 (CH); 121.73 (CH); 122.79 (CH); 125.34 (CH); 127.04 (CH); 128.27 (Cq); 129.84 (Cq); 138.77 (Cq); 140.55 (Cq); 141.16 (Cq); 142.08 (CH); 147.36 (Cq); 149.49 (Cq); IR (film): ν_{max} 1627; 1552; 1259; 1163; 1027 cm⁻¹; ESI-MS *m/z* (abund.): 454.97 [M]⁺ (100); Anal. calcd. (C₂₂H₁₉Cl₂F₃N₂O • CF₃SO₃H): C, 45.63; H, 3.33; N, 4.63; S, 5.30%. Found: C, 46.70; H, 3.38; N, 4.71; S, 4.96%.

***(E)*-1-Ethyl-4-(3-phenethylphenylimino)-1,4-dihydropyridin-3-amine trifluoromethanesulfonate, 2.132**

Method B - Yellow oil; 97%; ¹H-NMR (CDCl₃, 400.13 MHz) δ 1.53 (3H, t, *J* = 7.2 Hz, CH₃); 2.91 (4H, br.s, CH₂CH₂); 3.65 (2H, br.s, NH₂); 4.13 (2H, q, *J* = 7.2 Hz, NCH₂); 6.71 (1H, d, *J* = 6.8 Hz, Ar-*H*₅); 7.06-7.34 (9H, m, 8 Ar-*H* + Ar-*H*₆); 8.07 (1H, s, Ar-*H*₂); 8.33 (1H, s, Ar-*H*); ¹³C-NMR (CDCl₃, 100.61 MHz) δ 16.20 (CH₂CH₃); 37.58 (CH₂CH₂); 46.88 (CH₂CH₂); 54.30 (NCH₂); 105.74 (CH); 121.45 (Cq); 121.99 (Cq); 124.05 (CH); 125.94 (CH); 126.64 (CH); 128.36 (CH); 128.60 (CH); 129.65 (CH); 132.73 (CH); 134.17 (Cq); 137.18 (Cq); 141.36 (Cq); 143.49 (CH); 145.04 (CH); IR (film): ν_{max} 3437; 3354; 1634; 1532; 1491; 1252; 1163; 1027 cm⁻¹; ESI-MS *m/z* (abund.): 318.45 [M+H]⁺ (100); Anal. calcd. (C₂₁H₂₃N₃ • CF₃SO₃H): C, 56.52; H, 5.17; N, 8.99; S, 6.86%. Found: C, 55.70; H, 4.98; N, 8.69; S, 6.75%.

***(E)*-1-Methyl-4-(3-phenethylphenylimino)-1,4-dihydropyridin-3-amine hydroiodide, 2.133**

Method B - Yellowish oil; 50%; ¹H-NMR (CD₃OD, 400.13 MHz) δ 2.97 (4H, br.s, CH₂CH₂); 4.00 (3H, s, NCH₃); 6.69 (1H, d, *J* = 6.8 Hz, Ar-*H*₅); 7.04 (1H, br.s, Ar-*H*); 7.11-7.28 (7H, m, Ar-*H*); 7.40 (1H, t, *J* = 7.6 Hz, Ar-*H*); 7.69 (1H, dd, *J* = 6.8 and 1.6 Hz, Ar-*H*₆); 7.77 (1H, d, *J* = 1.6 Hz, Ar-*H*₂); ¹³C-NMR (CD₃OD, 100.61 MHz) δ 37.23 (CH₂CH₂); 37.31 (CH₂CH₂); 44.73 (NCH₃); 105.19 (CH); 121.35 (Cq); 124.09 (CH); 125.64 (CH); 125.91 (CH); 126.64 (CH); 128.00 (CH); 128.36 (CH); 129.60 (Cq); 133.96 (CH); 135.30 (Cq); 137.35 (Cq); 141.14 (Cq); 143.69 (CH); 144.75 (CH); IR (film): ν_{max} 3423; 3341; 1634; 1538; 1491; 1340; 1252; 1184; 1027 cm⁻¹; ESI-MS

m/z (abund.): 304.12 $[M+H]^+$ (100); Anal. calcd. ($C_{20}H_{21}N_3 \cdot HI$): C, 55.69; H, 5.14; N, 9.74%. Found: C, 55.14; H, 5.17; N, 9.56%.

(E)-1-Ethyl-4-(3-(4-(trifluoromethoxy)phenethyl)phenylimino)-1,4-dihydropyridin-3-amine trifluoromethanesulfonate, 2.134

Method B - Yellow oil; 70%; 1H -NMR (CD_3OD , 400.13 MHz) δ 1.53 (3H, t, $J = 7.2$ Hz, CH_3); 2.99 (4H, br.s, CH_2CH_2); 4.23 (2H, q, $J = 7.2$ Hz, NCH_2); 6.85 (1H, d, $J = 6.8$ Hz, Ar- H_5); 7.10 (1H, s, Ar H); 7.15-7.19 (4H, m, Ar- H); 7.27 (2H, d, $J = 7.6$ Hz, Ar- H); 7.41 (1H, t, $J = 7.6$ Hz, Ar- H); 7.78 (1H, d, $J = 7.2$ Hz, Ar- H_6); 7.82 (1H, s, Ar- H_2); ^{13}C -NMR (CD_3OD , 100.61 MHz) δ 15.13 (CH_2CH_3); 36.47 (CH_2CH_2); 37.00 (CH_2CH_2); 53.85 (NCH_2); 105.39 (CH); 120.55 (Cq); 121.57 (Cq); 122.01 (Cq); 124.14 (CH); 124.67 (CH); 126.68 (CH); 129.62 (CH); 129.86 (CH); 134.00 (CH); 134.20 (Cq); 137.54 (Cq); 140.58 (Cq); 143.47 (CH); 145.05 (CH); 147.36 (Cq); IR (film): ν_{max} 3382; 3272; 1627; 1545; 1259; 1163; 1027 cm^{-1} ; ESI-MS m/z (abund.): 402.53 $[M+H]^+$ (100); Anal. calcd. ($C_{22}H_{22}F_3N_3O \cdot CF_3SO_3H$): C, 50.09; H, 4.20; N, 7.62; S, 5.81%. Found: C, 50.34; H, 4.26; N, 7.66; S, 5.86%.

(E)-N-(3-Chloro-1-ethylpyridin-4(1H)-ylidene)-2-phenethylaniline trifluoromethanesulfonate, 2.135

Method B - Yellowish oil; 59%; 1H -NMR (CD_3OD , 400.13 MHz) δ 1.54 (3H, t, $J = 7.2$ Hz, CH_3); 2.87-2.96 (4H, m, CH_2CH_2); 4.28 (2H, q, $J = 7.2$ Hz, NCH_2); 6.37 (1H, d, $J = 7.2$ Hz, Ar- H_5); 7.03-7.16 (5H, m, Ar- H); 7.25 (1H, dd, $J = 7.6$ and 1.2 Hz, Ar- H); 7.40 (1H, td, $J = 7.6$ and 1.6 Hz, Ar- H); 7.46 (1H, td, $J = 7.6$ and 1.2 Hz, Ar- H); 7.53 (1H, dd, $J = 7.6$ and 1.6 Hz, Ar- H); 8.05 (1H, dd, $J = 7.2$ and 1.6 Hz, Ar- H_6); 8.69 (1H, d, $J = 1.6$ Hz, Ar- H_2); ^{13}C -NMR (CD_3OD , 100.61 MHz) δ 14.94 (CH_2CH_3); 32.83 (CH_2CH_2); 36.58 (CH_2CH_2); 53.86 (NCH_2); 107.22 (CH); 121.99 (Cq); 125.70 (CH); 127.24 (CH); 127.72 (CH); 128.03 (CH); 128.15 (CH); 128.95 (CH); 131.10 (CH); 134.36 (Cq); 139.10 (Cq); 141.04 (Cq); 141.25 (CH); 141.57 (CH); 153.70 (Cq); IR (film): ν_{max} 1641; 1559; 1491; 1266; 1191; 1020 cm^{-1} ; ESI-MS m/z (abund.): 337.32 $[M+H]^+$ (100). Anal. calcd. ($C_{21}H_{21}ClN_2 \cdot CF_3SO_3H$): C, 54.27; H, 4.55; N, 5.75; S, 6.59%. Found: C, 54.53; H, 4.55; N, 5.77; S, 6.27%.

(E)-N-(3-Chloro-1-ethylpyridin-4(1H)-ylidene)-4-phenethylaniline trifluoromethanesulfonate, 2.136

Method B - Yellowish oil; 53%; ¹H-NMR (CD₃OD, 400.13 MHz) δ 1.54 (3H, t, *J* = 7.6 Hz, CH₃); 2.94-3.04 (4H, m, CH₂CH₂); 4.29 (2H, q, *J* = 7.6 Hz, NCH₂); 6.96 (1H, d, *J* = 7.6 Hz, Ar-H5); 7.16-7.20 (3H, m, Ar-H); 7.24-7.31 (4H, m, Ar-H); 7.36 (2H, d, *J* = 8.4 Hz, Ar-H); 8.20 (1H, dd, *J* = 7.6 and 1.6 Hz, Ar-H6); 8.72 (1H, d, *J* = 1.6 Hz, Ar-H2); ¹³C-NMR (CD₃OD, 100.61 MHz) δ 14.91 (CH₂CH₃); 37.11 (CH₂CH₂); 37.37 (CH₂CH₂); 53.89 (NCH₂); 107.44 (CH); 117.26 (Cq); 125.27 (CH); 125.63 (CH); 127.95 (CH); 128.21 (CH); 130.03 (CH); 134.01 (Cq); 141.19 (Cq); 141.45 (CH); 141.60 (CH); 142.15 (Cq); 153.41 (Cq); IR (film): ν_{max} 1648; 1559; 1396; 1273; 1150; 1027 cm⁻¹; ESI-MS *m/z* (abund.): 337.32 [M+H]⁺ (100). Anal. calcd. (C₂₁H₂₁ClN₂ • CF₃SO₃H): C, 54.27; H, 4.55; N, 5.75; S, 6.59%. Found: C, 53.79; H, 4.53; N, 5.70; S, 6.25%.

(E)-N-(3-Chloro-1-ethylpyridin-4(1H)-ylidene)-3-(3-phenylpropyl)aniline trifluoromethanesulfonate, 2.137

Method B - Colourless oil; 33%; ¹H-NMR (CDCl₃, 400.13 MHz) δ 1.53 (3H, t, *J* = 7.2 Hz, CH₃); 1.94-1.97 (2H, m, CH₂CH₂CH₂); 2.65-2.69 (4H, m, CH₂CH₂CH₂); 4.36 (2H, q, *J* = 7.2 Hz, NCH₂); 7.16 (1H, d, *J* = 7.2 Hz, Ar-H5); 7.12-7.40 (9H, m, 8 Ar-H + Ar-H6); 8.18 (1H, d, *J* = 7.2 Hz, Ar-H); 8.45 (1H, s, Ar-H2); ¹³C-NMR (CDCl₃, 100.61 MHz) δ 16.28 (CH₂CH₃); 32.71 (CH₂CH₂CH₂); 35.14 (CH₂CH₂CH₂); 35.40 (CH₂CH₂CH₂); 54.65 (NCH₂); 107.97 (CH); 118.41 (Cq); 122.95 (CH); 124.92 (CH); 125.86 (CH); 128.37 (CH); 128.44 (CH); 130.00 (CH); 130.11 (CH); 135.24 (Cq); 140.59 (Cq); 141.17 (CH); 141.97 (CH); 145.08 (Cq); 152.66 (Cq); IR (film): ν_{max} 3217; 2914; 2364; 1641; 1561; 1484; 1266; 1150; 1027 cm⁻¹; ESI-MS *m/z* (abund.): 351.15 [M+H]⁺ (100). Anal. calcd. (C₂₂H₂₃ClN₂ • CF₃SO₃H): C, 55.14; H, 4.83; N, 5.59%. Found: C, 55.57; H, 5.02; N, 5.74%.

General procedure for pyridine *N*-oxides ^[330]

To a stirred solution of 4-chloropyridine (1 molar eq.) in dry chloroform (8.5 mL/mmol), 3-chloroperoxybenzoic acid (1.2 molar eq.) was added in small portions, and the mixture was heated under reflux for 6 hours. The mixture was cooled and extracted with NaOH 10% (3×20 mL); the organic layer dried over Na₂SO₄ and the solvent evaporated under reduced pressure. The crude product was purified by flash chromatography, CH₂Cl₂ : MeOH (9.5:0.5).

(E)-3-Chloro-4-(3-phenethylphenylimino)pyridin-1(4H)-ol, 2.138

Brown gum; 31%; ¹H-NMR (CDCl₃, 400.13 MHz) δ 2.97 (4H, br.s, CH₂CH₂); 6.50 (1H, br.s, NOH); 6.59 (1H, d, *J* = 7.6 Hz, Ar-H5); 6.88 (1H, s, Ar-H); 7.01 (1H, d, *J* = 8.0 Hz, Ar-H); 7.10-7.15 (3H, m, Ar-H); 7.24-7.38 (3H, m, Ar-H); 7.36 (1H, t, *J* = 8.0 Hz, Ar-H); 7.87 (1H, dd, *J* = 7.6 and 1.6 Hz, Ar-H6); 8.21 (1H, d, *J* = 1.6 Hz, Ar-H2); ¹³C-NMR (CDCl₃, 100.61 MHz) δ 37.55 (CH₂CH₂); 37.64 (CH₂CH₂); 108.17 (CH); 117.30 (Cq); 120.65 (Cq); 123.29 (CH); 126.07 (CH); 126.17 (CH); 128.44 (CH); 128.64 (CH); 129.99 (CH); 137.59 (Cq); 138.31 (Cq); 138.56 (CH); 140.93 (CH); 140.98 (CH); 143.70 (Cq); IR (film): ν_{max} 3423; 1634 cm⁻¹; ESI-MS *m/z* (abund.): 325.21 [M+H]⁺ (100); Anal. calcd. (C₁₉H₁₇ClN₂O • MeOH • 0.1 CH₂Cl₂): C, 66.08; H, 5.85; N, 7.67%. Found: C, 66.01; H, 5.93; N, 7.67%.

3,4,5-Trichloropyridine-N-oxide, 2.139

White solid; 73%; mp 131-135 °C; ¹H-NMR (CDCl₃, 400.13 MHz) δ 8.25 (2H, s).

7.4.7 Intermediates of 4(1H)-quinolonimines

7-Chloro-2-methyl-4(1H)-quinolone, 3.2

Ethyl acetoacetate (1 molar eq.) was added to PPA (1 mL/0.1 mmol). The viscous and transparent mixture was heated up to 100 °C, when it became progressively translucent. 3-Chloroaniline was then added and the temperature allowed to rise up to 150 °C. At this point the reaction was complete (TLC). The mixture was cooled down to room temperature and water was added. The mixture was treated with NaOH until pH 5. The precipitate was filtered off and the aqueous phase extracted with ethyl acetate (3×50 mL). A yellowish oil was obtained, corresponding to a mixture of **3.2** and its 5-chloro isomer, **3.3**; 87%; ¹H-NMR (CD₃OD, 400.13 MHz) δ 2.42 (3H, s, CH₃); 2.48 (3H, s, CH₃); 6.14 (1H, s, Ar-H3); 6.21 (1H, s, Ar-H3); 7.33 (1H, d, *J* = 7.6 Hz, Ar-H); 7.38 (1H, d, *J* = 9.0 Hz, Ar-H); 7.45 (1H, d, *J* = 8.0 Hz, Ar-H); 7.50-7.60 (2H, m, Ar-H); 8.18 (1H, d, *J* = 9.0 Hz, Ar-H).

General procedure for quinolinium triflates

The corresponding 4-chloroquinolines (1 molar eq.) were dissolved in dry toluene (0.5 mL/mmol). Ethyl or methyl trifluoromethanesulfonate (1-5 molar eq.) was added and the mixture

left reacting at room temperature for 24 hours. The precipitate was filtered off and washed with diethyl ether to afford pure triflate salts.

4,7-Dichloro-*N*-ethylquinolinium triflate, 3.4

White solid; 92%; mp 92-93 °C; ¹H-NMR (DMSO-*d*₆, 400.13 MHz) δ 1.74 (3H, t, *J* = 7.2 Hz, CH₃); 5.11 (2H, q, *J* = 7.2 Hz, CH₂); 8.18 (1H, dd, *J* = 9.2 and 1.6 Hz, Ar-*H*); 8.33 (1H, d, *J* = 6.4 Hz, Ar-*H*3); 8.72 (1H, d, *J* = 9.2 Hz, Ar-*H*); 8.80 (1H, d, *J* = 1.6 Hz, Ar-*H*); 9.41 (1H, d, *J* = 6.4 Hz, Ar-*H*2).

4-Chloro-*N*-ethyl-7-(trifluoromethyl)quinolinium triflate, 3.5

White solid; 95%; mp 134-136 °C; ¹H-NMR (CD₃OD, 400.13 MHz) δ 1.77 (3H, t, *J* = 7.2 Hz, CH₃); 5.24 (2H, q, *J* = 7.2 Hz, CH₂); 8.42 (1H, dd, *J* = 9.2 and 1.6 Hz, Ar-*H*); 8.51 (1H, d, *J* = 6.4 Hz, Ar-*H*3); 8.94-8.96 (2H, m, Ar-*H*); 9.56 (1H, d, *J* = 6.4 Hz, Ar-*H*2).

4-Chloro-*N*-methyl-7-(trifluoromethyl)quinolinium triflate, 3.6

White solid; 65%; mp 105-106 °C; ¹H-NMR (CD₃OD, 400.13 MHz) δ 4.65 (3H, s, CH₃); 8.19 (1H, d, *J* = 9.2 Hz, Ar-*H*); 8.32 (1H, d, *J* = 6.0 Hz, Ar-*H*3); 8.70-8.72 (2H, m, Ar-*H*); 9.35 (1H, d, *J* = 6.0 Hz, Ar-*H*2).

General procedure for nitrophenoxybenzenes

Phenol (1 molar eq.), 1-fluoro-4-nitrobenzene (2 molar eq.), Na₂CO₃ (2 molar eq.), and CuI (2 molar eq.) were suspended in DMF (3.5 mL) and heated. The reaction was followed by TLC, hexane : diethyl ether (9:1), and after completion (approximately 3-6 h), the desired product was extracted with dichloromethane (3×50 mL). The crude product was purified by flash chromatography, hexane : diethyl ether (100:1).

1-Nitro-4-(4-(trifluoromethoxy)phenoxy)benzene, 3.8

Yellow oil; 73%; ¹H-NMR (CDCl₃, 400.13 MHz) δ 7.06 (2H, d, *J* = 8.8 Hz, Ar-*H*); 7.14 (2H, d, *J* = 7.2 Hz, Ar-*H*); 7.30 (2H, d, *J* = 7.2 Hz, Ar-*H*); 8.24 (2H, d, *J* = 8.8 Hz, Ar-*H*); IR (film): ν_{max} 1606; 1555; 1485; 1294; 1077; 971; 875; 814 cm⁻¹.

1-Nitro-4-(phenoxy)benzene, 3.9

Yellow oil; 65%; $^1\text{H-NMR}$ (CD_3OD , 400.13 MHz) δ 7.07 (2H, d, $J = 9.2$ Hz, Ar- H); 7.13 (2H, d, $J = 8.0$ Hz, Ar- H); 7.30 (1H, t, $J = 7.2$ Hz, Ar- H); 7.48 (2H, d, $J = 8.0$ Hz, Ar- H); 8.23 (2H, d, $J = 9.2$ Hz, Ar- H); IR (film): ν_{max} 3113; 1581 1517; 1479; 1345; 1243; 872; 846; 791; 747 cm^{-1} .

1-Nitro-4-(3-(trifluoromethoxy)phenoxy)benzene, 3.10

Yellow oil; 81%; $^1\text{H-NMR}$ (CD_3OD , 400.13 MHz) δ 7.09-7.22 (5H, m, Ar- H); 7.56 (1H, m, Ar- H); 8.28 (2H, d, $J = 9.2$ Hz, Ar- H).

1-Nitro-4-(4-(trifluoromethyl)phenoxy)benzene, 3.11

Transparent oil; 71%; $^1\text{H-NMR}$ (CD_3OD , 400.13 MHz) δ 7.19 (2H, d, $J = 9.2$ Hz, Ar- H); 7.30 (2H, d, $J = 8.8$ Hz, Ar- H); 7.78 (2H, d, $J = 8.8$ Hz, Ar- H); 8.30 (2H, d, $J = 9.2$ Hz, Ar- H).

1-Nitro-4-(4-chlorophenoxy)benzene, 3.12

White needles; 75%; mp 64-65 $^\circ\text{C}$; $^1\text{H-NMR}$ (CD_3OD , 400.13 MHz) δ 7.12-7.16 (4H, m, Ar- H); 7.47 (2H, d, $J = 7.2$ Hz, Ar- H); 8.37 (2H, d, $J = 9.6$ Hz, Ar- H); IR (film): ν_{max} 1523; 1478; 1338; 1236 cm^{-1} .

1-Nitro-3-(4-(trifluoromethoxy)phenoxy)benzene, 3.13

Yellowish oil; 30%; $^1\text{H-NMR}$ (CDCl_3 , 400.13 MHz) δ 7.53-7.60 (2H, m, Ar- H); 7.65-7.70 (2H, m, Ar- H); 8.00 (2H, dd, $J = 8.8$ and 2.0 Hz, Ar- H); 8.09 (2H, d, $J = 8.0$ Hz, Ar- H).

General procedure for phenoxyanilines

Same procedure to the one described for the reduction of nitrostilbenes.

4-(4-(Trifluoromethoxy)phenoxy)benzenamine, 3.14

Yellow oil; 68%; $^1\text{H-NMR}$ (CDCl_3 , 400.13 MHz) δ 3.36 (2H, br.s, NH_2); 6.72 (2H, d, $J = 8.8$ Hz, Ar- H); 6.90 (2H, d, $J = 8.8$ Hz, Ar- H); 6.93 (2H, d, $J = 9.2$ Hz, Ar- H); 7.15 (2H, d, $J = 9.2$ Hz, Ar- H).

4-Phenoxybenzenamine, 3.15

Transparent oil; 75%; $^1\text{H-NMR}$ (CD_3OD , 400.13 MHz) δ 6.70-6.98 (4H, m, Ar-*H*); 6.88 (2H, d, $J = 8.2$ Hz, Ar-*H*); 7.00 (1H, t, $J = 7.6$ Hz, Ar-*H*); 7.27 (2H, t, $J = 8.0$ Hz, Ar-*H*).

4-(3-(Trifluoromethoxy)phenoxy)benzenamine, 3.16

Yellow oil; 85%; $^1\text{H-NMR}$ (CD_3OD , 400.13 MHz) δ 6.74-6.91 (7H, m, Ar-*H*); 7.35 (1H, m, Ar-*H*).

4-(4-(Trifluoromethyl)phenoxy)benzenamine, 3.17

White solid; 93%; mp 73-74 °C; $^1\text{H-NMR}$ (CD_3OD , 400.13 MHz) δ 6.80 (2H, d, $J = 8.8$ Hz, Ar-*H*); 6.87 (2H, d, $J = 8.8$ Hz, Ar-*H*); 7.01 (2H, d, $J = 8.4$ Hz, Ar-*H*); 7.59 (2H, d, $J = 8.4$ Hz, Ar-*H*); IR (film): ν_{max} 3203; 3191; 1511; 1414; 1332; 1102; 836 cm^{-1} .

4-(4-Chlorophenoxy)benzenamine, 3.18

1-Nitro-4-(4-chlorophenoxy)benzene (1 molar eq.) and tin 10-40 mesh (11.5 molar eq.) were suspended in ethanol (3.5 mL/mmol). Fuming HCl (0.9 mL/2.3 mL water) was added and the mixture stirred at reflux temperature for 1 hour. The reaction mixture was treated with NaOH 1N until pH \sim 5 and the product extracted with CH_2Cl_2 (200 mL). The solvent was evaporated under reduced pressure affording a white oil; 85%; $^1\text{H-NMR}$ (CD_3OD , 400.13 MHz) δ 6.88-6.90 (6H, m, Ar-*H*); 7.28 (2H, d, $J = 8.8$ Hz, Ar-*H*).

3-(4-(Trifluoromethoxy)phenoxy)benzenamine, 3.19

Translucid oil; 85%; $^1\text{H-NMR}$ (CDCl_3 , 400.13 MHz) δ 3.77 (2H, br.s., NH_2); 6.38-6.49 (6H, m, Ar-*H*); 7.09 (1H, d, $J = 8.0$ Hz, Ar-*H*); 7.12 (1H, d, $J = 8.0$ Hz, Ar-*H*).

7.4.8 4(1H)-Quinolonimines

Same procedure as the one described for the structure-base designed 4-pyridonimines.

(E)-N-(7-Chloro-1-ethylquinolin-4(1H)-ylidene)-3-(4-(trifluoromethoxy)phenetyl)aniline trifluoromethanesulfonate, 3.20

Yellow gum; 76%; $^1\text{H-NMR}$ (CDCl_3 , 400.13 MHz) δ 1.57 (3H, t, $J = 7.2$ Hz, CH_3); 2.89 (4H, br.s, CH_2CH_2); 4.48 (2H, q, $J = 7.2$ Hz, CH_2); 6.66 (1H, d, $J = 7.6$ Hz, Ar-*H*3); 7.10-7.18 (7H, m,

Ar-*H*); 7.30 (1H, m, Ar-*H*); 7.59 (1H, d, $J = 9.2$ Hz, Ar-*H*); 7.74 (1H, s, Ar-*H*); 8.17 (2H, d, $J = 7.6$ Hz, Ar-*H2*); 8.84 (1H, d, $J = 8.8$ Hz, Ar-*H*); ^{13}C -NMR (CDCl_3 , 100.61 MHz) δ 14.59 (CH_2CH_3); 36.70 (CH_2CH_2); 37.36 (CH_2CH_2); 50.26 (NCH_2); 100.94 (CH); 116.32 (Cq); 117.36 (CH); 120.87 (CH); 122.48 (CH); 125.03 (CH); 127.54 (CH); 127.82 (CH); 128.09 (CH); 128.21 (CH); 129.88 (CH); 136.62 (Cq); 138.54 (Cq); 140.01 (Cq); 141.50 (Cq); 143.41 (Cq); 145.60 (CH); 147.42 (Cq); 148.23 (Cq); 155.10 (Cq); IR (film): ν_{max} 1613; 1552; 1450; 1395; 1259; 1156; 1034 cm^{-1} ; ESI-MS m/z (abund.): 471.31 $[\text{M}+\text{H}]^+$ (100); 296.03 (98). Anal. Calcd. ($\text{C}_{26}\text{H}_{22}\text{ClF}_3\text{N}_2\text{O} \cdot \text{CF}_3\text{SO}_3\text{H}$): C, 52.22; H, 3.73; N, 4.51%. Found: C, 52.25; H, 3.75; N, 4.58%.

***E*-*N*-(1-Ethyl-7-(trifluoromethyl)quinolin-4(1*H*)-ylidene)-3-(4-(trifluoromethoxy)phenethyl)aniline trifluoromethanesulfonate, 3.21**

Brown gum; 81%; ^1H -NMR (CD_3OD , 400.13 MHz) δ 1.54 (3H, t, $J = 6.8$ Hz, CH_3); 3.00 (4H, br.s, CH_2CH_2); 4.56 (2H, q, $J = 6.8$ Hz, CH_2); 6.50 (1H, d, $J = 7.2$ Hz, Ar-*H3*); 7.06 (1H, s, Ar-*H*); 7.11-7.28 (6H, m, Ar-*H*); 7.43 (1H, t, $J = 7.6$ Hz, Ar-*H*); 7.92 (1H, d, $J = 8.4$ Hz, Ar-*H*); 8.16 (1H, d, $J = 7.2$ Hz, Ar-*H2*); 8.26 (1H, s, Ar-*H*); 8.73 (1H, d, $J = 8.4$ Hz, Ar-*H*); ^{13}C -NMR (CD_3OD , 100.61 MHz) δ 13.34 (CH_2CH_3); 36.51 (CH_2CH_2); 37.06 (CH_2CH_2); 49.06 (NCH_2); 101.39 (CH); 114.59 (Cq); 120.55 (Cq); 121.37 (CH); 121.62 (CH); 121.98 (CH); 122.77 (CH); 124.18 (CH); 126.12 (CH); 126.72 (CH); 129.71 (CH); 129.85 (CH); 134.11 (Cq); 134.44 (Cq); 138.24 (Cq); 140.61 (Cq); 141.43 (Cq); 143.51 (Cq); 145.18 (CH); 147.33 (Cq); 155.62 (Cq); IR (film): ν_{max} 1619; 1402; 1262; 1166 cm^{-1} ; ESI-MS m/z (abund.): 505.09 $[\text{M}+\text{H}]^+$ (100); Anal. Calcd. ($\text{C}_{27}\text{H}_{22}\text{F}_6\text{N}_2\text{O} \cdot 0.65 \text{CF}_3\text{SO}_3\text{H}$): C, 55.16; H, 3.79; N, 4.65%. Found: C, 55.17; H, 3.83; N, 4.66%.

***E*-*N*-(7-Chloro-1-ethylquinolin-4(1*H*)-ylidene)biphenyl-4-amine trifluoromethanesulfonate, 3.22**

Yellow solid; 100%; mp 94-96 $^\circ\text{C}$; ^1H -NMR (CD_3OD , 400.13 MHz) δ 1.58 (3H, t, $J = 7.2$ Hz, CH_3); 4.63 (2H, q, $J = 7.2$ Hz, CH_2); 6.95 (1H, d, $J = 7.6$ Hz, Ar-*H3*); 7.40 (1H, m, Ar-*H*); 7.50 (2H, t, $J = 7.6$ Hz, Ar-*H*); 7.55 (2H, d, $J = 8.4$ Hz, Ar-*H*); 7.70 (2H, d, $J = 7.6$ Hz, Ar-*H*); 7.84-7.88 (3H, m, Ar-*H*); 8.31 (1H, d, $J = 1.6$ Hz, Ar-*H*); 8.47 (1H, d, $J = 7.6$ Hz, Ar-*H2*); 8.64 (1H, d, $J = 9.0$ Hz, Ar-*H*); ^{13}C -NMR (CD_3OD , 100.61 MHz) δ 13.54 (CH_2CH_3); 50.00 (NCH_2); 100.85 (CH); 117.49 (CH); 118.80 (CH); 125.40 (CH); 125.69 (CH); 126.58 (CH); 127.52 (CH); 128.29 (CH); 128.68 (CH); 135.76 (Cq); 136.41 (Cq); 139.10 (Cq); 139.71 (Cq); 140.85 (Cq); 141.93 (Cq); 146.62 (CH); 155.42 (Cq); IR (film): ν_{max} 1620; 1545; 1491; 1395; 1252; 1157; 1034 cm^{-1} ; ESI-MS

m/z (abund.): 358.97 $[M+H]^+$ (100); Anal. Calcd. ($C_{23}H_{19}ClN_2 \cdot 1.1 CF_3SO_3H \cdot H_2O$): C, 53.23; H, 4.13; N, 5.15%. Found: C, 53.87; H, 4.07; N, 5.09%.

(E)-N-(1-Ethyl-7-(trifluoromethyl)quinolin-4(1H)-ylidene)biphenyl-4-amine trifluoromethanesulfonate, 3.23

Orange solid; 98%; mp 138-140 °C; 1H -NMR (CD_3OD , 400.13 MHz) δ 1.51 (3H, t, $J = 6.8$ Hz, CH_3); 4.17 (2H, q, $J = 6.8$ Hz, CH_2); 6.57 (1H, d, $J = 7.2$ Hz, Ar- $H3$); 7.30-7.38 (3H, m, Ar- H); 7.45 (2H, t, $J = 7.6$ Hz, Ar- H); 7.67 (2H, d, $J = 7.6$ Hz, Ar- H); 7.75 (2H, d, $J = 7.6$ Hz, Ar- H); 7.86 (1H, d, $J = 8.8$ Hz, Ar- H); 8.02 (1H, d, $J = 7.2$ Hz, Ar- $H2$); 8.16 (1H, s, Ar- H); 8.75 (1H, d, $J = 8.8$ Hz, Ar- H); ^{13}C -NMR (CD_3OD , 100.61 MHz) δ 13.28 (CH_2CH_3); 48.24 (N CH_2); 101.46 (CH); 111.12 (Cq); 114.12 (Cq); 121.02 (CH); 123.66 (CH); 123.92 (CH); 126.28 (CH); 126.41 (CH); 127.08 (CH); 128.04 (CH); 128.58 (CH); 138.38 (Cq); 140.19 (Cq); 142.51 (Cq); 144.49 (CH); 151.77 (Cq); 152.95 (Cq); 155.64 (Cq); IR (film): ν_{max} 1614; 1556; 1459; 1222; 1119 cm^{-1} ; ESI-MS m/z (abund.): 393 $[M+H]^+$ (100); Anal. Calcd. ($C_{24}H_{19}F_3N_2 \cdot 0.4 CF_3SO_3H$): C, 64.63; H, 4.36; N, 6.15%. Found: C, 64.77; H, 4.32; N, 6.19%.

(E)-4-Benzyl-N-(7-chloro-1-ethylquinolin-4(1H)-ylidene)aniline trifluoromethanesulfonate, 3.24

Yellow oil; 86%; mp 56-58 °C; 1H -NMR (CD_3OD , 400.13 MHz) δ 1.56 (3H, t, $J = 7.2$ Hz, CH_3); 4.07 (2H, s, CH_2); 4.62 (2H, q, $J = 7.2$ Hz, CH_2); 6.83 (1H, d, $J = 7.6$ Hz, Ar- $H3$); 7.20-7.33 (5H, m, Ar- H); 7.38 (2H, d, $J = 8.4$ Hz, Ar- H); 7.44 (2H, d, $J = 8.4$ Hz, Ar- H); 7.83 (1H, d, $J = 8.8$ Hz, Ar- H); 8.29 (1H, s, Ar- H); 8.42 (1H, d, $J = 7.6$ Hz, Ar- $H2$); 8.60 (1H, d, $J = 9.2$ Hz, Ar- H); ^{13}C -NMR (CD_3OD , 100.61 MHz) δ 13.52 (CH_2CH_3); 40.96 (CH_2); 49.96 (N CH_2); 100.69 (CH); 117.27 (Cq); 117.57 (Cq); 125.37 (CH); 125.62 (CH); 125.94 (CH); 127.62 (CH); 128.24 (CH); 128.33 (CH); 130.26 (CH); 134.95 (CH); 139.03 (Cq); 140.74 (Cq); 140.83 (Cq); 141.93 (Cq); 146.59 (CH); 155.53 (Cq); IR (film): ν_{max} 1619; 1542; 1440; 1389; 1255; 1160; 1032 cm^{-1} ; ESI-MS m/z (abund.): 373.02 $[M+H]^+$ (100); Anal. Calcd. ($C_{24}H_{21}ClN_2 \cdot 0.9 CF_3SO_3H$): C, 58.88; H, 4.35; N, 5.51%. Found: C, 58.28; H, 4.45; N, 5.27%.

(E)-N-(7-Chloro-1-ethylquinolin-4(1H)-ylidene)-4-phenoxyaniline trifluoromethanesulfonate, 3.25

Yellow oil; 92%; mp 52-54 °C; 1H -NMR (CD_3OD , 400.13 MHz) δ 1.56 (3H, t, $J = 7.2$ Hz, CH_3); 4.62 (2H, q, $J = 7.2$ Hz, CH_2); 6.82 (1H, d, $J = 7.6$ Hz, Ar- $H3$); 7.10 (2H, d, $J = 7.6$ Hz, Ar-

H); 7.16-7.22 (3H, m, Ar-*H*); 7.42-7.47.45 (4H, m, Ar-*H*); 7.83 (1H, d, $J = 9.2$ Hz, Ar-*H*); 8.28 (1H, s, Ar-*H*); 8.42 (1H, d, $J = 7.6$ Hz, Ar-*H*2); 8.60 (1H, d, $J = 9.2$ Hz, Ar-*H*); ^{13}C -NMR (CD₃OD, 100.61 MHz) δ 13.51 (CH₂CH₃); 49.86 (NCH₂); 100.64 (CH); 117.43 (Cq); 117.49 (Cq); 119.04 (CH); 119.39 (CH); 123.80 (CH); 125.65 (CH); 126.87 (CH); 127.50 (CH); 129.75 (CH); 132.32 (CH); 139.05 (Cq); 140.72 (Cq); 146.41 (CH); 155.79 (Cq); 156.57 (Cq); 157.21 (Cq); IR (film): ν_{max} 1620; 1552; 1491; 1436; 1245; 1164; 1027 cm⁻¹; ESI-MS m/z (abund.): 375.08 [M+H]⁺ (100); Anal. Calcd. (C₂₆H₂₂Cl₄N₂O • CF₃SO₃H): C, 54.91; H, 3.84; N, 5.34%. Found: C, 55.25; H, 3.95; N, 5.24%.

(*E*)-*N*-(7-Chloro-1-ethylquinolin-4(1*H*)-ylidene)-4-(4-chlorophenoxy)aniline trifluoromethanesulfonate, 3.26

Yellow oil; 83%; mp 61-63 °C; ^1H -NMR (CD₃OD, 400.13 MHz) δ 1.56 (3H, t, $J = 7.2$ Hz, CH₃); 4.62 (2H, q, $J = 7.2$ Hz, CH₂); 6.82 (1H, d, $J = 7.6$ Hz, Ar-*H*3); 7.08 (2H, d, $J = 8.8$ Hz, Ar-*H*); 7.20 (2H, d, $J = 8.8$ Hz, Ar-*H*); 7.40-7.46 (4H, m, Ar-*H*); 7.82 (1H, d, $J = 9.2$ Hz, Ar-*H*); 8.27 (1H, s, Ar-*H*); 8.42 (1H, d, $J = 7.6$ Hz, Ar-*H*2); 8.60 (1H, d, $J = 9.2$ Hz, Ar-*H*); ^{13}C -NMR (CD₃OD, 100.61 MHz) δ 13.52 (CH₂CH₃); 49.87 (NCH₂); 100.68 (CH); 117.48 (Cq); 117.50 (Cq); 119.73 (Cq); 120.29 (CH); 125.67 (CH); 126.96 (CH); 127.50 (CH); 127.82 (CH); 128.53 (CH); 128.64 (CH); 132.97 (Cq); 139.06 (Cq); 140.72 (Cq); 146.40 (CH); 155.52 (Cq); 156.64 (Cq); IR (film): ν_{max} 1620; 1552; 1477; 1239; 1157; 1034 cm⁻¹; ESI-MS m/z (abund.): 408.94 [M+H]⁺ (100); Anal. Calcd. (C₂₃H₁₈Cl₂N₂O • CF₃SO₃H): C, 51.53; H, 3.42; N, 5.01%. Found: C, 52.36; H, 3.43; N, 4.93%.

(*E*)-*N*-(7-Chloro-1-ethylquinolin-4(1*H*)-ylidene)-4-(4-(trifluoromethoxy)phenoxy)aniline trifluoromethanesulfonate, 3.27

Yellow solid; 75%; mp 78-81 °C; ^1H -NMR (CD₃OD, 400.13 MHz) δ 1.57 (3H, t, $J = 6.8$ Hz, CH₃); 4.63 (2H, q, $J = 6.8$ Hz, CH₂); 6.84 (1H, d, $J = 7.6$ Hz, Ar-*H*3); 7.18 (2H, d, $J = 8.8$ Hz, Ar-*H*); 7.23 (2H, d, $J = 7.2$ Hz, Ar-*H*); 7.35 (2H, d, $J = 8.8$ Hz, Ar-*H*); 7.46 (2H, d, $J = 7.2$ Hz, Ar-*H*); 7.84 (1H, d, $J = 8.4$ Hz, Ar-*H*); 8.30 (1H, s, Ar-*H*); 8.44 (1H, d, $J = 7.6$ Hz, Ar-*H*2); 8.60 (1H, d, $J = 8.4$ Hz, Ar-*H*); ^{13}C -NMR (CD₃OD, 100.61 MHz) δ 13.51 (CH₂CH₃); 49.90 (NCH₂); 100.67 (CH); 117.44 (Cq); 117.54 (Cq); 119.90 (Cq); 120.00 (CH); 122.69 (CH); 125.64 (CH); 127.06 (CH); 127.57 (CH); 132.95 (CH); 139.07 (CH); 140.79 (Cq); 141.75 (Cq); 145.03 (Cq); 146.48 (CH); 155.57 (Cq); 155.77 (Cq); 156.55 (Cq); IR (film): ν_{max} 1614; 1552; 1491; 1245; 1157; 1034 cm⁻¹;

ESI-MS m/z (abund.): 458.96 $[M+H]^+$ (100); Anal. Calcd. ($C_{26}H_{22}ClF_3N_2O \cdot CF_3SO_3H$): C, 49.31; H, 3.14; N, 4.60%. Found: C, 49.90; H, 3.26; N, 4.59%.

(E)-N-(7-Chloro-1-ethylquinolin-4(1H)-ylidene)-4-(4-(trifluoromethyl)phenoxy)aniline trifluoromethanesulfonate, 3.28

Yellow solid; 99%; mp 156-158 °C; 1H -NMR (CD_3OD , 400.13 MHz) δ 1.56 (3H, t, $J = 7.2$ Hz, CH_3); 4.59 (2H, q, $J = 7.2$ Hz, CH_2); 6.79 (1H, d, $J = 7.2$ Hz, Ar- $H3$); 7.22 (2H, d, $J = 8.8$ Hz, Ar- H); 7.28 (2H, d, $J = 8.8$ Hz, Ar- H); 7.46 (2H, d, $J = 8.8$ Hz, Ar- H); 7.72 (2H, d, $J = 8.8$ Hz, Ar- H); 7.80 (1H, d, $J = 8.4$ Hz, Ar- H); 8.23 (1H, s, Ar- H); 8.42 (1H, d, $J = 7.6$ Hz, Ar- $H2$); 8.59 (1H, d, $J = 8.4$ Hz, Ar- H); ^{13}C -NMR ($CDCl_3$, 100.61 MHz) δ 18.45 (CH_2CH_3); 53.96 (N CH_2); 104.95 (CH); 120.36 (Cq); 121.82 (Cq); 122.27 (Cq); 124.78 (CH); 130.54 (CH); 130.75 (CH); 131.05 (CH); 131.19 (CH); 131.30 (CH); 131.82 (CH); 142.65 (Cq); 145.08 (Cq); 149.23 (Cq); 149.30 (CH); 158.91 (Cq); 159.37 (Cq); 163.65 (Cq); IR (film): ν_{max} 1607; 1552; 1491; 1327; 1245; 1163; 1027 cm^{-1} ; ESI-MS m/z (abund.): 442.96 $[M+H]^+$ (100); Anal. Calcd. ($C_{24}H_{18}ClF_3N_2O \cdot 0.85 CF_3SO_3H$): C, 52.32; H, 3.33; N, 4.91%. Found: C, 52.07; H, 3.53; N, 4.85%.

(E)-N-(7-Chloro-1-methylquinolin-4(1H)-ylidene)-4-(4-(trifluoromethyl)phenoxy)aniline trifluoromethanesulfonate, 3.29

Yellow solid; 73%; mp 181-183 °C; 1H -NMR (CD_3OD , 400.13 MHz) δ 4.17 (3H, s, CH_3); 6.77 (1H, d, $J = 7.6$ Hz, Ar- $H3$); 7.22 (2H, d, $J = 8.4$ Hz, Ar- H); 7.27 (2H, d, $J = 8.4$ Hz, Ar- H); 7.47 (2H, d, $J = 8.4$ Hz, Ar- H); 7.71 (2H, d, $J = 8.4$ Hz, Ar- H); 7.81 (1H, d, $J = 8.8$ Hz, Ar- H); 8.16 (1H, s, Ar- H); 8.30 (1H, d, $J = 7.6$ Hz, Ar- $H2$); 8.69 (1H, d, $J = 8.8$ Hz, Ar- H); ^{13}C -NMR (CD_3OD , 100.61 MHz) δ 41.45 (N CH_3); 100.29 (CH); 117.52 (Cq); 117.71 (Cq); 118.04 (Cq); 120.96 (Cq); 125.49 (CH); 126.77 (CH); 127.01 (CH); 127.05 (CH); 127.08 (CH); 127.12 (CH); 127.25 (CH); 135.16 (Cq); 140.24 (Cq); 140.32 (Cq); 154.88 (CH); 155.83 (Cq); 160.37 (Cq); IR (film): ν_{max} 1620; 1402; 1327; 1245; 1156; 1061 cm^{-1} ; ESI-MS m/z (abund.): 428.97 $[M+H]^+$ (100); Anal. Calcd. ($C_{24}H_{18}ClF_3N_2O \cdot 0.85 CF_3SO_3H$): C, 51.48; H, 3.05; N, 5.03%. Found: C, 51.94; H, 2.97; N, 4.93%.

(E)-N-(7-Chloro-1-ethylquinolin-4(1H)-ylidene)-4-(3-(trifluoromethoxy)phenoxy)aniline trifluoromethanesulfonate, 3.30

Yellow oil; 85%; 1H -NMR (CD_3OD , 400.13 MHz) δ 1.56 (3H, t, $J = 7.2$ Hz, CH_3); 4.61 (2H, q, $J = 7.2$ Hz, CH_2); 6.81 (1H, d, $J = 7.2$ Hz, Ar- $H3$); 6.99 (1H, br.s, Ar- H); 7.10 (2H, m, Ar- H); 7.25

(2H, d, $J = 9.2$ Hz, Ar-*H*); 7.46 (2H, d, $J = 9.2$ Hz, Ar-*H*); 7.51 (1H, t, $J = 9.2$ Hz, Ar-*H*); 7.82 (1H, dd, $J = 8.8$ and 1.6 Hz, Ar-*H*); 8.26 (1H, s, Ar-*H*); 8.38 (1H, d, $J = 7.6$ Hz, Ar-*H*2); 8.60 (1H, d, $J = 8.8$ Hz, Ar-*H*); ^{13}C -NMR (CD_3OD , 100.61 MHz) δ 13.48 (CH_2CH_3); 49.72 (NCH_2); 100.69 (CH); 111.22 (CH); 115.52 (Cq); 116.89 (CH); 117.37 (CH); 120.44 (CH); 125.74 (CH); 126.89 (CH); 127.17 (CH); 127.33 (CH); 130.92 (CH); 139.11 (Cq); 140.58 (Cq); 146.13 (CH); 150.08 (Cq); 152.20 (Cq); 154.09 (Cq); 155.55 (Cq); 155.80 (Cq); 158.32 (Cq); IR (film): ν_{max} 1613; 1555; 1504; 1440; 1248; 1160; 1025 cm^{-1} ; ESI-MS m/z (abund.): 458.95 $[\text{M}+\text{H}]^+$ (100); Anal. Calcd. ($\text{C}_{26}\text{H}_{22}\text{ClF}_3\text{N}_2\text{O} \cdot 0.8 \text{CF}_3\text{SO}_3\text{H}$): C, 51.45; H, 3.27; N, 4.84%. Found: C, 51.23; H, 3.39; N, 4.79%.

(*E*)-*N*-(1-Ethyl-7-(trifluoromethyl)quinolin-4(1*H*)-ylidene)-4-(3-(trifluoromethoxy)phenoxy)aniline trifluoromethanesulfonate, 3.31

Yellow oil; 97%; ^1H -NMR (CD_3OD , 400.13 MHz) δ 1.47 (3H, t, $J = 7.2$ Hz, CH_3); 4.36 (2H, q, $J = 7.2$ Hz, CH_2); 6.33 (1H, d, $J = 7.6$ Hz, Ar-*H*3); 6.89 (1H, s, Ar-*H*); 6.99-7.01 (2H, m, Ar-*H*); 7.11-7.7.16 (4H, m, Ar-*H*); 7.43 (1H, t, $J = 8.4$ Hz, Ar-*H*); 7.73 (1H, d, $J = 8.4$ Hz, Ar-*H*); 7.78 (1H, d, $J = 7.6$ Hz, Ar-*H*2); 8.00 (1H, s, Ar-*H*); 8.69 (1H, d, $J = 8.4$ Hz, Ar-*H*); ^{13}C -NMR (CD_3OD , 100.61 MHz) δ 13.10 (CH_2CH_3); 47.85 (NCH_2); 101.22 (CH); 110.34 (CH); 113.43 (Cq); 114.66 (Cq); 116.02 (Cq); 119.17 (CH); 120.06 (CH); 120.75 (CH); 121.72 (CH); 122.33 (CH); 124.35 (CH); 125.10 (CH); 126.50 (CH); 130.66 (Cq); 138.49 (Cq); 142.92 (Cq); 143.51 (CH); 150.01 (Cq); 152.76 (Cq); 156.01 (Cq); 159.27 (Cq); IR (film): ν_{max} 1614; 1562; 1489; 1259; 1215; 1156; 1022; 875 cm^{-1} ; ESI-MS m/z (abund.): 493 $[\text{M}+\text{H}]^+$ (100); Anal. Calcd. ($\text{C}_{25}\text{H}_{18}\text{F}_6\text{N}_2\text{O}_2 \cdot 0.3 \text{CF}_3\text{SO}_3\text{H}$): C, 56.54; H, 3.43; N, 5.21%. Found: C, 56.00; H, 3.11; N, 5.37%.

(*E*)-*N*-(2-(Benzylthio)-1-ethyl-7-(trifluoromethyl)-2,3-dihydroquinolin-4(1*H*)-ylidene)-[1,1'-biphenyl]-4-amine, 3.33

Benzylthiol (2 molar eq.) was diluted in methanol (5 mL/mmol) and TEA (3 molar eq.) was added. The solution was stirred at 0 °C for five minutes, before adding **3.23** (1 molar eq.), and allowed to warm up to room temperature. The mixture was stirred for 24 hours, the solvent was evaporated under reduced pressure, and the crude product was purified by flash chromatography, CH_2Cl_2 : MeOH (9:1). Only the starting material **3.23** was recovered (97%).

7.4.9 Intermediates of flavones

General procedure for 4-phenoxybenzotrioles

Method A - Same procedure as for the synthesis of 1-nitrophenoxybenzenes.

Method B - Alcohol (1 molar eq.), 4-fluorobenzonitrile (1 molar eq.) and Na₂CO₃ (2 molar eq.) were suspended in DMF (3.5 mL/mmol) and heated. The reaction was followed by TLC, hexane : diethyl ether (9:1), and after completion (approximately 24 h), the desired product was extracted with dichloromethane (3×50 mL). The crude product was purified by flash chromatography, using hexane : diethyl ether (100:1) as eluent.

4-(4-Chlorophenoxy)benzotriole, 4.1

White solid; 100%; mp 67-68 °C; ¹H-NMR (CDCl₃, 400.13 MHz) δ 7.01-7.04 (4H, m, Ar-H); 7.40 (2H, d, *J* = 6.8 Hz, Ar-H); 7.63 (2H, d, *J* = 6.8 Hz, Ar-H); IR (film): ν_{max} 2241; 1581; 1485; 1402; 1242; 840 cm⁻¹.

4-(4-(Trifluoromethoxy)phenoxy)benzotriole, 4.2

Yellow oil; 100%; ¹H-NMR (CDCl₃, 400.13 MHz) δ 7.04 (2H, d, *J* = 9.0 Hz, Ar-H); 7.11 (2H, d, *J* = 9.0 Hz, Ar-H); 7.28 (2H, d, *J* = 9.0 Hz, Ar-H); 7.64 (2H, d, *J* = 9.0 Hz, Ar-H).

4-(4,4,4-Trifluorobutoxy)benzotriole, 4.3

Transparent oil; 94%; ¹H-NMR (CDCl₃, 400.13 MHz) δ 2.12 (2H, m, CH₂CH₂CH₂); 2.35 (2H, m, CH₂CH₂CF₃); 4.09 (2H, t, *J* = 6.0 Hz, CH₂CH₂CH₂CF₃); 6.96 (2H, d, *J* = 8.4 Hz, Ar-H); 7.62 (2H, d, *J* = 8.4 Hz, Ar-H).

4-(3-(Trifluoromethoxy)phenoxy)benzotriole, 4.4

Yellow oil; 100%; ¹H NMR (CDCl₃, 400.13 MHz) δ 6.97 (1H, br.s, Ar-H); 7.02 (1H, dd, *J* = 8.6 and 2.0 Hz, Ar-H); 7.05-7.14 (3H, m, Ar-H); 7.45 (1H, t, *J* = 8.2 Hz, Ar-H); 7.67 (2H, d, *J* = 9.0 Hz, Ar-H).

General procedure for 4-phenoxybenzoic acids

Method A - Benzotriole (1 molar eq.) was suspended in HCl 6N (10 mL/mmol) and heated to reflux temperature. The reaction was kept for 24 hours. The solvent was coevaporated with EtOH

under reduced pressure, and the crude product was purified by flash chromatography, CH₂Cl₂ : MeOH (9:1). No reaction occurred.

Method B - Benzonitrile (1 molar eq.) was suspended in water (2.5 mL/mmol), and H₂SO₄ (7.5 mL/mmol). After heating to reflux for 2 hours, the solvent was coevaporated with EtOH, under reduced pressure. The crude product was purified by flash chromatography, CH₂Cl₂ : MeOH (9:1). Hydrolysis to the amide occurred (*ca.* 1/3).

Method C - Benzonitrile (1 molar eq.) was suspended in NaOH 10% (10 mL/mmol). After heating to reflux for 6 hours, the reaction mixture was acidified with HCl and the white solid extracted with CH₂Cl₂ (3×15 mL). A mixture of starting material and its amide was isolated.

Method D ^[286] - Benzonitrile (1 molar eq.) and KOH in pellets (18 molar eq.) were suspended in MeOH (0.6 mL/mmol), and EtOH (2.6 mL/mmol). H₂O₂ 30% (1.0 mL/mmol) was added dropwise to avoid rapid heating and effervescence. After heating to reflux for 4 hours, the reaction mixture was acidified with concentrated HCl, and the solid extracted with CH₂Cl₂ (3×20 mL) to afford the required compound.

4-(4-Chlorophenoxy)benzoic acid, 4.5

White solid; 100%; mp 150-152°C; ¹H-NMR (CDCl₃, 400.13 MHz) δ 7.02-7.06 (4H, m, Ar-*H*); 7.39 (2H, d, *J* = 6.8 Hz, Ar-*H*); 8.10 (2H, d, *J* = 6.8 Hz, Ar-*H*); IR (film) ν_{max} 3409, 1675 cm⁻¹.

4-(4-(Trifluoromethoxy)phenoxy)benzoic acid, 4.6

White needles; 98%; mp 141-143 °C; ¹H-NMR (CDCl₃, 400.13 MHz) δ 7.05 (2H, d, *J* = 6.8 Hz, Ar-*H*); 7.12 (2H, d, *J* = 6.8 Hz, Ar-*H*); 7.28 (2H, d, *J* = 6.8 Hz, Ar-*H*); 8.12 (2H, d, *J* = 6.8 Hz, Ar-*H*).

4-(4,4,4-Trifluorobutoxy)benzoic acid, 4.7

Pinkish solid; 95%; mp 97-99 °C; ¹H-NMR (CDCl₃, 400.13 MHz) δ 2.12 (2H, m, CH₂CH₂CH₂); 2.35 (2H, m, CH₂CH₂CF₃); 4.09 (2H, t, *J* = 6.0 Hz, CH₂CH₂CH₂CF₃); 6.96 (2H, d, *J* = 8.4 Hz, Ar-*H*); 7.62 (2H, d, *J* = 8.4 Hz, Ar-*H*).

4-(3-(Trifluoromethoxy)phenoxy)benzoic acid, 4.8

Yellow gum; 96%; ¹H-NMR (CDCl₃, 400.13 MHz) δ 6.98 (1H, br.s, Ar-*H*); 7.03 (1H, dd, *J* = 8.2 and 2.0 Hz, Ar-*H*); 7.04-7.10 (3H, m, Ar-*H*); 7.43 (1H, t, *J* = 8.2 Hz, Ar-*H*); 8.13 (2H, d, *J* = 9.0 Hz, Ar-*H*).

Procedure for the synthesis of 2-acetylphenyl-3-(trifluoromethyl)benzoate, 4.10 ^[261]

1-(3-Trifluoromethyl)phenyl)ethanone (1 molar eq.) was dissolved in dry pyridine (2 mL/mol). 2-Hydroxyacetophenone (1 molar eq.) was added, and the mixture was stirred at room temperature for 3 hours. The mixture was acidified with HCl and extracted with ethyl acetate (3×20 mL). The crude product was purified by flash chromatography, CH₂Cl₂ : hexane (2:3) and CH₂Cl₂ : MeOH (4:1). A transparent oil was obtained; 30%; ¹H-NMR (CDCl₃, 400.13 MHz) δ 2.57 (3H, s, CH₃); 7.27 (1H, d, *J* = 8.0 Hz, Ar-*H*); 7.42 (1H, td, *J* = 7.8 and 1.2 Hz, Ar-*H*); 7.64 (1H, td, *J* = 7.8 and 1.6 Hz, Ar-*H*); 7.70 (1H, t, *J* = 7.8 Hz, Ar-*H*); 7.88-7.95 (2H, m, Ar-*H*); 8.42 (1H, d, *J* = 7.8 Hz, Ar-*H*); 8.50 (1H, s, Ar-*H*).

Procedure for the synthesis of 1-(3-Amino-5-chloro-2-hydroxyphenyl)ethanone, 4.26

Nitroacetophenone (1 molar eq.) and Sn 10-40 mesh (15 molar eq.) were suspended in EtOH (5 mL/mmol). HCl 30% (v/v) was added to the suspension and heated at reflux temperature for 1 hour. The mixture was cooled and diluted with water (20 mL/mmol). CH₂Cl₂ was added, and the aqueous phase basified up to pH 10. The aqueous phase was extracted with CH₂Cl₂ (4×50 mL), the combined extracts were dried over Na₂CO₃ and the solvent evaporated under reduced pressure. An orange solid was obtained; 94%; mp 84-85 °C; ¹H-NMR (CDCl₃, 400.13 MHz) δ 2.62 (3H, s, CH₃); 4.05 (2H, br.s, NH₂); 6.86 (1H, d, *J* = 2.4 Hz, Ar-*H*); 7.10 (1H, d, *J* = 2.4 Hz, Ar-*H*); 12.43 (1H, s, OH); IR (film) ν_{max} 3501; 3398; 1632; 1460; 1306 cm⁻¹.

Procedure for the synthesis of *N*-(3-acetyl-5-chloro-2-hydroxyphenyl)acetamide, 4.27

2-Hydroxyacetophenone **4.26** (1 molar eq.) was dissolved in dry pyridine (3 mL/mmol) and anhydride acetic was added (1.1 molar eq.). The mixture was refluxed for 6 hours, cooled to room temperature and acidified with concentrated HCl until pH 1. The aqueous phase was extracted with CH₂Cl₂ (3×50 mL), the combined extracts were dried (Na₂SO₄), and evaporated under reduced pressure. The crude product was purified by flash chromatography, hexane : ethyl acetate (4:1). Yellow solid; 74%; mp 125-127 °C; ¹H-NMR (CD₃OD, 400.13 MHz) δ 2.22 (3H, s, CH₃); 2.67 (3H, s, CH₃); 4.65 (1H, s, NH); 7.68 (1H, d, *J* = 2.4 Hz, Ar-*H*); 8.39 (1H, d, *J* = 2.4 Hz, Ar-*H*); IR (film) ν_{max} 3370; 1638; 1606; 1465; 1363; 1313; 1166; 856; 791 cm⁻¹.

Procedure for the synthesis of 1-(4-(bromomethyl)-5-chloro-2-hydroxyphenyl)ethanone, 4.29

Method A - Acetophenone (1 molar eq.), NBS (1.1 molar eq.) and a catalytic amount of AIBN were dissolved in benzene (20 mL/mmol). The mixture was refluxed for 2 hours and cooled to room temperature. The reaction mixture was poured into a saturated solution of Na₂CO₃, and was extracted with ethyl acetate (50 mL). The crude product was purified by flash chromatography, hexane : ethyl acetate (9:1). A 1:1 mixture of **4.29** and acetophenone was recovered; ¹H-NMR (CDCl₃, 400.13 MHz) δ 2.65 (3H, s, CH₃); 4.51 (2H, s, CH₂); 7.11 (1H, s, Ar-H); 7.76 (1H, s, Ar-H); 12.10 (1H, s, OH).

Method B – Identical to method A, except for: NBS was used in greater excess (1.5 molar eq.) and reflux was carried out for 24 hours. An untractable mixture was obtained.

Procedure for the synthesis of N-methoxy-N-methyl-4-(4-(trifluoromethoxy)phenoxy)benzamide, 4.38

Compound **4.6** (1 molar eq.) was dissolved in TEA (1 molar eq.) and TBTU (1.1 molar eq.), and stirred at room temperature for 30 minutes. *N,O*-dimethylhydroxylamine (1.2 molar eq.) in TEA (1.2 molar eq.) were added, and the final mixture kept stirring at room temperature for 24 hours. CH₂Cl₂ (50 mL/mmol) was poured, and the organic phase washed in sequence with HCl 3N, Na₂CO₃ and brine. The organic phase was dried (Na₂SO₄), and the solvent evaporated under reduced pressure. Yellow oil; 100%; ¹H-NMR (CDCl₃, 400.13 MHz) δ 3.37 (3H, s, CH₃); 3.53 (3H, s, OCH₃); 7.00 (2H, d, *J* = 8.0 Hz, Ar-H); 7.06 (2H, d, *J* = 8.4 Hz, Ar-H); 7.23 (2H, d, *J* = 8.4 Hz, Ar-H); 7.74 (2H, d, *J* = 8.0 Hz, Ar-H).

Procedure for the synthesis of 4-(4-(trifluoromethoxy)phenoxy)benzaldehyde, 4.39

Compound **4.40** (1 molar eq.) was dissolved in dry THF (20 mL/mmol), and LiAlH₄ (1.2 molar eq.) added slowly. The mixture was stirred for 1 hour at -5 °C, after which it was diluted with CH₂Cl₂ (50 mL/mmol), and washed in sequence with solutions of KHSO₄ 1N (20 mL), HCl 3N (20 mL), saturated solution of NaHSO₄ (20 mL) and brine (20 mL). The organic phase was dried (Na₂SO₄) and the solvent evaporated under reduced pressure. Transparent oil; 97%; ¹H-NMR (CDCl₃, 400.13 MHz) δ 7.08-7.14 (4H, m, Ar-H); 7.29 (2H, d, *J* = 8.4 Hz, Ar-H); 7.89 (2H, d, *J* = 8.4 Hz, Ar-H); 9.96 (1H, s, CHO).

Chalcones

General procedure

Method A - 8-Nitroacetophenone (1 molar eq.) and benzaldehyde (1 molar eq.) were dispersed in ethanol (20 mL/mmol). NaOH 1N (2 molar eq.) was added, and the mixture refluxed for 40 minutes. After cooling to room temperature, concentrated HCl was poured dropwise until pH 1. The resulting precipitate was filtered off and washed with ice-cold water. The crude product was crystallized from EtOH.

Method B - Identical to method A except NaOH was added in greater excess (6 molar eq.), and the reaction carried out at room temperature for 24 hours.

(E)-1-(5-Chloro-2-hydroxy-3-nitrophenyl)-3-phenylprop-2-en-1-one, 4.34

From method B - Yellow solid; 100%, mp 165-168 °C; ¹H-NMR (CDCl₃, 400.13 MHz) δ 7.42-7.50 (3H, m, Ar-H); 7.53 (1H, d, *J* = 15.6 Hz, CH); 7.68; (2H, d, *J* = 6.0 Hz, Ar-H); 7.94 (1H, d, *J* = 15.6 Hz, CH); 8.10 (1H, d, *J* = 2.4 Hz, Ar-H); 8.20 (1H, d, *J* = 2.4 Hz, Ar-H).

(E)-1-(5-Chloro-2-hydroxy-3-nitrophenyl)-3-(4-(4-(trifluoromethoxy)phenoxy)phenyl)prop-2-en-1-one, 4.37

From method B - Orange needles; 89%; mp 125-126 °C; ¹H-NMR (CDCl₃, 400.13 MHz) δ 7.07 (2H, d, *J* = 8.0 Hz, Ar-H); 7.11 (2H, d, *J* = 8.8 Hz, Ar-H); 7.28 (2H, d, *J* = 8.8 Hz, Ar-H); 7.46 (1H, d, *J* = 15.4 Hz, CH); 7.70 (2H, d, *J* = 8.0 Hz, Ar-H); 7.97 (1H, d, *J* = 15.4 Hz, CH); 8.12 (1H, s, Ar-H); 8.23 (1H, s, Ar-H); 13.33 (1H, s, OH); ¹³C-NMR (CDCl₃, 100.61 MHz) δ 118.56 (CH); 119.17 (CH); 120.90 (CH); 122.89 (CH); 123.59 (Cq); 125.80 (Cq); 126.71 (Cq); 128.05 (Cq); 129.05 (Cq); 130.35 (CH); 131.13 (CH); 135.39 (CH); 137.60 (Cq); 147.17 (CH); 154.12 (Cq); 156.06 (Cq); 160.33 (Cq); 190.99 (C=O); IR (film): ν_{\max} 3409; 1645; 1562; 1492; 1453; 1352; 1248; 1217; 1172; 1063 cm⁻¹; ESI-MS *m/z* (abund.): 480 [M+H]⁺ (100); Anal. Calcd. For (C₂₂H₁₃ClF₃NO₆): C, 55.07; H, 2.73%. Found: C, 56.24; H, 2.82%.

7.4.10 Flavones

General procedure

Method A ^[288] - DBU (2.2 molar eq.) was added to a solution of 2-hydroxyacetophenone (1 molar eq.) and benzoyl chloride (1.1 molar eq.) in dry pyridine (4 mL/mmol). The mixture was

stirred for 6 hours at reflux, cooled to room temperature and poured into HCl 1N (20-25 mL) containing ice. The solution was extracted with dichloromethane (3×50 mL) and the combined extracts were dried upon Na₂SO₄ and evaporated to dryness under reduced pressure. The crude product was purified by flash chromatography eluting with hexane : ethyl acetate (9:1).

Method B - Benzoic acid (1 molar eq.) was dissolved in SOCl₂ (8 mL/mmol) and heated at reflux temperature for 24 hours. The solvent was evaporated and the crude product used as such in the following step. DBU (2.2 molar eq.) was added to a solution of the 2-hydroxyacetophenone (1.5 molar eq.) and benzoyl chloride (1.0 molar eq.) in dry pyridine (4 mL/mmol). The mixture was stirred for 6 hours at reflux, cooled to room temperature and poured into HCl 1N (20-25 mL) containing ice. The solution was extracted with dichloromethane (3×50 mL), the combined extracts were dried (Na₂CO₃) and evaporated to dryness under reduced pressure. The crude product was purified by flash chromatography, hexane : ethyl acetate (9:1).

Method C - Equal to method B, but with 2-hydroxyacetophenone in greater excess (2 molar eq.)

Method D - Equal to method B, but with MW-assisted heating, i.e. potency of 100W to a maximum of 150 °C for 40 minutes.

2-((3-Trifluoromethyl)phenyl)-4H-chromen-4-one, 4.11

From method A - Pale yellow solid; 32%; mp 145-147; ¹H-NMR (CDCl₃, 400.13 MHz) δ 6.92 (1H, s, Ar-H3); 7.48 (1H, t, *J* = 7.2 Hz, Ar-H); 7.65 (1H, d, *J* = 8.0 Hz, Ar-H); 7.71 (1H, t, *J* = 8.0 Hz, Ar-H); 7.77 (1H, m, Ar-H); 8.83 (1H, d, *J* = 7.6 Hz, Ar-H); 8.13 (1H, d, *J* = 7.6 Hz, Ar-H); 8.23 (1H, s, Ar-H); 8.27 (1H, dd, *J* = 1.6 and 8.0 Hz, Ar-H).

2-(4-(4-Chlorophenoxy)phenyl)-4H-chromen-4-one, 4.12

From method B - Pale yellow solid; 30%; mp 132-133 °C; ¹H-NMR (CDCl₃, 400.13 MHz) δ 6.80 (1H, s, Ar-H3); 7.07 (2H, d, *J* = 8.8 Hz, Ar-H); 7.31 (2H, d, *J* = 8.8 Hz, Ar-H); 7.40 (2H, d, *J* = 8.8 Hz, Ar-H); 7.45 (1H, t, *J* = 7.2 Hz, Ar-H); 7.59 (1H, d, *J* = 7.2 Hz, Ar-H); 7.73 (1H, t, *J* = 7.2 Hz, Ar-H); 7.93 (2H, d, *J* = 8.8 Hz, Ar-H); 8.27 (1H, d, *J* = 7.2 Hz, Ar-H); ¹³C-NMR (CDCl₃, 100.61 MHz) δ 106.94 (CH); 118.02 (CH); 118.31 (CH); 121.22 (Cq); 123.93 (Cq); 125.27 (CH); 125.74 (CH); 126.51 (CH); 128.24 (CH); 129.67 (Cq); 130.12 (CH); 133.77 (CH); 154.37 (Cq); 156.21 (Cq); 160.34 (Cq); 162.86 (Cq); 178.38 (C=O); IR (film): ν_{max} 1638; 1472; 1402; 1364; 1243 cm⁻¹; ESI-MS *m/z* (abund.): 349 [M+H]⁺ (100); Anal. Calcd. (C₂₁H₁₃ClO₃ • 0.1 AcOEt): C, 71.88; H, 3.89%. Found: C, 72.14; H, 3.76%.

6-Chloro-2-(4-(4-chlorophenoxy)phenyl)-4H-chromen-4-one, 4.13

From method C - Pale yellow solid; 15%; mp 165-167 °C; ¹H-NMR (CDCl₃, 400.13 MHz) δ 6.78 (1H, s, Ar-H3); 7.05 (2H, d, *J* = 8.8 Hz, Ar-H); 7.11 (2H, d, *J* = 8.8 Hz, Ar-H); 7.39 (2H, d, *J* = 8.8 Hz, Ar-H); 7.55 (1H, d, *J* = 8.8 Hz, Ar-H); 7.67 (1H, dd, *J* = 8.8 and 2.4 Hz, Ar-H); 7.91 (2H, d, *J* = 8.8 Hz, Ar-H); 8.21 (1H, d, *J* = 2.4 Hz, Ar-H); ¹³C-NMR (CDCl₃, 100.61 MHz) δ 106.77 (CH); 118.28 (Cq); 119.74 (Cq); 121.30 (CH); 124.88 (CH); 125.21 (CH); 126.03 (CH); 128.29 (CH); 129.79 (Cq); 130.15 (CH); 131.22 (Cq); 133.94 (CH); 154.22 (Cq); 154.51 (Cq); 160.59 (Cq); 163.15 (Cq); 177.11 (C=O); IR (film): ν_{max} 1625; 1479; 1434; 1351; 1236; 824 cm⁻¹; ESI-MS *m/z* (abund.): 383 [M+H]⁺ (100); Anal. Calcd. (C₂₁H₁₂Cl₂O₃): C, 65.82; H, 3.16%. Found: C, 66.17; H, 3.07%.

7-Chloro-2-(4-(4-chlorophenoxy)phenyl)-4H-chromen-4-one, 4.14

From method C - Yellow solid; 32%; mp 179-181 °C; ¹H-NMR (CDCl₃, 400.13 MHz) δ 6.75 (1H, s, Ar-H3); 7.06 (2H, d, *J* = 7.2, Ar-H); 7.12 (2H, d, *J* = 8.0, Ar-H); 7.40 (2H, d, *J* = 7.2, Ar-H); 7.41 (1H, dd, *J* = 8.4 and 2.0 Hz, Ar-H); 8.62 (1H, d, *J* = 2.0, Ar-H); 7.91 (2H, d, *J* = 8.0 Hz, Ar-H); 8.19 (1H, d, *J* = 8.4 Hz, Ar-H); ¹³C-NMR (CDCl₃, 100.13 MHz) δ 107.07 (CH); 118.14 (Cq); 118.29 (CH); 121.31 (CH); 122.47 (CH); 126.01 (CH); 126.12 (CH); 127.12 (CH); 128.25 (CH); 129.80 (Cq); 130.15 (Cq); 139.75 (Cq); 154.33 (Cq); 156.29 (Cq); 160.59 (Cq); 163.18 (Cq); 177.48 (C=O); IR (film): ν_{max} 1645; 1479; 1415; 1364; 1242 cm⁻¹; ESI-MS *m/z* (abund.): 383 [M+H]⁺ (100); Anal. Calcd. (C₂₁H₁₂Cl₂O₃): C, 65.82; H, 3.16%. Found: C, 65.56; H, 3.09%.

2-(4-(4-Chlorophenoxy)phenyl)-7-methyl-4H-chromen-4-one, 4.15

From method C - White solid; 11%; mp 138-139 °C; ¹H-NMR (CDCl₃, 400.13 MHz) δ 2.54 (3H, s, CH₃); 6.76 (1H, s, Ar-H3); 7.06 (2H, d, *J* = 7.2 Hz, Ar-H); 7.11 (2H, d, *J* = 7.2 Hz, Ar-H); 7.26 (1H, dd, *J* = 8.0 and 1.2 Hz, Ar-H); 7.38-7.40 (3H, m, Ar-H); 7.91 (2H, d, *J* = 7.2 Hz, Ar-H); 8.13 (1H, d, *J* = 8.0 Hz, Ar-H); ¹³C-NMR (CDCl₃, 100.61 MHz) δ 21.88 (CH₃); 106.85 (CH); 117.80 (CH); 118.30 (CH); 121.20 (Cq); 121.66 (CH); 125.45 (CH); 126.64 (CH); 126.74 (CH); 128.15 (CH); 129.62 (Cq); 130.10 (Cq); 145.10 (Cq); 154.40 (Cq); 156.34 (Cq); 160.21 (Cq); 162.56 (Cq); 178.33 (C=O); IR (film): ν_{max} 1632; 1485; 1421; 1370; 1243; 827 cm⁻¹; ESI-MS *m/z* (abund.): 363 [M+H]⁺ (100); Anal. Calcd. (C₂₂H₁₅ClO₃): C, 72.83; H, 4.17%. Found: C, 72.59; H, 4.16%.

6-Chloro-2-(4-(4-chlorophenoxy)phenyl)-7-methyl-4H-chromen-4-one, 4.16

From method C - Yellow solid; 21%; mp 185-187 °C; ¹H-NMR (CDCl₃, 400.13 MHz) δ 2.54 (3H, s, CH₃); 6.76 (1H, s, Ar-H3); 7.06 (2H, d, *J* = 7.2 Hz, Ar-H); 7.10 (2H, d, *J* = 7.2 Hz, Ar-H); 7.39 (2H, d, *J* = 7.2 Hz, Ar-H); 7.48 (1H, s, Ar-H); 7.90 (2H, d, *J* = 7.2 Hz, Ar-H); 8.20 (1H, s, Ar-H); ¹³C-NMR (CDCl₃, 100.61 MHz) δ 20.88 (CH₃); 106.69 (CH); 118.28 (CH); 119.87 (CH); 121.26 (CH); 122.98 (CH); 125.42 (CH); 126.24 (Cq); 128.22 (CH); 129.74 (Cq); 130.14 (Cq); 131.93 (Cq); 142.98 (Cq); 154.29 (Cq); 154.45 (Cq); 160.45 (Cq); 162.88 (Cq); 177.18 (C=O); IR (film): ν_{max} 1630; 1481; 1400; 1237; 1163; 827 cm⁻¹; ESI-MS *m/z* (abund.): 397 [M+H]⁺ (100); Anal. Calcd. (C₂₂H₁₄Cl₂O₃): C, 66.52; H, 3.55%. Found: C, 65.72; H, 3.50%.

6-Chloro-7-methyl-2-(4-(4-trifluoromethoxy)phenoxy)phenyl-4H-chromen-4-one, 4.17

From method C - Pinkish solid; 40%; mp 171-173 °C; ¹H-NMR (CDCl₃, 400.13 MHz) δ 2.55 (3H, s, CH₃); 6.76 (1H, s, Ar-H3); 7.12-7.14 (4H, m, Ar-H); 7.28 (2H, d, *J* = 8.0 Hz, Ar-H); 7.48 (1H, s, Ar-H8); 7.91 (2H, d, *J* = 7.2 Hz, Ar-H); 8.20 (1H, s, Ar-H5); ¹³C-NMR (CDCl₃, 100.13 MHz) δ 20.89 (CH₃); 106.75 (CH); 118.45 (CH); 119.87 (CH); 120.92 (CH); 122.85 (Cq); 122.91 (CH); 122.95 (Cq); 122.99 (Cq); 125.43 (CH); 126.43 (Cq); 128.25 (CH); 131.95 (Cq); 143.00 (Cq); 145.45 (Cq); 154.19 (Cq); 160.30 (Cq); 162.84 (Cq); 177.17 (C=O); IR (film): ν_{max} 1630; 1503; 1251; 1163; 1037; 904; 830 cm⁻¹; ESI-MS *m/z* (abund.): 447 [M+H]⁺ (100); Anal. Calcd. (C₂₃H₁₄ClF₃O₄): C, 61.83; H, 3.16%. Found: C, 61.86; H, 3.10%.

2-([1,1'-Biphenyl]-4-yl)-6-chloro-7-methyl-4H-chromen-4-one, 4.18

From method C - Yellow solid; 27%; mp 197-199 °C; ¹H-NMR (CDCl₃, 400.13 MHz) δ 2.56 (3H, s, CH₃); 6.87 (1H, s, Ar-H3); 7.44 (1H, tt, *J* = 1.2 and 7.2 Hz, Ar-H); 7.50-7.54 (3H, m, Ar-H and Ar-H8); 7.68 (2H, d, *J* = 8.0 Hz, Ar-H); 7.78 (2H, d, *J* = 6.8 Hz, Ar-H); 8.01 (2H, d, *J* = 6.8 Hz, Ar-H); 8.22 (1H, s, Ar-H5); ¹³C-NMR (CDCl₃, 100.13 MHz) δ 20.91 (CH₃); 107.24 (CH); 119.97 (CH); 123.09 (Cq); 125.44 (CH); 126.76 (CH); 127.18 (CH); 127.72 (CH); 128.29 (Cq); 129.04 (CH); 129.07 (CH); 130.30 (Cq); 131.96 (Cq); 139.69 (Cq); 143.05 (Cq); 144.55 (Cq); 154.54 (Cq); 177.29 (C=O); IR (film): ν_{max} 1630; 1451; 1407; 1244; 1051; 908; 827 cm⁻¹; ESI-MS *m/z* (abund.): 347 [M+H]⁺ (100); Anal. Calcd. (C₂₂H₁₅ClO₂ • 0.2 CH₂Cl₂): C, 73.29; H, 4.27%. Found: C, 73.66; H, 4.31%.

2-([1,1'-Biphenyl]-4-yl)-6-chloro-8-nitro-4H-chromen-4-one, 4.19

From method D - $^1\text{H-NMR}$ (CDCl_3 , 400.13 MHz) δ 7.00 (1H, s, Ar-*H3*); 7.45 (1H, t, $J = 7.2$ Hz, Ar-*H*); 7.53 (2H, t, $J = 7.2$ Hz, Ar-*H*); 7.69 (2H, d, $J = 8.0$ Hz, Ar-*H*); 7.82 (2H, d, $J = 8.0$ Hz, Ar-*H*); 8.11 (2H, d, $J = 8.0$ Hz, Ar-*H*); 8.41 (1H, s, Ar-*H*); 8.52 (1H, s, Ar-*H*).

6-Chloro-7-methyl-2-(4-(4,4,4-trifluorobutoxy)phenyl)-4H-chromen-4-one, 4.20

From method C - Yellow solid; 15%; mp 161-162 °C; $^1\text{H-NMR}$ (CDCl_3 , 400.13 MHz) δ 2.13 (2H, m, $\text{CH}_2\text{CH}_2\text{CH}_2$); 2.36 (2H, m, $\text{CH}_2\text{CH}_2\text{CF}_3$); 2.54 (3H, s, CH_3); 4.13 (2H, t, $J = 6.0$ Hz, $\text{CH}_2\text{CH}_2\text{CH}_2\text{CF}_3$); 6.74 (1H, s, Ar-*H3*); 7.03 (2H, d, $J = 8.6$ Hz, Ar-*H*); 7.48 (1H, s, Ar-*H8*); 7.88 (2H, d, $J = 8.6$ Hz, Ar-*H*); 8.19 (1H, s, Ar-*H5*); $^{13}\text{C-NMR}$ (CDCl_3 , 100.13 MHz) δ 20.87 (CH_3); 22.09 (CH_2); 29.82 (CH_2); 30.52 (CH_2); 66.27 (CF_3); 106.08 (CH); 114.91 (Cq); 119.85 (CH); 123.00 (CH); 124.16 (Cq); 125.40 (CH); 128.08 (CH); 131.80 (Cq); 142.81 (Cq); 154.45 (Cq); 161.44 (Cq); 163.34 (Cq); 177.24 (C=O); IR (film): ν_{max} 1638; 1504; 1408; 1243; 1019 cm^{-1} ; ESI-MS m/z (abund.): 397 $[\text{M}+\text{H}]^+$ (100); Anal. Calcd. ($\text{C}_{20}\text{H}_{16}\text{ClF}_3\text{O}_3$): C, 60.54; H, 4.06%. Found: C, 60.49; H, 3.93%.

2-(4-(3-(Trifluoromethoxy)phenoxy)phenyl)-4H-chromen-4-one, 4.21

From method C - Yellow solid; 37%; mp 86-87%; $^1\text{H-NMR}$ (CDCl_3 , 400.13 MHz) δ 6.81 (1H, s, Ar-*H3*); 6.99-7.10 (3H, m, Ar-*H*); 7.18 (2H, d, $J = 8.8$, Ar-*H*); 7.41-7.48 (2H, m, Ar-*H*); 7.59 (1H, d, $J = 7.6$ Hz, Ar-*H*); 7.73 (1H, ddd, $J = 8.6, 7.2$ and 1.6 Hz, Ar-*H*); 7.96 (2H, d, $J = 8.8$ Hz, Ar-*H*); 8.26 (1H, dd, $J = 7.6$ and 1.6 Hz, Ar-*H*); $^{13}\text{C-NMR}$ (CDCl_3 , 100.13 MHz) δ 107.09 (CH); 112.58 (CH); 116.45 (CH); 117.67 (CH); 118.03 (Cq); 118.39 (CH); 118.89 (CH); 123.93 (Cq); 125.30 (CH); 125.76 (CH); 127.08 (Cq); 128.33 (CH); 130.61 (CH); 130.85 (Cq); 133.81 (CH); 156.22 (Cq); 157.02 (Cq); 159.58 (Cq); 162.77 (Cq); 178.40 (C=O); IR (film): ν_{max} 1632; 1587; 1478; 1370; 1262; 1172 cm^{-1} ; ESI-MS m/z (abund.): 399 $[\text{M}+\text{H}]^+$ (100); Anal. Calcd. ($\text{C}_{22}\text{H}_{13}\text{F}_3\text{O}_4$): C, 66.34; H, 3.29%. Found: C, 66.40; H, 3.22%.

2-([1,1'-Biphenyl]-4-yl)-3-bromo-7-bromomethyl-6-chloro-4H-chromen-4-one, 4.31

Compound **4.18** (1 molar eq.), NBS (1.2 molar eq.) and benzoyl peroxide (0.1 molar eq.) were suspended in CCl_4 (5 mL/mmol). The mixture was heated to reflux for 24 hours and then cooled to room temperature. The organic phase was washed with water and evaporated to dryness under reduced pressure. The crude product was purified by flash chromatography, hexane: ethyl acetate (9:1). Yellow solid; 27%; mp 262-265 °C; $^1\text{H-NMR}$ (CDCl_3 , 400.13 MHz) δ 4.67 (2H, s, CH_2);

7.45 (1H, t, $J = 7.0$ Hz, Ar-*H*); 7.53 (2H, t, $J = 7.4$ Hz, Ar-*H*); 7.69-7.71 (3H, m, Ar-*H*); 7.79 (2H, d, $J = 8.6$ Hz, Ar-*H*); 7.99 (2H, d, $J = 8.6$ Hz, Ar-*H*); 8.34 (1H, s, Ar-*H*); ^{13}C -NMR (CDCl_3 , 100.13 MHz) δ 29.00 (CH_2); 109.14 (Cq); 120.61 (CH); 122.43 (Cq); 127.07 (CH); 127.27 (CH); 127.36 (CH); 128.31 (CH); 129.04 (CH); 129.88 (CH); 131.04 (Cq); 131.46 (Cq); 139.72 (Cq); 141.76 (Cq); 144.34 (Cq); 153.85 (Cq); 162.21 (Cq); 171.90 (C=O); IR (film): ν_{max} 1651; 1613; 1549; 1453; 1409; 1332; 1076 cm^{-1} ; ESI-MS m/z (abund.): 505 $[\text{M}+\text{H}]^+$ (100); Anal. Calcd. ($\text{C}_{22}\text{H}_{13}\text{Br}_2\text{ClO}_2$): C, 52.37; H, 2.60%. Found: C, 52.01; H, 2.51%.

2-([1,1'-Biphenyl]-4-yl)-3-bromo-6-chloro-7-methyl-4*H*-chromen-4-one, 4.32 ^[290]

Compound **4.18** (1 molar eq.), NBS (1.2 molar eq.) and ZrCl_4 (0.1 molar eq.) were suspended in CH_2Cl_2 (4 mL/mmol). The suspension was stirred at room temperature for 24 hours and water was added. The aqueous phase was extracted with CH_2Cl_2 (4×50 mL), and the combined extracts were evaporated to dryness under reduced pressure. The crude product was purified by flash chromatography, hexane : ethyl acetate (9:1). Yellow solid; 10%; mp 190-192 °C; ^1H -NMR (CDCl_3 , 400.13 MHz) δ 2.55 (3H, s, CH_3); 7.41-7.48 (2H, m, Ar-*H*); 7.52 (2H, t, $J = 7.6$ Hz, Ar-*H*); 7.66-7.72 (2H, m, Ar-*H*); 7.78 (2H, d, $J = 8.6$ Hz, Ar-*H*); 7.97 (2H, d, $J = 8.6$ Hz, Ar-*H*); 8.28 (1H, s, Ar-*H*); ^{13}C -NMR (CDCl_3 , 100.13 MHz) δ 20.98 (CH_3); 109.02 (Cq); 119.67 (CH); 120.78 (Cq); 126.04 (CH); 126.97 (CH); 127.26 (CH); 128.24 (CH); 129.02 (CH); 129.87 (CH); 131.35 (Cq); 132.46 (Cq); 139.80 (Cq); 143.66 (Cq); 144.12 (Cq); 153.92 (Cq); 161.66 (Cq); 172.06 (C=O); IR (film): ν_{max} 1651; 1606; 1542; 1409 cm^{-1} ; HRMS calc. ($\text{C}_{22}\text{H}_{14}\text{BrClO}_2$): 423.9866 / 425.9845. Found: 423.9861 / 425.9839.

7.4.11 Intermediates for isoflavones

Procedure for the synthesis of 3-iodo-4*H*-chromen-4-one, 4.40 ^[296]

2-Hydroxyacetophenone (1 molar eq.) was diluted in DMF-DMA (1.5 molar eq.) and the resulting mixture was stirred at 95 °C for 3 hours. After evaporation of the solvent, the obtained solid was dissolved in CHCl_3 (4 mL/mmol) and successively treated with pyridine (1 molar eq.) and I_2 (2 molar eq.). The resulting mixture was stirred at room temperature for 24 hours. The reaction was treated with saturated aqueous $\text{Na}_2\text{S}_2\text{O}_3$ solution and stirred for 30 minutes at room temperature. The aqueous phase was extracted with CH_2Cl_2 (4×30 mL). The collected organic extracts were dried (Na_2SO_4), filtered, and concentrated under reduced pressure. The crude product

was purified by flash chromatography, hexane : ethyl acetate (9.5:0.5). White needles; 97%; mp 76-77 °C; ¹H-NMR (CDCl₃, 400.13 MHz) δ 7.45-7.50 (2H, m, Ar-*H*); 7.73 (1H, m, Ar-*H*); 8.26 (1H, dd, *J* = 8.6 and 1.6 Hz, Ar-*H*); 8.32 (1H, s, Ar-*H*2); IR (film) ν_{\max} 3061; 1651; 1555; 1460; 1318; 1064; 862; 759 cm⁻¹.

Procedure for the synthesis of 3-(4-fluorophenyl)-4*H*-chromen-4-one, 4.42 ^[296]

Na₂CO₃ (3 molar eq.) boronic acid (1.2 molar eq.) and Pd-C 10% w/w (5 mol% of the limiting reagent) were added to a solution of 4.40 (1 molar eq.) in DME (3 mL/mmol) and H₂O (3 mL/mmol). The resulting mixture was stirred for 1 hour at 45 °C and then the catalyst was filtered off, washed with water and CH₂Cl₂. The aqueous phase was extracted with CH₂Cl₂ (4×25 mL) and the combined extracts were dried (Na₂SO₄), filtered and concentrated under reduced pressure. Orange solid; 93%; mp 191-193 °C; ¹H-NMR (CDCl₃, 400.13 MHz) δ 7.14-7.19 (2H, m, Ar-*H*); 7.47 (1H, ddd, *J* = 8.0, 7.6, and 0.8 Hz, Ar-*H*); 7.52 (1H, dd, *J* = 8.0 and 0.8 Hz, Ar-*H*); 7.57 (2H, m, Ar-*H*); 7.73 (1H, ddd, *J* = 7.6, 7.2 and 1.6 Hz, Ar-*H*); 8.04 (1H, s, Ar-*H*2); 8.34 (1H, dd, *J* = 8.0 and 1.6 Hz, Ar-*H*); IR (film) ν_{\max} 1638; 1460; 1230 cm⁻¹.

Procedure for the synthesis of 1-(4-bromophenoxy)-3-(trifluoromethoxy)benzene, 4.45

Identical to the procedure reported for S_NAr reactions with reflux for 48 hours. Yellow oil; 38%; ¹H-NMR (CDCl₃, 400.13 MHz) δ 6.85 (1H, br.s, Ar-*H*); 6.90 (1H, ddd, *J* = 8.2, 2.4 and 0.8 Hz, Ar-*H*); 6.96 (1H, m, Ar-*H*); 7.01-7.13 (4H, m, Ar-*H*); 7.34 (1H, t, *J* = 8.2 Hz, Ar-*H*).

7.5 Computational Approach

7.5.1 Quantum mechanical calculations

Each structure was drawn with GaussView 3.0 ^[331] and fully optimized *in vacuo* without imposing any constraints. All calculations were performed with the Gaussian 03 package ^[332]. Geometry optimizations were first carried out at the semi-empirical level of theory, AM1 ^[333]. A more refined minimization was then achieved at a quantum mechanical level, using DFT ^[334] with the hybrid B3LYP functional, which is a combination of Becke's three parameter (B3) exchange functional ^[335] with the Lee, Yang, and Parr (LYP) correlation functional ^[336] and the 6-31G(d,p)

basis set, which adds polarized functions to both heavy atoms and hydrogen atoms. This hybrid functional and basis set has been described to calculate accurate energies ^[173]. The resulting geometries were found to be local minima on their potential energy by calculating harmonic frequencies. Molecular frontier orbitals, HOMO and LUMO, and MEPs of all optimized structures were visualized with Molekel 4.3 ^[337]. These MEP outlines provide a measure of the overall size of the molecule and the colour-coded surface gives location of the negative and positive electrostatic potentials, as a function of attraction or repulsion of a positively-charged test probe, respectively. MEP isoenergy contours were generated in the range of -0.15 and +0.15 e/au³.

7.5.2 Molecular docking and virtual screening

Protein preparation and molecular docking

The cytochrome *bc*₁ from the baker's yeast (PDB code 1KYO) ^[43] was used. This presents the dimeric and functional protein with the iron-sulfur cluster in close contact with cytochrome *b*, which is crucial for electron transfer. The protein preparation was carried out using UCSF Chimera ^[338]. Hydrogens were added to aminoacid residues, partial charges were assigned with Antechamber ^[339], the energy was minimized and the output saved as mol2 file. Histidine 181 at the Q_o site was kept protonated, as good evidence of such state is available for stigmatellin binding ^[63]. Docking was performed with the GOLD 3.02 or 4.01 ^[192] packages that search the best ligand interaction pose, inside the binding pocket, using a genetic algorithm. Docked ligands were ranked with the GoldScore ^[193] scoring function included in the software, and defined by the following components: protein-ligand hydrogen bond energy, protein-ligand van der Waals energy, ligand internal van der Waals energy and ligand torsional strain energy. This fitness function has been optimized to predict the ligand binding position and conformation of the ligands. Default settings were used and 10,000 docking runs performed for each ligand:

a) Population settings

Maxops	87000
Popsiz	100
select_pressure	100
n_islands	5
niche_siz	2

b) GA settings

pt_crosswt	95
allele_mutatewt	95
migratewt	10

c) Search settings

start_vdw_linear_cutoff	4.000
initial_virtual_pt_match_max	3.000

Database filtration

The ZINC database contains over 8.5 million compounds and was used in this study. Database filtration was performed to collect only drug-like compounds for the docking studies, by applying the Lipinski rule of five ^[319]. The database was further reduced using a 90% diversity set, which afforded 136,966 compounds for virtual screening.

As for the MOE database, only the drug-like subset, comprising over 600,000 compounds was used.

Pharmacophore modeling and screening

The pharmacophore was generated from the bioactive pose of GW844520, using the unified scheme in MOE to identify the pharmacophoric features. The algorithm uses active compounds to derive the pharmacophore without taking their biological data into account. Two different models were constructed and validated including the following features: hydrophobic centroid, amoteric centre, hydrogen-bond acceptor and its projection, hydrogen-bond donor and its projection. The radius of each feature was varied until a good selection of active molecules within a training set of 14 compounds was achieved. In order to fully validate the models, it was sought that the RMSD values would rank accordingly to the IC₅₀s against the T9-96 strain ^[19].

A conformational search using MOE was carried out to generate conformers for all compounds of the databases. In brief, this algorithm employs a parallelized fragment-based approach, in which molecules are divided into overlapping fragments. Each fragment is then submitted to a stochastic conformational search. The resulting fragment conformers are minimized and then assembled by superimposing common atoms. 250 conformations were generated for each compound, using the MMFF94x forcefield and a strain limit of 4 kcal/mol was employed to limit redundant conformers. No other input filters were applied. Virtual screening was then carried out for the two databases and only the lowest RMSD result for each hit was saved to advance to the docking studies.

Receptor-based screening and docking

In the first stage of the screen, 500 runs on a 7-8 times speed up setting were conducted for each of the *ca.* 2000 compounds that matched the pharmacophore query. The top 100 results (10%) from each database were selected for the second phase of the receptor-based screen. This was performed with 250 runs under default settings. For both screening rounds only the top 5 poses of each compound were stored and the results from the second phase of screening were visually inspected with PyMol^[46] based on the following criteria: (i) hydrogen bond with histidine 181 and glutamate 272; (ii) hydrophobic interactions and complementarity between ligand and binding pocket.

The active compounds from the *in vitro* tests were subjected to the third docking round, consisting of 10,000 runs in default settings, in order to better predict the molecular interactions within the Q_o site of cytochrome *bc*₁.

7.6 Hematin binding studies

Titration of hematin was carried out in buffered 40% DMSO at apparent pH 5.5. Chloroquine, clopidol and compounds **3.20-31** were prepared in the following way: stock solutions were obtained by dissolving accurately weighed hematin, chloroquine, clopidol and **3.20-31**, in UV-spectroscopy grade DMSO, to a concentration of 1-5 mM, and stored in the fridge and dark. A buffered 40% (v/v) DMSO solution was prepared in 250 mL volumetric flasks using DMSO (100 ml), aqueous HEPES 1M (5 ml) and completing up to the mark with deionized water. Aqueous buffered DMSO 40% (v/v) solutions of hematin, chloroquine, clopidol and **3.20-31** were prepared daily by mixing an accurately measured sample of the stock solution *ca.* 500 μ L (*via* microsyringe) and diluting to 1 mL with buffered 40% (v/v) DMSO solution. Hematin solutions of 10 μ M were prepared with buffered 40% (v/v) DMSO solution, and transferred to the titration and reference cells. Solutions of chloroquine, clopidol and **3.20-31** were initially added to the cuvette in amounts as small as 2 μ L, gradually increasing the volume in subsequent additions, until the final concentrations were higher than the hematin concentration, which is given by a plateau. After each addition the cuvette was stirred for one minute before the absorbance was taken. UV-Visible titrations were performed in a thermostated (20 °C) cell holder. Scans were run between 300 nm and 500 nm to incorporate the Soret band of the porphyrin. The UV-Visible spectra obtained after each titrated addition was analyzed and stacked against the corresponding absorbances. Dissociation constants of the ligands, complexed with the FPIX-OH, were determined by fitting the experimental data to the appropriate equation models^[245], using least squares nonlinear regression analysis with GraphPad Prism

computer program (GraphPad software, Version 5.00, San Diego, CA). Models were analyzed by χ^2 parameters. Association constants were calculated from dissociation constants.

APPENDICES

Appendix 1

Appendix 1.1 Energy-minimized structures

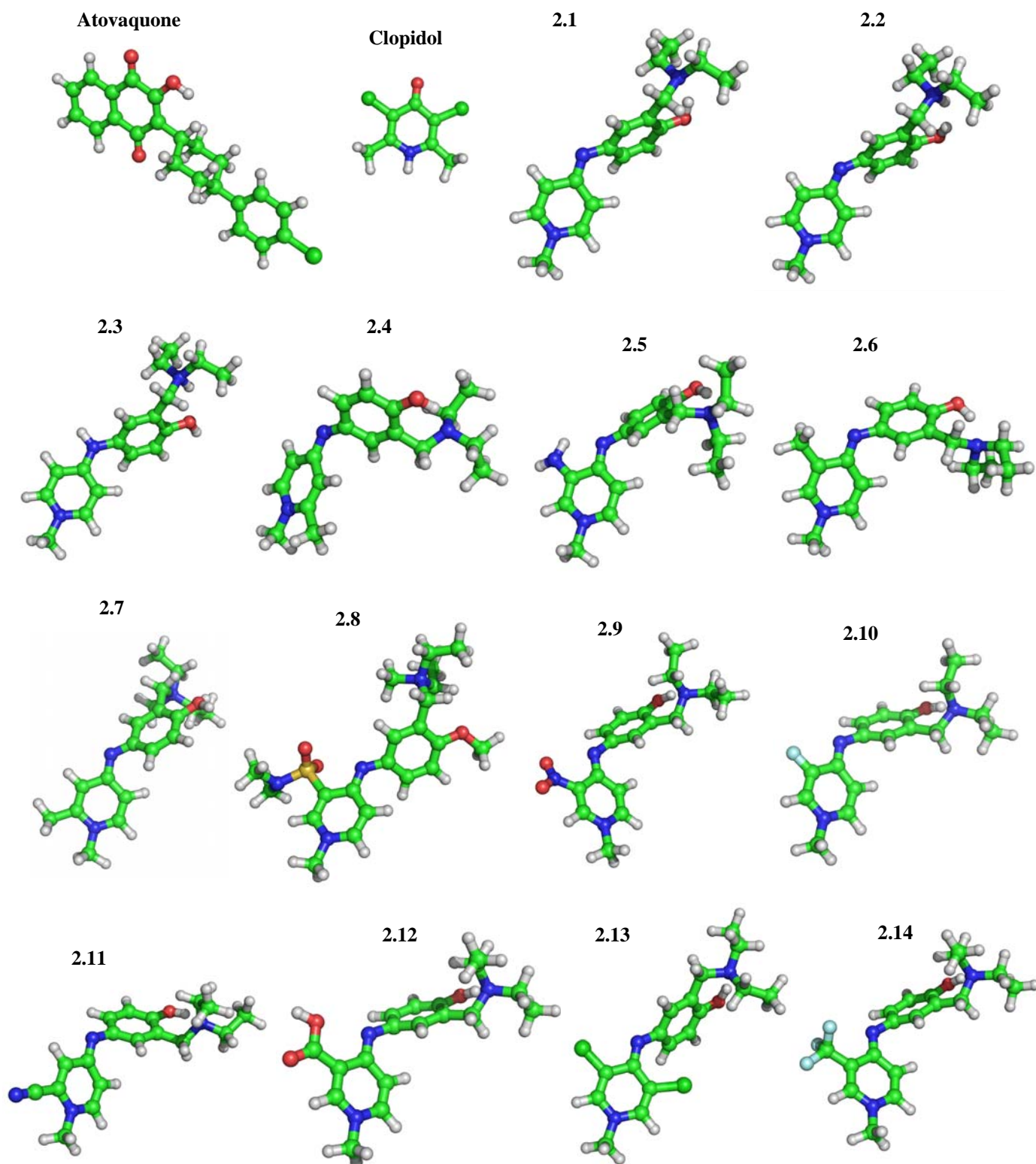


Figure A1.1 Energy-minimized structures of atovaquone, clopidol and compounds 2.1-17.

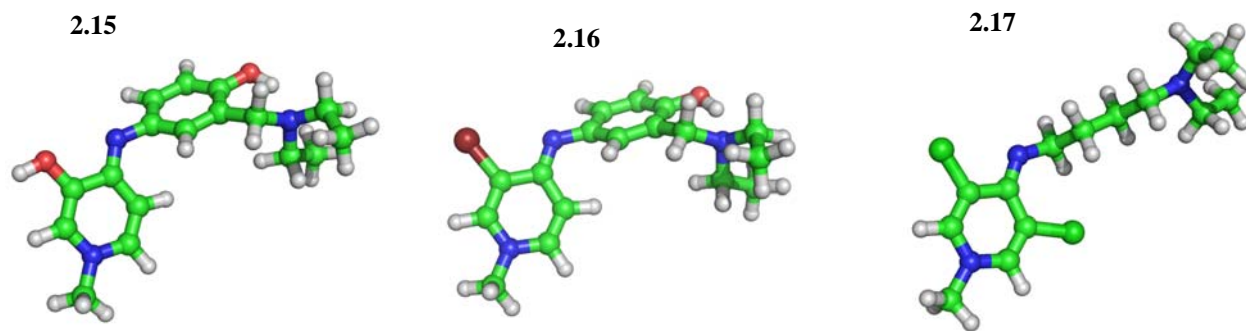


Figure A1.1 (cont.) Energy-minimized structures of atovaquone, clopidol and compounds 2.1-17.

Appendix 1.2 Docking pose of the synthesized Mannich-base 4-pyridonimines

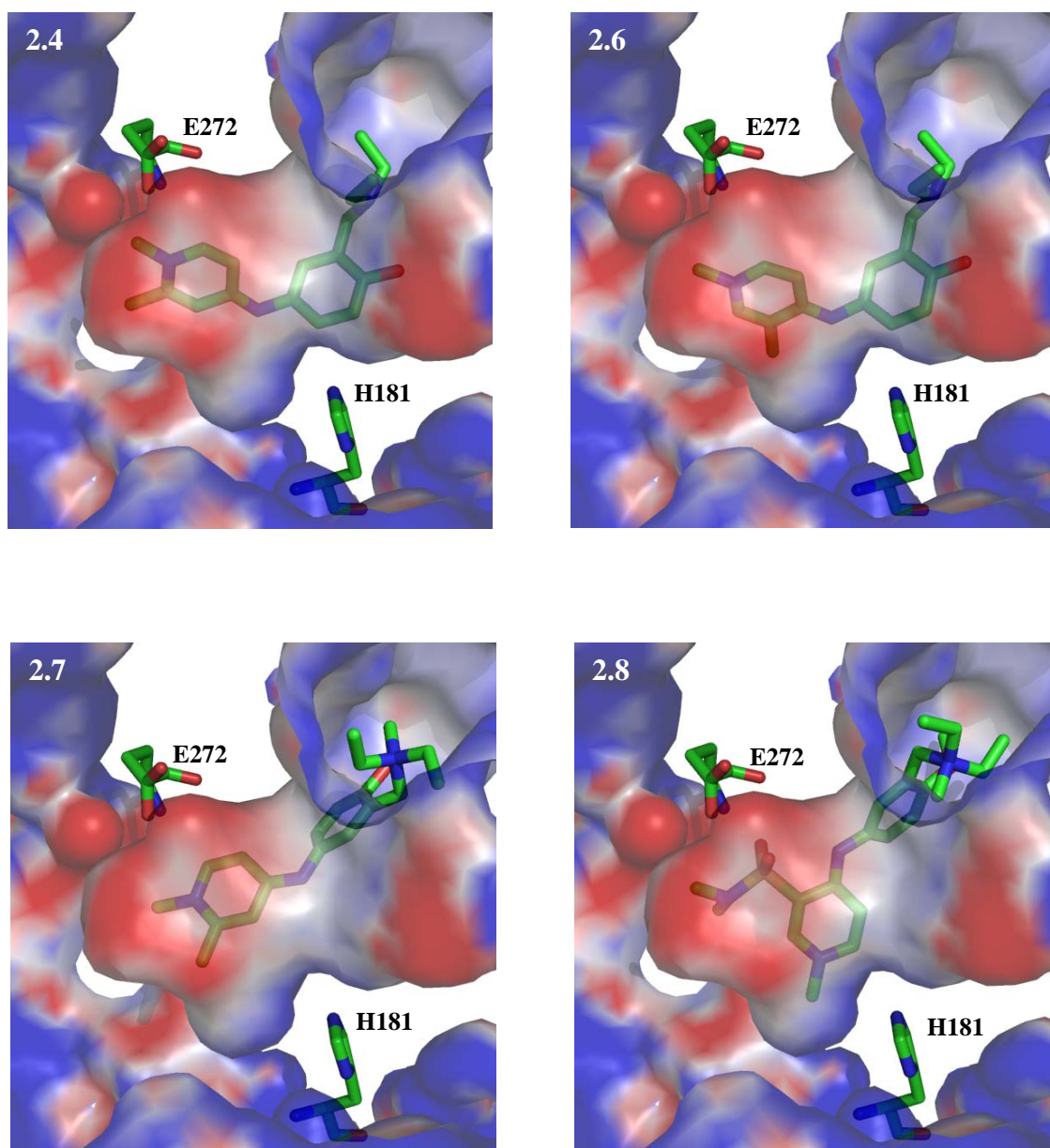


Figure A1.2 Docking poses of 2.4, 2.6-8.

Appendix 1.3 X-Ray data for compound 2.8*Crystal data*

$2 \cdot \text{C}_{21}\text{H}_{34}\text{N}_4\text{O}_3\text{S}_2^+ \cdot 4\text{I}^- \cdot 5\text{H}_2\text{O}$	$a = 12.7930(5) \text{ \AA}$
Mr = 1442.86	$b = 13.5539(6) \text{ \AA}$
Triclinic, P1	$c = 16.8386(7) \text{ \AA}$
$\alpha = 96.670(2)^\circ$	Mo $K\alpha$ radiation
$\beta = 97.667(2)^\circ$	$\mu = 2.33 \text{ mm}^{-1}$
$\gamma = 98.224(1)^\circ$	T = 100(2) K
$V = 2836.5(2) \text{ \AA}^3$	$0.35 \times 0.2 \times 0.08 \text{ mm}$
Z = 2	

Data collection

Bruker APEXII CCD	49577 measured reflections
diffractometer	11468 independent reflections
Absorption correction: multi-scan	8753 reflections with $I > 2 \sigma(I)$
(SADABS; Bruker, 2005)	$R_{\text{int}} = 0.050$
$T_{\text{min}} = 0.575, T_{\text{max}} = 0.830$	

Refinement

$R[F^2 > 2\sigma(F^2)] = 0.043$	H atoms treated by a mixture of
$wR(F^2) = 0.116$	independent and constrained
$S = 1.00$	refinement
11468 reflections	$\Delta\rho_{\text{max}} = 2.07 \text{ e \AA}^{-3}$
654 parameters	$\Delta\rho_{\text{min}} = -1.42 \text{ e \AA}^{-3}$
17 restraints	

Appendix 2

Appendix 2.1 X-Ray data for compound 3.22

Crystal data

$C_{23}H_{19}ClN_2$	$a = 13.3804(4) \text{ \AA}$
$M_r = 358.85$	$b = 9.1438(4) \text{ \AA}$
Monoclinic, $P2_1/c$	$c = 15.6064(5) \text{ \AA}$
$\alpha = 90^\circ$	Mo $K\alpha$ radiation
$\beta = 113.239(2)^\circ$	$\mu = 0.23 \text{ mm}^{-1}$
$\gamma = 90^\circ$	$T = 100(2) \text{ K}$
$V = 1754.49(10) \text{ \AA}^3$	$0.32 \times 0.1 \times 0.06 \text{ mm}$
$Z = 4$	

Data collection

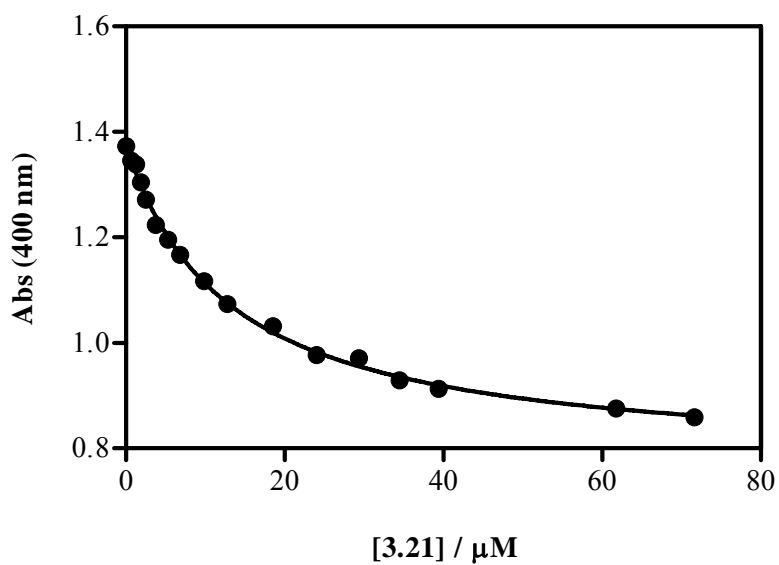
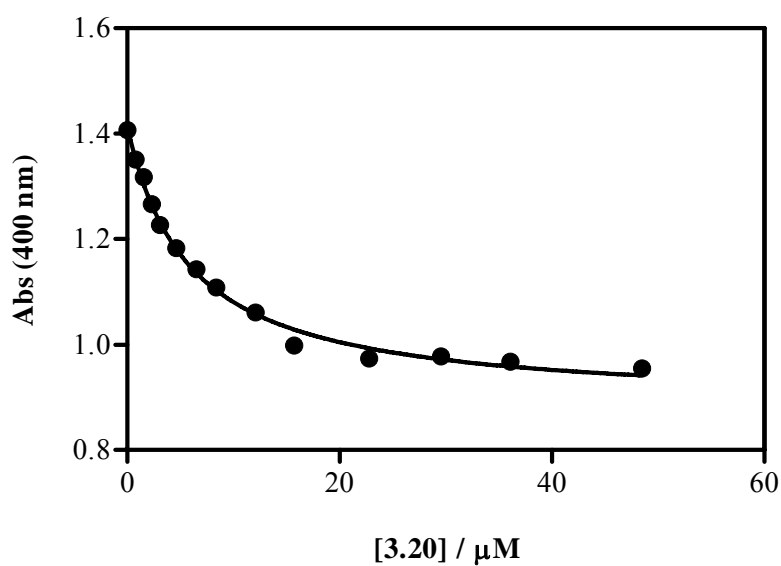
Bruker APEXII CCD	52897 measured reflections
diffractionmeter	5115 independent reflections
Absorption correction: multi-scan	3814 reflections with $I > 2 \sigma(I)$
(SADABS; Bruker, 2005)	$R_{int} = 0.059$
$T_{min} = 0.908, T_{max} = 0.986$	

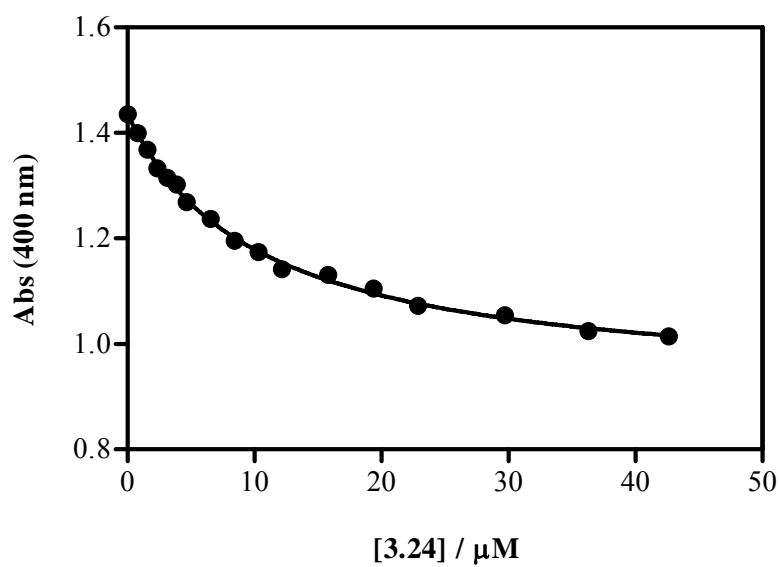
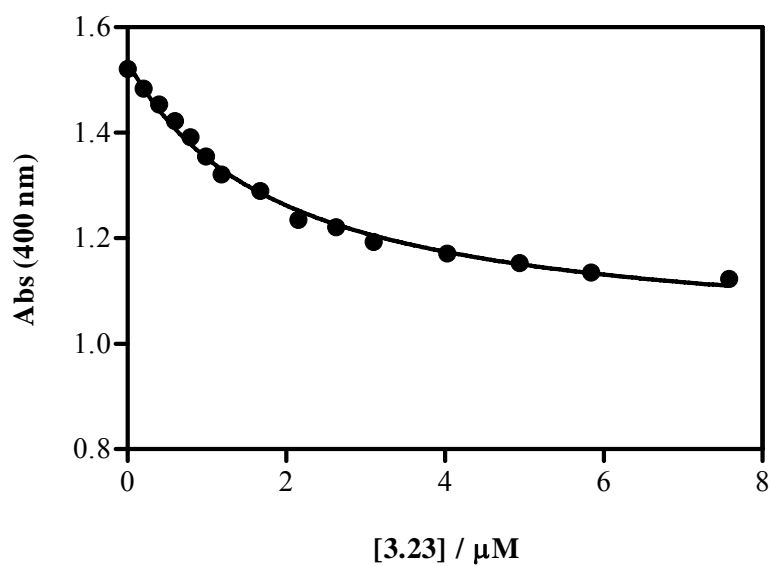
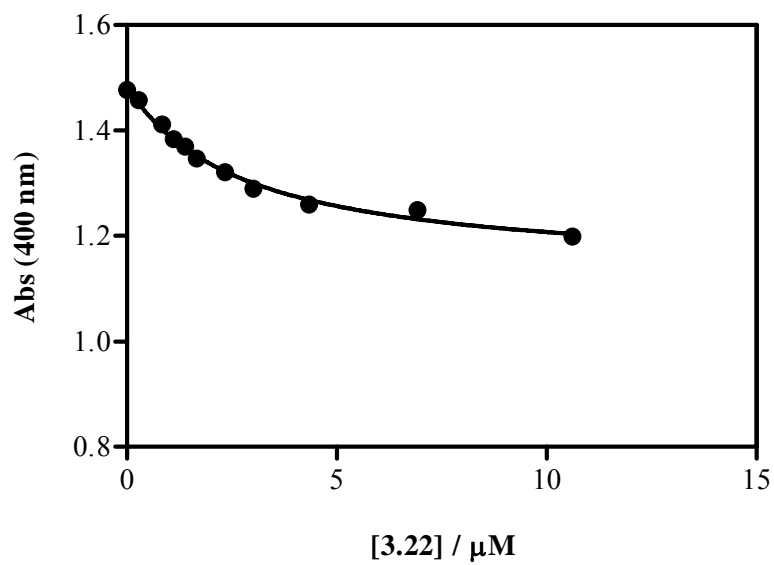
Refinement

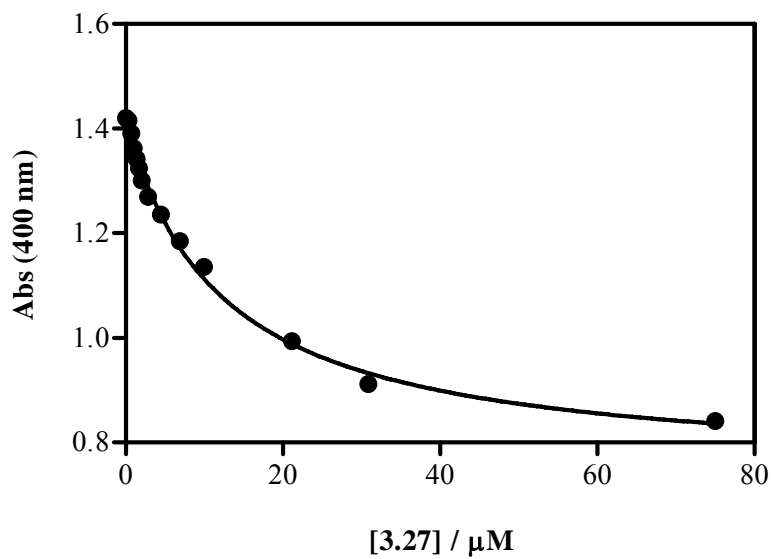
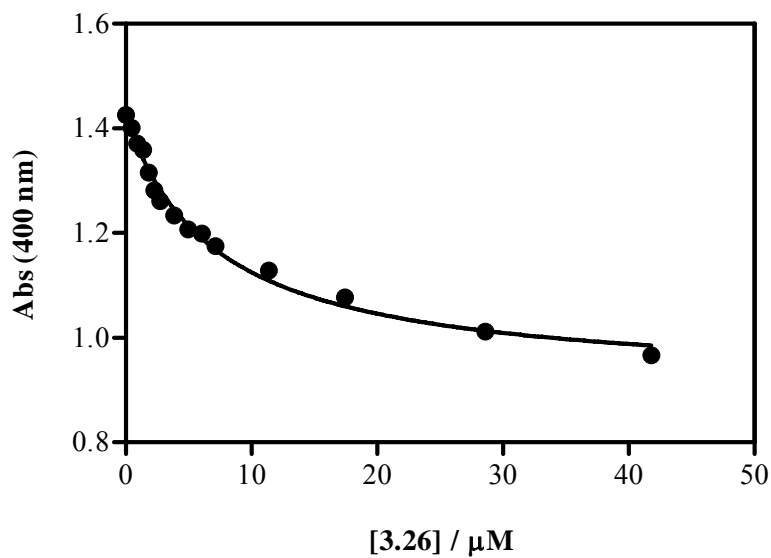
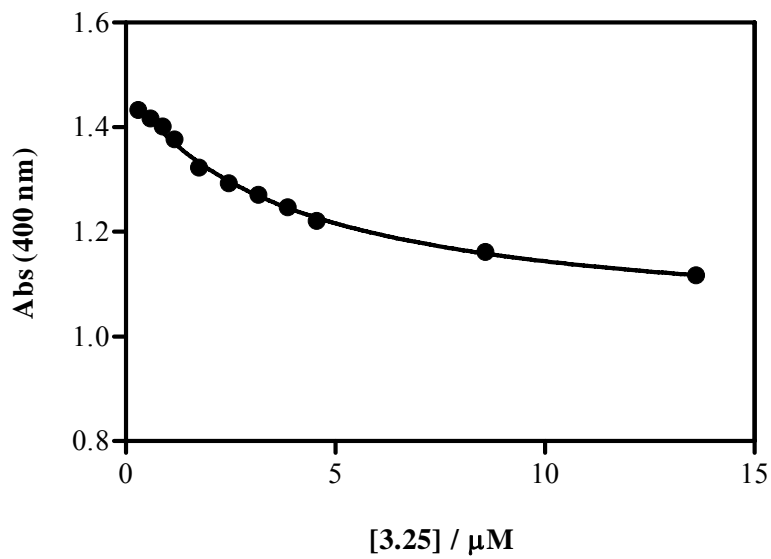
$R[F^2 > 2\sigma(F^2)] = 0.040$	H atoms parameters constrained
$wR(F^2) = 0.097$	$\Delta\rho_{max} = 0.38 \text{ e \AA}^{-3}$
$S = 1.00$	$\Delta\rho_{min} = -0.33 \text{ e \AA}^{-3}$
5115 reflections	
236 parameters	

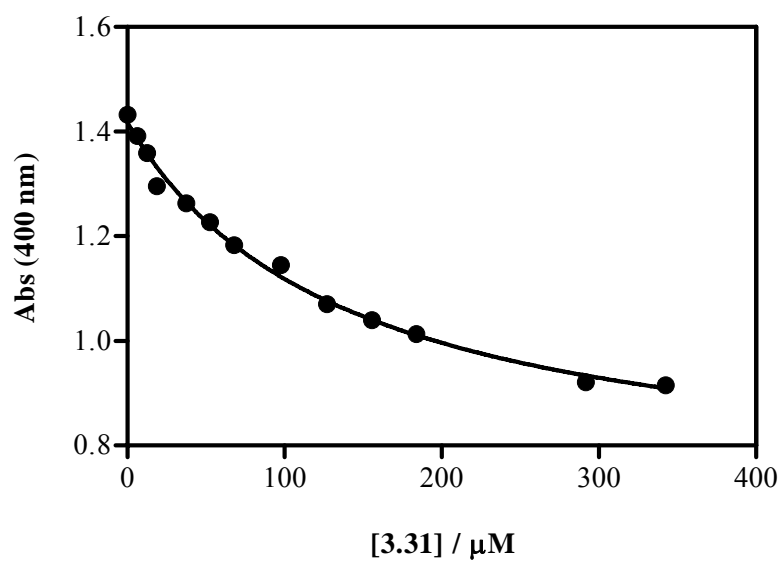
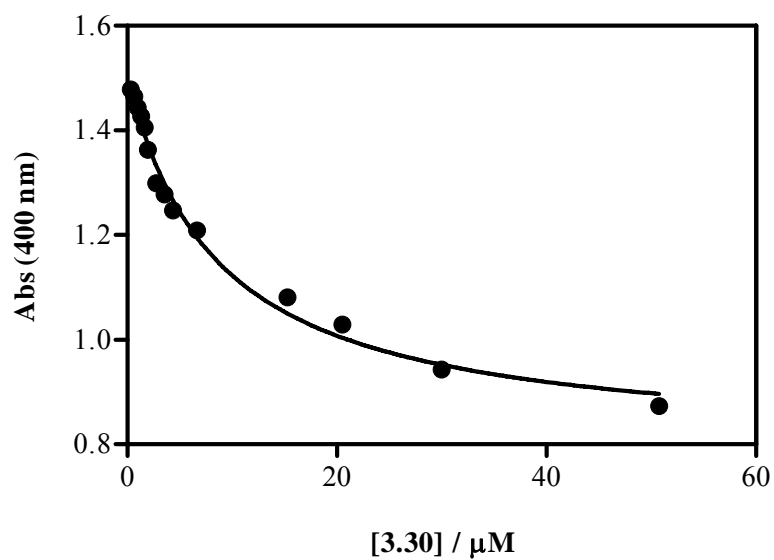
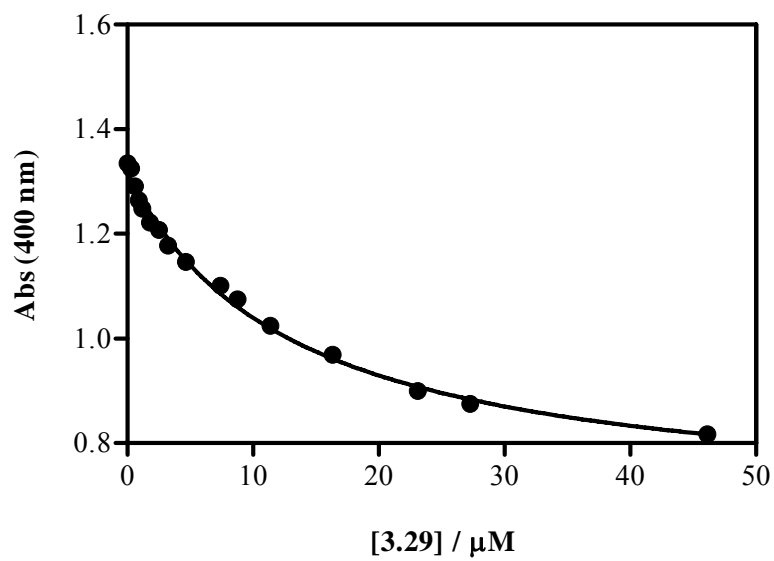
Appendix 2.2 Hematin titration with 4-quinolonimines

Titration of hematin with increasing concentrations of 4-quinolonimines (20 °C, apparent pH 5.5, HEPES buffer with 40% DMSO). The variation of absorbance of hematin at 400 nm is represented as a function of the compound concentration. The solid line represents the best fit curve for the 1:1 stoichiometry model. The curves were corrected for dilution and absorbance of the ligand at 400 nm.



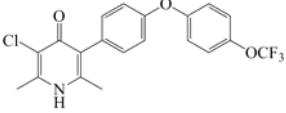
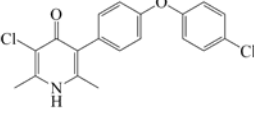
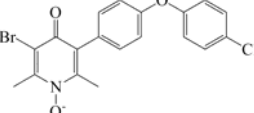
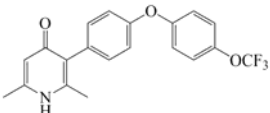
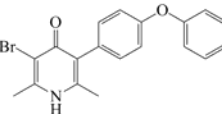
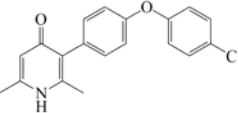
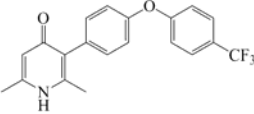
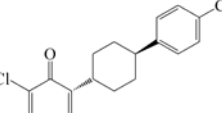
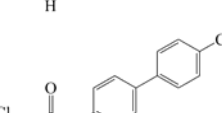
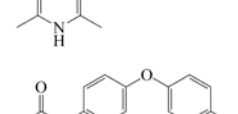
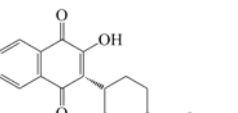




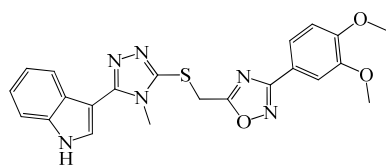


Appendix 3

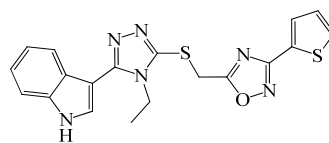
Appendix 3.1 Pharmacophore model validation, RMSD

Compound	Structure	IC ₅₀ (nM)	RMSD
1.113		30	0.4232
1.103		60	0.4799
1.125		450	0.4940
1.112		160	0.5192
1.110		150	0.5200
1.102		250	0.5390
1.107		500	0.5399
1.97		50	0.6050
1.98		40	0.6279
1.126		2,200	0.6355
1.1		3	0.8734

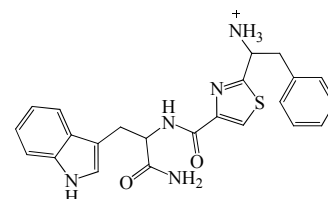
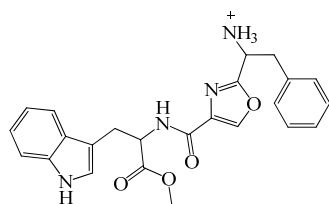
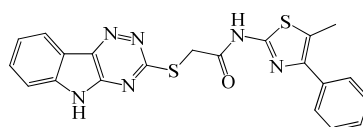
Appendix 3.2 MOE database: top 100 ligands



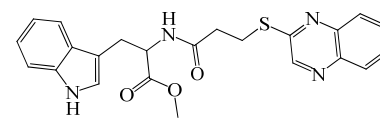
ChemBridge 7970346



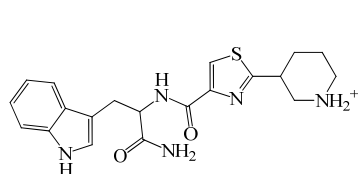
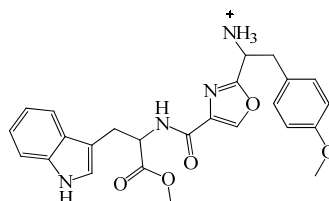
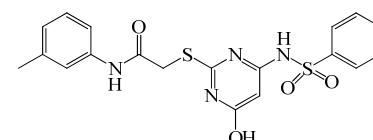
ChemBridge 7968477

EMC MicroCollections
013A0622EMC MicroCollections
009B0601

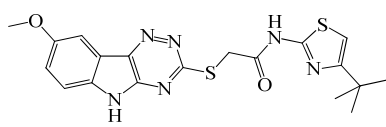
Art-Chem UZI/9122198



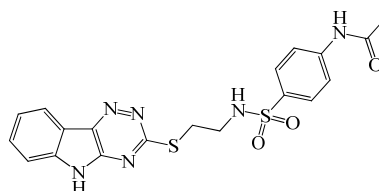
Cerep CER0145385

EMC MicroCollections
013A0628EMC MicroCollections
009B4857

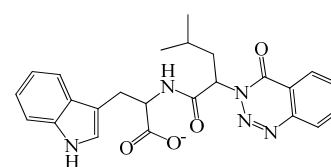
Asinex ASN 02749479



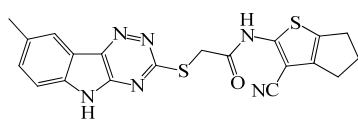
Asinex ASN 07197549



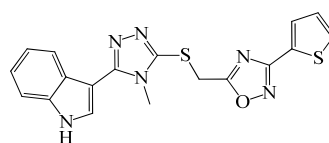
Asinex ASN 03798817



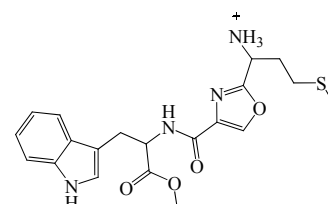
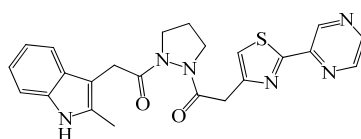
InterBioScreen STOCK5S-43288



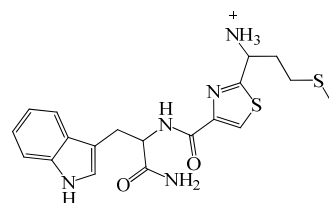
Asinex BAS 02053174



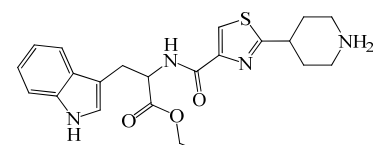
Chembridge 7950509

EMC MicroCollections
009B4832

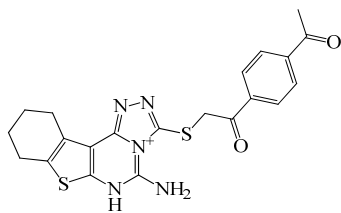
Tripos 1511-17379



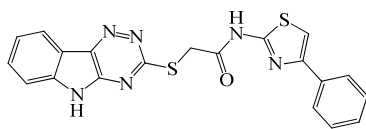
EMC MicroCollections 013A0626



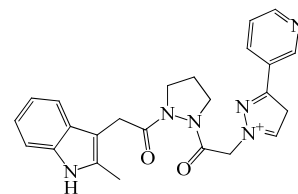
EMC MicroCollections 013A0767



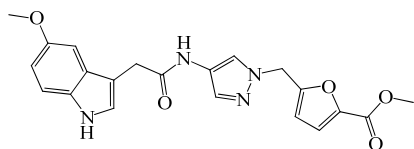
InterBioScreen STOCK4S-58358



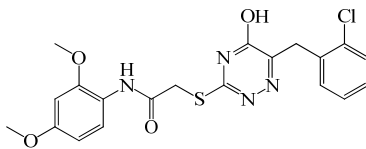
Lithuania 594407



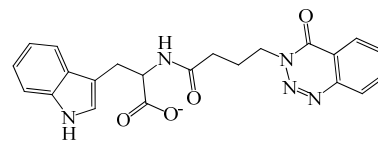
Tripos 1511-17511



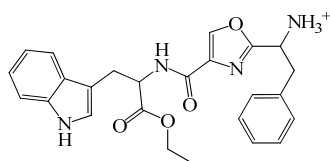
Tripos 1519-01887



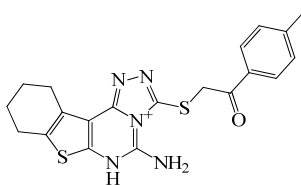
InnovaPharm STT-00186784



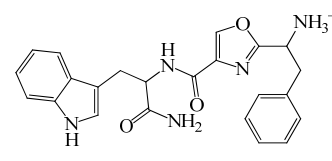
InterBioScreen STOCK5S-46555



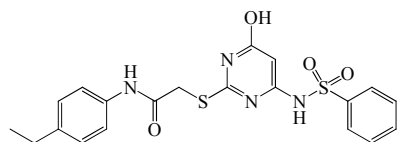
EMC Microcollections 009B0600



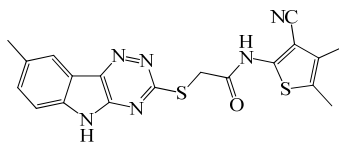
InterBioScreen STOCK4S-80261



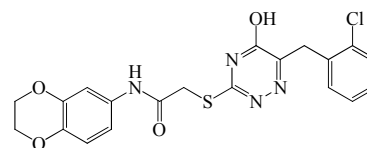
EMC Microcollections 009B2134



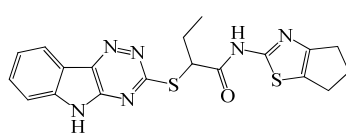
Asinex ASN 02790201



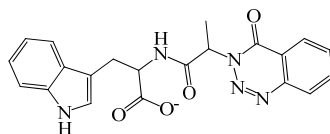
Asinex ASN 02053172



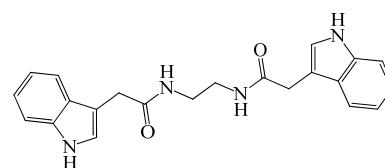
InnovaPharm STT-00186782



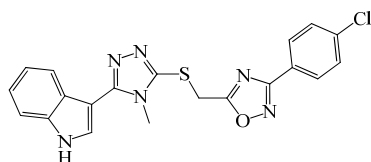
Art-Chem UZI/1736617



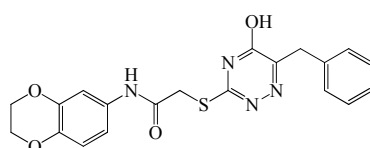
InterBioScreen STOCK5S-58077



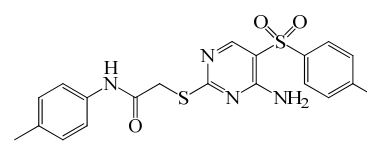
Specs AE-473/30364027



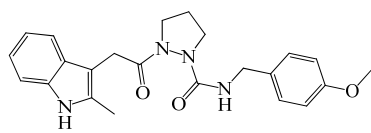
Chembridge 7963129



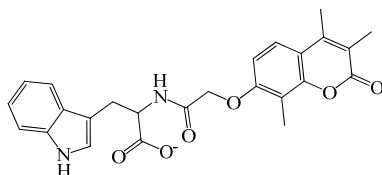
InnovaPharm STT-00186788



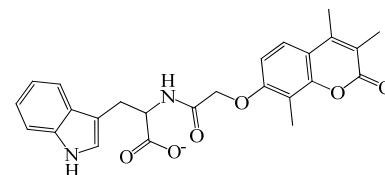
Life Chemicals F3062-0276



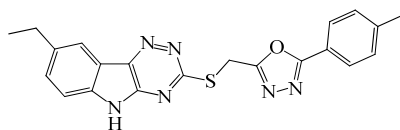
Tripos 1511-07681



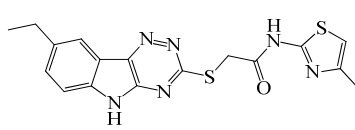
EMC Microcollections 013A0768



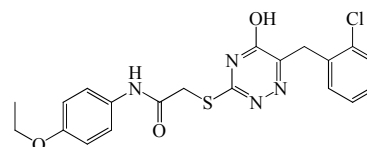
EMC Microcollections 013A0768



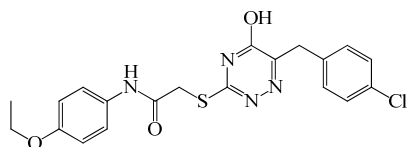
Asinex ASN 03212108



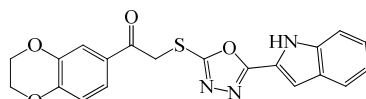
Asinex ASN 03212115



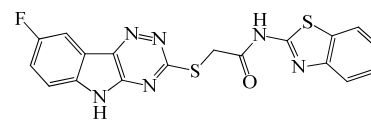
InnovaPharm STT-00186777



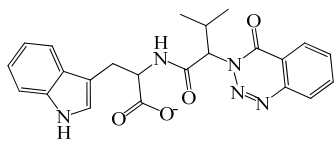
InnovaPharm STT-00186813



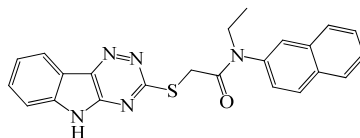
Asinex ASN 04889212



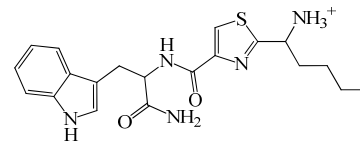
Asinex ASN 03160693



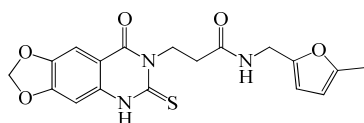
InterBioScreen STOCK5S-58971



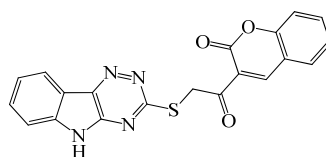
Enamine T0510-8279



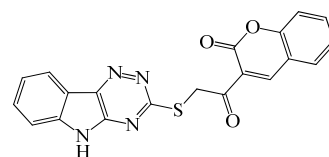
EMC Microcollections 013A0623



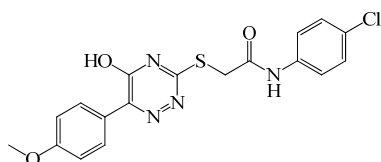
Life Chemicals F0920-6732



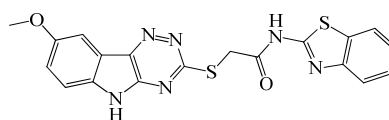
InterBioScreen STOCK5S-40792



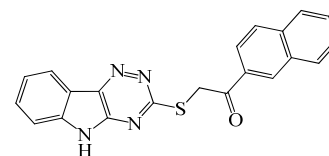
InterBioScreen STOCK5S-40792



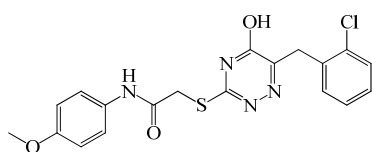
InnovaPharm STT-00186622



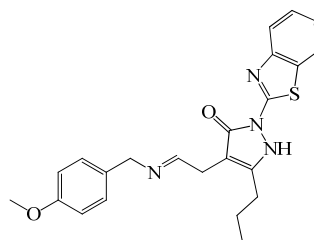
Asinex ASN 03160605



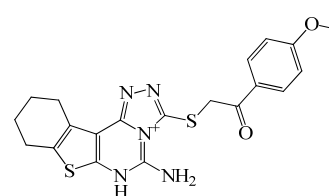
Enamine T0512-3423



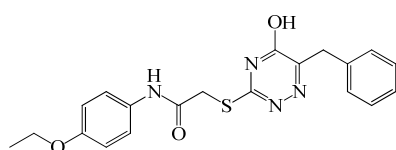
InnovaPharm STT-00186774



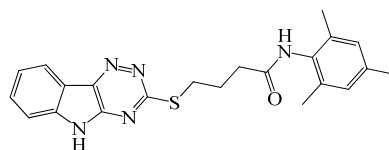
Specs AK-968/12513158



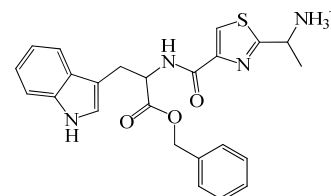
InterBioScreen STOCK4S-66444



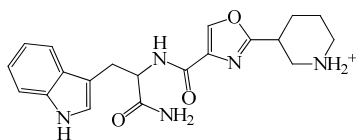
InnovaPharm STT-00186764



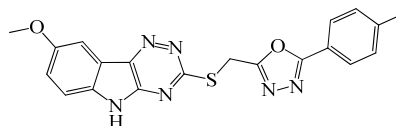
Asinex ASN 02992471



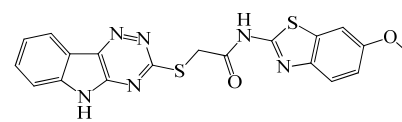
EMC Microcollections 013A0631



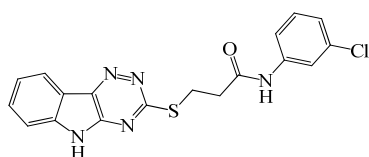
EMC Microcollections 009B2097



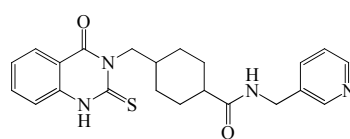
Asinex ASN 03160595



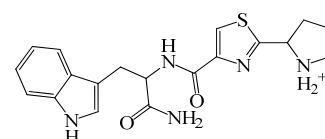
Asinex ASN 03160694



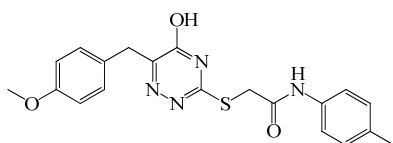
InterBioScreen STOCK5S-59598



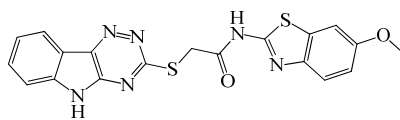
Chembridge 7758134



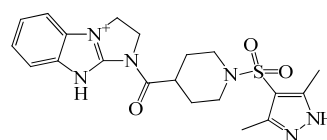
EMC Microcollections 013A0629



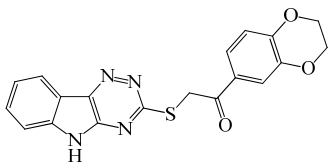
InnovaPharm STT-00186673



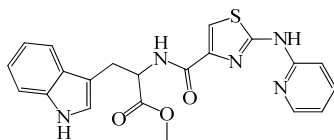
Asinex BAS 03160695



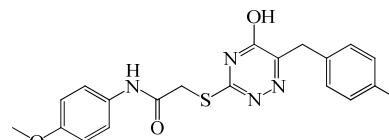
Life Chemicals F0920-6197



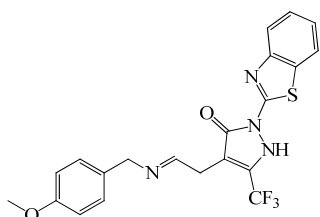
InterBioScreen STOCK5S-29891



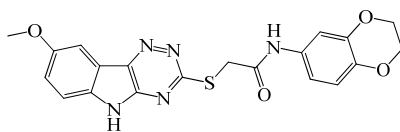
Cerep CER0147847



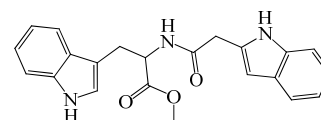
InnovaPharm STT-00186883



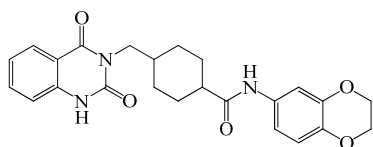
Toslab 701420



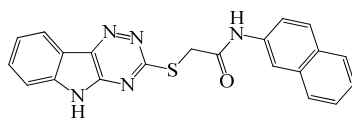
Asinex ASN 03160516



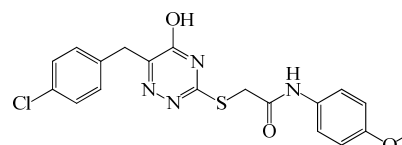
Otava 0120630216



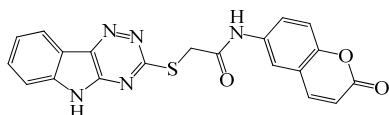
InterBioScreen STOCK5S-74052



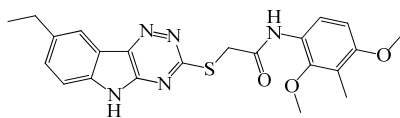
Asinex BAS 02914285



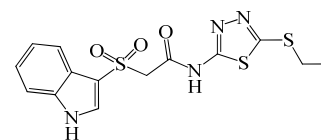
InnovaPharm STT-00186807



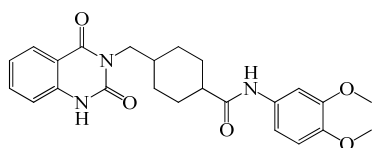
InterBioScreen STOCK5S-39753



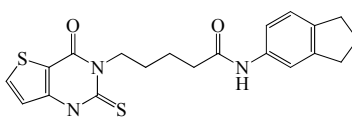
Asinex ASN 03212029



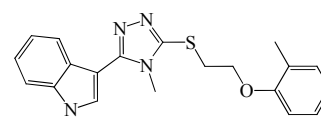
Life Chemicals F0590-0012



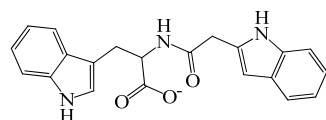
InterBioScreen STOCK5S-61476



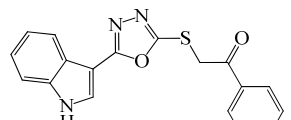
Life Chemicals F0921-6857



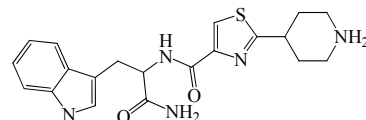
Chembridge 7969627



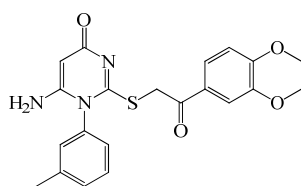
Otava 0120630217



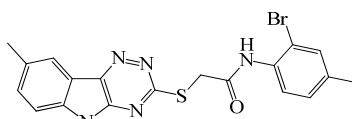
Asinex ASN 04889142



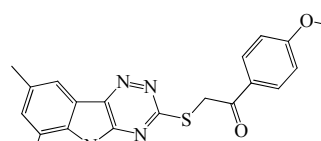
EMC Microcollections 013A0627



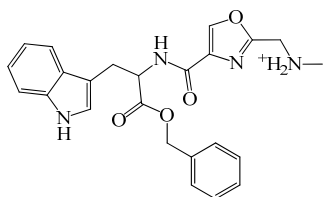
Art-Chem UZI/1727733



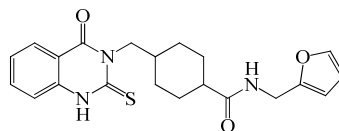
Asinex BAS 02053165



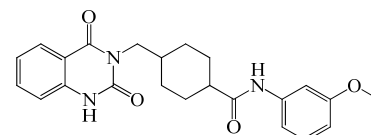
Specs AG-690/40697085



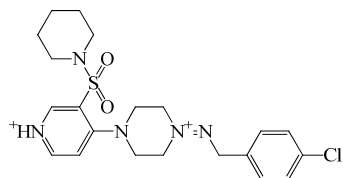
EMC Microcollections 009B4523



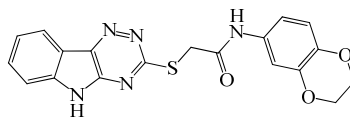
Chembridge 7755240



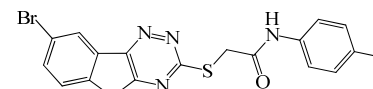
InterBioScreen STOCK5S-77798



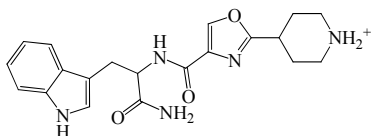
Specs AJ-333/36118051



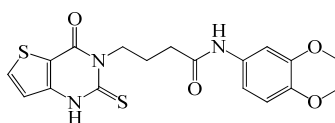
Asinex ASN 03160518



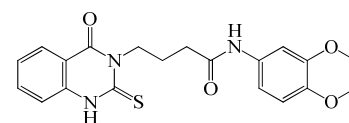
FCHC 26750



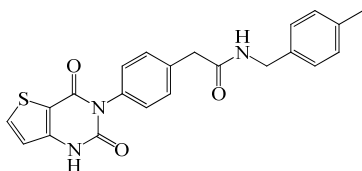
EMC Microcollections 009B2107



Life Chemicals F0921-6863

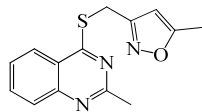


Life Chemicals F0913-3656

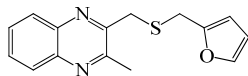


Chemdiv C172-0342

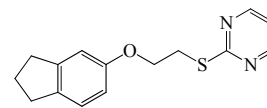
Appendix 3.3 ZINC database: top 100 ligands



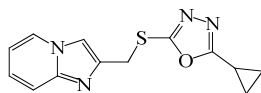
ZINC05315199



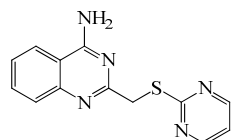
ZINC04520610



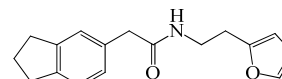
ZINC02845115



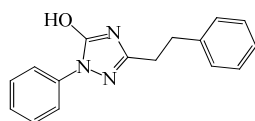
ZINC12573560



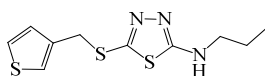
ZINC08163848



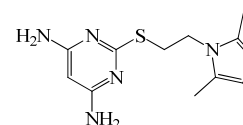
ZINC12898566



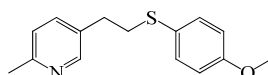
ZINC03845665



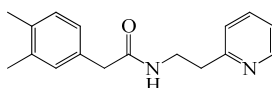
ZINC07777904



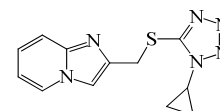
ZINC08782544



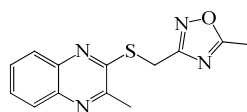
ZINC00185229



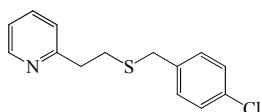
ZINC05689355



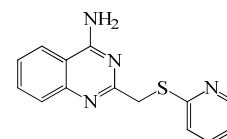
ZINC08307782



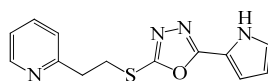
ZINC12951978



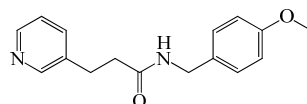
ZINC02810247



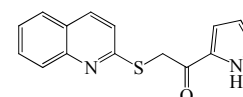
ZINC11225615



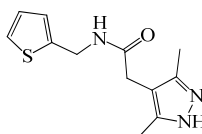
ZINC11120276



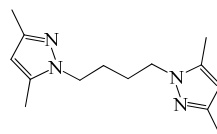
ZINC08720961



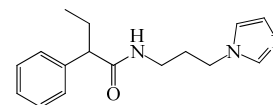
ZINC10961832



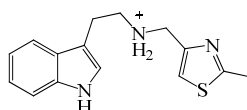
ZINC09721954



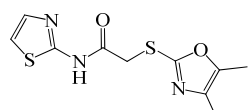
ZINC02481864



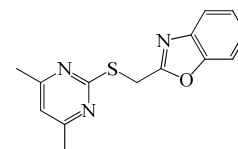
ZINC12418900



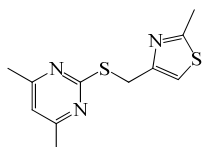
ZINC09596533



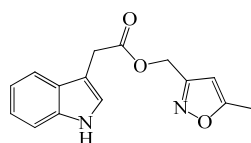
ZINC08333407



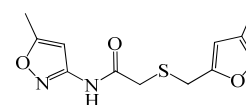
ZINC07049304



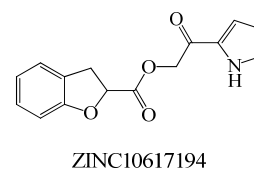
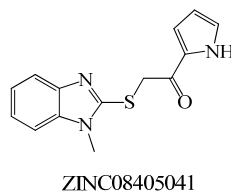
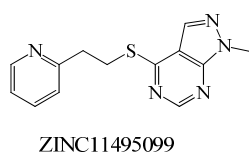
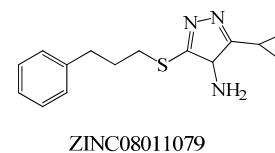
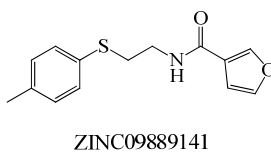
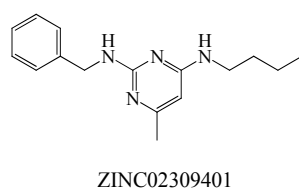
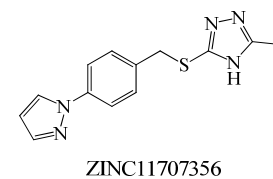
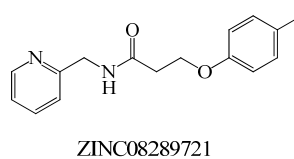
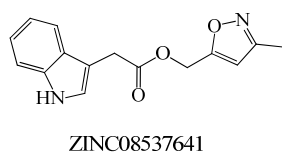
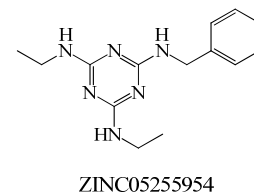
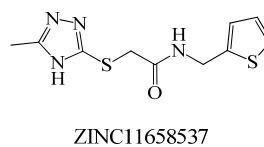
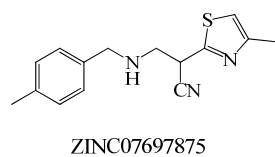
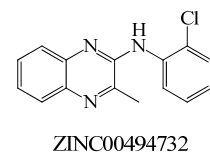
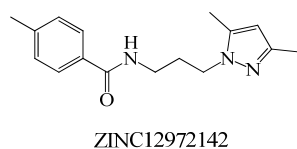
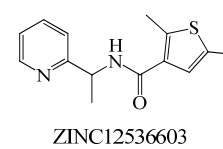
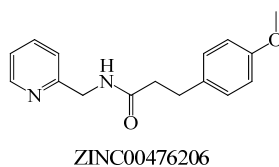
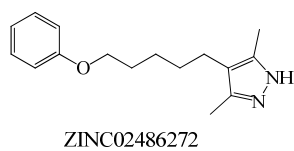
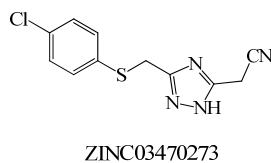
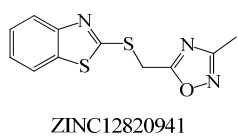
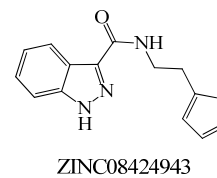
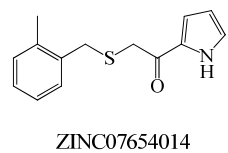
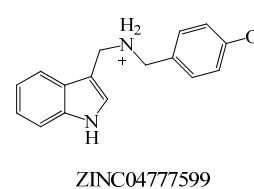
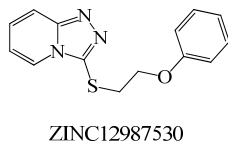
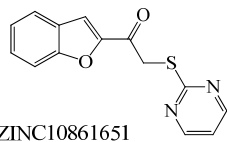
ZINC03194649

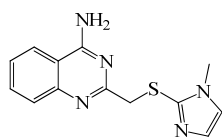


ZINC05280955

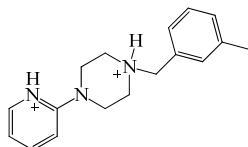


ZINC12592125

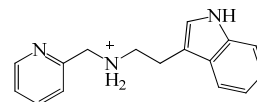




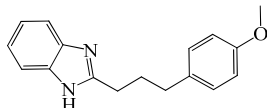
ZINC09115448



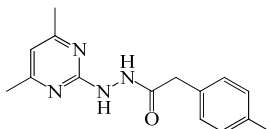
ZINC00241163



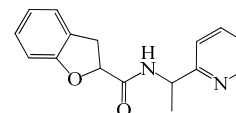
ZINC05590121



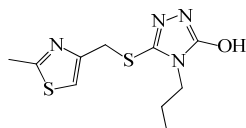
ZINC00073702



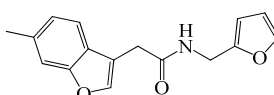
ZINC11334357



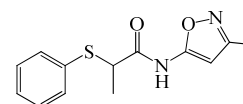
ZINC12545289



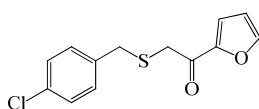
ZINC07531399



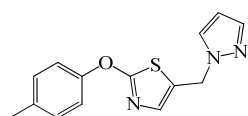
ZINC06703391



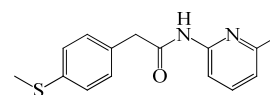
ZINC10999326



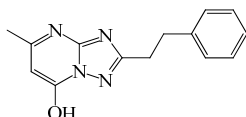
ZINC03265502



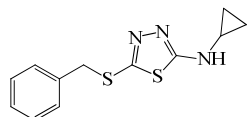
ZINC04050744



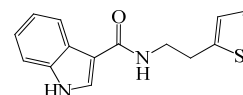
ZINC08737145



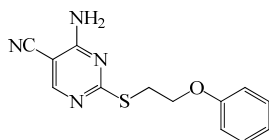
ZINC08686322



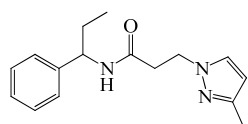
ZINC07577301



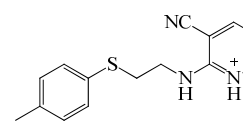
ZINC12360154



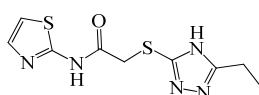
ZINC06715998



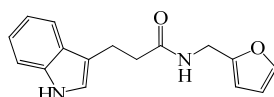
ZINC02805391



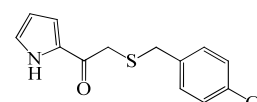
ZINC08730497



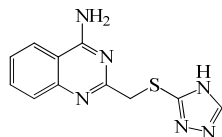
ZINC05002171



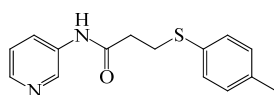
ZINC00269721



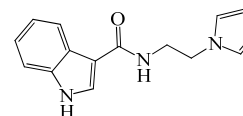
ZINC07483468



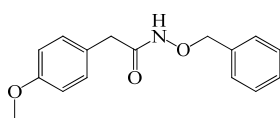
ZINC08726028



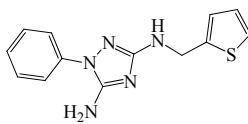
ZINC00555080



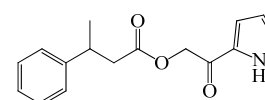
ZINC09419598



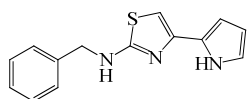
ZINC08096673



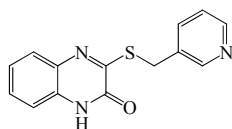
ZINC02489310



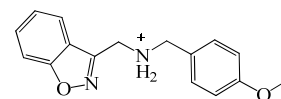
ZINC04412858



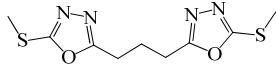
ZINC06948179



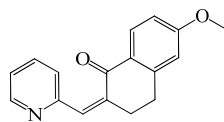
ZINC12360086



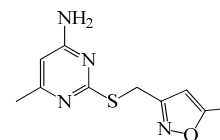
ZINC13346202



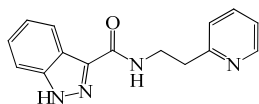
ZINC00087144



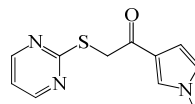
ZINC00214509



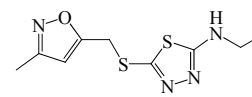
ZINC07372397



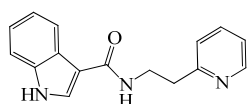
ZINC05827808



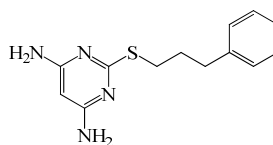
ZINC06903107



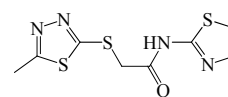
ZINC12593098



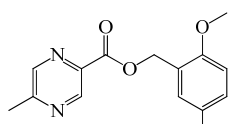
ZINC12360153



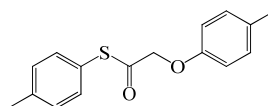
ZINC05229339



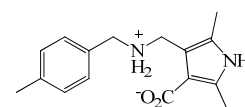
ZINC00303702



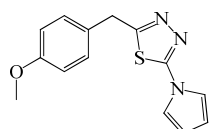
ZINC07753659



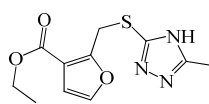
ZINC00305945



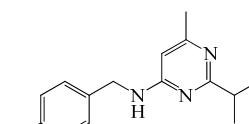
ZINC06806711



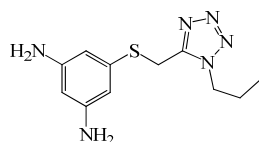
ZINC00034396



ZINC11699266



ZINC12854640



ZINC07692757

REFERENCES

- [1] Bjorkman, A.; Bhattarai, A., Public health impact of drug resistant *Plasmodium falciparum* malaria. *Acta Trop.* **2005**, *94*, 163-169.
- [2] Talisuna, A. O.; Bloland, P.; D'Alessandro, U., History, Dynamics, and Public Health Importance of Malaria Parasite Resistance. *Clin. Microbiol. Rev.* **2004**, *17*, 235–254.
- [3] WHO, World Malaria Report 2009. **2009**.
- [4] Marsh, K., Malaria disaster in Africa. *Lancet* **1998**, *352*, 924-925.
- [5] Sachs, J.; Malaney, P., The economical and social burden of malaria. *Nature* **2002**, *415*, 680-685.
- [6] Rey, L., *Parasitologia*. 3rd edition; Guanabara Koogan: 2001; p 335-348.
- [7] Wellems, T.; Plowe, C., Chloroquine-Resistant Malaria. *J. Infect. Dis.* **2001**, *184*, 770-776.
- [8] Srivastava, I. K.; Morrisey, J.; Darrouzet, E.; Daldal, F.; Vaidya, A. B., Resistance mutations reveal the atovaquone-binding domain of cytochrome *b* in malaria parasites. *Mol. Microbiol.* **1999**, *33*, 704-711.
- [9] Wu, Y.; Kickman, L.; Wellems, T., Transformation of *Plasmodium falciparum* malaria parasites by homologous integration of plasmids that confer resistance to pyrimethamine. *Proc. Natl. Acad. Sci. U.S.A.* **1996**, *93*, 1130-1134.
- [10] Triglia, T.; Wang, P.; Sims, P.; Hyde, J.; Cowman, A., Allelic exchange at the endogenous genomic locus in *Plasmodium falciparum* proves the rule of dihydropteroate synthase in sulfadoxine-resistant malaria. *EMBO J.* **1998**, *17*, 3807-3815.
- [11] Wang, C. C., Parasite Enzymes as Potential Targets for Antiparasitic Chemotherapy. *J. Med. Chem.* **1984**, *27*, 1-9.
- [12] Olliaro, P. L.; Yuthavong, Y., An Overview of Chemotherapeutic Targets for Antimalarial Drug Discovery. *Pharmacol. Ther.* **1999**, *81*, 91-110.
- [13] Mather, M. W.; Henry, K. W.; Vaidya, A. B., Mitochondrial Drug Targets in Apicomplexan Parasites. *Curr. Drug Targets* **2007**, *8*, 49-60.
- [14] Mather, M. W.; Vaidya, A. B., Mitochondria in malaria and related parasites: ancient, diverse and streamlined. *J. Bioenerg. Biomembr.* **2008**, *40*, 425-433.
- [15] Basselin, M.; Hunt, S.; Abdala-Valencia, H.; Kaneshiro, E. S., Ubiquinone Synthesis in Mitochondrial and Microsomal Subcellular Fraction of *Pneumocystis* spp.: Differential Sensitivities to Atovaquone. *Eukaryotic Cell* **2005**, *4*, 1483-1492.
- [16] Gardner, M. J.; Hall, N.; Fung, E.; White, O.; Berriman, M.; Hyman, R. W.; Carlton, J. M.; Pain, A.; Nelson, K. E.; Bowman, S.; Paulsen, I. T.; James, K.; Eisen, J. A.; Rutherford, K.; Salzberg, S. L.; Craig, A.; Kyes, S.; Chan, M.-S.; Nene, V.; Shallom, S. J.; Suh, B.; Peterson, J.; Angiuoli, S.; Pertea, M.; Allen, J.; Selengut, J.; Haft, D.; Mather, M. W.;

- Vaidya, A. B.; Martin, D. M. A.; Fairlamb, A. H.; Fraunholz, M. J.; Roos, D. S.; Ralph, S. A.; McFadden, G. I.; Cummings, L. M.; Subramanian, G. M.; Mungall, C.; Venter, J. C.; Carucci, D. J.; Hoffman, S. L.; Newbold, C.; Davis, R. W.; Fraser, C. M.; Barrell, B., Genome sequence of the human malaria parasite *Plasmodium falciparum*. *Nature* **2002**, *419*, 498-511.
- [17] Srivastava, I. K.; Rottenberg, H.; Vaidya, A. B., Atovaquone, a broad spectrum antiparasitic drug, collapses mitochondrial membrane potential in a malarial parasite. *J. Biol. Chem.* **1997**, *272*, 3961-3966.
- [18] Kongkathip, N.; Pradidphol, N.; Hasitapan, K.; Grigg, R.; Kao, W.-C.; Hunte, C.; Fisher, N.; Warman, A. J.; Biagini, G. A.; Kongsaree, P.; Chuawong, P.; Kongkathip, B., Transforming Rhinacanthin Analogues from Potent Anticancer Agents into Potent Antimalarial Agents. *J. Med. Chem.* **2010**, *53*, 1211-1221.
- [19] Yeates, C. L.; Batchelor, J. F.; Capon, E. C.; Cheesman, N. J.; Fry, M.; Hudson, A. T.; Pudney, M.; Trimming, H.; Woolven, J.; Bueno, J. M.; Chicharro, J.; Fernández, E.; Fiandor, J. M.; Gargallo-Viola, D.; Heras, F. G.; Herreros, E.; León, M. L., Synthesis and Structure–Activity Relationships of 4-Pyridones as Potential Antimalarials. *J. Med. Chem.* **2008**, *51*, 2845-2852.
- [20] Biagini, G. A.; Fisher, N.; Berry, N.; Stocks, P. A.; Meunier, B.; Williams, D. P.; Bonar-Law, R.; Bray, P. G.; Owen, A.; O'Neill, P. M.; Ward, S. A., Acridinediones: Selective and Potent Inhibitors of Malaria Parasite Mitochondrial bc_1 Complex. *Mol. Pharmacol.* **2008**, *73*, 1347-1355.
- [21] Mitchell, P., Possible molecular mechanisms of the protonmotive function of cytochrome systems. *J. Theor. Biol.* **1976**, *62*, 327-367.
- [22] Hunte, C.; Palsdottir, C.; Trumpower, B. L., Protonmotive pathways and mechanisms in the cytochrome bc_1 complex. *FEBS Lett.* **2003**, *545*, 39-46.
- [23] Eschermann, A.; Galkin, A.; Oettmeier, W.; Brandt, U.; Kerscher, S., HDQ (1-hydroxy-2-dodecyl-4-(1*H*)quinolone), a high affinity inhibitor for mitochondrial alternative NADH dehydrogenase: evidence for a ping-pong mechanism. *J. Biol. Chem.* **2005**, *280*, 3138-3142.
- [24] Suraveratum, N.; Krungkrai, S. R.; Leangaramgul, P.; Prapunwattana, P.; Krungkrai, J., Purification and characterization of *Plasmodium falciparum* succinate dehydrogenase. *Mol. Biochem. Parasit.* **2000**, *105*, 215-222.
- [25] Christopherson, R. I.; Lyons, S. D.; Wilson, P. K., Inhibitors of de Novo Nucleotide Biosynthesis as Drugs. *Acc. Chem. Res.* **2002**, *35*, 961-971.

- [26] Gutteridge, W. E.; Dave, D.; Richards, W. H., Conversion of dihydroorotate to orotate in parasitic protozoa. *Biochim. Biophys. Acta* **1979**, *582*, 390-401.
- [27] Baldwin, J.; Farajallah, A. M.; Malmquist, N. A.; Rathod, P. K.; Phillips, M. A., Malarial Dihydroorotate Dehydrogenase. *J. Biol. Chem.* **2002**, *277*, 41827-41834.
- [28] Painter, H. J.; Morrissey, J. M.; Mather, M. W.; Vaidya, A. B., Specific role of mitochondrial electron transport in blood-stage *Plasmodium falciparum*. *Nature* **2007**, *446*, 88-91.
- [29] Schütz, M.; Brugna, M.; Lebrun, E.; Baymann, F.; Huber, R.; Stetter, K.-O.; Hauska, G.; Toci, R.; Lemesle-Meunier, D.; Tron, P.; Schmidt, C.; Nitschke, W., Early Evolution of Cytochrome *bc* Complexes. *J. Mol. Biol.* **2000**, *300*, 663-675.
- [30] Meunier, D. L.; Brivet-Chevillotte, P.; Rago, J. P. d.; Slonimski, P. P.; Bruel, C.; Tron, T.; Forget, N., Cytochrome *b*-deficient Mutants of the Ubiquinol-cytochrome *c* Oxidoreductase in *Saccharomyces cerevisiae*. *J. Biol. Chem.* **1993**, *268*, 15626-15632.
- [31] Gao, X.; Wen, X.; Yu, C.; Esser, L.; Tsao, S.; Quinn, B.; Zhang, L.; Yu, L.; Xia, D., The Crystal Structure of Mitochondrial Cytochrome *bc*₁ in Complex with Famoxadone: The Role of Aromatic-Aromatic Interaction in Inhibition. *Biochemistry* **2002**, *41*, 11692-11702.
- [32] Darrouzet, E.; Valkova-Valchanova, M.; Moser, C. C.; Dutton, P. M.; Daldal, F., Uncovering the [2Fe2S] domain movement in cytochrome *bc*₁ and its implications for energy conversion. *Proc. Natl. Acad. Sci. USA* **2000**, *97*, 4567-4572.
- [33] Fisher, N.; Bourges, I.; Hill, P.; Brasseur, G.; Meunier, B., Disruption of the interaction between the Rieske iron-sulfur protein and cytochrome *b* in the yeast *bc*₁ complex owing to a human disease associated mutation within cytochrome *b*. *Eur. J. Biochem.* **2004**, *271*, 1292-1298.
- [34] Brandt, U.; Haase, U.; Schägger, H.; von Jagow, G., Significance of the "Rieske" Iron-Sulfur Protein for Formation and Function of the Ubiquinol-Oxidation Pocket of Mitochondrial Cytochrome *c* Reductase (*bc*₁ Complex). *J. Biol. Chem.* **1991**, *266*, 19958-19964.
- [35] Kim, H.; Xia, D.; Yu, C.-A.; Xia, J.-Z.; Kachurin, A. M.; Zhang, L.; Yu, L.; Deizenhofer, J., Inhibitor binding changes domain mobility in the iron-sulfur protein in the mitochondrial *bc*₁ complex from bovine heart. *Proc. Natl. Acad. Sci. USA* **1998**, *95*, 8026-8033.
- [36] Crofts, A. R.; Lhee, S.; Crofts, S. B.; Cheng, J.; Rose, S., Proton pumping in the *bc*₁ complex: A new gating mechanism that prevents short circuits. *Biochim. Biophys. Acta* **2006**, *1757*, 1019-1034.
- [37] Moser, C. C.; Farid, T. A.; Chobot, S. E.; Dutton, P. L., Electron tunneling chains of mitochondria. *Biochim. Biophys. Acta* **2006**, *1757*, 1096-1109.

- [38] Trumpower, B. L., A concerted, alternating sites mechanism of ubiquinol oxidation by the dimeric cytochrome *bc*₁ complex. *Biochim. Biophys. Acta* **2002**, *1555*, 166-173.
- [39] Zhang, Z.; Huang, L.; Shulmeister, V. M.; Chi, Y.-I.; Kim, K. K.; Hung, L. W.; Crofts, A. R.; Berry, E. A.; Kim, S. H., Electron transfer by domain movement in cytochrome *bc*₁. *Nature* **1998**, *392*, 677-684.
- [40] Vaidya, A. B., Mitochondrial and plastid functions as antimalarial drug targets. *Curr. Drug Targets* **2004**, *4*, 11-23.
- [41] Hunte, C.; Koepke, J.; Lange, C.; Rossmann, T.; Michel, H., Structure at 2.3 Å resolution of the cytochrome *bc*₁ complex from the yeast *Saccharomyces cerevisiae* co-crystallized with an antibody Fv fragment. *Structure* **2000**, *8*, 669-684.
- [42] Esser, L.; Quinn, B.; Li, Y.-F.; Zhang, M.; Elberry, M.; Yu, L.; Yu, C.-A.; Xia, D., Crystallographic Studies of Quinol Oxidation Site Inhibitors: A Modified Classification of Inhibitors for the Cytochrome *bc*₁ Complex. *J. Mol. Biol.* **2004**, *341*, 281-302.
- [43] Lange, C.; Hunte, C., Crystal structure of the yeast cytochrome *bc*₁ complex with its bound substrate cytochrome *c*. *Proc. Natl. Acad. Sci. USA* **2003**, *99*, 2800-2805.
- [44] Solmaz, S. R. N.; Hunte, C., Structure of complex III with bound cytochrome *c* in reduced state and definition of a minimal core interface for electron transfer. *J. Biol. Chem.* **2008**, *283*, 17542-17549.
- [45] Palsdottir, H.; Lojero, C. G.; Trumpower, B.; Hunte, C., Structure of the Yeast Cytochrome *bc*₁ Complex with a Hydroxyquinone Anion Q_o Site Inhibitor Bound. *J. Biol. Chem.* **2003**, *278*, 31303-31311.
- [46] DeLano, W. L., *The PyMol Molecular Graphics System*, DeLano Scientific: Palo Alto, CA, USA.
- [47] von Jagow, G.; Link, T. A., Use of Specific Inhibitors on the Mitochondrial *bc*₁ Complex. *Method Enzymol.* **1986**, *126*, 253-271.
- [48] Fry, M.; Pudney, M., Site of action of the antimalarial hydroxynaphthoquinone, 2-[trans-4-(4'-chlorophenyl)cyclohexyl]-3-hydroxy-1,4-naphthoquinone (566C80). *Biochem. Pharmacol.* **1992**, *43*, 1545-53.
- [49] Mather, M. W.; Darrouzet, E.; Valkova-Valchanova, M.; Cooley, J. W.; McIntosh, M. T.; Daldal, F.; Vaidya, A. B., Uncovering the Molecular Mode of Action of the Antimalarial Drug Atovaquone Using a Bacterial System. *J. Biol. Chem.* **2005**, *280*, 27458-27465.
- [50] Krungkrai, J.; Krungkrai, S. R.; Suraveratum, N.; Prapunwattana, P., Mitochondrial Ubiquinol-Cytochrome *c* Reductase and Cytochrome *c* Oxidase: Chemotherapeutic Targets in Malarial Parasites. *Biochem. Mol. Biol. Inter.* **1997**, *42*, 1007-1014.

- [51] Wichmann, O.; Muehlberger, N.; Jelinek, T.; Alifrangis, M.; Peyerl-Hoffmann, G.; Mühlen, M.; Grobusch, M. P.; Gascon, J.; Matteelli, A.; Laferl, H.; Bisoffi, Z.; Ehrhardt, S.; Cuadros, J.; Hatz, C.; Gjørup, I.; McWhinney, P.; Beran, J.; Cunha, S. d.; Schulze, M.; Kollaritsch, H.; Kern, P.; Fry, G.; Richter, J., Screening for Mutations Related to Atovaquone/Proguanil Resistance in Treatment Failures and Other Imported Isolates of *Plasmodium falciparum* in Europe. *J. Infect. Dis.* **2004**, *190*, 1541-1546.
- [52] Kessl, J. J.; Ha, K. H.; Merritt, A. K.; Lange, B. B.; Hill, P.; Meunier, B.; Meshnick, S. R.; Trumpower, B. L., Cytochrome *b* Mutations That Modify the Ubiquinol-binding Pocket of the Cytochrome *bc*₁ Complex and Confer Anti-malarial Drug Resistance in *Saccharomyces cerevisiae*. *J. Biol. Chem.* **2005**, *280*, 17142-17148.
- [53] Siregar, J. E.; Syafruddin, D.; Matsuoka, H.; Kita, K.; Marzuki, S., Mutation underlying resistance of *Plasmodium berghei* to atovaquone in the quinone binding domain 2 (Q_o2) of the cytochrome *b* gene. *Parasitol. Int.* **2008**, *57*, 229-232.
- [54] Schwöbel, B.; Alifrangis, M.; Salanti, A.; Jelinek, T., Different mutation of atovaquone resistance to *Plasmodium falciparum* *in vitro* and *in vivo*: rapid detection of codon 268 polymorphisms in the cytochrome *b* as potential *in vivo* resistance marker. *Malaria J.* **2003**, *2*, 5-11.
- [55] Syafruddin, D.; Siregar, J. E.; Marzuki, S., Mutations in the cytochrome *b* gene of *Plasmodium berghei* conferring resistance to atovaquone. *Mol. Biochem. Parasitol.* **1999**, *104*, 185-194.
- [56] Fisher, N.; Meunier, B., Molecular basis of resistance to cytochrome *bc*₁ inhibitors. *FEMS Yeast Res.* **2008**, *8*, 183-192.
- [57] Peters, J. M.; Chen, N.; Gatton, M.; Korsinczky, M.; Fowler, E. V.; Manzetti, S.; Saul, A.; Cheng, Q., Mutations in Cytochrome *b* Resulting in Atovaquone Resistance Are Associated with Loss of Fitness in *Plasmodium falciparum*. *Antimicrob. Agents Chemother.* **2002**, *46*, 2435-2441.
- [58] Kessl, J. J.; Lange, B. B.; Merbitz-Zahradnik, T.; Zwicker, K.; Hill, P.; Meunier, B.; Pálsdóttir, H.; Hunte, C.; Meshnick, S.; Trumpower, B. L., Molecular Basis for Atovaquone Binding to the Cytochrome *bc*₁ Complex. *J. Biol. Chem.* **2003**, *278*, 31312-31318.
- [59] Kessl, J. J.; Moskalev, N. V.; Bribble, G. W.; Nasr, M.; Meshnick, S. R.; Trumpower, B. L., Parameters determining the relative efficacy of hydroxynaphthoquinone inhibitors of the cytochrome *bc*₁ complex. *Biochim. Biophys. Acta* **2007**, *1767*, 319-326.

- [60] Kessler, J. J.; Hill, P.; Lange, B. B.; Meshnick, S. R.; Meunier, B.; Trumpower, B., Molecular Basis for Atovaquone Resistance in *Pneumocystis jirovecii* Modeled in the Cytochrome *bc*₁ complex of *Saccharomyces cerevisiae*. *J. Biol. Chem.* **2004**, *279*, 2817-2824.
- [61] Kessler, J. J.; Meshnick, S. R.; Trumpower, B. L., Modeling the molecular basis of atovaquone resistance in parasites and pathogenic fungi. *Trends Parasitol.* **2007**, *23*, 494-501.
- [62] Korsinczky, M.; Chen, N.; Kotecka, B.; Saul, A.; Rieckmann, K.; Cheng, Q., Mutations in *Plasmodium falciparum* Cytochrome *b* That Are Associated with Atovaquone Resistance Are Located at a Putative Drug-Binding Site. *Antimicrob. Agents Chemother.* **2000**, *44*, 2100-2108.
- [63] Ritter, M.; Palsdottir, H.; Abe, M.; Mäntele, W.; Hunte, C.; Miyoshi, H.; Hellwig, P., Direct Evidence for the Interaction of Stigmatellin with a Protonated Acidic Group in the *bc*₁ Complex from *Saccharomyces cerevisiae* as Monitored by FTIR Difference Spectroscopy and ¹³C Specific Labelling. *Biochemistry* **2004**, *43*, 8439-8446.
- [64] Suswam, E.; Kyle, D.; Lang-Unnasch, N., *Plasmodium falciparum*: The Effects of Atovaquone Resistance on Respiration. *Exp. Parasitol.* **2001**, *98*, 180-187.
- [65] Canfield, C. J.; Pudney, M.; Gutteridge, W. E., Interactions of Atovaquone with Other Antimalarial Drugs against *Plasmodium falciparum* *in Vitro*. *Exp. Parasitol.* **1995**, *80*, 373-381.
- [66] Fleck, S. L.; Pudney, M.; Sinden, R. E., The effect of atovaquone (566C80) on the maturation and viability of *Plasmodium falciparum* gametocytes *in vitro*. *T. Roy. Soc. Trop. Med. H.* **1996**, *90*, 309-312.
- [67] Latter, V. S.; Hudson, A. T.; Richards, W. H. G.; Randall, A. W., Antiprotozoal Agents. USP 5,053,418, **1991**.
- [68] Fieser, L. F.; Richardson, A. P., Naphthoquinone Antimalarials. II. Correlation of Structure and Activity Against *P. lophurae* in Ducks. *J. Am. Chem. Soc.* **1948**, *70*, 3156-3165.
- [69] Fieser, L. F.; Brown, R. H., Naphthoquinone Antimalarials. XXIII. Bz-Substituted Derivatives. *J. Am. Chem. Soc.* **1949**, *71*, 3615-3617.
- [70] Fieser, L. F.; Berlinger, E.; Bondhus, F. J.; Chang, F. C.; Dauben, W. G.; Ettliger, M. G.; Fawaz, G.; Fields, M.; Fieser, M.; Heidelberger, C.; Heymann, H.; Seligman, A. M.; Vaughan, W. R.; Wilson, A. G.; Wilson, E.; Wu, M.-I.; Leffler, M. T.; Hamlin, K. E.; Hathaway, R. J.; Matson, E. J.; Moore, E. E.; Moore, M. B.; Rapala, R. T.; Zaugg, H. E., Naphthoquinone Antimalarials. I. General Survey. *J. Am. Chem. Soc.* **1948**, *70*, 3151-3155.

- [71] Moser, C. M.; Paulshock, M., Naphthoquinone Antimalarials. XXVI. Thioether Naphthoquinones. *J. Am. Chem. Soc.* **1950**, *72*, 5419-5423.
- [72] Heymann, H.; Fieser, L. F., Naphthoquinone Antimalarials. XXI. Antisuccinate Oxidase Activity. *J. Biol. Chem.* **1948**, *176*, 1359-1362.
- [73] Hughes, L. M.; Covian, R.; Gribble, G. W.; Trumpower, B. L., Probing binding determinants in centre P of the cytochrome *bc₁* complex using novel hydroxy-naphthoquinones. *Biochim. Biophys. Acta* **2010**, *1797*, 38-43.
- [74] Paulshock, M.; Moser, C. M., Naphthoquinone Antimalarials. XXV. Naphthoquinones with Oxygen in the Side Chain. *J. Am. Chem. Soc.* **1950**, *72*, 5073-5077.
- [75] Fawaz, G.; Fieser, L. F., Naphthoquinone Antimalarials. XXIV. A New Synthesis of Lapinone. *J. Am. Chem. Soc.* **1950**, *72*, 996-1000.
- [76] Fieser, L. F.; Heymann, H., Naphthoquinone Antimalarials XXII. Relative Antirespiratory Activities (*Plasmodium lophurae*). *J. Biol. Chem.* **1948**, *176*, 1363-1370.
- [77] Fieser, L. F.; Nazer, M. Z., Naphthoquinone Antimalarials. XXX. 2-Hydroxy-3-[ω -(1-adamantyl)alkyl]-1,4-naphthoquinones. *J. Med. Chem.* **1967**, *10*, 517-521.
- [78] Fieser, L. F.; Pfaffenbach, J. P., Naphthoquinone Antimalarials. XXIX. 2-Hydroxy-3-(ω -cyclohexylalkyl)-1,4-naphthoquinones. *J. Med. Chem.* **1967**, *10*, 513-17.
- [79] Prescott, B., Potential Antimalarial Agents. Derivatives of 2-Chloro-1,4-naphthoquinone. *J. Med. Chem.* **1969**, *12*, 181-182.
- [80] Boehm, P.; Cooper, K.; Hudson, A. T.; Elphick, J. P.; McHardy, N., *In vitro* activity of 2-alkyl-3-hydroxy-1,4-naphthoquinones against *Theileria parva*. *J. Med. Chem.* **1981**, *24*, 295-299.
- [81] Schlitzer, M., Malaria Chemotherapeutics Part I: History of Antimalarial Drug Development, Currently Used Therapeutics, and Drugs in Clinical Development. *ChemMedChem* **2007**, *2*, 944-986.
- [82] Hudson, A. T.; Randall, A. W.; Fry, M.; Ginger, C. D.; Hill, B.; Latter, V. S.; McHardy, N.; Williams, R. B., Novel anti-malarial hydroxynaphthoquinones with potent broad spectrum anti-protozoal activity. *Parasitology* **1985**, *90*, 45-55.
- [83] Hudson, A. T.; Yeates, C. L., 1,4-Naphthoquinone derivatives with anti-protozoal and anti-parasitic activity. WO 93/20044, **1993**.
- [84] Hudson, A. T., Naphthoquinone derivatives for the treatment of parasitic infections. WO 93/07156, **1993**.
- [85] Khambay, B. P. S.; Simmonds, M. S. J., Use of naphthoquinone compounds as antiprotozoal agents. WO 97/18800, **1997**.

- [86] Weiss, C. R.; Moideen, S. V. K.; Croft, S. L.; Houghton, P. J., Activity of Extracts and Isolated Naphthoquinones from *Kigelia pinnata* against *Plasmodium falciparum*. *J. Nat. Prod.* **2000**, *63*, 1306-1309.
- [87] Zani, C. L.; Chiari, E.; Krettli, A. U.; Murta, S. M. F.; Cunningham, M. L.; Fairlamb, A. H.; Romana, A. J., Anti-Plasmodial and Anti-Trypanosomal Activity of Synthetic Naphtho[2,3-*b*]thiophen-4,9-quinones. *Bioorg. Med. Chem.* **1997**, *5*, 2185-2192.
- [88] Kapadia, G. J.; Azuine, M. A.; Balasubramanian, V.; Sridhar, R., Aminonaphthoquinones - A Novel Class of Compounds with Potent Antimalarial Activity Against *Plasmodium falciparum*. *Pharmacol. Res.* **2001**, *43*, 363-367.
- [89] Baramée, A.; Coppin, A.; Mortuaire, M.; Pelinski, L.; Tomavo, S.; Brocard, J., Synthesis and *in vitro* activities of ferrocenic aminohydroxynaphthoquinones against *Toxoplasma gondii* and *Plasmodium falciparum*. *Bioorg. Med. Chem.* **2006**, *14*, 1294-1302.
- [90] Price, C. C.; Jackson, W. G., Synthesis of 4-Hydroxyquinolines. VII. 3-(Di-*n*-butylaminomethyl)-7-methoxy-2-methyl-4-quinolinol. *J. Am. Chem. Soc.* **1946**, *68*, 1282-1283.
- [91] Baker, R. H.; Dodson, R. M., The Synthesis of 3-(3-Cyclohexylpropyl)-4-quinolinol. *J. Am. Chem. Soc.* **1946**, *68*, 1283-1284.
- [92] Hermans, B.; Janssen, M.; Verhoeven, H.; Knaeps, A.; Offenwert, T. V.; Mostmans, J.; Willems, J.; Maes, B.; Vanparijis, O., Structure and Anticoccidial Activity of a New Series of 4-Hydroxyquinoline-3-carboxylates. *J. Med. Chem.* **1973**, *16*, 1047-1050.
- [93] Puri, S. K.; Dutta, G. P., Quinoline esters as potential antimalarial drugs: effect on relapses of *Plasmodium cynomolgi* infections in monkeys. *T. Roy. Soc. Trop. Med. H.* **1990**, *84*, 759-760.
- [94] Burckhalter, J. H.; Mikolasek, D. G., Antimalarial Agents. IX. 3-Alkylquinolones as Potential Repository Drugs. *J. Pharm. Sci.* **1967**, *56*, 236-239.
- [95] Kyle, D. E.; Gerena, L.; Pitzer, K.; Gettyacamin, M., Antimalarial Activity of 4(1*H*)-Quinolones. *Am. J. Trop. Med. Hyg.* **2005**, *73*, 147.
- [96] Casey, A. C., 4(1*H*)-Quinolones. 2. Antimalarial Effect of Some 2-Methyl-3-(1'-alkenyl)- or -3-alkyl-4(1*H*)-quinolones. *J. Med. Chem.* **1974**, *17*, 255-256.
- [97] Casey, A. C. *Synthesis of some 4-quinolones and related structures for evaluation as potential antimalarial agents*; Bridgeport University: Bridgeport, CT, 30 November 1974, 1974; pp 1-45.

- [98] Bhattacharjee, A. K.; Gerena, L.; Gettyacamin, M.; Pitzer, K.; Milhous, W. K.; Kyle, D. E., *In silico* pharmacophore for antimalarial activity of the 4(1*H*)-quinolones to aid discovery of novel causal prophylactic drug candidates. *Am. J. Trop. Med. Hyg.* **2007**, *77*, 144.
- [99] Winter, R. W.; Kelly, J. X.; Smilkstein, M. J.; Dodean, R.; Hinrichs, D.; Riscoe, M. K., Antimalarial quinolones: Synthesis, potency, and mechanistic studies. *Exp. Parasitol.* **2008**, *118*, 487–497.
- [100] Winter, R. W.; Kelly, J.; Smilkstein, M.; Dodean, R.; Bagby, G.; Rathbun, R.; Levin, J.; Hinrichs, D.; Riscoe, M., Evaluation and lead optimization of antimalarial acridones. *Exp. Parasitol.* **2006**, *114*, 47-56.
- [101] Basco, L. K.; Mitaku, S.; Skaltsounis, A.-L.; Ravelomanantsoa, N.; Tillequin, F.; Koch, M.; Bras, J. L., *In Vitro* Activities of Furoquinoline and Acridone Alkaloids against *Plasmodium falciparum*. *Antimicrob. Agents Chemother.* **1994**, *38*, 1169-1171.
- [102] Schmidt, L. H., Antimalarial Properties of Floxacrine, a Dihydroacridinedione Derivative. *Antimicrob. Agents Chemother.* **1979**, *16*, 475-485.
- [103] Berman, J.; Brown, L.; Miller, R.; Andersen, S. L.; McGreevy, P.; Schuster, B. G.; Ellis, W.; Ager, A.; Rossan, R., Antimalarial Activity of WR 243251, a Dihydroacridinedione. *Antimicrob. Agents Chemother.* **1994**, *38*, 1753-1756.
- [104] Werbel, L. L., 7-Chloro-3-substituted aryl-3,4-dihydro-1,9(2*H*,10*H*) and 10-hydroxy acridinedioneimines having antimalarial activity. USP 4,291,034, **1981**.
- [105] Davidson, D. E.; Ager, A. L.; Brown, J. L.; Chapple, F. E.; Whitmire, R. E.; Rossan, R. E., New tissue schizonticidal antimalarial drugs. *Bull. World Health Organ.* **1981**, *59*, 463-479.
- [106] Dorn, A.; Scovill, J. P.; Ellis, W. Y.; Matile, H.; Ridley, R. G.; Vennerstrom, J. L., Short Report: Floxacrine Analog WR 243251 Inhibits Hematin Polymerization. *Am. J. Trop. Med. Hyg.* **2001**, *65*, 19-20.
- [107] Kesten, S. J.; Degman, M. J.; Hung, J.; McNamara, D. J.; Ortwine, D. F.; Uhlendorf, S. E.; Werbel, L. M., Antimalarial Drugs. 64. Synthesis and Antimalarial Properties of 1-Imino Derivatives of 7-Chloro-3-substituted-3,4-dihydro-1,9(2*H*,10*H*)-acridinediones and Related Structures. *J. Med. Chem.* **1992**, *35*, 3429-3447.
- [108] Markley, L.; Van Heertum, J.; Doorenbos, H., Antimalarial Activity of Clopidol, 3,5-dichloro-2,6-dimethyl-4-pyridinol, and Its Esters, Carbonates, and Sulfonates. *J. Med. Chem.* **1972**, *15*, 1188-1189.
- [109] Fry, M.; Williams, R. B., Effects of Decoquinatate and Clopidol on Electron Transport in Mitochondria of *Eimeria tenella* (Apicomplexa: Coccidia). *Biochem. Pharmacol.* **1984**, *33*, 229-240.

- [110] Markley, L.; Eckman, M., Synthesis and Anticoccidial Activity of 3-fluoro-5-chloro- and -bromo-2,6-dimethyl-4-pyridinol. *J. Med. Chem.* **1973**, *16*, 297-298.
- [111] Bathurst, I.; Hentschel, C., Medicines for Malaria Venture: sustaining antimalarial drug development. *Trends Parasitol.* **2006**, *22*, 301-307.
- [112] Biagini, G. A.; O'Neill, P. M.; Bray, P. G.; Ward, S. A., Current drug development portfolio for antimalarial therapies. *Curr. Opin. Pharmacol.* **2005**, *5*, 473-478.
- [113] Batchelor, J. F.; Yeates, C. L., Heterocyclic compounds. WO 91/13873, **1991**.
- [114] Improved murine model of malaria using *P. falciparum* competent strains and non-myelodepleted NOD-*scid* *IL2R γ* ^{null} mice engrafted with human erythrocytes. *Antimicrob. Agents Chemother.* **2009**, *53*, 4533-4536.
- [115] Xiang, H.; Mcsurdy-Freed, J.; Moorthy, G. S.; Hugger, E.; Bambal, R.; Han, C.; Ferrer, S.; Gargallo, D.; Davis, C. B., Preclinical drug metabolism and pharmacokinetic evaluation of GW844520, a novel anti-malarial mitochondrial electron transport inhibitor *J. Pharm. Sci.* **2006**, *95*, 2657-2672.
- [116] Almela, M. J.; Torres, P. A.; Lozano, S.; Herreros, E., Characterization of the phospholipidogenic potential of 4(1*H*)-pyridone antimalarial derivatives. *Toxicol. in Vitro* **2009**, *23*, 1528-1534.
- [117] Ferrer, S.; Garcia, A.; Jiménez-Díaz, B.; Rodriguez, B.; Romanos, E.; Mulet, T.; Viera, S.; Gómez, V.; Angulo-Barturen, I.; Parrowe, H.; Xiang, H.; Davis, C.; Gómez-de-las-Heras, F.; Pompliano, D.; Gargallo, D., Comparative Multi-Dose Pharmacokinetic Modelling and Determination of Non-Recrudescence Level for *Plasmodium yoelli* infection in Mouse of Antimalarial 4(1*H*)-Pyridones. *Am. J. Trop. Med. Hyg.* **2006**, *75*, 155.
- [118] Roman, J. M. F.; Calderon, J. M. B.; Rubio, A. M., Novel Heterocyclic Compounds. WO 2006/094799, **2006**.
- [119] Calderon, J. M. B.; Gonzalo, J. C.; Garcia, M. L.; Chinchon, M. P. M., Novel Heterocyclic Compounds. WO 2007/138048, **2007**.
- [120] MMV in <http://www.mmv.org/research-development/project-portfolio>, accessed 14th July 2010.
- [121] Zheng, Y.-J., Molecular basis for the enantioselective binding of a novel class of cytochrome *bc*₁ complex inhibitors. *J. Mol. Graph. Model.* **2006**, *25*, 71-76.
- [122] Roberts, A. G.; Bowman, M. K.; Kramer, D. M., The Inhibitor DBMIB Provides Insight into the Functional Architecture of the Q_o Site in the Cytochrome *b₆f* Complex. *Biochemistry* **2004**, *43*, 7707-7716.

- [123] Fisher, N.; Brown, A. C.; Sexton, G.; Cook, A.; Windass, J.; Meunier, B., Modeling the Q_o site of crop pathogens in *Saccharomyces cerevisiae* cytochrome *b*. *Eur. J. Biochem.* **2004**, *271*, 2264-2271.
- [124] Uchiro, H.; Nagasawa, K.; Sawa, T.; Hasegawa, D.; Kotake, T.; Sugiura, Y.; Kobayashi, S.; Ootogurob, K.; Omura, S., Remarkable Influence of the Aromatic Substructure in 9-Methoxystrobilurin Derivatives on their Antifungal Activity. *Bioorg. Med. Chem. Lett.* **2002**, *12*, 2699-2702.
- [125] Brandt, U.; Djafarzadeh-Andababili, R., Binding of MOA-stilbene to the mitochondrial cytochrome *bc*₁ complex is affected by the protonation state of a redox-Bohr group of the 'Rieske' iron-sulfur protein. *Biochim. Biophys. Acta* **1997**, *1321*, 238-242.
- [126] Zheng, Y.-J.; Shapiro, R.; Marshall, W. J.; Jordan, D. B., Synthesis and Structural Analysis of the Active Enantiomer of Famoxadone, a Potent Inhibitor of Cytochrome *bc*₁. *Bioorg. Med. Chem. Lett.* **2000**, *10*, 1059-1062.
- [127] Chen, H.; Taylor, J. L.; Abrams, S. R., Design and synthesis of β -methoxyacrylate analogues via click chemistry and biological evaluations. *Bioorg. Med. Chem. Lett.* **2007**, *17*, 1979-1983.
- [128] Brandt, U.; Schagger, H.; von Jagow, G., Characterisation of binding of the methoxyacrylate inhibitors to mitochondrial cytochrome *c* reductase *Eur. J. Biochem.* **1988**, *173*, 499-506.
- [129] Pember, S. O.; Fleck, L. C.; Moberg, W. K.; Walker, M. P., Mechanistic differences in inhibition of ubiquinol cytochrome *c* reductase by the proximal Q_o-site inhibitors famoxadone and methoxyacrylate stilbene. *Arch. Biochem. Biophys.* **2005**, *435*, 280-290.
- [130] Alzeer, J.; Chollet, J.; Matile, H.; Ridley, R. G., β -Alkoxyacrylate against malaria. WO 99/02150, **1999**.
- [131] Alzeer, J.; Chollet, J.; Heinze-Krauss, I.; Hubschwerlen, C.; Matile, H.; Ridley, R. G., Phenyl β -Methoxyacrylates: A New Antimalarial Pharmacophore. *J. Med. Chem.* **2000**, *43*, 560-568.
- [132] Liu, M.; Wilairat, P.; Go, M.-L., Antimalarial Alkoxyated and Hydroxylated Chalcones: Structure-Activity Relationship Analysis. *J. Med. Chem.* **2001**, *44*, 4443-4452.
- [133] Liu, M.; Wilairat, P.; Croft, S. L.; Tand, A. L.-C.; Goa, M.-L., Structure-Activity Relationships of Antileishmanial and Antimalarial Chalcones. *Bioorg. Med. Chem.* **2003**, *11*, 2729-2738.
- [134] Gutteridge, C. E.; Nichols, D. A.; Curtis, S. M.; Thota, D. S.; Vo, J. V.; Gerena, L.; Montip, G.; Asher, C. O.; Diaz, D. S.; DiTusa, C. A.; Smith, K. S.; Bhattacharjee, A. K., *In vitro* and

- in vivo* efficacy and *in vitro* metabolism of 1-phenyl-3-aryl-2-propen-1-ones against *Plasmodium falciparum*. *Bioorg. Med. Chem. Lett.* **2006**, *16*, 5682-5686.
- [135] Gutteridge, C. E.; Vo, J. V.; Tillett, C. B.; Vigilante, J. A.; Dettmer, J. R.; Patterson, S. L.; Werbovets, K. A.; Capers, J.; Nichols, D. A.; Bhattacharjee, A. K.; Gerena, L., Antileishmanial and Antimalarial Chalcones: Synthesis, Efficacy and Cytotoxicity of Pyridinyl and Naphthalenyl Analogs. *Med. Chem.* **2007**, *3*, 115-119.
- [136] Narender, T.; Shweta; Tanvir, K.; Rao, M. S.; Srivastava, K.; Puri, S. K., Prenylated chalcones isolated from *Crotalaria* genus inhibits *in vitro* growth of the human malaria parasite *Plasmodium falciparum*. *Bioorg. Med. Chem. Lett.* **2005**, *15*, 2453-2455.
- [137] Go, M.-L., Novel Antiplasmodial Agents. *Med. Res. Rev.* **2003**, *23*, 456-487.
- [138] Valla, A.; Valla, B.; Cartier, D.; Guillou, R. L.; Labia, R.; Florent, L.; Charneau, S.; Schrevel, J.; Potier, P., New syntheses and potential antimalarial activities of new 'retinoid-like chalcones'. *Eur. J. Med. Chem.* **2006**, *41*, 142-146.
- [139] Nowakowska, Z., A review of anti-infective and anti-inflammatory chalcones. *Eur. J. Med. Chem.* **2007**, *42*, 125-137.
- [140] Kita, K.; Shiomi, K.; Omura, S., Advances in drug discovery and biochemical studies. *Trends Parasitol.* **2007**, *23*, 223-229.
- [141] Charris, J. E.; Lobo, G. M.; Camacho, J.; Ferrer, R.; Barazarte, A.; Domínguez, J. N.; Gamboa, N.; Rodrigues, J. R.; Angel, J. E., Synthesis and Antimalarial Activity of (*E*)-2-(2'-Chloro-3'-Quinolinylmethylidene)-5,7-Dimethoxyindanones. *Lett. Drug Des. Discov.* **2007**, *4*, 49-54.
- [142] Zhai, L.; Blom, J.; Chen, M.; Christensen, S. B.; Kharazmi, A., The Antileishmanial Agent Licochalcone A Interferes with the Function of Parasite Mitochondria. *Antimicrob. Agents Chemother.* **1995**, *39*, 2742-2748.
- [143] Domínguez, J. N.; Charris, J. E.; Lobo, G.; Domínguez, N. G. d.; Moreno, M. M.; Riggione, F.; Sanchez, E.; Olson, J.; Rosenthal, P. J., Synthesis of quinolinyl chalcones and evaluation of their antimalarial activity. *Eur. J. Med. Chem.* **2001**, *36*, 555-560.
- [144] Mi-Ichi, F.; Miyadera, H.; Kobayashi, T.; Takamiya, S.; Waki, S.; Iwata, S.; Shibata, S.; Kita, K., Parasite Mitochondria as a Target of Chemotherapy: Inhibitory Effect of Licochalcone A on the *Plasmodium falciparum* Respiratory Chain. *Ann. N.Y. Acad. Sci.* **2005**, *1056*, 46-54.
- [145] Vaidya, A. B.; Lashgari, M. S.; Pologe, L. G.; Morrissey, J., Structural features of *Plasmodium falciparum* cytochrome *b* that may underlie susceptibility to 8-aminoquinolines and hydroxynaphthoquinones. *Mol. Biochem. Parasit.* **1993**, *58*, 33-43.

- [146] Elderfield, R. C.; Kupchan, S. M.; Rosenberg, C. C., The Effect of Pamaquin on the Oxygen Consumption of Liver Slices. *J. Am. Chem. Soc.* **1949**, *71*, 1915-1916.
- [147] Skelton, F. S.; Pardini, R. S.; Heidker, J. C.; Folkers, K., Coenzyme Q. CVIII. Inhibition of coenzyme Q systems by chloroquine and other antimalarials. *J. Am. Chem. Soc.* **1968**, *90*, 5334-5336.
- [148] Ball, M. D.; Bartlett, M. S.; Shaw, M.; Smith, J. W.; Nasr, M.; Meshnick, S. R., Activities and Conformational Fitting of 1,4-Naphthoquinone Derivatives and Other Cyclic 1,4-Diones Tested *In Vitro* against *Pneumocystis carinii*. *Antimicrob. Agents Chemother.* **2001**, *45*.
- [149] Vale, N.; Moreira, R.; Gomes, P., Primaquine revisited six decades after its discovery. *Eur. J. Med. Chem.* **2009**, *44*, 937-953.
- [150] Dueñas-Romero, A. M.; Loiseau, P. M.; Saint-Pierre-Chazalet, M., Interaction of sitamaquine with membrane lipids of *Leishmania donovani* promastigotes. *Biochim. Biophys. Acta* **2007**, *1768*, 246-252.
- [151] Elderfield, R. C.; Kremer, C. B.; Kupchan, S. M.; Birstein, O.; Cortes, G., Synthesis of Certain 8-(5-Alkylamino-1-methylpentylamino)-Derivatives of Quinoline. *J. Am. Chem. Soc.* **1947**, *69*, 1258-1260.
- [152] Wetter, W. P.; Jr., C. D. B., 8-(ω -Aminoalkylamino)quinolines as potential prophylactic antimalarials. *J. Med. Chem.* **1974**, *17*, 620-624.
- [153] Carroll, F. I.; Berrang, B.; Linn, C. P.; Charles E. Twine, J., Synthesis of Some 4-Substituted 8-Amino-6-methoxyquinolines as Potential Antimalarials. *J. Med. Chem.* **1979**, *22*, 694-699.
- [154] Carroll, F. I.; Berrang, B. D.; Linn, C. P., Synthesis of 2,4-Disubstituted 6-Methoxy-8-aminoquinoline analogues as Potential Antiparasitics. *J. Med. Chem.* **1980**, *23*, 581-584.
- [155] Carroll, F. I.; Berrang, B. D.; Linn, C. P., 4,5-Disubstituted primaquine analogues as potential antimalarial agents. *J. Med. Chem.* **1986**, *29*, 1796-1798.
- [156] Carroll, F. I.; Berrang, B. D.; Linn, C. P., Synthesis of 4-alkyl- and 4-(β -alkylvinyl)derivatives of primaquine as potential antimalarials. *J. Med. Chem.* **1979**, *22*, 1363-1367.
- [157] Yan, S.-J.; Chien, P.-L.; Cheng, C. C., Synthesis and antimalarial activity of 8-[(1-alkyl-4-aminobutyl)amino]-6-methoxy-4-methylquinolines. *J. Med. Chem.* **1981**, *24*, 215-217.
- [158] Jain, M.; Vangapandu, S.; Sachdeva, S.; Singh, S.; Singh, P. P.; Jena, G. B.; Tikoo, K.; Ramarao, P.; Kaul, C. L.; Jain, R., Discovery of a Bulky 2-tert-Butyl Group Containing Primaquine Analogue That Exhibits Potent Blood-Schizontocidal Antimalarial Activities and Complete Elimination of Methemoglobin Toxicity. *J. Med. Chem.* **2004**, *47*, 285-287.

- [159] Smilkstein, M. J.; Forquer, I.; Kanazawa, A.; Kelly, J. X.; Winter, R. W.; Hinrichs, D. J.; Kramer, D. M.; Riscoe, M. K., A drug-selected *Plasmodium falciparum* lacking the need for conventional electron transport. *Mol. Biochem. Parasitol.* **2008**, *159*, 64-68.
- [160] von Jagow, G.; Ohnishi, T., The chromone inhibitor stigmatellin - binding to the ubiquinol oxidation center at the C-side of the mitochondrial membrane. *FEBS Lett.* **1985**, *185*, 311-315.
- [161] Kim, H.; Esser, L.; Hossain, M. B.; Xia, D.; Yu, C.-A.; Rizo, J.; Helm, D. v. d.; Deisenhofer, J., Structure of Antimycin A1, a Specific Electron Transfer Inhibitor of Ubiquinol-Cytochrome *c* Oxidoreductase. *J. Am. Chem. Soc.* **1999**, *121*, 4902-4903.
- [162] Huang, L.-s.; Cobessi, D.; Tung, E. Y.; Berry, E. A., Binding of the Respiratory Chain Inhibitor Antimycin to the Mitochondrial *bc*₁ Complex: A New Crystal Structure Reveals an Altered Intramolecular Hydrogen-bonding Pattern. *J. Mol. Biol.* **2005**, *351*, 573-597.
- [163] Gao, X.; Wen, X.; Esser, L.; Quinn, B.; Yu, L.; Yu, C.-A.; Xia, D., Structural Basis for the Quinone Reduction in the *bc*₁ Complex: A Comparative Analysis of Crystal Structures of Mitochondrial Cytochrome *bc*₁ with Bound Substrate and Inhibitors at the Q_i Site. *Biochemistry* **2003**, *42*, 9067-9080.
- [164] Bolgunas, S.; Clark, D. A.; Hanna, W. S.; Mauvais, P. A.; Pember, S. O., Potent Inhibitors of the Q_i Site of the Mitochondrial Respiration Complex III. *J. Med. Chem.* **2006**, *49*, 4762-4766.
- [165] Dickie, J. P.; Loomans, M. E.; Farley, T. M.; Strong, F. M., The Chemistry of Antimycin A. XI. *N*-Substituted 3-Formamidosalicylic Amides. *J. Med. Chem.* **1963**, *6*, 424-427.
- [166] Tokutake, N.; Miyoshi, H.; Satoh, T.; Hatano, T.; Iwamura, H., Structural factors of antimycin A molecule required for inhibitory action. *Biochim. Biophys. Acta* **1994**, *1185*, 271-278.
- [167] Tokutake, N.; Miyoshi, H.; Nakazato, H.; Iwamura, H., Inhibition of electron transport of rat-liver mitochondria by synthesized antimycin A analogs. *Biochim. Biophys. Acta* **1993**, *1142*, 262-268.
- [168] Moser, U. K.; Walter, P., Funiculosin, a new specific inhibitor of the respiratory chain in rat liver mitochondria. *FEBS Lett.* **1975**, *50*, 279-282.
- [169] Brasseur, G.; Brivet-Chevillotte, P., Specificities of the two center N inhibitors of mitochondrial *bc*₁ complex, antimycin and funiculosin: strong involvement of cytochrome asparagine-208 in funiculosin binding. *FEBS Lett.* **1994**, *354*, 23-29.
- [170] Nelson, B. D.; Walter, P.; Ernster, L., Funiculosin: an antibiotic with antimycin-like inhibitory properties. *Biochim. Biophys. Acta* **1977**, *460*, 157-162.

- [171] Patani, G. A.; LaVoie, E. J., Bioisoterism: A rational approach in drug design. *Chem. Rev.* **1996**, *96*, 3147-3176.
- [172] Lopes, F.; Capela, R.; Gonçalves, J. O.; Horton, P. N.; Hursthouse, M. B.; Iley, J.; Casimiro, C. M.; Bom, J.; Moreira, R., Amidomethylation of amodiaquine: antimalarial *N*-Mannich base derivatives. *Tetrahedron Lett.* **2004**, *45*, 7663-7666.
- [173] Foresman, J. B.; Frisch, A., *Exploring Chemistry with Electronic Structure Methods*. 2nd edition; Gaussian, Inc.: Pittsburgh, PA, **1996**.
- [174] Cavali, A.; Carloni, P.; Recanatini, M., Target-related applications of first principles quantum chemical methods in drug design. *Chem. Rev.* **2006**, *106*, 3497-3519.
- [175] Bhattacharjee, A. K.; Karle, J. M., Molecular electronic Properties of a Series of 4-Quinolincarbinolamines Define Antimalarial Activity Profile. *J. Med. Chem.* **1996**, *39*, 4622-4629.
- [176] Portela, C.; Afonso, C. M. M.; Pinto, M. M. M.; Ramos, M. J., Definition of an electronic profile of compounds with inhibitory activity against hemozoin aggregation in malaria parasite. *Bioorg. Med. Chem.* **2004**, *12*, 3313-3321.
- [177] Portela, C.; Afonso, C. M. M.; Pinto, M. M. M.; Ramos, M. J., Receptor-drug association studies in the inhibition of the hemozoin aggregation process of malaria. *FEBS Lett.* **2003**, *27435*, 217-222.
- [178] Portela, C.; Afonso, C. M. M.; Pinto, M. M. M.; Ramos, M. J., Computational studies of new potential antimalarial compounds - Stereoelectronic complementarity with the receptor. *J. Comput. Aid. Mol. Des.* **2003**, *17*, 583-595.
- [179] Bhattacharjee, A. K.; Karle, J. M., Functional correlation of molecular electronic properties with potency of synthetic carbinolamine antimalarial agents. *Bioorg. Med. Chem.* **1998**, *6*, 1927-1933.
- [180] Semeniuk, A.; Niedospial, A.; Kalinowska-Tluscik, J.; Nitek, W.; Oleksyn, B. J., Molecular geometry of antimalarial amodiaquine in different crystalline environments. *J. Mol. Struct.* **2008**, *875*, 32-41.
- [181] Hilal, S.; Karickhoff, S. W.; Carreira, L. A., A Rigorous Test for SPARC's Chemical Reactivity Models: Estimation of More Than 4300 Ionization pKa's. *Quant. Struc. Act. Rel.* **1995**, *14*, 348-355.
- [182] Humphrey, W.; Dalke, A.; Schulten, K., VMD - Visual Molecular Dynamics. *J. Mol. Graphics* **1996**, *14*, 33-38.
- [183] Fleming, I., *Frontier Orbitals and Organic Chemical Reactions*. 1st edition; John Wiley & Sons Ltd.: Chichester, 1976; p 249.

- [184] Hudson, R. F., The perturbation treatment of chemical reactivity. *Angew. Chem. Int. Edn.* **1973**, *12*, 36-56.
- [185] Aihara, J.-I., Reduced HOMO-LUMO Gap as an Index of Kinetic Stability for Polycyclic Aromatic Hydrocarbons. *J. Phys. Chem. A* **1999**, *103*, 7487-7495.
- [186] Murray, J. S.; Zilles, B. A.; Jayaswuya, K.; Politzer, D., *J. Am. Chem. Soc.* **1986**, *108*, 915-918.
- [187] Dukhovich, F. S.; Darkhovskii, M. B., Molecular electrostatic potential as a factor of drug-receptor recognition. *J. Mol. Recognit.* **2003**, *16*, 191-202.
- [188] Totrov, M.; Abagyan, R., Flexible ligand docking to multiple receptor conformations: a practical alternative. *Curr. Opin. Struct. Biol.* **2008**, *18*, 178-184.
- [189] Sousa, S. F.; Fernandes, P. A.; Ramos, M. J., Protein-Ligand Docking: Current Status and Future Challenges. *Proteins* **2006**, *65*, 15-26.
- [190] Cozzini, P.; Kellogg, G. E.; Spyraakis, F.; Abraham, D. J.; Costantino, G.; Emerson, A.; Fanelli, F.; Gohlke, H.; Kuhn, L. A.; Morris, G. M.; Orozco, M.; Pertinhez, T. A.; Rizzi, M.; Sotriffer, C. A., Target flexibility: An emerging consideration in drug discovery and design. *J. Med. Chem.* **2008**, *51*, 6237-6255.
- [191] Taylor, R. D.; Jewsbury, P. J.; Essex, J. W., A review of protein-small molecule docking methods. *J. Comput. Aid. Mol. Des.* **2002**, *16*, 151-166.
- [192] Jones, G.; Willett, P.; Glen, R. C., Molecular recognition of receptor sites using a genetic algorithm with a description of desolvation. *J. Mol. Biol.* **1995**, *245*, 43-53.
- [193] Jones, G.; Willett, P.; Glen, R. C.; Leach, A. R.; Taylor, R., Development and validation of a genetic algorithm for flexible docking. *J. Mol. Biol.* **1997**, *267*, 727-748.
- [194] Eldridge, M. D.; Murray, C. W.; Auton, T. R.; Paolini, G. V.; Mee, R. P., Empirical scoring functions: I. The development of a fast empirical scoring function to estimate the binding affinity of ligands in receptor complexes. *J. Comput. Aided Mol. Des.* **1997**, *11*, 425-445.
- [195] Perola, E.; Walters, W. P.; Charifson, P. S., A detailed comparison of current docking and scoring methods on systems of pharmaceutical relevance. *Proteins* **2004**, *56*, 235-249.
- [196] Verdonk, M. L.; Chessari, G.; Cole, J. C.; Hartshorn, M. J.; Murray, C. W.; Nissink, J. W. M.; Taylor, R. D.; Taylor, R., Modeling water molecules in protein-ligand docking using GOLD. *J. Med. Chem.* **2005**, *48*, 6504-6515.
- [197] de Beer, S. B. A.; Vermeulen, N. P. E.; Oostenbrink, C., The role of water molecules in computational drug design. *Curr. Top. Med. Chem.* **2010**, *10*, 55-66.
- [198] Roberts, B. C.; Mancera, R. L., Ligand-Protein docking with water molecules. *J. Chem. Inf. Model.* **2008**, *48*, 397-408.

- [199] Abagyan, R.; Totrov, M., High-throughput docking for lead generation. *Curr. Opin. Chem. Biol.* **2001**, *5*, 375-382.
- [200] Gamo, F.-J.; Sanz, L. M.; Vidal, J.; Cozar, C. d.; Alvarez, E.; Lavandera, J.-L.; Vanderwall, D. E.; Green, D. V. S.; Kumar, V.; Hasan, S.; Brown, J. R.; Peishoff, C. E.; Cardon, L. R.; Garcia-Bustos, J. F., Thousands of chemical starting points for antimalarial lead identification. *Nature* **2010**, *465*, 305-310.
- [201] Raynes, K. J.; Stocks, P. A.; O'Neill, P. M.; Park, B. K.; Ward, S. A., New 4-Aminoquinoline Mannich Base Antimalarials. 1. Effect of an Alkyl Substituent in the 5'-Position of the 4'-Hydroxyanilino Side Chain. *J. Med. Chem.* **1999**, *42*, 2747 - 2751.
- [202] Schock, R. U., Some Displacement Reactions of 4,7-Dichloro-1-methylquinolinium Ion *J. Am. Chem. Soc.* **1957**, *79*, 1670-1672.
- [203] Hawley, S. R.; Bray, P. G.; O'Neill, P. M.; Park, B. P.; Ward, S. A., The role of drug accumulation in 4-aminoquinoline antimalarial potency: The influence of structural substitution and physicochemical properties. *Biochem. Pharmacol.* **1996**, *52*, 723-733.
- [204] Chrystiuk, E.; A., W., A single transition-state in the transfer of the methoxycarbonyl group between isoquinoline and substituted pyridines in aqueous solution. *J. Am. Chem. Soc.* **1987**, *109*, 3040-3046.
- [205] Pytela, O.; Vetesnik, V., Dissociation constants of monosubstituted diphenylamines and an optimized construction of acidity function. *Coll. Czech. Chem. Commun.* **1983**, *48*, 2368-2375.
- [206] Gervasini, A.; Aurou, A., Thermodynamics of adsorbed molecules for a new acid-base topochemistry of alumina. *J. Phys. Chem.* **1993**, *97*, 2628-2639.
- [207] Bordwell, F.; Algrim, D. J., Acidities of anilines in dimethyl sulfoxide solution. *J. Am. Chem. Soc.* **1988**, *110*, 2964-2968.
- [208] Vlasov, V. M.; Os'kina, I. A.; Starichenko, V. F., Oxidation Potentials and Basicities of Amide Anions and Rate Constants of Their Reactions With Aryl Halides in Dimethylsulfoxide. *Russ. J. Org. Chem.* **1997**, *33*, 660-664.
- [209] Joule, J. A.; Mills, K., *Heterocyclic Chemistry*. 4th edition; Blackwell Publishing: 2000.
- [210] Djedouani, A.; Boufas, S.; Allain, M.; Bouet, G.; Khan, M., Zwitterionic 6-methyl-2-oxo-3-[1-(ureidoimino)ethyl]-2H-pyran-4-olate monohydrate *Acta Cryst. E* **2008**, *64*, o1785.
- [211] Wang, Y.; Zhang, J.; Chen, H.; Luo, S., (S)-1-(2-Ammonio-3-methylbutyl)-1,2-dihydropyridin-2-iminium dibromide. *Acta Cryst. E* **2008**, *64*, o1025.
- [212] Semenov, A.; Olson, J. E.; Rosenthal, P. J., Antimalarial Synergy of Cysteine and Aspartic Protease Inhibitors. *Antimicrob. Agents Chemother.* **1998**, *42*, 2254-2258.

- [213] Hawley, S. R.; Bray, P. G.; Mungthin, M.; Atkinson, J. D.; O'Neill, P. M.; Ward, S. A., Relationship between antimalarial drug activity, accumulation, and inhibition of heme polymerization in *Plasmodium falciparum* in vitro. *Antimicrob. Agents Chemother.* **1998**, *42*, 682-686.
- [214] Ketcham, R.; Jamboktar, D.; Martinelli, L., The preparation of *cis*-4-nitro-4'-methoxystilbene via the Wittig Reaction. *J. Org. Chem.* **1962**, *27*, 4666-4667.
- [215] Mylona, A.; Nikokavouras, J.; Takakis, I. M., Stereoselectivity Differences in Wittig Reactions of Semistabilized Ylides. *J. Org. Chem.* **1988**, *53*, 3838-3841.
- [216] Tewari, R. S.; Gupta, K. C.; Kendurkar, P. S., Synthesis of Some New Exocyclic Olefins via Phosphonium Ylides. *J. Chem. Eng. Data* **1977**, *22*, 351-352.
- [217] Hwang, J.-J.; Lin, R.-L.; Shieh, R.-L.; Jwo, J.-J., Study of Wittig reaction of benzyltriphenylphosphonium salt and benzaldehyde via ylide-mediated phase transfer catalysis. Substituent and solvent effects. *J. Mol. Catal. A: Chem.* **1999**, *142*, 125-139.
- [218] Zhang, X.-M.; Fry, A. J.; Bordwell, F. G., Equilibrium Acidities and Homolytic Bond Dissociation Enthalpies of the Acidic C-H Bonds in P-(Para-substituted benzyl)triphenylphosphonium Cations and Related Cations. *J. Org. Chem.* **1996**, *61*, 4101-4106.
- [219] Harrowven, D. C.; Guy, I. L.; Howell, M.; Packham, G. T., The Synthesis of a Combretastatin A-4 Based Library and Discovery of New Cooperative ortho-Effects in Wittig Reactions Leading to (*Z*)-Stilbenes. *Synlett* **2006**, *18*, 2977-2980.
- [220] Dunne, E. C.; Coyne, E. J.; Crowley, P. B.; Gilheany, D. G., Co-operative ortho-effects on the Wittig reaction. Interpretation of stereoselectivity in the reaction of ortho-halo-substituted benzaldehydes and benzyliidenetriphenylphosphoranes. *Tetrahedron Lett.* **2002**, *43*, 2449-2453.
- [221] Thiemann, T.; Watanabe, M.; Tanaka, Y.; Mataka, S., Solvent-free Wittig olefination with stabilized phosphoranes - scope and limitations. *New J. Chem.* **2004**, *28*, 578-584.
- [222] Siegel, B., Mechanism of base-promoted phosphonium salt hydrolysis. Kinetics and multiple substituent effects for a nucleophilic attack at phosphorous. *J. Am. Chem. Soc.* **1978**, *101*, 2265-2268.
- [223] Mandal, P. K.; McMurray, J. S., Pd-C-Induced Catalytic Transfer Hydrogenation with Triethylsilane. *J. Org. Chem.* **2007**, *72*, 6599-6601.
- [224] Boukherroub, R.; Chatgililoglu, C.; Manuel, G., PdCl₂-Catalyzed Reduction of Organic Halides by Triethylsilane. *Organometallics* **1996**, *15*, 1508-1510.

- [225] Bierer, D. E.; Fort, D. M.; Mendez, C. D.; Luo, J.; Imbach, P. A.; Dubenko, L. G.; Jolad, S. D.; Gerber, R. E.; Litvak, J.; Lu, Q.; Zhang, P.; Reed, M. J.; Waldeck, N.; Bruening, R. C.; Noamesi, B. K.; Hector, R. F.; Carlson, T. J.; King, S. R., Ethnobotanical-Directed Discovery of the Antihyperglycemic Properties of Cryptolepine: Its Isolation from *Cryptolepis sanguinolenta*, Synthesis, and in Vitro and in Vivo Activities. *J. Med. Chem.* **1998**, *41*, 894-901.
- [226] Takezawa, Y.; Tanaka, K.; Yori, M.; Tashiro, S.; Shiro, M.; Shionoya, M., Soft Metal-Mediated Base Pairing with Novel Synthetic Nucleosides Possessing an O,S-Donor Ligand *J. Org. Chem.* **2008**, *73*, 6092-6098.
- [227] Tee, O. S.; Paventi, M., Kinetics and mechanism of the bromination of 4-pyridone and related derivatives in aqueous solution. *Can. J. Chem.* **1983**, *61*, 2556-2562.
- [228] O'Leary, M. H.; Stach, R. W., The mechanism of nucleophilic substitution of *N*-methyl-4-substituted pyridinium salts. *J. Org. Chem.* **1972**, *37*, 1491-1493.
- [229] Ploemen, I. H. J.; Prudêncio, M.; Douradinha, B. G.; Ramesar, J.; Fonager, J.; Gemert, G.-J. v.; Luty, A. J. F.; Hermsen, C. C.; Sauerwein, R. W.; Baptista, F. G.; Mota, M. M.; Waters, A. P.; Que, I.; Lowik, C. W. G. M.; Khan, S. M.; Janse, C. J.; Franke-Fayard, B. M. D., Visualisation and Quantitative Analysis of the Rodent Malaria Liver Stage by Real Time Imaging. *PloS ONE* **2009**, *4*, e7881.
- [230] Cogswell, F. B., The Hypnozoite and Relapse in Primate Malaria. *Clin. Microbiol. Rev.* **1992**, *5*, 26-35.
- [231] Tetko, I. V.; Tanchuk, V. Y., Application of associative neural networks for prediction of lipophilicity in ALOGPS 2.1 program. *J. Chem. Inf. Com. Sci.* **2002**, *42*, 1136-1145.
- [232] Kostakis, I. K.; Magiatis, P.; Pouli, N.; Marakos, P.; Skaltsounis, A.-L.; Pratsinis, H.; Léonce, S.; Pierré, A., Design, synthesis and antiproliferative activity of some new pyrazole-fused amino derivatives of the pyranoxanthenone, pyranothioxanthenone, and pyranoacridone ring systems: a new class of cytotoxic agents. *J. Med. Chem.* **2002**, *45*, 2599-2609.
- [233] Cheng, M.-K.; Modi, C.; Cookson, J. C.; Hutchinson, I.; Heald, R. A.; McCarroll, A. J.; Missailidis, S.; Tanious, F.; Wilson, W. D.; Mergny, J.-L.; Laughton, C. A.; Stevens, M. F. G., Antitumor polycyclic acridines. 20.¹ Search for DNA quadruplex binding selectivity in a series of 8,13-dimethylquino[4,3,2-*kl*]acridinium salts: telomere-targeted agents. *J. Med. Chem.* **2008**, *51*, 963-975.
- [234] Effland, R. C.; Klein, J. T.; Davis, L.; Olsen, G. E. *N*-heteroaryl-4-quinolinamines, a process for their preparation and their use as medicaments. EP 0397040A2, **1990**.

- [235] Boschelli, D. H.; Wang, Y. D.; Ye, F.; Wu, B.; Zhang, N.; Dutia, M.; Powell, D. W.; Wissner, A.; Arndt, K.; Weber, J. M.; Boschelli, F., Synthesis and Src Kinase Inhibitory Activity of a Series of 4-Phenylamino-3-quinolinecarbonitriles. *J. Med. Chem.* **2001**, *44*, 822-833.
- [236] Michne, W. M.; Guiles, J. W.; Treasurywala, A. M.; Castonguay, L. A.; Weigelt, C. A.; Oconnor, B.; Volberg, W. A.; Grant, A. M.; Chadwick, C. C.; Krafte, D. S.; Hill, R. J., Novel inhibitors of potassium ion channels on human T lymphocytes. *J. Med. Chem.* **1995**, *38*, 1877-1883.
- [237] Kuo, G.-H.; Eissenstat, M. A.; Wentland, M. P.; Robinson, R. G.; Klingbeil, K. M.; Danz, D. W.; Coughlin, S. A., Potent mammalian topoisomerase II inhibitors: 1-cyclopropyl-6,8-difluoro-1,4-dihydro-7-(2,6-dimethyl-4-pyridinyl)-4-substituted quinolines. *Bioorg. Med. Chem. Lett.* **1995**, *5*, 399-404.
- [238] Kumar, S.; Guha, M.; Choubey, V.; Maity, P.; Bandyopadhyay, U., Antimalarial drugs inhibiting hemozoin (β -hematin) formation: A mechanistic update. *Life Sci.* **2007**, *80*, 813-828.
- [239] Foley, M.; Tilley, L., Quinoline Antimalarials: Mechanisms of Action and Resistance and Prospects for New Agents. *Pharmacol. Ther.* **1998**, *79*, 55-87.
- [240] Solomonov, I.; Osipova, M.; Feldman, Y.; Baetz, C.; Kjaer, K.; Robinson, I. K.; Webster, G. T.; McNaughton, D.; Wood, B. R.; Weissbuch, I.; Leiserowitz, L., Crystal Nucleation, Growth, and Morphology of the Synthetic Malaria Pigment β -Hematin and the Effect Thereon by Quinoline Additives: The Malaria Pigment as a Target of Various Antimalarial Drugs. *J. Am. Chem. Soc.* **2007**, *129*, 2615-2627.
- [241] Dodean, R. A.; Kelly, J. X.; Peyton, D.; Gard, G. L.; Riscoe, M. K.; Winter, R. W., Synthesis and heme-binding correlation with antimalarial activity of 3,6-bis-(ω -*N,N*-diethylaminoamyoxy)-4,5-difluoroxanthone. *Bioorg. Med. Chem.* **2008**, *16*, 1174-1183.
- [242] Dascombe, M. J.; Drew, M. G. B.; Morris, H.; Wilairat, P.; Auparakkitanon, S.; Moule, W. A.; Alizadeh-Shekalgourabi, S.; Evans, P. G.; Lloyd, M.; Dyas, A. M.; Carr, P.; Ismail, F. M. D., Mapping Antimalarial Pharmacophores as a Useful Tool for the Rapid Discovery of Drugs Effective in Vivo: Design, Construction, Characterization, and Pharmacology of Metaquine. *J. Med. Chem.* **2005**, *48*, 5423-5436.
- [243] de Dios, A. C.; Casabianca, L. B.; Kosar, A.; Roepe, P. D., Structure of the Amodiaquine-FPIX μ Oxo Dimer Solution Complex at Atomic Resolution. *Inorg. Chem.* **2004**, *43*, 8078-8084.

- [244] Egan, T., Interactions of quinoline antimalarials with hematin in solution. *J. Inorg. Biochem.* **2006**, *100*, 916-926.
- [245] Egan, T. F.; Mavuso, W. W.; Ross, D. C.; Marques, H. M., Thermodynamic factors controlling the interaction of quinoline antimalarial drugs with ferriprotoporphyrin IX. *J. Inorg. Biochem.* **1997**, *68*, 137-145.
- [246] Wang, Z.-X.; Jiang, R.-F., A novel two-site binding equation presented in terms of the total ligand concentration. *FEBS Lett.* **1996**, *392*, 245-249.
- [247] Vippagunta, S. R.; Dorn, A.; Ridley, R. G.; Vennerstrom, J. L., Characterization of chloroquine-hematin μ -oxo dimer binding by isothermal titration calorimetry. *Biochim. Biophys. Acta* **2000**, *1475*, 133-140.
- [248] O'Neill, P. M.; Park, B. K.; Shone, A. E.; Maggs, J. L.; Roberts, P.; Stocks, P. A.; Biagini, G. A.; Bray, P. G.; Gibbons, P.; Berry, N.; Winstanley, P. A.; Mukhtar, A.; Bonar-Law, R.; Hindley, S.; Bambal, R. B.; Davis, C. B.; Bates, M.; Hart, T. K.; Gresham, S. L.; Lawrence, R. M.; Brigandi, R. A.; Gomez-delas-Heras, F. M.; Gargallo, D. V.; Ward, S. A., Candidate Selection and Preclinical Evaluation of *N*-tert-Butyl Isoquine (GSK369796), An Affordable and Effective 4-Aminoquinoline Antimalarial for the 21st Century. *J. Med. Chem.* **2009**, *52*, 1408–1415.
- [249] Bachhawat, K.; Thomas, C. J.; Surolia, N.; Surolia, A., Interaction of Chloroquine and Its Analogues with Heme: An Isothermal Titration Calorimetric Study. *Biochem. Biophys. Res. Commun.* **2000**, *276*, 1075–1079.
- [250] Wiesner, J.; Ortmann, R.; Jomaa, H.; Schlitzer, M., New Antimalarial Drugs. *Angew. Chem. Int. Edn.* **2003**, *42*, 5274 – 5293.
- [251] Meyer, N. D.; Haemers, A.; Mishra, L.; Pandey, H.-K.; Pieters, L. A. C.; Berghe, D. A. V.; Vlietinck, A. J., 4'-Hydroxy-3-methoxyflavones with potent antipicornavirus activity. *J. Med. Chem.* **1991**, *34*, 736-746.
- [252] Shen, Y.; Zhang, J.; Sheng, R.; Dong, X.; He, Q.; Yang, B.; Hu, Y., Synthesis and biological evaluation of novel flavonoid derivatives as dual binding acetylcholinesterase inhibitors. *J. Enzyme Inhib. Med. Chem.* **2009**, *24*, 372-380.
- [253] Beutler, J. A.; Hamel, E.; Vlietinck, A. J.; Haemers, A.; Rajan, P.; Roitman, J. N.; Cardelina II, J. H.; Boyd, M. R., Structure-activity requirements for flavone cytotoxicity and binding to tubulin. *J. Med. Chem.* **1998**, *41*, 2333-2338.
- [254] Shawa, A. Y.; Chang, C.-Y.; Liao, H.-H.; Lu, P.-J.; Chen, H.-L.; Yang, C.-N.; Li, H.-Y., Synthesis of 2-styrylchromones as a novel class of antiproliferative agents targeting carcinoma cells. *Eur. J. Med. Chem.* **2009**, *44*, 2552–2562.

- [255] Menichincheri, M.; Ballinari, D.; Bargiotti, A.; Bonomini, L.; Ceccarelli, W.; D'Alessio, R.; Fretta, A.; Moll, J.; Polucci, P.; Soncini, C.; Tibolla, M.; Trosset, J.-Y.; Vanotti, E., Catecholic Flavonoids Acting as Telomerase Inhibitors. *J. Med. Chem.* **2004**, *47*, 6466-6475.
- [256] Wanich, S.; Yenjai, C., Amino and Nitro Derivatives of 5,7-Dimethoxyflavone from *Kaempferia parviflora* and Cytotoxicity against KB Cell Line. *Arch. Pharm. Res.* **2009**, *32*, 1185-1189.
- [257] Ragazzoni, P. A.; Iley, J.; Missailidis, S., Structure-activity Studies of the Binding of the Flavonoid Scaffold to DNA. *Anticancer Res.* **2009**, *29*, 2289-2294.
- [258] Furuta, T.; Kimura, T.; Kondo, S.; Mihara, H.; Wakimoto, T.; Nukaya, H.; Tsuji, K.; Tanaka, K., Concise total synthesis of flavone C-glycoside having potent anti-inflammatory activity. *Tetrahedron* **2004**, *60*, 9375-9379.
- [259] Horvath, A.; Nussbaumer, P.; Wolff, B.; Billich, A., 2-(1-Adamantyl)-4-(thio)chromenone-6-carboxylic acids: potent reversible inhibitors of human steroid sulfatase. *J. Med. Chem.* **2004**, *47*, 4268-4276.
- [260] Mavel, S.; Dikic, B.; Palakas, S.; Emond, P.; Greguric, I.; Garcia, A. G. d.; Mattner, F.; Garrigos, M.; Guilloteau, D.; Katsifis, A., Synthesis and biological evaluation of a series of flavone derivatives as potential radioligands for imaging the multidrug resistance-associated protein 1 (ABCC1/MRP1). *Bioorg. Med. Chem.* **2006**, *14*, 1599-1607.
- [261] Ono, M.; Watanabe, R.; Kawashima, H.; Kawai, T.; Watanabe, H.; Haratake, M.; Saji, H.; Nakayama, M., ¹⁸F-labeled flavones for *in vivo* imaging of β -amyloid plaques in Alzheimer's brains. *Bioorg. Med. Chem.* **2009**, *17*, 2069-2076.
- [262] Ono, M.; Yoshida, N.; Ishibashi, K.; Haratake, M.; Arano, Y.; Mori, H.; Nakayama, M., Radioiodinated Flavones for *in Vivo* Imaging of β -Amyloid Plaques in the Brain. *J. Med. Chem.* **2005**, *48*, 7253-7260.
- [263] Dekermendjian, K.; Kahnberg, P.; Witt, M.-R.; Sterner, O.; Nielsen, M.; Liljefors, T., Structure-Activity Relationships and Molecular Modeling Analysis of Flavonoids Binding to the Benzodiazepine Site of the Rat Brain GABA_A Receptor Complex. *J. Med. Chem.* **1999**, *42*, 4343-4350.
- [264] Gurung, S. K.; Kim, H. P.; Park, H., Inhibition of Prostaglandin E₂ Production by Synthetic Wogonin Analogs. *Arch. Pharm. Res.* **2009**, *32*, 1503-1508.
- [265] Cushman, M.; Zhu, H.; Geahlen, R. L.; Krakert, A. J., Synthesis and Biochemical Evaluation of a Series of Aminoflavones as Potential Inhibitors of Protein-Tyrosine Kinases p56^{lck}, EGFR, and p60^{v-src}. *J. Med. Chem.* **1994**, *37*, 3353-3362.

- [266] Ares, J. J.; Outt, P. E.; Randall, J. L.; Murray, P. D.; Weisshaar, P. S.; O'Brien, L. M.; Ems, B. L.; Kakodkar, S. V.; Kelm, G. R.; Kershaw, W. C.; Werchowksi, K. M.; Parkinson, A., Synthesis and Biological Evaluation of Substituted Flavones as Gastroprotective Agents. *J. Med. Chem.* **1995**, *38*, 4937-4943.
- [267] Auffret, G.; Labaied, M.; Frappier, F.; Rasoanaivo, P.; Grellier, P.; Lewin, G., Synthesis and antimalarial evaluation of a series of piperazinyl flavones. *Bioorg. Med. Chem. Lett.* **2007**, *17*, 959-963.
- [268] Lim, S. S.; Kim, H.-S.; Lee, D.-U., *In vitro* antimalarial activity of flavonoids and chalcones. *Bull. Korean Chem. Soc.* **2007**, *28*, 2495-2497.
- [269] Boonphong, S.; Baramée, A.; Kittakoop, P.; Puangsombat, P., Antitubercular and antiplasmodial prenylated flavones from the roots of *Artocarpus altilis*. *Chiang Mai J. Sci.* **2007**, *34*, 339-344.
- [270] Widyawaruyanti, A.; Subehan; Kalauni, S. K.; Awale, S.; Nindatu, M.; Zaini, N. C.; Syafruddin, D.; Asih, P. B. S.; Tezuka, Y.; Kadota, S., New prenylated flavones from *Artocarpus champeden* and their antimalarial activity *in vitro*. *J. Nat. Prod.* **2007**, *61*, 410-413.
- [271] Tasdemir, D.; Lack, G.; Brun, R.; Rüedi, P.; Scapozza, L.; Perozzo, R., Inhibition of *Plasmodium falciparum* Fatty Acid Biosynthesis: Evaluation of FabG, FabZ, and FabI as Drug Targets for Flavonoids. *J. Med. Chem.* **2006**, *49*, 3345-3353.
- [272] Salvi, M.; Brunati, A. M.; Clari, G.; Toninello, A., Interaction of genistein with the mitochondrial electron transport chain results in opening of the membrane transition pore. *Biochim. Biophys. Acta* **2002**, *1556*, 187-196.
- [273] Awuah, E.; Capretta, A., Access to flavones via a microwave-assisted, one-pot Sonogashira-carbonylation, annulation reaction. *Org. Lett.* **2009**, *11*, 3210-3213.
- [274] Miao, H.; Yang, Z., Regiospecific carbonylative annulation of iodophenol acetates and acetylenes to construct flavones by a new catalyst of palladium-thiourea-dppp complex. *Org. Lett.* **2000**, *2*, 1765-1768.
- [275] Torii, S.; Okumoto, H.; Xu, L. H.; Sadakane, M.; Shostakovskiy, M. V.; Ponomaryov, A. B.; Kalinin, V. N., Syntheses of chromones and quinolones via Pd-catalyzed carbonylation of *o*-iodophenols and anilines in the presence of acetylenes. *Tetrahedron* **1993**, *49*, 6773-6784.
- [276] Hirao, I.; Yamagushi, M.; Hamada, M., A convenient synthesis of 2- and 2,3-substituted 4H-chromen-4-ones. *Synthesis* **1984**, *12*, 1076-1078.

- [277] Ganguly, A. K.; Kaur, S.; Mahata, P. K.; Biswas, D.; Pramanik, B. N.; Chan, T. M., Synthesis and properties of 3-acyl- γ -pyrones, a novel class of flavones and chromones. *Tetrahedron Lett.* **2005**, *46*, 4119-4121.
- [278] Enders, D.; Geibel, G.; Osborne, S., Diastereo- and enantioselective total synthesis of stigmatellin A. *Chem. Eur. J.* **2000**, *6*, 1302-1309.
- [279] Fitzmaurice, R. J.; Etheridge, Z. C.; Jumel, E.; Woolfson, D. N.; Caddick, S., Microwave enhanced palladium catalysed coupling reactions: a diversity-oriented synthesis approach to functionalised flavones. *Chem. Commun.* **2006**, *46*, 4814-4816.
- [280] Pathak, V. N.; Gupta, R.; Varshney, B., A 'One Pot' Synthesis of 2-Aryl-4*H*-1-benzopyran-4-ones Under Coupled Microwave Phase Transfer Catalysis (PTC) and Ultrasonic Irradiation PTC. *J. Heterocyclic Chem.* **2008**, *45*, 589-592.
- [281] Ghani, S. B. A.; Weaver, L.; Zidan, Z. H.; Ali, H. M.; Keevil, C. W.; Brown, R. C. D., Microwave-assisted synthesis and antimicrobial activities of flavonoid derivatives. *Bioorg. Med. Chem. Lett.* **2008**, *18*, 518-522.
- [282] Cabrera, M.; Simoens, M.; Falchi, G.; Lavaggi, M. L.; Piro, O. E.; Castellano, E. E.; Vidal, A.; Azqueta, A.; Monge, A.; Ceráin, A. L. d.; Sagrera, G.; Seoane, G.; Cerecetto, H.; González, M., Synthetic chalcones, flavanones, and flavones as antitumoral agents: Biological evaluation and structure-activity relationships. *Bioorg. Med. Chem.* **2007**, *15*, 3356-3367.
- [283] Fougereuse, A.; Gonzalez, E.; Brouillard, R., A Convenient Method for Synthesizing 2-Aryl-3-hydroxy-4-oxo-4*H*-1-benzopyrans or Flavonols. *J. Org. Chem.* **2000**, *65*, 583-586.
- [284] Gobbi, S.; Rampa, A.; Bisi, A.; Belluti, F.; Piazzini, L.; Valenti, P.; Caputo, A.; Zampiron, A.; Carrara, M., Synthesis and Biological Evaluation of 3-Alkoxy Analogues of Flavone-8-acetic Acid. *J. Med. Chem.* **2003**, *46*, 3662-3669.
- [285] Menezes, M. J.; Manjrekar, S.; Pai, V.; Patre, R. E.; Tilve, S. G., A facile microwave assisted synthesis of flavones. *Ind. J. Chem.* **2009**, *48*, 1311-1314.
- [286] Sawyer, J. S.; Schmittling, E. A.; Palkowitz, J. A.; Smith-III, W. J., Synthesis of Diaryl Ethers, Diaryl Thioethers, and Diarylamines Mediated by Potassium Fluoride-Alumina and 18-Crown-6: Expansion of Scope and Utility. *J. Org. Chem.* **1998**, *63*, 6338-6343.
- [287] Prihod'ko, R.; Sychev, M.; Kolomitsyn, I.; J. Stobbelaar, P.; Hensen, E. J. M.; van Santen, R. A., Layered double hydroxides as catalysts for aromatic nitrile hydrolysis. *Microp. Mesop. Mater.* **2002**, *56*, 241-255.

- [288] Riva, C.; de Toma, C.; Donadel, L.; Boi, C.; Pennini, R.; Motta, G.; Leonardi, A., New DBU (1,8-diazabicyclo[5.4.0]undec-7-ene) assisted one-pot synthesis of 2,8-disubstituted 4*H*-1-benzopyran-4-ones. *Synthesis* **1997**, *2*, 195-201.
- [289] Tang, L.; Zhang, S.; Yang, J.; Gao, W.; Cui, J.; Zhuang, T., A Novel Approach to the Synthesis of 6-Amino-7-hydroxyflavone. *Molecules* **2004**, *9*, 842-848.
- [290] Shibatomi, K.; Zhang, Y.; Yamamoto, H., Lewis acid catalyzed benzylic bromination. *Chem. Asian J.* **2008**, *3*, 1581-1584.
- [291] Itagaki, Y.; Kurokawa, T.; Sasaki, S.-I., The mass spectra of chalcones, flavones and isoflavones. *Bull. Chem. Soc. Jap.* **1966**, *39*, 538-543.
- [292] Burnham, W. S.; Sidwell, R. W.; Tolman, R. L.; Stout, M. G., Synthesis and antiviral activity of 4'-hydroxy-5,6,7,8-tetramethoxyflavone. *J. Med. Chem.* **1972**, *15*, 1075-1076.
- [293] Mills, C. J.; Mateeva, N. N.; Redda, K. K., Synthesis of Novel Substituted Flavonoids. *J. Heterocyclic Chem.* **2006**, *43*, 59-64.
- [294] Lorenz, M.; Kabir, M. S.; Cook, J. M., A two step synthesis of BzR/GABAergic active flavones via a Wacker-related oxidation. *Tetrahedron Lett.* **2010**, *51*, 1095-1098.
- [295] Movassagh, B.; Balalaie, S.; Shaygana, P., A new and efficient protocol for preparation of thiol esters from carboxylic acids and thiols in the presence of 2-(1*H*-benzotriazole-1-yl)-1,1,3,3-tetramethyluronium tetrafluoroborate (TBTU). *Arkivoc* **2007**, *8*, 47-52.
- [296] Felpin, F.-X.; Lory, C.; Sow, H.; Acherar, S., Practical and efficient entry to isoflavones by Pd(0)/C-mediated Suzuki-Miyayra reaction. Total synthesis of geranylated isoflavones. *Tetrahedron* **2007**, *63*, 3010-3016.
- [297] Wong, K.-T.; Chien, Y.-Y.; Liao, Y.-L.; Lin, C.-C.; Chou, M.-Y.; Leung, M.-K., Efficient and convenient nonaqueous workup procedure for the preparation of arylboronic esters. *J. Org. Chem.* **2002**, *67*, 1041-1044.
- [298] Bissantz, C.; Kuhn, B.; Stahl, M., A Medicinal Chemist's Guide to Molecular Interactions. *J. Med. Chem.* **2010**, *53*, 5061-5084.
- [299] Lu, Y.; Shi, T.; Wang, Y.; Yang, H.; Yan, X.; Luo, X.; Jiang, H.; Zhu, W., Halogen Bonding-A Novel Interaction for Rational Drug Design? *J. Med. Chem.* **2009**, *52*, 2854-2862.
- [300] Cunha-Rodrigues, M.; Portugal, S.; Prudêncio, M.; Gonçalves, L. A.; Casalou, C.; Buger, D.; Sauerwein, R.; Haas, W.; Mota, M. M., Genistein-supplemented diet decreases malaria liver infection in mice and constitutes a potential prophylactic strategy. *PLoS ONE* **2008**, *3*, e2732.
- [301] Sun, H., Pharmacophore-based virtual screening. *Curr. Med. Chem.* **2008**, *15*, 1018-1024.

- [302] Schneider, G.; Fechner, U., Computer-based *de novo* design of drug-like molecules. *Nat. Rev. Drug Discov.* **2005**, *4*, 649-663.
- [303] Bleicher, K. H.; Böhm, H.-J.; Müller, K.; Alanine, A. I., Hit and lead generation: beyond high-throughput screening. *Nat. Rev. Drug Discov.* **2003**, *2*, 369-278.
- [304] Adane, L.; Patel, D. S.; Bharatam, P. V., Shape- and chemical feature-based 3D-pharmacophore model generation and virtual screening: Identification of potential leads for *P. falciparum* DHFR enzyme inhibition. *Chem. Biol. Drug Des.* **2010**, *75*, 115-126.
- [305] Bhattacharjee, A. K.; Hartell, M. G.; Nichols, D. A.; Hicks, R. P.; Stanton, B.; van Hamont, J. E.; Milhous, W. K., Structure-activity relationship study of antimalarial indolo[2,1,b]quinazoline-6,12-diones (tryptanthrins. Three dimensional pharmacophore modeling and identification of new antimalarial candidates. *Eur. J. Med. Chem.* **2004**, *39*, 59-67.
- [306] Acharya, B. N.; Saraswat, D.; Kaushik, M. P., Pharmacophore based discovery of potential antimalarial agent targeting haem detoxification pathway. *Eur. J. Med. Chem.* **2008**, *43*, 2840-2852.
- [307] Bhattacharjee, A. K., *In silico* three-dimensional pharmacophores for aiding the discovery of the Pfmrk (*Plasmodium* cyclin-dependent protein kinases) specific inhibitors for the therapeutic treatment of malaria. *Expert. Opin. Drug Discov.* **2007**, *2*, 1115-1127.
- [308] Desai, P. V.; Patny, A.; Sabnis, Y.; Tekwani, B.; Gut, J.; Rosenthal, P.; Srivastava, A.; Avery, M., Identification of Novel Parasitic Cysteine Protease Inhibitors Using Virtual Screening. 1. The ChemBridge Database. *J. Med. Chem.* **2004**, *47*, 6609-6615.
- [309] Desai, P. V.; Patny, A.; Gut, J.; Rosenthal, P. J.; Tekwani, B.; Srivastava, A.; Avery, M., Identification of Novel Parasitic Cysteine Protease Inhibitors by Use of Virtual Screening. 2. The Available Chemical Directory. *J. Med. Chem.* **2006**, *49*, 1576-1584.
- [310] Li, H.; Huang, J.; Chen, L.; Liu, X.; Chen, T.; Zhu, J.; Lu, W.; Shen, X.; Li, J.; Hilgenfeld, R.; Jiang, H., Identification of Novel Falcipain-2 Inhibitors as Potential Antimalarial Agents through Structure-Based Virtual Screening. *J. Med. Chem.* **2009**, *52*, 4936-4940.
- [311] Nicola, G.; Smith, C. A.; Lucumi, E.; Kuo, M. R.; Karagyozev, L.; Fidock, D. A.; Sacchettini, J. C.; Abagyan, R., Discovery of novel inhibitors targeting enoyl-acyl carrier protein reductase in *Plasmodium falciparum* by structure-based virtual screening. *Biochem. Biophys. Res. Comm.* **2007**, *358*, 686-691.
- [312] Eckert, H.; Bajorath, J., Molecular similarity analysis in virtual screening: foundations, limitations and novel approaches. *Drug Discov. Today* **2007**, *12*, 225-233.

- [313] Klebe, G., Virtual ligand screening: strategies, perspectives and limitations. *Drug Discov. Today* **2006**, *11*, 580-594.
- [314] ChemicalComputingGroup *MOE: Molecular Operating Environment*, 2008.10; Montreal, 2008.
- [315] Wolber, G.; Seidel, T.; Bendix, F.; Langer, T., Molecule-pharmacophore superpositioning and pattern matching in computational drug design. *Drug Discov. Today* **2008**, *13*, 23-29.
- [316] Chen, I.-J.; Foloppe, N., Conformational sampling of druglike molecules with MOE and Catalyst: implications for pharmacophore modeling and virtual screening. *J. Chem. Inf. Model.* **2008**, *48*, 1773-1791.
- [317] Irwin, J. J.; Shoichet, B. K., ZINC - A Free Database of Commercially Available Compounds for Virtual Screening. *J. Chem. Inf. Model.* **2005**, *45*, 177-182.
- [318] Lipinski, C. A.; Lombardo, F.; Dominy, B. W.; Feeney, P. J., Experimental and computational approaches to estimate solubility and permeability in drug discovery and development settings. *Adv. Drug Delivery Rev.* **1997**, *23*, 3-25.
- [319] Lipinski, C. A., Drug-like properties and the causes of poor solubility and poor permeability. *J. Pharmacol. Toxicol. Methods* **2000**, *44*, 235-249.
- [320] Alvarez, J.; Soichet, B., *Virtual Screening in Drug Discovery*. Taylor & Francis: Boca Raton, FL, 2005; p 451.
- [321] Shahinas, D.; Liang, M.; Datti, A.; Pillai, D. R., A repurposing strategy identifies novel synergistic inhibitors of *Plasmodium falciparum* Heat Shock Protein 90. *J. Med. Chem.* **2010**, *53*, 3552-3557.
- [322] Davis, M. A.; Duffy, S.; Avery, V. M.; Camp, D.; Hooper, J. N. A.; Quinn, R. J., (+)-7-Bromotrypargine: an antimalarial β -carboline from Australian marine sponge *Ancorina* sp. *Tetrahedron Lett.* **2010**, *51*, 583-585.
- [323] Kkokong, J. L.; Smith, P. P.; Matsabis, G. M., 1,2,4-Triazino-[5,6*b*]indole derivatives: effects of the trifluoromethyl group on in vitro antimalarial activity. *Bioorg. Med. Chem.* **2005**, *13*, 2935-2942.
- [324] Lambert, P. F.; Ahlquist, P. G.; Pyeon, D.; Huang, H. S., Drugs to prevent HPV infection. WO 2009/148961, **2009**.
- [325] Zhu, S.; Zhang, Q.; Gudise, C.; Wei, L.; Smith, E.; Zeng, Y., Synthesis and biological evaluation of febrifugine analogues as potential antimalarial agents. *Bioorg. Med. Chem.* **2009**, *17*, 4496-4502.

- [326] Jiang, S.; Zeng, Q.; Gettayacamin, M.; Tungtaeng, A.; Wannaying, S.; Lim, A.; Hansukjariya, P.; Okunji, C. O.; Zhu, S.; Fang, D., Antimalarial Activities and Therapeutic Properties of Febrifugine Analogs. *Antimicrob. Agents Chemother.* **2005**, *49*, 1169-1176.
- [327] Kikuchi, H.; Tasaka, H.; Hirai, S.; Takaya, Y.; Iwabuchi, Y.; Ooi, H.; Hatakeyama, S.; Kim, H.-S.; Wataya, Y.; Oshima, Y., Potent Antimalarial Febrifugine Analogues against the *Plasmodium Malaria Parasite*. *J. Med. Chem.* **2002**, *45*, 2563-2570.
- [328] Suping, J.; Thomas, H. H.; Vilbur, M., Antimalarial activities of febrifugine analogues. WO 2004/000319, **2004**.
- [329] Kim, H. S.; Chung, Y. M.; Park, Y. J.; Kim, J. N., Reinvestigation for the Synthesis of 1,2-Isoindolo-1,(2H),3,4-tetrahydro- β -carbonile. *Bull. Korean Chem. Soc.* **2000**, *21*, 371-372.
- [330] Cartwright, D.; Ferguson, J. R.; Giannopoulos, T.; Varvounis, G.; Wakefield, B. J., Abnormal Nucleophilic Substitution in 3-Trichloromethylpyridine, its *N*-Oxide and 3,5-Bis(trichloromethyl)pyridine. *Tetrahedron* **1995**, *51*, 12791-12796.
- [331] Dennington, R.; Keith, T.; Millam, J.; Eppinnett, K.; Hovell, W. L.; Gilliland, R. *GaussView 3.0*, Semichem, Inc.: Shawnee Mission, KS, 2003.
- [332] Frisch, M. J.; Trucks, G. W.; Schlegel, H. B.; Scuseria, G. E.; Robb, M. A.; Cheeseman, J. R.; J. A. Montgomery, J.; Vreven, T.; Kudin, K. N.; Burant, J. C.; Millam, J. M.; Iyengar, S. S.; Tomasi, J.; Barone, V.; Mennucci, B.; Cossi, M.; Scalmani, G.; Rega, N.; Petersson, G. A.; Nakatsuji, H.; Hada, M.; Ehara, M.; Toyota, K.; Fukuda, R.; Hasegawa, J.; Ishida, M.; Nakajima, T.; Honda, Y.; Kitao, O.; Nakai, H.; Klene, M.; Li, X.; Knox, J. E.; Hratchian, H. P.; Cross, J. B.; Bakken, V.; Adamo, C.; Jaramillo, J.; Gomperts, R.; Stratmann, R. E.; Yazyev, O.; Austin, A. J.; Cammi, R.; Pomelli, C.; Ochterski, J. W.; Ayala, P. Y.; Morokuma, K.; Voth, G. A.; Salvador, P.; Dannenberg, J. J.; Zakrzewski, V. G.; Dapprich, S.; Daniels, A. D.; Strain, M. C.; Farkas, O.; Malick, D. K.; Rabuck, A. D.; Raghavachari, K.; Foresman, J. B.; Ortiz, J. V.; Cui, Q.; Baboul, A. G.; Clifford, S.; Cioslowski, J.; Stefanov, B. B.; Liu, G.; Liashenko, A.; Piskorz, P.; Komaromi, I.; Martin, R. L.; Fox, D. J.; Keith, T.; Al-Laham, M. A.; Peng, C. Y.; Nanayakkara, A.; Challacombe, M.; Gill, P. M. W.; Johnson, B.; Chen, W.; Wong, M. W.; Gonzalez, C.; Pople, J. A. *Gaussian 03*, Revision C.02; Gaussian Inc.: Wallingford CT, 2004.
- [333] Dewar, M. J. S.; Zoebisch, E. G.; Healy, E. F.; Stewart, J. J. P., AM1: A New General Purpose Quantum Mechanical Molecular Model. *J. Am. Chem. Soc.* **1985**, *107*, 3902-3909.
- [334] Becke, A. D., Density-functional exchange-energy approximation with correct asymptotic behavior. *Phys. Rev. A* **1988**, *38*, 3098-3100.

- [335] Becke, A. D., Density functional thermochemistry. III. The role of exact exchange. *J. Chem. Phys.* **1993**, *98*, 5648-5652.
- [336] Lee, C. T.; Yang, W.; Parr, R. G., Development of the Colle-Salvetti correlation-energy formula into a functional of the electron density. *Phys. Rev. B* **1988**, *37*, 785-789.
- [337] Portmann, S.; Lüthi, H. T., MOLEKEL: an interactive molecular graphics tool. *Chimia* **2000**, *54*, 766-770.
- [338] Pettersen, E. F.; Goddard, T. D.; Huang, C. C.; Couch, G. S.; Greenblatt, D. M.; Meng, E. C.; Ferrin, T. E., UCSF Chimera - A Visualization System for Exploratory Research and Analysis. *J. Comput. Chem.* **2004**, *25*, 1605-1612.
- [339] Wang, J.; Wang, W.; Kollman, P. A.; Case, D. A., Automatic atom type and bond type perception in molecular mechanical calculations. *J. Mol. Graph. Model.* **2006**, *25*, 247-260.

Publications resulting from this thesis

- I Rodrigues, T.; Moreira, R.; Dacunha-Marinho B.; Lopes F., Bis{(E)-3-[(diethylmethylammonio)methyl]-N-[3-(N,N-dimethylsulfamoyl)-1-methylpyridin-4-ylidene]-4-methoxyanilinium} tetraiodide pentahydrate. *Acta Cryst. E* **2009**, *65*, o283-o284.
- II Rodrigues, T.; Guedes, R. C.; dos Santos, D. J. V. A.; Carrasco M.; Gut, J.; Rosenthal, P. J.; Moreira, R.; Lopes, F. Design, synthesis and structure-activity relationships of (1*H*-pyridin-4-ylidene)amines as potential antimalarials. *Bioorg. Med. Chem. Lett.* **2009**, *19*, 3476-3480.
- III Rodrigues, T.; Lopes, F.; Moreira, R., Inhibitors of the Mitochondrial Electron Transport Chain and *de novo* Pyridimidine Biosynthesis as Antimalarials: The Present Status. *Curr. Med. Chem.* **2010**, *17*, 929-956.
- IV Rodrigues, T.; dos Santos, D. J. V. A.; Moreira, R.; Lopes, F.; Guedes, R. C., A Quantum Mechanical Study of Novel Potential Inhibitors of Cytochrome *bc*₁ as Antimalarial Compounds. *Int. J. Quantum Chem.* **2010**, DOI 10.1002/qua22741.
- V Rodrigues, T.; Lopes, F.; Moreira, R., Microwave-assisted Wittig reaction of semistabilized nitro-substituted benzyltriphenyl-phosphorous ylides with aldehydes in phase transfer conditions. *Synth. Commun.* **2010**, *accepted*.
- VI Rodrigues, T.; Guedes, R. C.; dos Santos, J. V. A.; Gut, J.; Rosenthal, P. J.; Biagini, G. A.; O'Neill, P. M.; Moreira, R.; Lopes, F., Identification of novel antimalarial leads through virtual screening. *In preparation*.
- VII Rodrigues, T.; Guedes, R. C.; dos Santos, D. J. V. A.; Gut, J.; Rosenthal, P. J.; Moreira, R.; Lopes, F. Design, synthesis and SAR of novel 4(1*H*)-quinolonimines with potent antiplasmodial activity. *In preparation*.
- VIII Rodrigues, T.; da Cruz, F. P.; Prudêncio, M.; Gut, J.; Rosenthal, P. J.; Moreira, R.; Lopes, F. Design and synthesis of flavones with activity against the liver stage of *Plasmodium* sp. *In preparation*.